



日中笹川医学奨学金制度
第41期（学位取得コース）

中間報告書

2019年4月～2020年3月

公益財団法人 日中医学協会

目 次

No.	氏名	所属機関	研究先	指導責任者	頁数
G1	趙 申 チウ シン (課程博士)	北海道大学大学院歯学院 博士課程学生 研究テーマ：PTH間欠投与による骨血管の組織学的変化	北海道大学大学院歯学研究院 口腔顎顔面外科学教室	鄭 漢忠 教授	……P1
G2	常 立甲 ジョウ リツコウ (課程博士)	石家荘市第四医院 主管技師 研究テーマ：精神疾患の病因解明と新規治療法の開発	千葉大学 社会精神保健教育研究センター	橋本 謙二 副センター長・教授	……P32
G3	朱 俊 シュ シュン (論文博士)	江蘇省蘇北人民医院 主治医師 研究テーマ：骨髄由来免疫制御細胞のマウス角膜移植に及ぼす影響	順天堂大学大学院医学研究科 眼科学	村上 晶 教授	……P136
G4	孟 雪 モウ セツ (論文博士)	中国医科大学附属盛京医院 主治医師 研究テーマ：次世代シークエンサーを用いた頭頸部癌の特異的癌遺伝子の創出	順天堂大学大学院医学研究科 耳鼻咽喉科学	池田 勝久 主任教授	……P145
G5	蔣 元源 ショウ ゲンゲン (課程博士)	南京市口腔医院 住院医師 研究テーマ：咀嚼と下顎骨軟骨組織の病理学的変化の関係について	昭和大学大学院歯学研究科 歯科矯正学講座	槇 宏太郎 教授	休学中
G6	劉 雨桐 リュウ ウトウ (課程博士)	西安交通大学外国語学院 学生 研究テーマ：日本人医療通訳者と外国人医療通訳者の特性比較研究	杏林大学大学院 国際協力研究科	宮首 弘子 教授	……P169
G7	許 婧 キョウ セイ (課程博士)	貴州省医科大学附属医院 主治医師 研究テーマ：SGLT-2 阻害薬と糖尿病性腎臓病	金沢医科大学 糖尿病・内分泌内科	古家 大祐 教授	……P175
G8	盧 雪婧 ロ セツセイ (課程博士)	京都大学大学院医学研究科 博士課程学生 研究テーマ：脂肪摂食後GIP分泌のメカニズム	京都大学大学院医学研究科 糖尿病・内分泌・栄養内科学	稲垣 暢也 教授	……P198
G9	張 含鳳 チウ ガンフウ (課程博士)	四川省腫瘤医院 主管護師 研究テーマ：中国の生後年齢にある男性がん患者の妊娠性温存をめざした支援プログラムの効果	広島大学大学院医系科学研究科 保健学分野	宮下 美香 教授	……P204
G10	崔 力萌 サイ リキモウ (課程博士)	北京市預防医学研究中心 研究員 研究テーマ：福島県富岡町における環境放射能モニタリングと住民の被ばく線量評価	長崎大学 原爆後障害医療研究所	高村 昇 教授	……P210

日中笹川医学奨学金制度(学位取得コース)中間評価書

課程博士：指導教官用



第41期 研究者番号： G4101

作成日： 2020年3月9日

氏名	趙申	Zhao Shen	性別	M	生年月日	1989. 07. 07
所属機関(役職)	北海道大学大学院歯学院(博士課程学生)					
研究先(指導教官)	北海道大学大学院歯学研究院口腔顎顔面外科学教室(鄭漢忠教授)					
研究テーマ	PTH間欠投与による骨血管の組織学的変化 Histological alternation of blood vessel in bone by intermittent PTH administration					
専攻種別	<input type="checkbox"/> 論文博士			<input checked="" type="checkbox"/> 課程博士		

研究者評価(指導教官記入欄)

成績状況	優 学業成績係数=	取得単位数
		30単位以上
学生本人が行った研究の概要	PTH間欠投与によるマウス長管骨における骨特異的血管の組織学的変化に関する研究を行った。PTH(Parathyroid Hormone)の間欠投与は骨造成を促進することが知られているが、PTHの間欠投与が骨特異的な血管や血管の周囲の他の細胞にどのような影響を及ぼすのかは明らかではない。そのため趙申君は6週齢のマウスに2週間連日PTHの投与を行い、その後固定してマウスの大腿骨と脛骨を免疫組織学的に検索した。	
総合評価	【良かった点】 PTHの間欠投与により骨芽細胞と骨特異的血管に影響を及ぼすことを明らかにしたこと。	
	【改善すべき点】 間欠投与その後どれほどで投与の効果が消失するのかは不明であること。	
	【今後の展望】 PTHの間欠投与と中止を繰り返すことにより、PTHの影響はより明らかになるものと考えられる。	
学位取得見込	2020年3月取得見込み	

評価者(指導教官名) 鄭漢忠



日中笹川医学奨学金制度(学位取得コース)中間報告書

研究者用



第41期 研究者番号: G4101 作成日: 2020年3月10日

氏名	Zhao Shen	趙申	性別	M	生年月日	1989. 07. 07
所属機関(役職)	北海道大学大学院歯学院(博士課程学生)					
研究先(指導教官)	北海道大学大学院歯学研究院口腔顎顔面外科学教室(鄭漢忠教授)					
研究テーマ	PTH間欠投与による骨血管の組織学的変化 Histological alternation of blood vessel in bone by intermittent PTH administration					
専攻種別	論文博士	<input type="checkbox"/>	課程博士	<input checked="" type="checkbox"/>		

1. 研究概要

1) 目的 (Goal) & 戦略 (Approach)

Intermittent administration of parathyroid hormone (PTH) promotes preosteoblastic proliferation and differentiation into osteoblasts, which are coupled with osteoclasts, finally resulting in enhanced bone formation. Endomucin-high-positive bone-specific blood vessels have been reported to interact with osteoblastic cells to form new bones. However, it is still veiled whether PTH can affect the distribution of bone-specific blood vessels and other cell-types which surround the blood vessels. In this study, we have attempted to histologically examine bone-specific blood vessels after the intermittent PTH administration.

2) 材料と方法 (Materials and methods)

Six weeks-old C57BL/6J mice half received vehicle as control group, half received 20 µg/kg/day of human PTH [1-34] (hPTH) as PTH group for 2 weeks. Mice were fixed with aldehyde solution, and the femora and tibiae were used for immunohistochemical analyses of endomucin, αSMA, ALP (alkaline phosphatase), EphB4, ephrinB2 and PTH receptor staining. Histomorphometry of statistical analysis were also measured by the diameter and area of endomucin-positive blood vessel and the number of endomucin-, αSMA-, EphB4-, and ephrinB2-positive blood vessel. Gene expression of endomucin, αSMA, EphB4, ephrinB2 and PTH receptor of the control and PTH-administered bone were also examined by RT-PCR.

3) 実験結果 (Results)

In the control group, numbers of endomucin-positive/EphB4-positive blood vessels were observed, while few numbers of αSMA-reactive blood vessels were seen. After PTH administration, the numbers of endomucin-positive/EphB4-positive blood vessels increased, and the vascular diameters were markedly-expanded when compared to the control group. Of note, numbers of blood vessels which accompany αSMA-positive cells were increased in the PTH group, and were divided into two histologically distinct types: the blood vessels surrounded by ALP-reactive/αSMA-positive cells that were closed to the bone surface, and the blood vessels associated only with αSMA-positive cells that showed a long cell shape with extending thin cytoplasmic processes.

4) 考察 (Discussion)

By intermittent PTH administration, the number of endomucin-positive blood vessels increased, and their diameter significantly expanded. The number of αSMA-positive, ephrinB2-positive and EphB4-positive blood vessels also increased. αSMA (+)/ALP (+) cells and αSMA (+)/ALP (-) cells are located on the periphery of blood vessel. To summarize, the intermittent administration of hPTH (1-34) may affect not only osteoblastic cells but also bone-specific blood vessels.

5) 参考文献 (References)

- Schweser KM, Crist BD (2017) Osteoporosis: a discussion on the past 5 years. *Curr Rev Musculoskelet Med* 10: 265 - 274
- Kim SC, Kim DH, Mogun H, Eddings W, Polinski JM, Franklin JM, Solomon DH (2016) Impact of the U.S. food and drug administration's safety-related announcements on the use of bisphosphonates after hip fracture. *J Bone Miner Res* 31: 1536 - 1540
- Orwoll E, Scheele W, Paul S, Adami S, Syversen U, Diez-Perez A, Kaufman JM, Clancy AD, Gaich GA (2003) The effect of teriparatide [human parathyroid hormone (1-34)] therapy on bone density in men with osteoporosis. *J Bone Miner Res* 18: 9 - 17
- Skipitz R, Aspenberg P (2004) Parathyroid hormone—a drug for orthopedic surgery? *Acta Orthop Scand* 75: 654 - 662

5. Luiz de Freitas PH, Li M, Ninomiya T, Nakamura M, Ubaidus S, Oda K, Udagawa N, Maeda T, Takagi R, Amizuka N (2009) Intermittent PTH administration stimulates pre-osteoblastic proliferation without leading to enhanced bone formation in osteoclast-less c-fos(-/-) mice. *J Bone Miner Res* 24: 1586 - 1597
6. Yamamoto T, Hasegawa T, Sasaki M, Hongo H, Tsuboi K, Shimizu T, Ohta M, Haraguchi M, Takahata T, Oda K, Freitas PHL, Takakura A, Takao-Kawabata R, Isogai Y, Amizuka N (2016) Frequency of teriparatide administration affects the histological pattern of bone formation in young adult male mice. *Endocrinology* 157: 2604 - 2620
7. Kusumbe AP, Ramasamy SK, Adams RH (2014) Coupling of angiogenesis and osteogenesis by a specific vessel subtype in bone. *Nature* 507: 323 - 328
8. Ramasamy SK, Kusumbe AP, Wang L, Adams RH (2014) Endothelial Notch activity promotes angiogenesis and osteogenesis in bone. *Nature* 507: 376 - 380
9. Sivaraj KK, Adams RH (2016) Blood vessel formation and function in bone. *Development* 143: 2706 - 2715
10. Armulik A, Genove G, Betsholtz C (2011) Pericytes: developmental, physiological, and pathological perspectives, problems, and promises. *Dev Cell* 21: 193 - 215
11. Aizman I, Holland WS, Yang C, Bates D (2016) alphaSMA Expression in Large Colonies of Colony-Forming Units-Fibroblast as an Early Predictor of Bone Marrow MSC Expandability. *Cell Med* 8: 79 - 85
12. Ramasamy SK (2017) Structure and functions of blood vessels and vascular niches in bone. *Stem Cells Int* 2017: 5046953
13. Matthews BG, Grcevic D, Wang L, Hagiwara Y, Roguljic H, Joshi P, Shin DG, Adams DJ, Kalajzic I (2014) Analysis of alphaSMA-labeled progenitor cell commitment identifies notch signaling as an important pathway in fracture healing. *J Bone Miner Res* 29: 1283 - 1294
14. Kusumbe AP, Ramasamy SK, Itkin T, Mae MA, Langen UH, Betsholtz C, Lapidot T, Adams RH (2016) Age-dependent modulation of vascular niches for haematopoietic stem cells. *Nature* 532: 380 - 384
15. Kunisaki Y, Bruns I, Scheiermann C, Ahmed J, Pinho S, Zhang D, Mizoguchi T, Wei Q, Lucas D, Ito K, Mar JC, Bergman A, Frenette PS (2013) Arteriolar niches maintain haematopoietic stem cell quiescence. *Nature* 502: 637 - 643
16. Mendez-Ferrer S, Michurina TV, Ferraro F, Mazloom AR, Macarthur BD, Lira SA, Scadden DT, Ma'ayan A, Enikolopov GN, Frenette PS (2010) Mesenchymal and haematopoietic stem cells form a unique bone marrow niche. *Nature* 466: 829 - 834
17. Rundle CH, Xing W, Lau KW, Mohan S (2016) Bidirectional ephrin signaling in bone. *Osteoporos Sarcopenia* 2: 65 - 76
18. Zhao C, Irie N, Takada Y, Shimoda K, Miyamoto T, Nishiwaki T, Suda T, Matsuo K (2006) Bidirectional ephrinB2-EphB4 signaling controls bone homeostasis. *Cell Metab* 4: 111 - 121
19. Ng YS, Ramsauer M, Loureiro RM, D'Amore PA (2004) Identification of genes involved in VEGF-mediated vascular morphogenesis using embryonic stem cell-derived cystic embryoid bodies. *Lab Invest* 84: 1209 - 1218
20. Allan EH, Hausler KD, Wei T, Gooi JH, Quinn JM, Crimeen-Irwin B, Pompolo S, Sims NA, Gillespie MT, Onyia JE, Martin TJ (2008) EphrinB2 regulation by PTH and PTHrP revealed by molecular profiling in differentiating osteoblasts. *J Bone Miner Res* 23: 1170 - 1181
21. Du JH, Lin SX, Wu XL, Yang SM, Cao LY, Zheng A, Wu JN, Jiang XQ (2019) The function of Wnt ligands on osteocyte and bone remodeling. *J Dent Res* 98: 930 - 938.
22. Baron R, Hesse E (2012) Update on bone anabolics in osteoporosis treatment: rationale, current status, and perspectives. *J Clin Endocrinol Metab* 97: 311 - 325
23. Portal-Nunez S, Lozano D, Esbrit P (2012) Role of angiogenesis on bone formation. *Histol Histopathol* 27: 559 - 566
24. Grüneboom A, Hawwari I, Weidner D, Culemann S, Müller S, Henneberg S, Brenzel A, Merz S, Bornemann L, Zec K, Wuelling M, Kling L, Hasenberg M, Voortmann S, Lang S, Baum W, Ohs A, Kraff O, Quick HH, Jäger M, Landgraaber S, Dudda M, Danuser R, Stein JV, Rohde M, Gelse K, Garbe AI, Adamczyk A, Westendorf AM, Hoffmann D, Christiansen S, Engel DR, Vortkamp A, Krönke G, Herrmann M, Kamradt T, Schett G, Hasenberg A, Gunzer M (2019) A network of trans-cortical capillaries as mainstay for blood circulation in long bones. *Nature Metabolism* 1:236 - 250
25. Jiang L, Zhang W, Wei L, Zhou Q, Yang G, Qian N, Tang Y, Gao Y, Jiang X (2018) Early effects of parathyroid hormone on vascularized bone regeneration and implant osseointegration in aged rats. *Biomaterials* 179:15 - 28
26. Rey A, Manen D, Rizzoli R, Ferrari SL, Caverzasio J (2007) Evidences for a role of p38 MAP kinase in the stimulation of alkaline phosphatase and matrix mineralization induced by parathyroid hormone in osteoblastic cells. *Bone* 41: 59 - 67
27. Nakajima A, Shimoji N, Shiomi K, Shimizu S, Moriya H, Einhorn TA, Yamazaki M (2002) Mechanisms for the enhancement of fracture healing in rats treated with intermittent low-dose human parathyroid hormone (1-34). *J Bone Miner Res* 17: 2038 - 2047
28. Hirota S, Takaoka K, Hashimoto J, Nakase T, Takemura T, Morii E, Fukuyama A, Morihana K, Kitamura Y, Nomura S (1994) Expression of mRNA of murine bone-related proteins in ectopic bone induced by murine bone morphogenetic protein-4. *Cell and tissue research* 277: 27 - 32
29. Marini M, Rosa I, Ibba-Manneschi L, Manetti M (2018) Telocytes in skeletal, cardiac and smooth muscle interstitium: morphological and functional aspects. *Histol Histopathol* 33:1151 - 1165

2. 執筆論文 Publication of thesis ※記載した論文を添付してください。Attach all of the papers listed below.

論文名 1 Title						
掲載誌名 Published journal						
	年	月	巻(号)	頁 ~	頁	言語 Language
第1著者名 First author			第2著者名 Second author			第3著者名 Third author
その他著者名 Other authors						
論文名 2 Title						
掲載誌名 Published journal						
	年	月	巻(号)	頁 ~	頁	言語 Language
第1著者名 First author			第2著者名 Second author			第3著者名 Third author
その他著者名 Other authors						
論文名 3 Title						
掲載誌名 Published journal						
	年	月	巻(号)	頁 ~	頁	言語 Language
第1著者名 First author			第2著者名 Second author			第3著者名 Third author
その他著者名 Other authors						
論文名 4 Title						
掲載誌名 Published journal						
	年	月	巻(号)	頁 ~	頁	言語 Language
第1著者名 First author			第2著者名 Second author			第3著者名 Third author
その他著者名 Other authors						
論文名 5 Title						
掲載誌名 Published journal						
	年	月	巻(号)	頁 ~	頁	言語 Language
第1著者名 First author			第2著者名 Second author			第3著者名 Third author
その他著者名 Other authors						

3. 学会発表 Conference presentation ※筆頭演者として総会・国際学会を含む主な学会で発表したものを記載

※Describe your presentation as the principal presenter in major academic meetings including general meetings

学会名 Conference	日本解剖学会第65回東北・北海道連合支部学術集会			
演題 Topic	The biological effect of bone-specific blood vessels by intermittent PTH administration in mice.			
開催日 date	2019 年 9 月 8 日	開催地 venue	北海道江別市	
形式 method	<input type="checkbox"/> 口頭発表 Oral <input type="checkbox"/> ポスター発表 Post	言語 Language	<input type="checkbox"/> 日本語 <input type="checkbox"/> 英語 <input type="checkbox"/> 中国語	
共同演者名 Co-presenter	Hasegawa T., Tei K., Amizuka N			
学会名 Conference				
演題 Topic				
開催日 date	年 月 日	開催地 venue		
形式 method	<input type="checkbox"/> 口頭発表 Oral <input type="checkbox"/> ポスター発表 Post	言語 Language	<input type="checkbox"/> 日本語 <input type="checkbox"/> 英語 <input type="checkbox"/> 中国語	
共同演者名 Co-presenter				
学会名 Conference				
演題 Topic				
開催日 date	年 月 日	開催地 venue		
形式 method	<input type="checkbox"/> 口頭発表 Oral <input type="checkbox"/> ポスター発表 Post	言語 Language	<input type="checkbox"/> 日本語 <input type="checkbox"/> 英語 <input type="checkbox"/> 中国語	
共同演者名 Co-presenter				
学会名 Conference				
演題 Topic				
開催日 date	年 月 日	開催地 venue		
形式 method	<input type="checkbox"/> 口頭発表 Oral <input type="checkbox"/> ポスター発表 Post	言語 Language	<input type="checkbox"/> 日本語 <input type="checkbox"/> 英語 <input type="checkbox"/> 中国語	
共同演者名 Co-presenter				

4. 受賞（研究業績 Award (Research achievement)

名称 Award name	国名 Country	受賞年 Year of	年 月
名称 Award name	国名 Country	受賞年 Year of	年 月

5. 本研究テーマに関わる他の研究助成金受給 Other research grants concerned with your research

受給実績 Receipt record	<input type="checkbox"/> 有 <input checked="" type="checkbox"/> 無
助成機関名称 Funding agency	
助成金名称 Grant name	
受給期間 Supported	年 月 ~ 年 月
受給額 Amount received	円
受給実績 Receipt record	<input type="checkbox"/> 有 <input checked="" type="checkbox"/> 無
助成機関名称 Funding agency	
助成金名称 Grant name	
受給期間 Supported	年 月 ~ 年 月
受給額 Amount received	円

6. 他の奨学金受給 Another awarded scholarship

受給実績 Receipt record	<input type="checkbox"/> 有 <input checked="" type="checkbox"/> 無
助成機関名称 Funding agency	
奨学金名称 Scholarship	
受給期間 Supported	年 月 ~ 年 月
受給額 Amount received	円

7. 研究活動に関する報道発表 Press release concerned with your research activities

※記載した記事を添付してください。 Attach a copy of the article described below

報道発表 Press release	<input type="checkbox"/> 有 <input checked="" type="checkbox"/> 無	発表年月日 Date of release
発表機関 Released medium		
発表形式 Release method	・新聞 ・雑誌 ・Web site ・記者発表 ・その他 ()	
発表タイトル Released title		

8. 本研究テーマに関する特許出願予定 Patent application concerned with your research theme

出願予定 Scheduled	<input type="checkbox"/> 有 <input checked="" type="checkbox"/> 無	出願国 Application
出願内容(概要) Application contents		

9. その他 Others

--

指導責任者 (署名)

鄭 漢 忠



博士論文

**Histological alteration of bone specific-blood vessels in murine long
bones with intermittent PTH administration**

(PTH 間歇投与によるマウス長管骨における骨特異
的血管の組織学的変化)

令和2年3月申請

北海道大学
大学院歯学研究科口腔医学専攻

趙 申

Histological alteration of bone specific-blood vessels in murine long bones with intermittent PTH administration

Zhao Shen

Oral and Maxillofacial Surgery, Graduate School of Dental Medicine, Hokkaido University, Sapporo, Japan

Abbreviated Title: *Blood vessels in PTH-administered bone*

#Address for correspondence:

Zhao Shen

Oral and Maxillofacial Surgery,
Graduate School of Dental Medicine, Hokkaido University

Kita 13 Nishi 7 Kita-ku

Sapporo, 060-8586, Japan

Tel/Fax: +81-11-706-4283

E-mail: zhaoshen@den.hokudai.ac.jp

Abstract

It is well known that the intermittent administration of parathyroid hormone (PTH) promotes bone formation, but it remains to be unveiled if PTH could affect the distribution of bone-specific blood vessels and other cell-types surrounding the blood vessels. In this study, we have attempted to histologically examine bone-specific blood vessels after intermittent PTH administration. Six-week-old C57BL/6J mice received vehicle (control group) or 20 µg/kg/day of hPTH [1–34] (PTH group) for two weeks. The mice were then fixed and their femora and tibiae were examined for the immunohistochemical profile. The gene expression of bone was also examined by RT-PCR. In the control femoral metaphysis, there were many endomucin-positive/EphB4-positive blood vessels and few αSMA-reactive blood vessels. In the PTH administered femoral metaphysis, the numbers of endomucin-positive/EphB4-positive blood vessels and their diameters were significantly expanded when compared to those of the control groups. Interestingly, blood vessels accompanied with αSMA-positive cells were significantly increased in number in the PTH group, and were histochemically divided into two distinct types: the one surrounded by ALP-reactive/αSMA-positive cells close to the bone surface, and the others accompanied merely with αSMA-positive cells that showed a long cell shape extending thin cytoplasmic processes. In summary, the intermittent administration of PTH may affect both osteoblastic cells and bone-specific blood vessels.

210 words

Keywords: *blood vessel, bone, parathyroid hormone (PTH), endomucin, vascular smooth muscle cell*

Introduction

Osteoporosis is a typical symptom in geriatric disease. For years, the first-line drug in therapy for osteoporosis has remained bisphosphonates [1]. However, it has been reported that bisphosphonates could be associated with severe complications such as osteonecrosis of the jaw or atypical femur fractures [2]. Over the last decade, teriparatide, which is a recombinant form of parathyroid hormone (PTH), has become the preferred drug for the treatment of osteoporosis [1, 3]. The anabolic action of PTH has also been demonstrated in clinical trials: PTH increased bone mass and reduced the fracture rate in patients with osteoporosis [4]. In our previous study, we have demonstrated that intermittent PTH administration promotes preosteoblastic proliferation and osteoblastic bone formation, both of which are finely tuned by cell coupling with osteoclasts, and finally induced new bone formation [5, 6].

Recently, Kusumbe and Ramasamy demonstrated two new disparate subtypes of endothelial cells in bone according to distribution and function: type H and type L [7]. The type H bone-specific subtype is a blood vessel that features CD31 and endomucin double strong positivity located underneath the growth plate in the metaphysis, while the type L subtype showed CD31 and endomucin low positivity in diaphysis [7, 8]. Endomucin^{high}-positive bone-specific blood vessels have been shown to reciprocally interact with osteoblastic cells [7]. Endomucin^{high}-positive endothelial cells have been reported to secrete noggin, supporting osteoblasts and chondrocytes, which secrete vascular endothelial growth factor (VEGF) sustaining angiogenesis in reverse [7, 8]. This may implicate the reciprocal interaction of blood vessels and osteoblastic cells in bone in a normal state.

It is well-known that blood vessels consist of various cell-types, being roughly divided into inner vascular endothelial cells and outer perivascular cells [9]. A vascular smooth muscle cell is a type of perivascular cell that always covers arteries/veins including arterioles and venules and appears to regulate vessel caliber [10]. α -Smooth muscle actin (α SMA) is a specific marker of vascular smooth muscle cells and myofibroblasts [11]. The nutrient arteries and arterioles surrounded by vascular smooth muscle cells invade from the periosteum into the bone and run in the inner bone marrow region of the diaphyses of long bones [12]. However, the peripheral vascular smooth muscle cells gradually disappear to form sinusoidal capillaries that extend from the sinusoidal capillaries toward the chondro-osseous

junctions, where they are not covered by peripheral vascular smooth muscle cells and are sometimes surrounded by discontinuous basement membranes [10]. Therefore, perivascular cells including vascular smooth muscle cells will not always be adjacent to vascular endothelial cells, depending on the micro-circumstance of the blood vessels. It is assumed that perivascular cells such as vascular smooth muscle cells may not be fully differentiated but still possess the potential to differentiate into other cell types [10, 11, 13]. Indeed, it has been reported that arteries in bone are covered by α SMA-positive smooth muscle cells that have the potential to differentiate into different mesenchymal lineages [14–16].

Recently, considerable reports have supported the importance of the interactions between EphB4 and ephrinB2 in the cardiovascular system and skeletal system [17, 18]. EphB4 is a marker for veins, while ephrinB2 is a marker for arteries. Since previous reports have suggested EphB4/ephrinB2 action as a coupling factor in bone [17], it may be possible for EphB4-positive veins/ephrinB2-reactive arteries to affect the activities of osteoblastic cells. Thus, PTH-driven anabolic effects may affect both osteoblastic cells and vascular endothelial cells and the surrounding perivascular cells including vascular smooth muscle cells. Alternately, it might be possible that PTH would directly affect vascular endothelial cells of bone-specific blood vessels and surrounding vascular smooth muscle cells. However, the biological effects of PTH on bone-specific blood vessels including vascular endothelial cells and surrounding vascular smooth muscle cells remain unknown.

Therefore, in this study we have attempted to histochemically examine the bone-specific blood vessels in long bone after intermittent PTH administration *in vivo*.

Materials and methods

Animals

Six-week-old male C57BL/6J mice (n = 12, Japan CLEA, Tokyo, Japan) were divided into a control group and PTH group following the principles for animal care and research use set by Hokkaido University (approved No: 15-0032). The control group received vehicle (0.9% saline) while the PTH group received hPTH [1–34] (Sigma-Aldrich Co., LLC., St. Louis, MO). According to our previous report [6], the mice received 20 µg/kg/day of hPTH [1–34] twice per day. Intraperitoneal injections were performed at 8:00 am and 8:00 pm for two weeks. Mice were kept under standard conditions.

Specimen preparation

Before fixation, mice were anesthetized with an intraperitoneal injection of chloral hydrate for bodyweight determination. Then, all mice were perfused with 4% paraformaldehyde diluted in 0.1 M cacodylate buffer (pH 7.4) through the cardiac left ventricle. After perfusion with 4% paraformaldehyde solution, the femora and tibiae were extracted promptly and immersed in the same solution for 24 hours at 4°C. After washing in phosphate-buffered saline (PBS) for three days, all the samples were decalcified with 10% or 4.13% EDTA-2Na for paraffin-specimens and epoxy resin-specimens, respectively. For paraffin-embedded specimens, samples were dehydrated in ascending ethanol solutions, soaked in xylene, and finally embedded in paraffin. For epoxy resin-embedded specimens, samples were post-fixed with 1% osmium tetroxide in a 0.1 M cacodylate buffer for eight hours at 4°C, dehydrated in ascending acetone solutions, and finally embedded with epoxy resin (Epon 812).

Histological and immunohistochemical detection

Dewaxed paraffin sections were examined for endomucin, αSMA, EphB4 and ephrin B2 as previously examined [5]. The sections were treated for endogenous peroxidase inhibition with 0.3% H₂O₂ in PBS for 30 mins, and subsequently for nonspecific staining blocking by 1% bovine serum albumin (BSA; Serologicals Proteins Inc. Kankakee, IL) in PBS (1% BSA-PBS) for 20 mins at room temperature. Then, sections were incubated with rat antibody against endomucin (Santa Cruz Biotechnology, Inc., Dallas, TX) at a dilution of 1:100 and 4°C overnight. Following

several washings in PBS, they were incubated with horseradish peroxidase (HRP)-conjugated anti-rat IgG (Zymed Laboratories Inc., South San Francisco, CA) at a dilution of 1:100. To detect α SMA, the dewaxed sections treated with 1% BSA–PBS were incubated with mouse antibody against α SMA (Thermo Fisher Scientific Inc., Cheshire, UK) at a dilution of 1:400 and 4°C overnight. Then, the sections were incubated with HRP-conjugated rabbit anti-mouse IgG (Bethyl Laboratories, Inc., Montgomery, TX). For the detection of EphB4 and ephrinB2, the dewaxed sections were reacted with goat antibody against mouse EphB4 (R&D Systems Inc., Minneapolis, MN) at a dilution of 1:50 or with goat antibody against mouse ephrinB2 (R&D Systems Inc., Minneapolis, MN) at a dilution of 1:50 and 4°C overnight. After several washings in PBS, they were incubated with HRP-conjugated rabbit anti-goat IgG (American Qualex Scientific Products, Inc., San Clemente, CA) for 1 h. Immune complexes of all sections were visualized using 3, 3'-diaminobenzidine tetrahydrochloride (Dojindo Laboratories, Kumamoto, Japan). Then, specimens were observed under a Nikon Eclipse Ni microscope (Nikon Instruments Inc. Tokyo, Japan), and light microscopic images were acquired with a digital camera (Nikon DXM1200C, Nikon).

Double immunohistochemical and immunofluorescence staining

For α SMA/endomucin double immunohistochemical staining procedures, dewaxed paraffin sections were incubated with 1% BSA–PBS and then with mouse antibody against α SMA (Thermo Fisher Scientific Inc.) at a dilution of 1:400 with 1% BSA–PBS. After that, they were incubated with fluorescein (FITC)-conjugated goat anti-mouse IgG (MP Biomedicals. LLC., Solon, OH) at a dilution of 1:100 with 1% BSA–PBS and then incubated with rat antibody against endomucin at a dilution of 1:100 at 4°C after washing with PBS. Sections were subsequently reacted with Alexa 594-conjugated rabbit anti-rat IgG (Thermo Fisher Scientific Inc., Cheshire, UK) at a dilution of 1: 100. For the detection of α SMA and ALP, dewaxed paraffin sections were incubated with 1% BSA–PBS and then with mouse antibody against α SMA (Thermo Fisher Scientific Inc.) at a dilution of 1:400 with 1% BSA–PBS; then, they were incubated with fluorescein (FITC)-conjugated goat anti-mouse IgG (MP Biomedicals. LLC., Solon, OH) at a dilution of 1:100. After PBS washing, the sections were reacted with rabbit polyclonal antisera against TNALP at a dilution of 1:300 with 1% BSA–PBS; then, they were incubated with Alexa Fluor

594-conjugated goat anti-rabbit IgG (Thermo Fisher Scientific, Inc, Waltham, MA) at a dilution of 1:100 with 1% BSA-PBS for 1 h. All sections were embedded by VECTASHIELD hard-set mounting medium with DAPI (Vector Laboratories, Inc. Burlingame, CA) and observed under light microscopy.

Toluidine blue staining

Semi-thin sections were prepared with an ultramicrotome and were then stained with toluidine blue staining and observed under a Nikon microscope. Light microscopy images were acquired with a digital camera.

Static parameters for bone histomorphometry

A 800×1000 µm Region of Interest (ROI) located underneath the growth plate of femoral metaphysis was employed to assess the following static parameters: number of endomucin-positive, αSMA-positive, EphB4-positive, and ephrinB2-positive blood vessels, maximum diameter (length of longest line joining two points of blood vessel's outline and passing through the centroid)/minimum diameter (length of the shortest line joining two points in the blood vessel's outline and passing through the centroid)/mean diameter (average length of diameters measured at 2 degree intervals and passing through the blood vessel's centroid) of the endomucin-immunopositive blood vessels, area of the endomucin-reactive blood vessels. Images of the ROI stained for endomucin/αSMA, EphB4, ephrinB2 from the control groups and PTH groups (n = 6 for each group) were used to determine the number of each kind of vessel and the external diameter of the endomucin-immunoreactive blood vessel within the ROI were measured with Image-Pro Plus 6.2 (Media Cybernetics, Inc., Bethesda MD); the results were later statistically analyzed as follows.

RT-PCR assessment

Total RNA was extracted from fresh frozen femora and tibiae using TRIzol reagent (Life Technologies Co., Carlsbad, CA). For RT-PCR, total RNA was reverse transcribed to cDNA using SuperScript VILO cDNA Synthesis Kit (Life Technologies). For PCR amplification, the following primer sets were used: (forward) 5'- TGTCTTACCACCATGGAGAAGG -3' and (reverse) 5'- GTGGATGCAGGGATGATGTTCTG -3' for GAPDH, (forward) 5'- CTATGAAAATAACAGTGCCAAATACTCCAA -3' and (reverse) 5'-

AGGATCCATCACGATGTCAGTTCTTGGTTT -3' for endomucin, and (forward) 5'-
GTATGTGGCTATTCAGGCTG -3' and (reverse) 5'-
CTTCTGCATCCTGTCAGCAA -3' for α -SMA, (forward) 5'-
CCCAAATAGGAGACGAGTCC -3' and (reverse) 5'-
CTCAAAAGGAGGTGGTCCAG -3' for EphB4, and (forward) 5'-
TCCAGGAGGGACTCTGTGTGGAAG -3' and (reverse)
5'-CGGGGTATTCTCCTTCTTAATTGT -3' for ephrinB2. PCR products were
electrophoresed on a 2% agarose gel containing ethidium bromide and visualized with
UV light.

Statistical analysis

All statistical analyses were carried out using SPSS version 18.0.0 and analyzed for statistical significance by Student's t-test. Data values were presented as mean \pm SE. For the study, any p-value of 0.05 was considered statistically significant.

Results

Altered distribution of bone specific-blood vessels after intermittent PTH administration

Metaphyseal trabeculae and the trabecular bone mass were increased in femora of the PTH group compared with the control group (**Figure 1A–B**). After PTH administration, the number of endomucin-positive blood vessels appeared to increase histologically and their diameters seemed to expand compared to the control groups (**Figure 1C–D**). Therefore, we measured the cross-sectioned maximum diameter, the minimum diameter, and the mean diameter of the endomucin-reactive blood vessels in the ROI of 800 μm x 1,000 μm (**Figure 1E**). One consequence of intermittent PTH administration is that the indices of the maximum and mean diameter of the endomucin-immunoreactive blood vessels were significantly higher than those of the control specimens. The average maximum diameter of the endomucin-immunoreactive blood vessels in the control group were 224.53 ± 10.06 μm and the average mean diameter of the endomucin-reactive blood vessels was 121.37 ± 4.76 μm . In the PTH group, the average maximum diameter and mean diameter of the endomucin-reactive blood vessels were 339.22 ± 14.58 μm ($p < 0.01$ vs. control) and 144.01 ± 4.63 μm ($p < 0.05$ vs. control), respectively. There was no significant difference in the minimum diameter of the endomucin-positive blood vessels between the control group and the PTH group as shown in **Figure 1E**. The average minimum diameter of the endomucin-reactive blood vessels was 73.16 ± 2.94 μm in the control group and 73.26 ± 2.32 μm in the PTH group. Additionally, we examined the cross-section areas of the endomucin-immunopositive blood vessels in the ROI (**Figure 1F**). After intermittent PTH administration, the area of the endomucin-reactive blood vessels had significantly increased: The cross-sectioned areas of the endomucin-immunopositive blood vessels were $19,841.02 \pm 2,585.61$ μm^2 in the control group and $28,652.31 \pm 2,413.11$ μm^2 in the PTH group ($p < 0.05$).

Immunolocalization of αSMA -immunoreactive, EphB4-immunoreactive and ephrinB2-immunoreactive cells in PTH-administrated blood vessels

The number of αSMA -immunopositive cells was markedly-increased in the vicinity of endomucin-reactive blood vessels after PTH administration. There was a huge number of αSMA -reactive blood vessels in the metaphyses by PTH administration,

while there seemed a few α SMA-positive blood vessels in the control counterparts (**Figure 2A–C**). In addition, the numbers of EphB4-positive blood vessels and ephrinB2-positive arteries increased in PTH-treated metaphyses when compared with those in the control specimens (**Figure 2 D–I**).

Using the immunostained sections, we counted the number of each type of blood vessel in the ROI underneath the growth plate. After intermittent PTH administration, the numbers of endomucin-positive, α SMA-positive, EphB4-positive, and ephrinB2-positive blood vessels were significantly increased (**Figure 2J**). The numbers of endomucin-positive, α SMA-positive, EphB4-positive, and ephrinB2-positive blood vessels in the control group were 50.17 ± 18.45 , 3.50 ± 2.17 , 63.00 ± 18.01 , and 4.00 ± 1.55 , respectively. The numbers of endomucin-positive, α SMA-positive, EphB4-positive, and ephrinB2-positive blood vessels in the PTH group were 82.33 ± 14.63 , 26.67 ± 7.58 , 147 ± 42.37 , and 21.5 ± 4.84 , respectively ($p < 0.01$ vs. control). When examined by RT-PCR, the gene expressions of endomucin, α SMA, EphB4, and ephrinB2 in the femora consistently appeared elevated after PTH administration (**Figure 2K**).

The distribution of α SMA-immunoreactive cells surrounding endomucin-immunoreactive blood vessels in PTH-administered metaphyses

Some α SMA-immunopositive cells seemed closely associated with endomucin-positive vascular endothelial cells, being identical to vascular smooth muscle cells. However, the others were located somewhat apart from the blood vessels, and therefore appeared to be cell-types other than vascular smooth muscle cells (**Figure 3A–D**). To define the characteristics of α SMA-positive cells not identical to vascular smooth muscle cells, we examined the double immunodetection of ALP and α SMA, and consequently divided them into two distinct cell-types (**Figure 3E–H**): the α SMA-positive cells bearing ALP-reactivity located in close proximity to the blood vessels in the intertrabecular regions (**Figure 3E and G**), and the α SMA-positive but ALP-negative cells that extend long cell bodies and thin cytoplasmic processes (**Figure 3F and H**). Taken together, three α SMA-positive cell-types appeared after PTH administration: α SMA-positive vascular smooth muscle cells, α SMA/ALP double-positive cells close but not adjacent to blood vessels, and α SMA-positive/ALP-negative cells that extend their straightly extending cytoplasmic processes. Thus, it appears that the cellular population surrounding the

blood vessels changes after PTH administration. Therefore, we examined the corresponding region using semi-thin sections (**Figure 4**). Two distinct cell-types were shown to be located around blood vessels in the femoral metaphysis of the PTH-administered mice (**Figure 4B–D**). One was the cells revealing a long cell-shape with thin cytoplasmic processes distant from bone, and the other was the cells containing several cell organelles in the somehow translucent cytoplasm.

Discussion

In this study, we have attempted to histologically demonstrate the altered distribution of bone-specific blood vessels in murine bone after intermittent PTH administration. Our main histological findings can be summarized as follows:

- 1) Intermittent PTH administration increased the number of endomucin-positive blood vessels and significantly expanded their diameter.
- 2) The numbers of α SMA-positive, ephrinB2-positive, and EphB4-positive blood vessels also increased after PTH administration.
- 3) α SMA-positive cells were markedly-increased in number and can be distinctively divided into the first type, α SMA-positive vascular smooth muscle cells closely surrounding the endomucin-reactive vascular endothelial cells, the second type, α SMA/ALP double-positive cells close but not adjacent to blood vessels, and the third type, α SMA-positive but ALP-negative cells extending their straightly extending cytoplasmic processes.

To our knowledge, this is the first report to suggest that the intermittent administration of PTH affects bone-specific blood vessels in bone.

One may wonder why we have employed regimens of two- and four-times administration of PTH each day. Using murine models, we have recently demonstrated that the high frequency of intermittent PTH administration (two or four times per day) promotes bone remodeling by stimulating both bone resorption and formation, while low-frequency PTH administration (once a day or per two days) caused both remodeling-based/mini-modeling-based bone formation [6]. In addition, we have reported that high-frequency PTH administration stimulated preosteoblastic proliferation and subsequent osteoblastic differentiation by mediating cell coupling with osteoclasts [5]. Therefore, the anabolic effects of PTH appear to be based on accelerated preosteoblastic proliferation and finely-tuned cell coupling with osteoclasts.

These cellular events take place in the region of mature osteoblasts including preosteoblastic cells, bone marrow-stromal cells, and blood vessels rather than in the region of the osteocytic network embedded in bone, although many investigators have suggested that PTH-driven anabolic action is reportedly mediated by the sclerostin/Wnt pathway of osteocytes [21, 22]. In accordance with our previous

reports, we decided to employ high-frequency PTH administration in this study rather than low-frequency to ensure adequate regimens to examine the bone specific-blood vessels and the surrounding cells; consequently, we were able to observe the significant alteration of bone specific-blood vessels by PTH.

Regarding the biological actions of blood vessels in bone, many studies have paid close attention to the intimate connection between blood vessels and bone tissues [23]. Since bone is highly vascularized tissue, it has been previously assumed that blood vessels serve as a tunnel by which to transmit oxygen, nutrition, growth factors, and hormones into the bone and take part in the hematopoiesis of neighboring bone marrow [9]. Recently, it has been demonstrated that there is a network of trans-cortical capillaries as a mainstay for blood circulation in long bone [24]. Literally, Kusumbe and Ramasamy et al. reported a bone-specific subtype of blood vessels featuring CD31^{high}/endomucin^{high}, and illuminated that angiogenesis also plays an important role in bone development and remodeling [7, 8]. Endomucin^{high}-positive blood vessels in the metaphyses of long bone have been shown to reciprocally interact with osteoblastic cells requiring various cytokines, microRNA, and signaling pathways. Thus, while recent studies on bone/blood vessel interaction have progressed, few reports have elucidated the biological action of PTH on bone-specific blood vessels.

In the present study, intermittent PTH administration increased the number of endomucin-immunoreactive/EphB4-positive blood vessels and the maximum/mean diameters and area of endomucin-positive blood vessels in the metaphyses of murine femora and tibiae. Since most blood vessels in this area are capillaries that are not surrounded by vascular smooth muscle cells, the enlargement of blood vessels in this area seems non-ascribable to the relaxation of vascular smooth muscle cells but is rather probably due to morphological changes in the capillaries. In addition, we assume that the reason why blood vessels increased in number might be due to angiogenesis stimulated by PTH. Another interpretation may be that PTH mainly reacts to the development and remodeling of bone by the classical Wnt/ β -catenin pathway [22], which might be able to react to the angiogenesis by the VEGF-relevant pathway. However, further investigation is necessary to define the cellular mechanism of the increased numbers and diameters of capillaries after PTH administration.

We have observed that three α SMA-positive cell-types appear after PTH administration: the first is α SMA-positive vascular smooth muscle cells closely

surrounding the endomucin-reactive vascular endothelial cells, the second is α SMA/ALP double-positive cells close but not adjacent to blood vessels, and the third is α SMA-positive but ALP-negative cells extending their straightly extending cytoplasmic processes. The first appears to be vascular smooth muscle cells, but the other two might be other cell-types. Since the control vascular endothelial cells were hardly accompanied by α SMA-positive vascular smooth muscle cells in the metaphyses, it seems likely that undifferentiated perivascular cells might differentiate into vascular smooth muscle cells by PTH administration. α SMA-positive/ALP-reactive cells that were located close but not adjacent to endomucin-positive/ α SMA-reactive blood vessels seem different to vascular smooth muscle cells even though they showed α SMA-immunoreactivity. It has been previously reported that arteries in bone were covered by α SMA-positive/NG2-reactive vascular smooth muscle cells [14], possessing the potential to differentiate into other mesenchymal lineages [7, 8]. Therefore, α SMA-positive/ALP-reactive cells close to the blood vessels might be derived from vascular smooth muscle cells that have differentiated from perivascular cells. Alternately, perivascular cells may have directly differentiated into α SMA-positive/ALP-reactive cells. A previous study indicated that PTH may promote vascularized bone regeneration and directly improve blood vessel formation and the osteogenic potential of aged bone marrow mesenchymal stem cells [25]. Since ALP is an important bone metabolic marker expressed in the osteoblastic lineage [26–28] that also comes from bone marrow mesenchymal cells, these cells may be able to differentiate into preosteoblasts/osteoblasts. Taken together, it may be possible for PTH to stimulate perivascular cells to differentiate into either vascular smooth muscle cells or an ALP-positive osteoblastic lineage.

Regarding α SMA-positive/ALP-negative cells with long cell bodies and thin cytoplasmic processes located in middle of the intertrabecular region, this cell-type extends long cytoplasmic processes linearly parallel to the bone surface. Judging from the cell shape and long cytoplasmic processes, this may be a kind of telocyte that was discovered in 2003 [29]. Telocytes are fibroblast-like cells extending extremely long but thin prolongations. There has not yet been any report of the discovery of telocytes in bone and further examination is warranted. Taken together, bone specific-blood vessels may play an important role in the bone formation process.

In summary, the intermittent administration of PTH may affect both osteoblastic

cells and bone-specific blood vessels.

References

1. Schweser KM, Crist BD (2017) Osteoporosis: a discussion on the past 5 years. *Curr Rev Musculoskelet Med* 10: 265–274
2. Kim SC, Kim DH, Mogun H, Eddings W, Polinski JM, Franklin JM Solomon DH (2016) Impact of the U.S. food and drug administrations safety-related announcements on the use of bisphosphonates after hip fracture. *J Bone Miner Res* 31: 1536–1540
3. Orwoll E, Scheele W, Paul S, Adami S, Syversen U, Diez-Perez A, Kaufman JM, Clancy AD, Gaich GA (2003) The effect of teriparatide [human parathyroid hormone (1–34)] therapy on bone density in men with osteoporosis. *J Bone Miner Res* 18: 9–17
4. Skripitz R, Aspenberg P (2004) Parathyroid hormone--a drug for orthopedic surgery? *Acta Orthop Scand* 75: 654–662
5. Luiz de Freitas PH, Li M, Ninomiya T, Nakamura M, Ubaidus S, Oda K, Udagawa N, Maeda T, Takagi R, Amizuka N (2009) Intermittent PTH administration stimulates pre-osteoblastic proliferation without leading to enhanced bone formation in osteoclast-less c-fos(-/-) mice. *J Bone Miner Res* 24: 1586–1597
6. Yamamoto T, Hasegawa T, Sasaki M, Hongo H, Tsuboi K, Shimizu T, Ohta M, Haraguchi M, Takahata T, Oda K, Freitas PHL, Takakura A, Takao-Kawabata R, Isogai Y, Amizuka N (2016) Frequency of teriparatide administration affects the histological pattern of bone formation in young adult male mice. *Endocrinology* 157: 2604–2620
7. Kusumbe AP, Ramasamy SK, Adams RH (2014) Coupling of angiogenesis and osteogenesis by a specific vessel subtype in bone. *Nature* 507: 323–328
8. Ramasamy SK, Kusumbe AP, Wang L, Adams RH (2014) Endothelial Notch activity promotes angiogenesis and osteogenesis in bone. *Nature* 507: 376–380
9. Sivaraj KK, Adams RH (2016) Blood vessel formation and function in bone. *Development* 143: 2706–2715
10. Armulik A, Genove G, Betsholtz C (2011) Pericytes: developmental, physiological, and pathological perspectives, problems, and promises. *Dev Cell* 21: 193–215

11. Aizman I, Holland WS, Yang C, Bates D (2016) alphaSMA Expression in Large Colonies of Colony-Forming Units-Fibroblast as an Early Predictor of Bone Marrow MSC Expandability. *Cell Med* 8: 79–85
12. Ramasamy SK (2017) Structure and functions of blood vessels and vascular niches in bone. *Stem Cells Int* 2017: 5046953
13. Matthews BG, Greevic D, Wang L, Hagiwara Y, Roguljic H, Joshi P, Shin DG, Adams DJ, Kalajzic I (2014) Analysis of alphaSMA-labeled progenitor cell commitment identifies notch signaling as an important pathway in fracture healing. *J Bone Miner Res* 29: 1283–1294
14. Kusumbe AP, Ramasamy SK, Itkin T, Mae MA, Langen UH, Betsholtz C, Lapidot T, Adams RH (2016) Age-dependent modulation of vascular niches for haematopoietic stem cells. *Nature* 532: 380–384
15. Kunisaki Y, Bruns I, Scheiermann C, Ahmed J, Pinho S, Zhang D, Mizoguchi T, Wei Q, Lucas D, Ito K, Mar JC, Bergman A, Frenette PS (2013) Arteriolar niches maintain haematopoietic stem cell quiescence. *Nature* 502: 637–643
16. Mendez-Ferrer S, Michurina TV, Ferraro F, Mazloom AR, Macarthur BD, Lira SA, Scadden DT, Maayan A, Enikolopov GN, Frenette PS (2010) Mesenchymal and haematopoietic stem cells form a unique bone marrow niche. *Nature* 466: 829–834
17. Rundle CH, Xing W, Lau KW, Mohan S (2016) Bidirectional ephrin signaling in bone. *Osteoporos Sarcopenia* 2: 65–76
18. Zhao C, Irie N, Takada Y, Shimoda K, Miyamoto T, Nishiwaki T, Suda T, Matsuo K (2006) Bidirectional ephrinB2-EphB4 signaling controls bone homeostasis. *Cell Metab* 4: 111–121
19. Ng YS, Ramsauer M, Loureiro RM, D'Amore PA (2004) Identification of genes involved in VEGF-mediated vascular morphogenesis using embryonic stem cell-derived cystic embryoid bodies. *Lab Invest* 84: 1209–1218
20. Allan EH, Hausler KD, Wei T, Gooi JH, Quinn JM, Crimeen-Irwin B, Pompolo S, Sims NA, Gillespie MT, Onyia JE, Martin TJ (2008) EphrinB2 regulation by PTH and PTHrP revealed by molecular profiling in differentiating osteoblasts. *J Bone Miner Res* 23: 1170–1181
21. Du JH, Lin SX, Wu XL, Yang SM, Cao LY, Zheng A, Wu JN, Jiang XQ (2019) The function of Wnt ligands on osteocyte and bone remodeling. *J Dent Res* 98:

930–938.

22. Baron R, Hesse E (2012) Update on bone anabolics in osteoporosis treatment: rationale, current status, and perspectives. *J Clin Endocrinol Metab* 97: 311–325
23. Portal-Nunez S, Lozano D, Esbrit P (2012) Role of angiogenesis on bone formation. *Histol Histopathol* 27: 559–566
24. Grüneboom A, Hawwari I, Weidner D, Culemann S, Müller S, Henneberg S, Henneberg S, Brenzel A, Merz S, Bornemann L, Zec K, Wuelling M, Kling L, Hasenberg M, Voortmann S, Lang S, Baum W, Ohs A, Kraff O, Quick HH, Jäger M, Landgraeber S, Dudda M, Danuser R, Stein JV, Rohde M, Gelse K, Garbe AI, Adamczyk A, Westendorf AM, Hoffmann D, Christiansen S, Engel DR, Vorkamp A, Krönke G, Herrmann M, Kamradt T, Schett G, Hasenberg A, Gunzer M (2019) A network of trans-cortical capillaries as mainstay for blood circulation in long bones. *Nature Metabolism* 1:236–250
25. Jiang L, Zhang W, Wei L, Zhou Q, Yang G, Qian N, Tang Y, Gao Y, Jiang X (2018) Early effects of parathyroid hormone on vascularized bone regeneration and implant osseointegration in aged rats. *Biomaterials* 179:15–28
26. Rey A, Manen D, Rizzoli R, Ferrari SL, Caverzasio J (2007) Evidences for a role of p38 MAP kinase in the stimulation of alkaline phosphatase and matrix mineralization induced by parathyroid hormone in osteoblastic cells. *Bone* 41: 59–67
27. Nakajima A, Shimoji N, Shiomi K, Shimizu S, Moriya H, Einhorn TA, Yamazaki M (2002) Mechanisms for the enhancement of fracture healing in rats treated with intermittent low-dose human parathyroid hormone (1-34). *J Bone Miner Res* 17: 2038–2047
28. Hirota S, Takaoka K, Hashimoto J, Nakase T, Takemura T, Morii E, Fukuyama A, Morihana K, Kitamura Y, Nomura S (1994) Expression of mRNA of murine bone-related proteins in ectopic bone induced by murine bone morphogenetic protein-4. *Cell and tissue research* 277: 27–32
29. Marini M, Rosa I, Ibbá-Manneschi L, Manetti M (2018) Telocytes in skeletal, cardiac and smooth muscle interstitium: morphological and functional aspects. *Histol Histopathol* 33:1151–1165

Figure legends

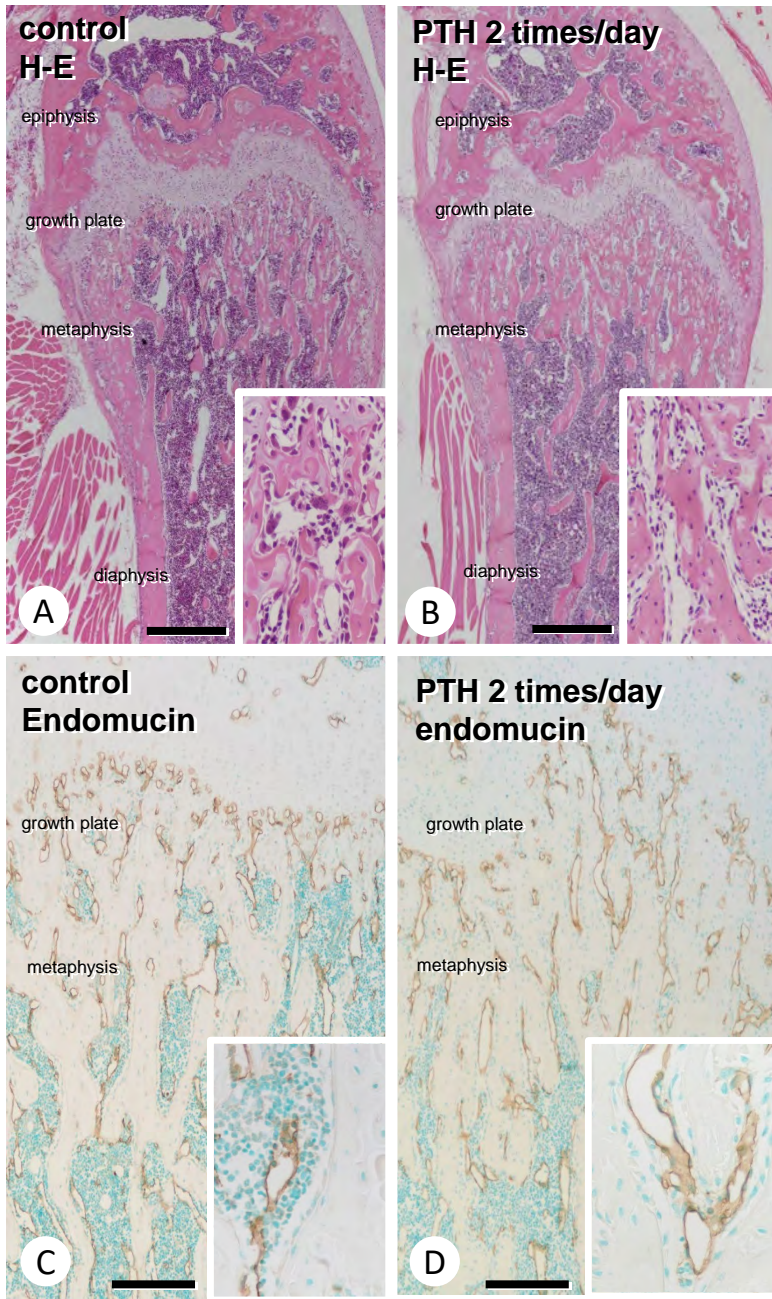
Fig. 1 HE staining of the control mice's femora (A) and PTH-administered mice's femora (B). The bone mass increased in the PTH-administered mice (B) compared to the control groups (A). In the metaphysis of the femora, the diameter of the endomucin-positive blood vessels (brown color) tended to expand in PTH mice (D) compared to control mice (C). Graph E showed the index of the luminal diameter of endomucin-positive blood vessels. After PTH administration, the maximum and mean diameter of the endomucin-positive blood vessels were significantly increased compared to the control group (* $p < 0.05$, ** $p < 0.01$). Graph F demonstrated the total areas of the endomucin-positive blood vessels in the ROI. The area of the endomucin-positive blood vessels was significantly expanded after PTH injection ($p < 0.05$). Bars: A, B: 500 μm C, D: 200 μm

Fig. 2 In the metaphysis, both αSMA -positive blood vessels (brown color) and αSMA -immunopositive cells close to the endomucin-reactive blood vessels tended to increase in PTH-administered groups (B and C) compared to the control group (A). Figures D–F demonstrated the immunolocalization of EphB4 (brown color) and Figures G–I showed the immunolocalization of ephrinB2 (brown color) in the control and PTH-administered groups. The number of endomucin-, αSMA -, EphB4-, and ephrinB2-positive blood vessels were significantly increased in PTH mice, respectively (J, $p < 0.01$). The gene expressions of *Endomucin*, *α -sma*, *Ephrinb2*, and *Ephb4* were also increased by RT-PCR analysis (K). BV: blood vessel
Bars: A, B: 200 μm C–I: 50 μm

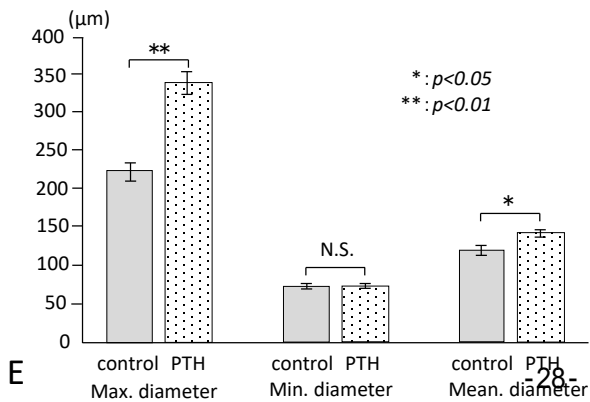
Fig. 3 After PTH administration, αSMA -immunoreactivity (brown color: A and B; green color: C and D) were localized on the vascular smooth muscle cells associated with endomucin-positive vascular endothelial cells and other types of cells other than the blood vessels (arrows: B and D). ALP (blue color: E and F; red color: G and H) and αSMA (brown color: E and F; green color: G and H) double staining demonstrated 1) ALP-positive/ αSMA -positive cells close to the blood vessels (G), and 2) ALP-negative/ αSMA -positive cells extending long cell bodies and thin cytoplasmic

processes in the PTH-administered groups (arrows, H). BV: blood vessel
Bars: A, B: 200 μm C–I: 50 μm

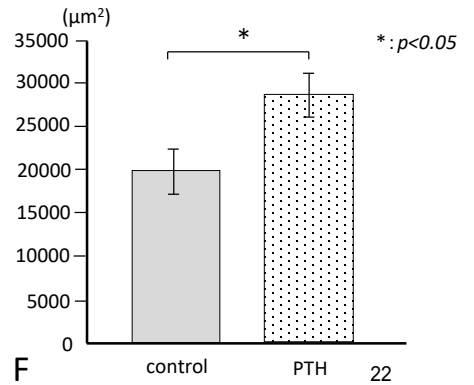
Fig. 4 The semi-thin section obtained from the PTH group demonstrated two different type of cells in the bone marrow region over the osteoblasts (C–D). One is the spindle cell that reveals a long shape with thin cytoplasmic processes distant from the bone (inset, D), and the other is cuboidal cells that appeared to contain several cell organelles (arrows, D). ob: osteoblast; BV: blood vessel.
Bars: A, B: 50 μm C, D: 20 μm



Index of luminal diameter of blood vessels

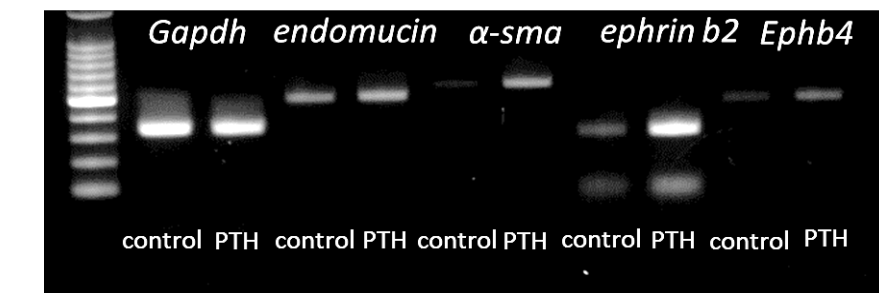
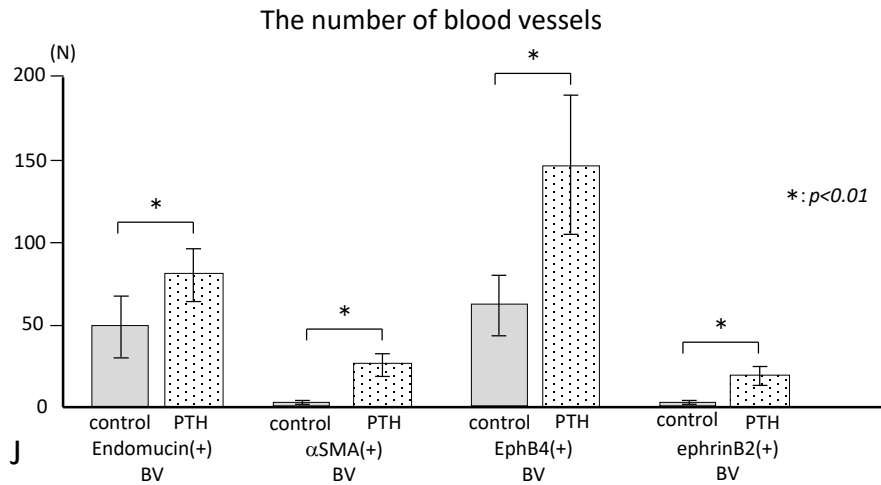
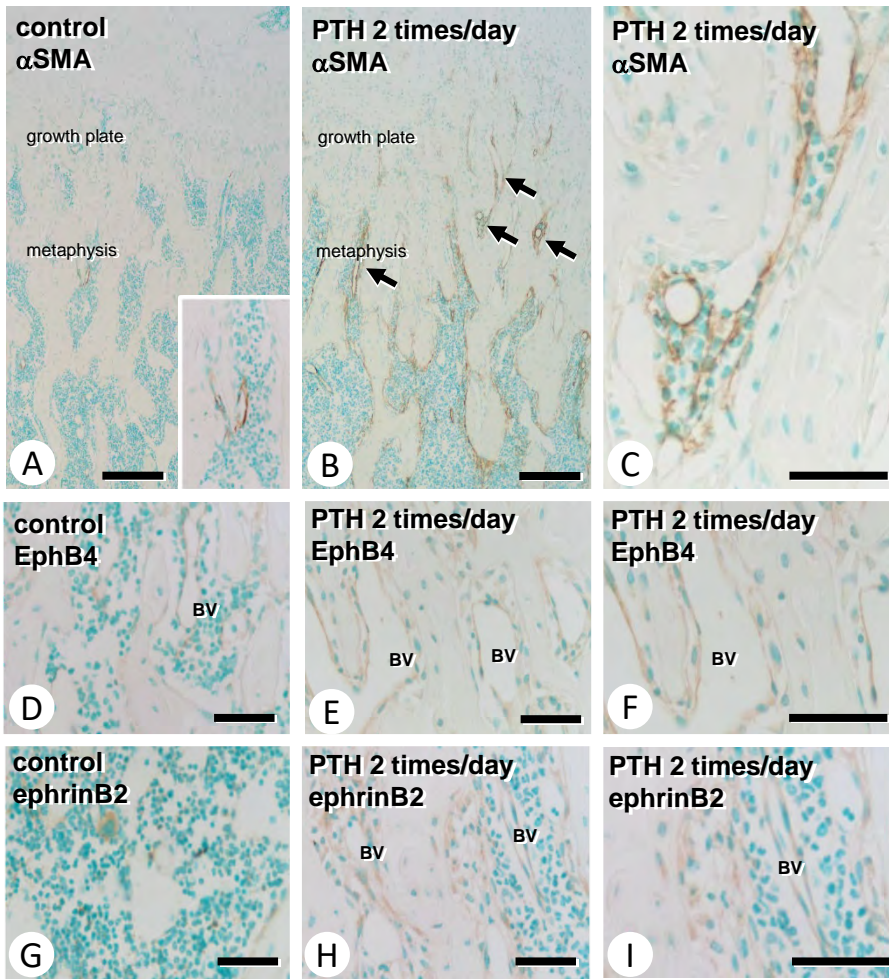


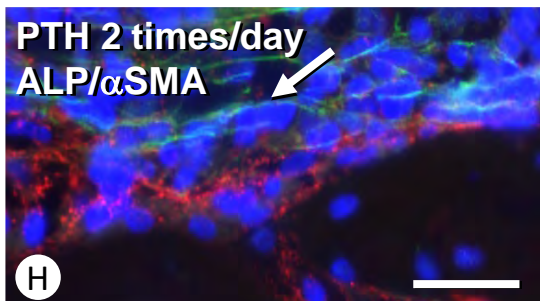
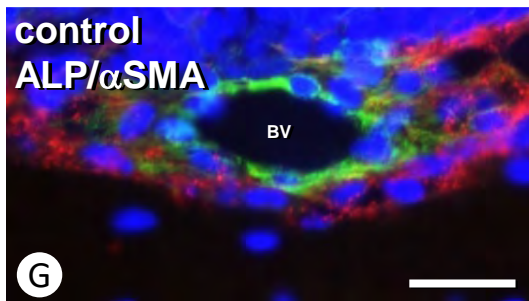
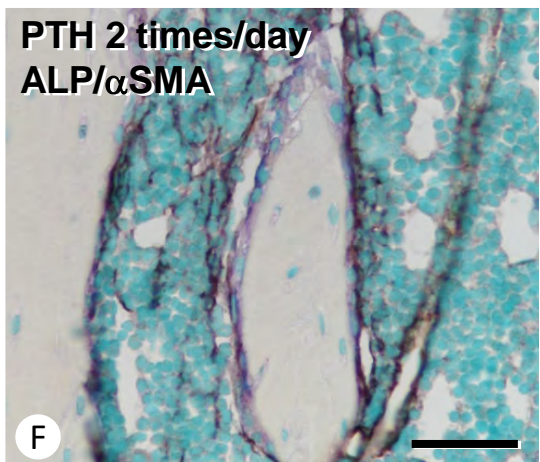
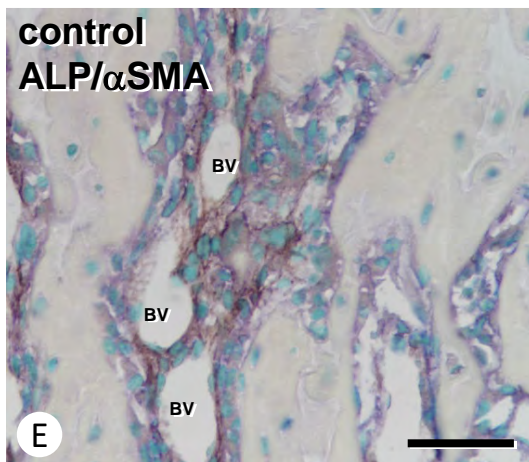
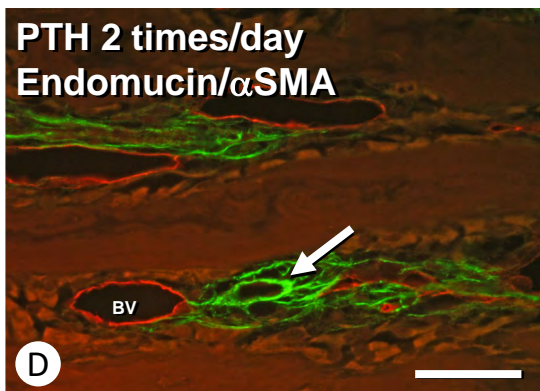
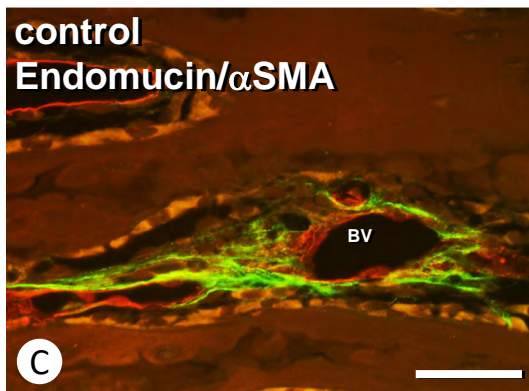
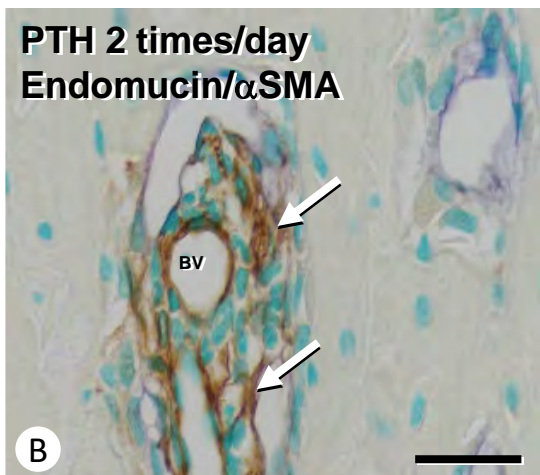
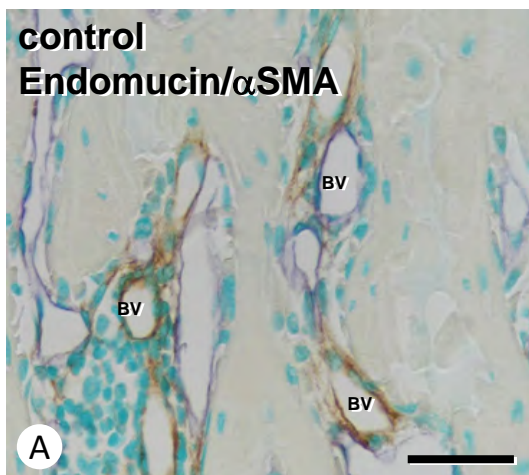
Total areas of blood vessels

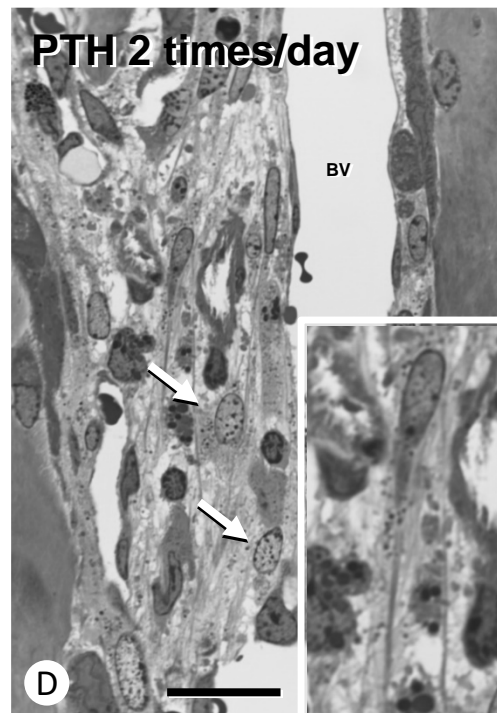
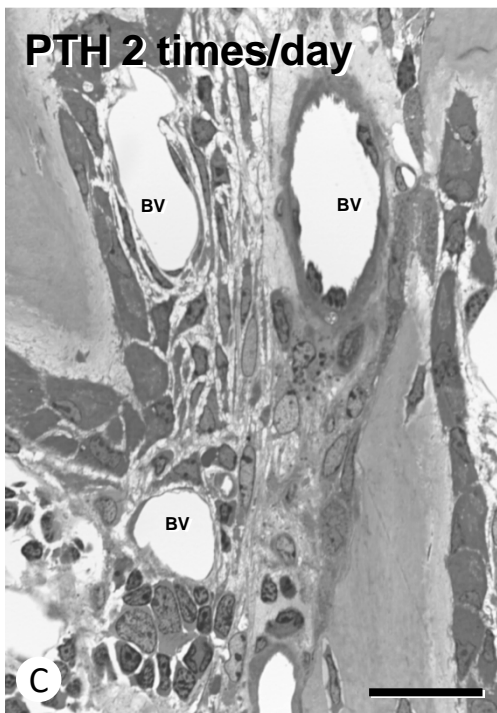
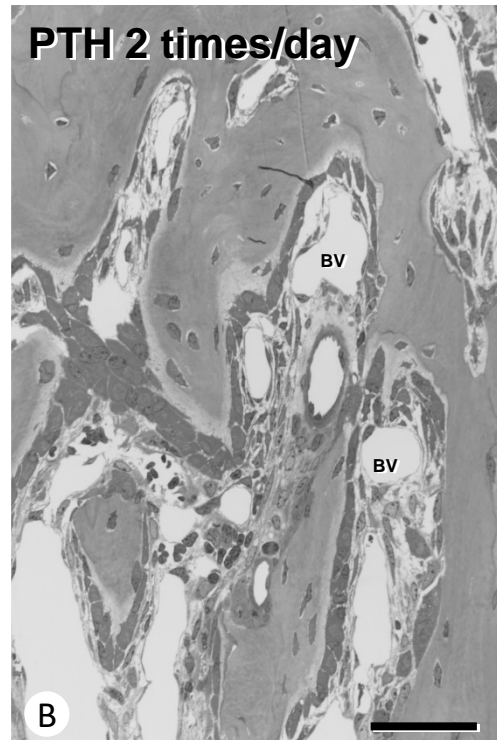
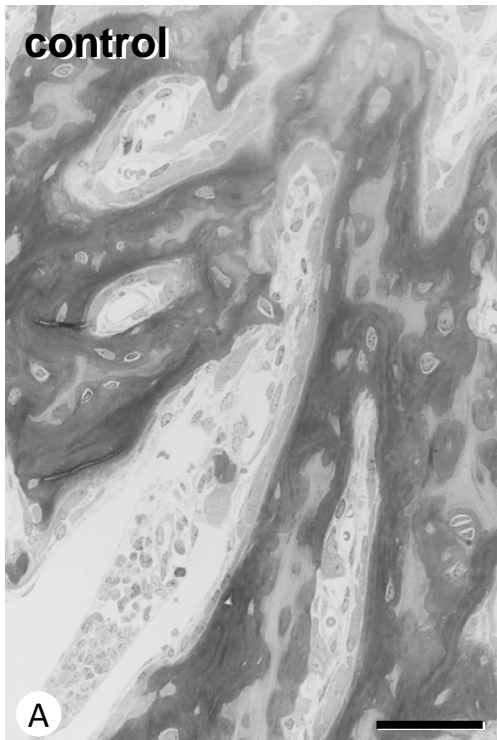


E

F







日中笹川医学奨学金制度(学位取得コース)中間評価書

課程博士：指導教官用



第 41 期 研究者番号： G4102

作成日：2020年3月3日

氏名	常立甲	Chang Lijia	性別	M	生年月日	1984. 08. 28
所属機関(役職)	石家荘市第四医院(主管技師)					
研究先(指導教官)	千葉大学社会精神保健教育研究センター(橋本 謙二副センター長・教授)					
研究テーマ	精神疾患の病因解明と新規治療法の開発 Study of pathogenesis of psychiatric disorders and the development of novel therapeutic methods					
専攻種別	<input type="checkbox"/> 論文博士			<input checked="" type="checkbox"/> 課程博士		

研究者評価(指導教官記入欄)

成績状況	優 良 可 不可 学業成績係数=3.78	取得単位数
学生本人が行った研究の概要	うつ病の動物モデルを用いて、新規抗うつ薬R-ケタミンの抗うつ効果、副作用をRS-ケタミンおよびS-ケタミンと比較し、原著論文として発表した(Chang L, et al. Pharmacol Biochem Behav 2019)。また、R-ケタミンの抗うつ効果にドパミンD1受容体は寄与しないことを見出し、短報として発表した(Chang L, et al. Eur Arch Psychiatry Clin Neurosci 2020)。さらに英語BOOK特集にケタミン総説を発表した(Chang L. and Hashimoto K. in press)。	
総合評価	【良かった点】 既に筆頭著者として、3本の論文を発表している。また論文投稿予定の論文データも揃っており、今年度中に論文を執筆する予定である。	
	【改善すべき点】 特に改善する点はないが、これまで通りに研究を継続すれば、さらに多くの論文業績が発表できると思う。	
	【今後の展望】 これまでに英語での論文発表を行っているので、次年度は、研究成果を国際会議で発表して海外の研究者と積極的に議論する人材に育てていただきたい。将来は、中国に帰国して活躍できる人材だと思う。さらに、常君の性格から、将来、日中の共同研究など日中交流の懸け橋になる人材になると思います。	
学位取得見込	既に原著論文を含む幾つかの論文を発表しており、学位取得見込みはある。	

評価者(指導教官名) 橋本 謙



日中笹川医学奨学金制度(学位取得コース)中間報告書 研究者用



第41期 研究者番号: G4102 作成日: 2020年03月02日

氏名	Chang Lijia	常 立甲	性別	M	生年月日 1984. 08. 28
所属機関(役職)	石家荘市第四医院 (主管技師)				
研究先(指導教官)	千葉大学社会精神保健教育研究センター(橋本 謙二副センター長・教授)				
研究テーマ	精神疾患の病因解明と新規治療法の開発 Study of pathogenesis of psychiatric disorders and the development of novel therapeutic methods				
専攻種別	論文博士	<input type="checkbox"/>	課程博士	<input checked="" type="checkbox"/>	

1. 研究概要(1)

1) 目的 (Goal) :

The N-methyl-D-aspartate receptor (NMDAR) antagonist (R,S)-ketamine produces rapid and sustained antidepressant effects in treatment-resistant patients with depression although intranasal use of (R,S)-ketamine in ketamine abusers is popular. On March 5, 2019, the US Food Drug Administration (FDA) approved Janssen Pharmaceutical Inc.'s (S)-ketamine nasal spray for treatment-resistant depression[1]. However, there are no reports showing the direct comparison of intranasal administration of (R,S)-ketamine and its two enantiomers for antidepressant and side effects in rodents. The purpose of this study is to compare the antidepressant and side effects of intranasal administration of (R,S)-ketamine and its two enantiomers (R)-ketamine and (S)-ketamine.

2) 戦略 (Approach) :

First, we compared the antidepressant effects of a single intranasal administration of (R,S)-ketamine, (R)-ketamine and (S)-ketamine in susceptible mice after chronic social defeat stress (CSDS). Second, we compared the side effects [i.e., locomotion, prepulse inhibition (PPI), conditioned place preference (CPP)] of intranasal administration of (R,S)-ketamine, (R)-ketamine and (S)-ketamine in mice.

3) 材料と方法 (Materials and methods) :

① Animals, Male adult C57BL/6 mice and male adult CD1 (ICR) mice were used. ② Materials, (R)-Ketamine hydrochloride and (S)-ketamine hydrochloride were prepared by recrystallization of (R,S)-ketamine. ③ Chronic social defeat stress (CSDS) model: The C57BL/6 mice were exposed to a different CD1 aggressor mouse for 10 min per day for consecutive 10 days. ④ Treatment and behavioral tests, the CSDS susceptible mice were divided to four groups. Subsequently, saline (0.5 ml/kg), (R,S)-ketamine (10 mg/kg), (R)-ketamine (10 mg/kg), or (S)-ketamine (10 mg/kg) was administered intranasally into CSDS susceptible mice. Behavioral tests, including locomotion test (LMT), tail suspension test (TST), forced swimming test (FST) and 1% sucrose preference test (SPT). ⑤ Side effects of behavioral tests, including Locomotion, Prepulse inhibition (PPI) test, Conditioned place preference (CPP) test. ⑥ Analysis was performed using PASW Statistics 20.

4) 実験結果 (Results) :

① The order of potency of antidepressant effects in a CSDS model was (R)-ketamine > (R,S)-ketamine > (S)-ketamine. ② The order of potencies of side effects (i.e., psychosis, abuse liability) in mice after intranasal administration was (S)-ketamine > (R,S)-ketamine > (R)-ketamine. Detail results were attached in the published paper.

5) 考察 (Discussion) :

① In the present study, we compared (R,S)-ketamine, and its two enantiomers in CSDS susceptible mice (for antidepressant effects) and control mice (for side effects). The order of potency of antidepressant effects after a single intranasal administration to CSDS susceptible mice is (R)-ketamine > (R,S)-ketamine > (S)-ketamine. Furthermore, the order of potency of side effects (i.e., psychosis and abuse liability) after intranasal administration is (S)-ketamine > (R,S)-ketamine > (R)-ketamine. Collectively, it is likely that (R)-ketamine would be a rapid-acting and sustained antidepressant without side effects compared to (R,S)-ketamine and (S)-ketamine. ② In this study, we found that antidepressant effects of (R,S)-ketamine and its two enantiomers in CSDS susceptible mice after a single intranasal administration may be less potent than those of a single i.p. administration[2-5]. Lower bioavailability of intranasal administration of (R,S)-ketamine and its two enantiomers may contribute to lower efficacy of intranasal administration compared to i.p. administration. Interestingly, the potency of antidepressant effects of (R,S)-ketamine and its two enantiomers was not correlated with the potencies of these compounds at the NMDAR, suggesting that NMDAR inhibition may not play a key role in the antidepressant effects of (R,S)-ketamine and its enantiomers[6]. ③ Due to its

1. 研究概要 (2)

serious side effects, clinical use of ketamine has remained limited[7-9], although it has been used as an off-label antidepressant in the USA[10]. In this study, we found that locomotion after a single intranasal administration of (R)-ketamine is lower than those of (R,S)-ketamine and (S)-ketamine, consistent with the previous reports[3]. Furthermore, we found that a single intranasal administration of (R)-ketamine did not cause PPI deficits in mice compared to (R,S)-ketamine and (S)-ketamine, consistent with the previous reports of i.p. administration[3]. Finally, we found that repeated intranasal administration of (R)-ketamine did not increase CPP scores in mice although (R,S)-ketamine and (S)-ketamine increased CPP scores, in a dose dependent manner, consistent with the previous reports of i.p. administration[2,11]. Unlike (R,S)-ketamine and (S)-ketamine, it seems that intranasal infusion of (R)-ketamine does not appear to cause psychotomimetic effects or have abuse potential in humans, based on the lack of behavioral abnormalities (e.g., PPI deficits, CPP) observed in mice after single or repeated intranasal administration[12]. Taken all together, it seems likely that (S)-ketamine contributes to the acute psychotomimetic and dissociative effects of (R,S)-ketamine, whereas (R)-ketamine may not be associated with these side effects [13]. ④ On March 5, 2019, the US FDA approved nasal spray of (S)-ketamine for treatment-resistant depression[1]. Due to the risk of serious adverse outcomes from sedation and dissociation caused by administration of (S)-ketamine, as well as the potential for abuse and misuse of the drug, FDA said that the drug will only be available through a restricted distribution system, under a Risk Evaluation and Mitigation Strategy (REMS). Patients will self-administer (S)-ketamine under the supervision of a health care provider in a certified doctor's office or clinic; the nasal spray cannot be taken home [1]. Given the lack of adverse side effects of (R)-ketamine, it is possible that patients may take (R)-ketamine to their home.

6) 参考文献 (References)

- [1] FDA News Release on March 5, 2019. FDA Approves New Nasal Spray Medication for Treatment-resistant Depression; Available Only at a Certified Doctor's Office or Clinic. <https://www.fda.gov/NewsEvents/Newsroom/PressAnnouncements/ucm632761.htm>
- [2] Yang, C., Shirayama, Y., Zhang, J.C., Ren, Q., Yao, W., Ma, M., Dong, C., Hashimoto, K., 2015. R-ketamine: a rapid-onset and sustained antidepressant without psychotomimetic side effects. *Transl. Psychiatry* 5, e632.
- [3] Yang, C., Qu, Y., Abe, M., Nozawa, D., Chaki, S., Hashimoto, K., 2017a. (R)-ketamine shows greater potency and longer lasting antidepressant effects than its metabolite (2R,6R)-hydroxynorketamine. *Biol. Psychiatry* 82, e43 - e44.
- [4] Yang, C., Qu, Y., Fujita, Y., Ren, Q., Ma, M., Dong, C., Hashimoto, K., 2017b. Possible role of the gut microbiota-brain axis in the antidepressant effects of (R)-ketamine in a social defeat stress model. *Transl. Psychiatry* 7, 1294.
- [5] Yang, C., Ren, Q., Qu, Y., Zhang, J.C., Ma, M., Dong, C., Hashimoto, K., 2018a. Mechanistic target of rapamycin-independent antidepressant effects of (R)-ketamine in a social defeat stress model. *Biol. Psychiatry* 83, 18 - 28.
- [6] Ebert, B., Mikkelsen, S., Thorkildsen, C., Borgbjerg, F.M., 1997. Norketamine, the main metabolite of ketamine, is a non-competitive NMDA receptor antagonist in the rat cortex and spinal cord. *Eur. J. Pharmacol.* 333, 99 - 104.
- [7] Domino, E.F., 2010. Taming the ketamine tiger. 1965. *Anesthesiology* 113, 678 - 684.
- [8] Sanacora, G., Frye, M.A., McDonald, W., Mathew, S.J., Turner, M.S., Schatzberg, A.F., Summergrad, P., Nemeroff, C.B., American Psychiatric Association (APA) Council of Research Task Force on Novel Biomarkers and Treatments, 2017. A consensus statement on the use of ketamine in the treatment of mood disorders. *JAMA Psychiatry* 74, 399 - 405.
- [9] Singh, I., Morgan, C., Curran, V., Nutt, D., Schlag, A., McShane, R., 2017. Ketamine treatment for depression: opportunities for clinical innovation and ethical foresight. *Lancet Psychiatry* 4, 419 - 426.
- [10] Wilkinson, S.T., Toprak, M., Turner, M.S., Levine, S.P., Katz, R.B., Sanacora, G., 2017. A survey of the clinical, off-label use of ketamine as a treatment for psychiatric disorders. *Am. J. Psychiatry* 174, 695 - 696.
- [11] Yang, C., Kobayashi, S., Nakao, K., Dong, C., Han, M., Qu, Y., Ren, Q., Zhang, J.C., Ma, M., Toki, H., Yamaguchi, J.I., Chaki, S., Shirayama, Y., Nakazawa, K., Manabe, T., Hashimoto, K., 2018b. AMPA receptor activation-independent antidepressant actions of ketamine metabolite (S)-norketamine. *Biol. Psychiatry* 84, 591 - 600.
- [12] Hashimoto, K., 2016a. R-ketamine: a rapid-onset and sustained antidepressant without risk of brain toxicity. *Psychol. Med.* 46, 2449 - 2451.
- [13] Zanos, P., Moaddel, R., Morris, P.J., Riggs, L.M., Highland, J.N., Georgiou, P., Pereira, E.F.R., Albuquerque, E.X., Thomas, C.J., Zarate Jr., C.A., Gould, T.D., 2018. Ketamine and ketamine metabolite pharmacology: insights into therapeutic mechanisms. *Pharmacol. Rev.* 70, 621 - 660.

2. 執筆論文 Publication of thesis ※記載した論文を添付してください。Attach all of the papers listed below.

論文名 1 Title	Comparison of antidepressant and side effects in mice after intranasal administration of (R,S)-ketamine, (R)-ketamine, and (S)-ketamine					
掲載誌名 Published journal	Pharmacology Biochemistry and Behavior					
	2019 年 6 月	181 巻(号)	53 頁 ~	59 頁	言語 Language	English
第1著者名 First author	Lijia Chang	第2著者名 Second author	Kai Zhang		第3著者名 Third author	Yaoyu Pu
その他著者名 Other authors	Youge Qu, Si-ming Wang, Zhongwei Xiong, Qian Ren, Chao Dong, Yuko Fujita, Kenji Hashimoto					
論文名 2 Title	Lack of dopamine D1 receptors in the antidepressant actions of (R)-ketamine in a chronic social defeat stress model					
掲載誌名 Published journal	European Archives of Psychiatry and Clinical Neuroscience					
	2020 年 3 月	270 (2) 巻(号)	271 頁 ~	275 頁	言語 Language	English
第1著者名 First author	Lijia Chang	第2著者名 Second author	Kai Zhang		第3著者名 Third author	Yaoyu Pu
その他著者名 Other authors	Youge Qu, Si-ming Wang, Zhongwei Xiong, Yukihiko Shirayama, Kenji Hashimoto					
論文名 3 Title	Antidepressant Actions of Ketamine and Its Two Enantiomers (Chapter Title)					
掲載誌名 Published journal	Ketamine from Abused Drug to Rapid-acting Antidepressant (Book Title) (In Press)					
	2020 年 1 月	巻(号)	頁 ~	頁	言語 Language	English
第1著者名 First author	Lijia Chang	第2著者名 Second author	Yan Wei		第3著者名 Third author	Kenji Hashimoto
その他著者名 Other authors						
論文名 4 Title	Essential Role of Microglial Transforming Growth factor- β 1 in Antidepressant Actions of (R)-ketamine and the Novel Antidepressant TGF- β 1					
掲載誌名 Published journal	Translational Psychiatry					
	2020 年 1 月	10:32 巻(号)	1 頁 ~	12 頁	言語 Language	English
第1著者名 First author	Kai Zhang	第2著者名 Second author	Chun Yang		第3著者名 Third author	Lijia Chang
その他著者名 Other authors	Akemi Sakamoto, Toru Suzuki, Yuko Fujita, Youge Qu, Siming Wang, Yaoyu Pu, Yunfei Tan, Xingming Wang, Tamaki Ishima, Yukihiko Shirayama, Masahiko Hatano, Kenji F Tanaka, Kenji Hashimoto					
論文名 5 Title	Antibiotic-induced Microbiome Depletion Is Associated With Resilience in Mice After Chronic Social Defeat Stress					
掲載誌名 Published journal	Journal of Affective Disorders					
	2020 年 1 月	260 巻(号)	448 頁 ~	457 頁	言語 Language	English
第1著者名 First author	Siming Wang	第2著者名 Second author	Youge Qu		第3著者名 Third author	Lijia Chang
その他著者名 Other authors	Yaoyu Pu, Kai Zhang, Kenji Hashimoto					

論文名 6 Title	A Historical Review of Antidepressant Effects of Ketamine and Its Enantiomers					
掲載誌名 Published journal	Pharmacology Biochemistry and Behavior					
	2020 年 3 月	190 卷 (号)	頁 ~	頁	言語 Language	English
第1 著者名 First author	Yan Wei	第2 著者名 Second author	Lijia Chang	第3 著者名 Third author	Kenji Hashimoto	
その他著者名 Other authors						
論文名 7 Title	Antibiotic-induced Microbiome Depletion Protects Against MPTP-induced Dopaminergic Neurotoxicity in the Brain					
掲載誌名 Published journal	Aging (Albany NY)					
	2019 年 9 月	11 (17) 卷 (号)	6915 頁 ~	6929 頁	言語 Language	English
第1 著者名 First author	Yaoyu Pu	第2 著者名 Second author	Lijia Chang	第3 著者名 Third author	Younge Qu	
その他著者名 Other authors	Siming Wang, Kai Zhang, Kenji Hashimoto					
論文名 8 Title	Abnormal composition of gut microbiota is associated with resilience versus susceptibility to inescapable electric stress					
掲載誌名 Published journal	Translational Psychiatry					
	2019 年 9 月	231 卷 (号)	1 頁 ~	9 頁	言語 Language	
第1 著者名 First author	Kai Zhang	第2 著者名 Second author	Yuko Fujita	第3 著者名 Third author	Lijia Chang	
その他著者名 Other authors	Younge Qu, Yaoyu Pu, Siming Wang, Yukihiro Shirayama & Kenji Hashimoto					
論文名 9 Title	(R)-Ketamine Rapidly Ameliorates the Decreased Spine Density in the Medial Prefrontal Cortex and Hippocampus of Susceptible Mice After Chronic Social Defeat Stress					
掲載誌名 Published journal	International Journal of Neuropsychopharmacology					
	2019 年 10 月	22(10) 卷 (号)	675 頁 ~	679 頁	言語 Language	English
第1 著者名 First author	Jiancheng Zhang	第2 著者名 Second author	Younge Qu	第3 著者名 Third author	Lijia Chang	
その他著者名 Other authors	Yaoyu Pu, Kenji Hashimoto					

3. 学会発表 Conference presentation ※筆頭演者として総会・国際学会を含む主な学会で発表したものを記載し
 ※Describe your presentation as the principal presenter in major academic meetings including general meetings
 or international meetings.

学会名 Conference	The Chiba-Otawa Joint Session of Pharmacology 2019		
演題 Topic	"Antidepressant actions of ketamine enantiomers"		
開催日 date	2019 年 7 月 24 日	開催地 venue	Chiba University Graduate School of Medicine
形式 method	<input checked="" type="checkbox"/> 口頭発表 Oral <input type="checkbox"/> ポスター発表 Poster		言語 Language <input type="checkbox"/> 日本語 <input checked="" type="checkbox"/> 英語 <input type="checkbox"/> 中国語
共同演者名 Co-presenter			
学会名 Conference			
演題 Topic			
開催日 date	年 月 日	開催地 venue	
形式 method	<input type="checkbox"/> 口頭発表 Oral <input type="checkbox"/> ポスター発表 Poster		言語 Language <input type="checkbox"/> 日本語 <input type="checkbox"/> 英語 <input type="checkbox"/> 中国語
共同演者名 Co-presenter			
学会名 Conference			
演題 Topic			
開催日 date	年 月 日	開催地 venue	
形式 method	<input type="checkbox"/> 口頭発表 Oral <input type="checkbox"/> ポスター発表 Poster		言語 Language <input type="checkbox"/> 日本語 <input type="checkbox"/> 英語 <input type="checkbox"/> 中国語
共同演者名 Co-presenter			
学会名 Conference			
演題 Topic			
開催日 date	年 月 日	開催地 venue	
形式 method	<input type="checkbox"/> 口頭発表 Oral <input type="checkbox"/> ポスター発表 Poster		言語 Language <input type="checkbox"/> 日本語 <input type="checkbox"/> 英語 <input type="checkbox"/> 中国語
共同演者名 Co-presenter			

4. 受賞 (研究業績) Award (Research achievement)

名称 Award name			
	国名 Country		受賞年 Year of 年 月
名称 Award name			
	国名 Country		受賞年 Year of 年 月

5. 本研究テーマに関わる他の研究助成金受給 Other research grants concerned with your research

受給実績 Receipt record	<input type="checkbox"/> 有 <input checked="" type="checkbox"/> 無
助成機関名称 Funding agency	
助成金名称 Grant name	
受給期間 Supported	年 月 ~ 年 月
受給額 Amount received	円
受給実績 Receipt record	<input type="checkbox"/> 有 <input checked="" type="checkbox"/> 無
助成機関名称 Funding agency	
助成金名称 Grant name	
受給期間 Supported	年 月 ~ 年 月
受給額 Amount received	円

6. 他の奨学金受給 Another awarded scholarship

受給実績 Receipt record	<input type="checkbox"/> 有 <input checked="" type="checkbox"/> 無
助成機関名称 Funding agency	
奨学金名称 Scholarship	
受給期間 Supported	年 月 ~ 年 月
受給額 Amount received	円

7. 研究活動に関する報道発表 Press release concerned with your research activities

※記載した記事を添付してください。 Attach a copy of the article described below

報道発表 Press release	<input type="checkbox"/> 有 <input checked="" type="checkbox"/> 無	発表年月日 Date of release	
発表機関 Released medium			
発表形式 Release method	・新聞 ・雑誌 ・Web site ・記者発表 ・その他 ()		
発表タイトル Released title			

8. 本研究テーマに関する特許出願予定 Patent application concerned with your research theme

出願予定 Scheduled	<input type="checkbox"/> 有 <input checked="" type="checkbox"/> 無	出願国 Application	
出願内容(概要) Application contents			

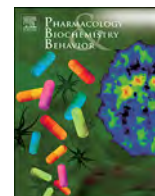
9. その他 Others

--

指導責任者(署名)

橋本謙





Comparison of antidepressant and side effects in mice after intranasal administration of (*R,S*)-ketamine, (*R*)-ketamine, and (*S*)-ketamine

Lijia Chang, Kai Zhang, Yaoyu Pu, Youge Qu, Si-ming Wang, Zhongwei Xiong, Qian Ren, Chao Dong, Yuko Fujita, Kenji Hashimoto*

Division of Clinical Neuroscience, Chiba University Center for Forensic Mental Health, Chiba 260-8670, Japan

ARTICLE INFO

Keywords:

Antidepressant
(*R*)-ketamine
(*R,S*)-ketamine
(*S*)-ketamine
Side effects

ABSTRACT

The *N*-methyl-D-aspartate receptor (NMDAR) antagonist (*R,S*)-ketamine produces rapid and sustained antidepressant effects in treatment-resistant patients with depression although intranasal use of (*R,S*)-ketamine in ketamine abusers is popular. In March 5, 2019, nasal spray of (*S*)-ketamine for treatment-resistant depression was approved as a new antidepressant by the US Food Drug Administration. Clinical study of (*R*)-ketamine is underway. In a chronic social defeat stress (CSDS) model, we compared the antidepressant effects of (*R,S*)-ketamine, (*R*)-ketamine, and (*S*)-ketamine after a single intranasal administration. Furthermore, we also compared the side effects (i.e., locomotion, prepulse inhibition (PPI), abuse liability) of these three compounds in mice. The order of potency of antidepressant effects after a single intranasal administration was (*R*)-ketamine > (*R,S*)-ketamine > (*S*)-ketamine. In contrast, the order of locomotor activity and prepulse inhibition (PPI) deficits after a single intranasal administration was (*S*)-ketamine > (*R,S*)-ketamine > (*R*)-ketamine. In the conditioned place preference (CPP) test, both (*S*)-ketamine and (*R,S*)-ketamine increased CPP scores in mice after repeated intranasal administration, in a dose dependent manner. In contrast, (*R*)-ketamine did not increase CPP scores in mice. These findings suggest that intranasal administration of (*R*)-ketamine would be a safer antidepressant than (*R,S*)-ketamine and (*S*)-ketamine.

1. Introduction

In 2000, Berman et al. (2000) reported a first double-blind, placebo-controlled study of the *N*-methyl-D-aspartate receptor (NMDAR) antagonist (*R,S*)-ketamine, demonstrating that (*R,S*)-ketamine exhibits rapid antidepressant effects in treatment-resistant patients with major depressive disorder (MDD). Subsequently, a number of groups replicated robust antidepressant effects of (*R,S*)-ketamine in treatment-resistant patients with MDD (Murrough et al., 2013; Su et al., 2017; Zarate et al., 2006;). Interestingly, (*R,S*)-ketamine could produce anti-suicidal effects in treatment-resistant patients with MDD (Grunebaum et al., 2018; Larkin and Beautrais, 2011; Murrough et al., 2015; Price et al., 2009). Several meta-analyses showed that (*R,S*)-ketamine exhibits rapid antidepressant and anti-suicidal ideation effects in treatment-resistant patients with MDD or bipolar disorder (Kishimoto et al., 2016; Newport et al., 2015; Wilkinson et al., 2018; Xu et al., 2016). Off-label use of (*R,S*)-ketamine (i.e., intravenous and intranasal administration) for antidepressant effects is increasing in the United State of America (USA) although the common adverse effects (e.g.,

psychotomimetic effects and dissociative effects) of (*R,S*)-ketamine are not resolved (Singh et al., 2017; Wilkinson et al., 2017; Zhu et al., 2016). Thus, although (*R,S*)-ketamine is the most attractive antidepressant in the treatment of severe depression, the precise mechanisms underlying its antidepressant actions remain elusive (Abdallah et al., 2018; Chaki, 2017a, 2017b; Duman, 2018; Gould et al., 2019; Hashimoto, 2016a, 2016b; Krystal et al., 2019; Monteggia and Zarate Jr, 2015; Murrough et al., 2017; Zanos et al., 2018; Zhang and Hashimoto, 2019a).

(*R,S*)-ketamine ($K_i = 0.53 \mu\text{M}$ for NMDAR) is a racemic mixture containing equal parts of (*R*)-ketamine (or arketamine) ($K_i = 1.4 \mu\text{M}$ for NMDAR) and (*S*)-ketamine (or esketamine) ($K_i = 0.30 \mu\text{M}$ for NMDAR) (Ebert et al., 1997). (*R*)-ketamine is reported to show greater potency and longer-lasting antidepressant effects than (*S*)-ketamine in several animal models of depression (Fukumoto et al., 2017; Yang et al., 2015, 2017a, 2017b, 2018a; Zanos et al., 2016; Zhang et al., 2014). Unlike (*S*)-ketamine, (*R*)-ketamine might not induce psychotomimetic side effects or exhibit abuse potential in rodents (Yang et al., 2015, 2016). In addition, unlike (*R,S*)-ketamine and (*S*)-ketamine, (*R*)-ketamine did not

* Corresponding author.

E-mail address: hashimoto@faculty.chiba-u.jp (K. Hashimoto).

<https://doi.org/10.1016/j.pbb.2019.04.008>

Received 2 April 2019; Received in revised form 25 April 2019; Accepted 25 April 2019

Available online 26 April 2019

0091-3057/ © 2019 Elsevier Inc. All rights reserved.

cause the expression of heat shock protein HSP-70 (a marker for neuronal injury) in the rat retrosplenial cortex after a single intraperitoneal (i.p.) administration (Tian et al., 2018). A positron emission tomography (PET) study showed a marked reduction of dopamine D_{2/3} receptor binding in conscious monkey striatum after a single intravenous (i.v.) infusion of (S)-ketamine but not that of (R)-ketamine, suggesting that (S)-ketamine-induced dopamine release might be associated with acute psychotomimetic and dissociative side effects in humans (Hashimoto et al., 2017). Therefore, it seems that (R)-ketamine could be a safer antidepressant in humans than (R,S)-ketamine and (S)-ketamine (Hashimoto, 2014, 2016a, 2016b, 2016c).

Fukumoto et al. (2017) reported that (R,S)-ketamine (10 mg/kg) and (R)-ketamine (10 mg/kg), but not (S)-ketamine (3 and 10 mg/kg), significantly reversed the depressive-like behavior induced by repeated treatments with corticosterone in rats at 24 h after a single i.p. administration, indicating that (S)-ketamine's antidepressant effects are less potent than (R,S)-ketamine and (R)-ketamine. On March 5, 2019, the US Food Drug Administration (FDA) approved Janssen Pharmaceutical Inc.'s (S)-ketamine nasal spray for treatment-resistant depression (FDA 2019). It is well known that bioavailability (17–29%) of intranasal administration of (R,S)-ketamine in humans is markedly lower than i.v. (100%) and intramuscular (i.m.) administration (93%) (Li and Vlisides, 2016; Peltoniemi et al., 2016; Zhang and Hashimoto, 2019a), suggesting lower efficacy and higher individual difference of intranasal administration compared to i.v. and i.m. administration. However, there are no reports showing the direct comparison of intranasal administration of (R,S)-ketamine and its two enantiomers for antidepressant and side effects in rodents.

The purpose of this study is to compare the antidepressant and side effects of intranasal administration of (R,S)-ketamine and its two enantiomers (R)-ketamine and (S)-ketamine. First, we compared the antidepressant effects of a single intranasal administration of (R,S)-ketamine, (R)-ketamine and (S)-ketamine in susceptible mice after chronic social defeat stress (CSDS). Second, we compared the side effects [i.e., locomotion, prepulse inhibition (PPI), conditioned place preference (CPP)] of intranasal administration of (R,S)-ketamine, (R)-ketamine and (S)-ketamine in mice.

2. Methods and Materials

2.1. Animals

Male adult C57BL/6 mice ($n = 400$), aged 8 weeks (body weight 20–25 g, Japan SLC, Inc., Hamamatsu, Japan) and male adult CD1 (ICR) mice ($n = 40$), aged 13–15 weeks (body weight > 40 g, Japan SLC, Inc., Hamamatsu, Japan) were used. Animals were housed under controlled temperatures and 12h/dark cycles (lights on between 07:00 and 19:00 h), with ad libitum food (CE-2; CLEA Japan, Inc., Tokyo, Japan) and water. The protocol was approved by the Chiba University Institutional Animal Care and Use Committee (Permission number: 29-420). This study was carried out in strict accordance with the recommendations in the Guide for the Care and Use of Laboratory Animals of the National Institutes of Health, USA. Animals were deeply anesthetized with isoflurane before being killed by cervical dislocation. All efforts were made to minimize suffering.

2.2. Materials

(R)-Ketamine hydrochloride and (S)-ketamine hydrochloride were prepared by recrystallization of (R,S)-ketamine (Ketalar®, ketamine hydrochloride, Daiichi Sankyo Pharmaceutical Ltd., Tokyo, Japan) and D-(–)-tartaric acid and L-(+)-tartaric acid, respectively (Zhang et al., 2014). The dose (10, 20 or 40 mg/kg as hydrochloride) of (R,S)-ketamine and its enantiomers dissolved in the physiological saline was used as previously reported (Chang et al., 2019; Yang et al., 2015, 2017a, 2017b, 2018a; Zhang et al., 2018). Other reagents were purchased

commercially.

2.3. Chronic social defeat stress (CSDS) model

The procedure of CSDS was performed as previously reported (Chang et al., 2019; Dong et al., 2017; Golden et al., 2011; Yang et al., 2015, 2017a, 2017b, 2018a; Xiong et al., 2018a, 2018b; Zhang et al., 2018). The C57BL/6 mice were exposed to a different CD1 aggressor mouse for 10 min per day for consecutive 10 days. When the social defeat session ended, the resident CD1 mouse and the intruder mouse were housed in one half of the cage separated by a perforated Plexiglas divider to allow visual, olfactory, and auditory contact for the remainder of the 24-h period. At 24 h after the last session, all mice were housed individually. On day 11, a social interaction test (SIT) was performed to identify subgroups of mice that were susceptible and unsusceptible to social defeat stress. This was accomplished by placing mice in an interaction test box (42 × 42 cm) with an empty wire-mesh cage (10 × 4.5 cm) located at one end. The movement of the mice was tracked for 2.5 min, followed by 2.5 min in the presence of an unfamiliar aggressor confined in the wire-mesh cage. The duration of the subject's presence in the “interaction zone” (defined as the 8-cm-wide area surrounding the wiremesh cage) was recorded by a stopwatch. The interaction ratio was calculated as time spent in an interaction zone with an aggressor/time spent in an interaction zone without an aggressor. An interaction ratio of 1 was set as the cutoff: mice with scores < 1 were defined as “susceptible” to social defeat stress and those with scores ≥ 1 were defined as “resilient”. Approximately 70–80% of mice were susceptible after CSDS. Susceptible mice were randomly divided in the subsequent experiments. Control C57BL/6 mice without CSDS were housed in the cage before the behavioral tests.

2.4. Treatment and behavioral tests

The CSDS susceptible mice were divided to four groups. Subsequently, saline (0.5 ml/kg), (R,S)-ketamine (10 mg/kg), (R)-ketamine (10 mg/kg), or (S)-ketamine (10 mg/kg) was administered intranasally into CSDS susceptible mice (Fig. 1A). Mice were restrained by hand, and saline or ketamine was administered intranasally into awake mice using Eppendorf micropipette (Eppendorf Japan, Tokyo, Japan). Behavioral tests, including locomotion test (LMT), tail suspension test (TST), forced swimming test (FST) and 1% sucrose preference test (SPT), were performed as reported previously (Dong et al., 2017; Yang et al., 2015, 2017a, 2017b, 2018a; Xiong et al., 2018a, 2018b; Zhang et al., 2018). LMT and TST were performed 2 and 4 h after a single injection, respectively. FST was performed 1 day after injection. SPT was performed 2, and 7 days after a single injection (Fig. 1A).

2.4.1. Locomotion

The locomotor activity was measured by an animal movement analysis system SCANETMV-40 (MELQUEST Co., Ltd., Toyama, Japan). The mice were placed in experimental cages (length × width × height: 560 × 560 × 330 mm). The cumulative locomotor activity counts were recorded for 60 min. Cages were cleaned between testing session.

2.4.2. TST

A small piece of adhesive tape placed approximately 2 cm from the tip of the tail for mouse. A single hole was punched in the tape and mice were hung individually, on a hook. The immobility time was recorded for 10 min. Mice were considered immobile only when they hung passively and completely motionless.

2.4.3. FST

The FST was conducted using an automated forced-swim apparatus (SCANET MV-40; MELQUEST Co., Ltd., Toyama, Japan). Mice were placed individually in a cylinder (diameter: 23 cm; height: 31 cm) containing 15 cm of water maintained at a temperature of

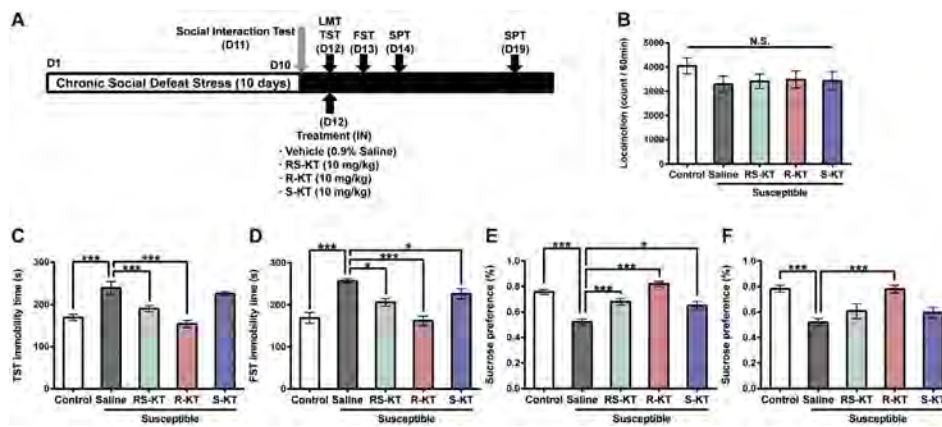


Fig. 1. Schedule of a CSDS model, treatment, and behavioral tests.

(A): CSDS was performed from day 1 to day 10, and the social interaction test (SIT) was performed on day 11. Saline (0.5 ml/kg), (*R,S*)-ketamine (10 mg/kg), (*R*)-ketamine (10 mg/kg), or (*S*)-ketamine (10 mg/kg) was administered intranasally into the susceptible mice on day 12. LMT and TST were performed 2 and 4 h after a single injection, respectively. SPT was performed 2, and 7 days after a single injection. (B): LMT (day 12). (C): TST (day 12). (D): FST (day 13). (E): SPT (day 14). (F): SPT (day 19). The values represent the mean \pm S.E.M. ($n = 15$ or 16). * $P < 0.05$, ** $P < 0.01$, *** $P < 0.001$ compared with saline-treated susceptible mice. N.S.: not significant. LMT: locomotion test. TST: tail suspension test. FST: forced swimming test. SPT: 1% sucrose preference test. R-KT: (*R*)-ketamine. RS-KT: (*R,S*)-ketamine. S-KT: (*S*)-ketamine.

$23^{\circ}\text{C} \pm 1^{\circ}\text{C}$. The immobility time was calculated using the activity time as (total) – (active) time by the apparatus analysis software. The immobility time of each mouse was recorded for a period of 6 min.

2.4.4. SPT

Mice were exposed to water and 1% sucrose solution for 48 h, followed by 4 h of water and food deprivation and a 1-hour exposure to two identical bottles (water and 1% sucrose solution). The bottles containing water and sucrose were weighed before and at the end of this period. The sucrose preference was calculated as a percentage of sucrose solution consumption to the total liquid consumption.

2.5. Side effects

2.5.1. Locomotion

After habituation (60 min) in the cage, saline (0.5 ml/kg), (*R,S*)-ketamine (10, 20 or 40 mg/kg), (*R*)-ketamine (10, 20 or 40 mg/kg), or (*S*)-ketamine (10, 20 or 40 mg/kg) was injected intranasally into male C57BL/6 mice. Locomotor activity was measured using an animal movement analysis system (SCANET MV-40, Melquest, Toyama, Japan). The system consisted of a rectangular enclosure (560 \times 560 mm). The side walls (height, 60 mm) of the enclosure were equipped with 144 pairs of photosensors located at 6-mm intervals at a height of 30 mm from the bottom edge. An animal was placed in the observation cage 60 min from a single dose of saline or compounds. A pair of photosensors was scanned every 0.1 s to detect the animal's movements. The intersection of paired photosensors (10 mm apart) in the enclosure was counted as one unit of locomotor activity. Data collected for 60 min after a single injection were used in this study.

2.5.2. Prepulse inhibition (PPI) test

Male C57BL/6 mice were tested for their acoustic startle reactivity (ASR) in a startle chamber (SR-LAB; San Diego Instruments, San Diego, CA, USA) using the standard methods described previously (Matsuura et al., 2015; Yang et al., 2015; Yang et al., 2018b). The test sessions were begun after an initial 10-min acclimation period in the chamber. The mice were subjected to one of six trials: (1) pulse alone, as a 40 ms broadband burst; a pulse (40 ms broadband burst) preceded by 100 ms with a 20 ms prepulse that was (2) 4 dB, (3) 8 dB, (4) 12 dB, or (5) 16 dB over background (65 dB); and (6) background only (no stimulus). The amount of PPI was expressed as the percentage decrease in the amplitude of the startle reactivity caused by presentation of the prepulse (% PPI). Saline (0.5 ml/kg), or (*R,S*)-ketamine (10, 20 or 40 mg/kg) [or (*R*)-ketamine (10, 20 or 40 mg/kg), (*S*)-ketamine (10, 20 or 40 mg/kg)] was administered intranasally 20 min (including the 10-min acclimation period) before the machine records. The PPI test lasted 20 min in

total.

2.5.3. Conditioned place preference (CPP) test

The place conditioning paradigm (Brain Science Idea Inc., Osaka, Japan) was used for studying ketamine-induced rewarding effects, as reported previously (Yang et al., 2015; Yang et al., 2018b). Male C57BL/6 mouse was allowed to move freely between transparent and black boxes for a 15 min session once a day, for 3 days (days 1–3) as preconditioning. On day 3, the time spent in each box was measured. There was no significant difference between time spent in the black compartment with a smooth floor and the white compartment with a textured floor, indicating that there was no place preference before conditioning. On days 4, 6, and 8, saline (0.5 ml/kg), or (*R,S*)-ketamine (10, 20 or 40 mg/kg) [or (*R*)-ketamine (10, 20 or 40 mg/kg), (*S*)-ketamine (10, 20 or 40 mg/kg)] was intranasally administered, and then mice were confined to either the transparent or black box for 30 min. On days 5, 7, and 9, mice were given saline and placed in the opposite ketamine-conditioning box for 30 min. On day 10, the post-conditioning test was performed without drug treatment, and the time spent in each box was measured for 15 min. A counterbalanced protocol was used in order to nullify any initial preference by the mouse. The CPP score was designated as the time spent in the drug-conditioning sites, minus the time spent in the saline-conditioning sites.

2.6. Statistical analysis

The data show as the mean \pm standard error of the mean (S.E.M.). Analysis was performed using PASW Statistics 20 (formerly SPSS Statistics; SPSS, Tokyo, Japan). The data were analyzed using the one-way analysis of variance (ANOVA), followed by *post-hoc* Fisher's Least Significant Difference (LSD) test. The PPI data were also analyzed using multivariate analysis of variance, followed by *post-hoc* Fisher's LSD test. The P -values of < 0.05 were considered statistically significant.

3. Results

3.1. Antidepressant effects of (*R,S*)-ketamine, (*R*)-ketamine and (*S*)-ketamine in CSDS susceptible mice

Locomotion showed no difference ($F_{4,72} = 0.735$, $P = 0.571$) among the five groups (Fig. 1B). One-way ANOVA of TST data showed a statistical significance ($F_{4,72} = 15.23$, $P < 0.001$) among the five groups (Fig. 1C). *Post-hoc* tests showed that (*R,S*)-ketamine (10 mg/kg) and (*R*)-ketamine (10 mg/kg) significantly attenuated the increased immobility times of TST in CSDS susceptible mice (Fig. 1C). However, (*S*)-ketamine (10 mg/kg) did not attenuate the increased immobility

time of TST in CSDS susceptible mice although (*S*)-ketamine slightly decreased the increased immobility time (Fig. 1C). One-way ANOVA of FST data showed a statistical significance ($F_{4,72} = 13.77$, $P < 0.001$) among the five groups (Fig. 1D). *Post-hoc* tests showed that three compounds (10 mg/kg) significantly attenuated the increased immobility times of FST in CSDS susceptible mice (Fig. 1D). One-way ANOVA of SPT data showed statistical significance (2 days after a single injection: $F_{4,72} = 20.78$, $P < 0.001$) among the five groups (Fig. 1E). *Post-hoc* tests showed that three compounds (10 mg/kg) significantly attenuated the decreased sucrose preference of SPT in CSDS susceptible mice (Fig. 1E). One-way ANOVA of SPT data showed statistical significance (7 days after a single injection: $F_{4,72} = 9.311$, $P < 0.001$) among the five groups (Fig. 1F). *Post-hoc* tests showed that sucrose preference of (*R*)-ketamine-treated group was significantly higher from saline-treated group. However, sucrose preference of (*R,S*)-ketamine-treated group and (*S*)-ketamine-treated group was not different from saline-treated group (Fig. 1E and F). Collectively, the order of potency of antidepressant effects in a CSDS model was (*R*)-ketamine > (*R,S*)-ketamine > (*S*)-ketamine.

3.2. Effects of (*R,S*)-ketamine, (*R*)-ketamine, and (*S*)-ketamine on locomotion in mice after a single intranasal administration

Effects of three compounds on locomotion of male mice were examined after a single intranasal administration. One-way ANOVA of the data showed statistical significances ($F_{9,70} = 8.931$, $P < 0.001$) among the ten groups (Fig. 2A). *Post-hoc* tests showed that a single intranasal administration of (*R,S*)-ketamine (20 and 40 mg/kg) or (*S*)-ketamine (10, 20 and 40 mg/kg) significantly increased locomotion compared to saline-treated group (Fig. 2A). Furthermore, locomotion of (*S*)-ketamine (40 mg/kg) treated mice was significantly higher than that of (*R,S*)-ketamine (40 mg/kg) or (*R*)-ketamine (40 mg/kg) treated mice. In contrast, all doses (10, 20 or 40 mg/kg) of (*R*)-ketamine did not alter locomotion in mice (Fig. 2A).

3.3. Effects of (*R,S*)-ketamine, (*R*)-ketamine, and (*S*)-ketamine on PPI in mice after a single intranasal administration

PPI test was performed to examine the effects of three compounds in mice. There were no changes in the acoustic startle response among the four groups for (*R,S*)-ketamine [Wilks lambda = 0.717, $P = 0.589$], (*R*)-ketamine [Wilks lambda = 0.629, $P = 0.226$], and (*S*)-ketamine [Wilks lambda = 0.588, $P = 0.405$] (Fig. 3A–3C).

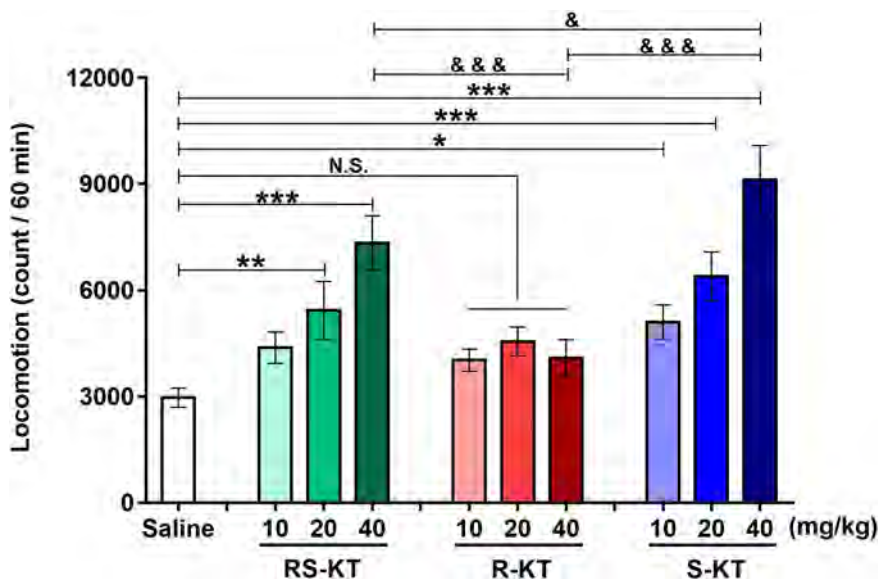


Fig. 2. Effects of (*R,S*)-ketamine, (*R*)-ketamine, and (*S*)-ketamine on locomotion after a single intranasal administration.

Saline (0.5 ml/kg), (*R,S*)-ketamine (10, 20, or 40 mg/kg), (*R*)-ketamine (10, 20, or 40 mg/kg), or (*S*)-ketamine (10, 20, or 40 mg/kg) was administered intranasally into male mice. Locomotor activity was measured 60 min after a single injection of the compounds. The values represent the mean \pm S.E.M. ($n = 8$). * $P < 0.05$, ** $P < 0.01$, *** $P < 0.001$ compared with saline-treated mice. & $P < 0.05$ compared to R-KT (40 mg/kg). &&& $P < 0.001$ compared to R-KT (40 mg/kg). N.S.: not significant. R-KT: (*R*)-ketamine. RS-KT: (*R,S*)-ketamine. S-KT: (*S*)-ketamine.

The MANOVA analysis of all PPI data of (*R,S*)-ketamine revealed that there was a significant effect [Wilks lambda = 0.497, $P = 0.042$]. Treatment with (*R,S*)-ketamine (10, 20 or 40 mg/kg) decreased PPI at all dB groups, in a dose dependent manner. Subsequent *post-hoc* tests indicated significant differences in PPI between the saline group and (*R,S*)-ketamine (40 mg/kg) group at all dB groups (Fig. 3A). In contrast, the MANOVA analysis of all PPI data of (*R*)-ketamine revealed that there was not a significant effect [Wilks lambda = 0.625, $P = 0.216$] (Fig. 3B). The MANOVA analysis of all PPI data of (*S*)-ketamine revealed that there was a significant effect [Wilks lambda = 0.299, $P < 0.001$]. Treatment with (*S*)-ketamine (10, 20 or 40 mg/kg) decreased PPI at all dB groups, in a dose dependent manner. Subsequent *post-hoc* tests indicated significant differences in PPI deficits between the saline group and (*S*)-ketamine (20 and 40 mg/kg) group at all dB groups. Furthermore, (*S*)-ketamine (10 mg/kg) significantly decreased PPI at 73 dB (Fig. 3C).

3.4. Effects of (*R,S*)-ketamine, (*R*)-ketamine, and (*S*)-ketamine on CPP scores in mice after repeated intranasal administration

In the conditioned place preference (CPP) test (Fig. 4A), both (*R,S*)-ketamine and (*S*)-ketamine, but not (*R*)-ketamine, increased CPP scores, in a dose dependent manner (Fig. 4). Repeated intranasal administration of (*R,S*)-ketamine (40 mg/kg), but not the low doses (10 and 20 mg/kg), significantly increased CPP scores ($F_{3,34} = 3.054$, $P = 0.042$) (Fig. 4B). In contrast, repeated intranasal administration of (*R*)-ketamine (10, 20 or 40 mg/kg) did not increase CPP scores ($F_{3,36} = 0.072$, $P = 0.974$) (Fig. 4C). Repeated intranasal administration of (*S*)-ketamine (20 and 40 mg/kg), but not the low dose (10 mg/kg), significantly increased CPP scores ($F_{3,36} = 14.0$, $P < 0.001$) (Fig. 4D).

Collectively, the order of potencies of side effects (i.e., psychosis, abuse liability) in mice after intranasal administration was (*S*)-ketamine > (*R,S*)-ketamine > (*R*)-ketamine.

4. Discussion

In the present study, we compared (*R,S*)-ketamine, and its two enantiomers, in CSDS susceptible mice (for antidepressant effects) and control mice (for side effects). The order of potency of antidepressant effects after a single intranasal administration to CSDS susceptible mice is (*R*)-ketamine > (*R,S*)-ketamine > (*S*)-ketamine. Furthermore, the order of potency of side effects (i.e., psychosis and abuse liability) after

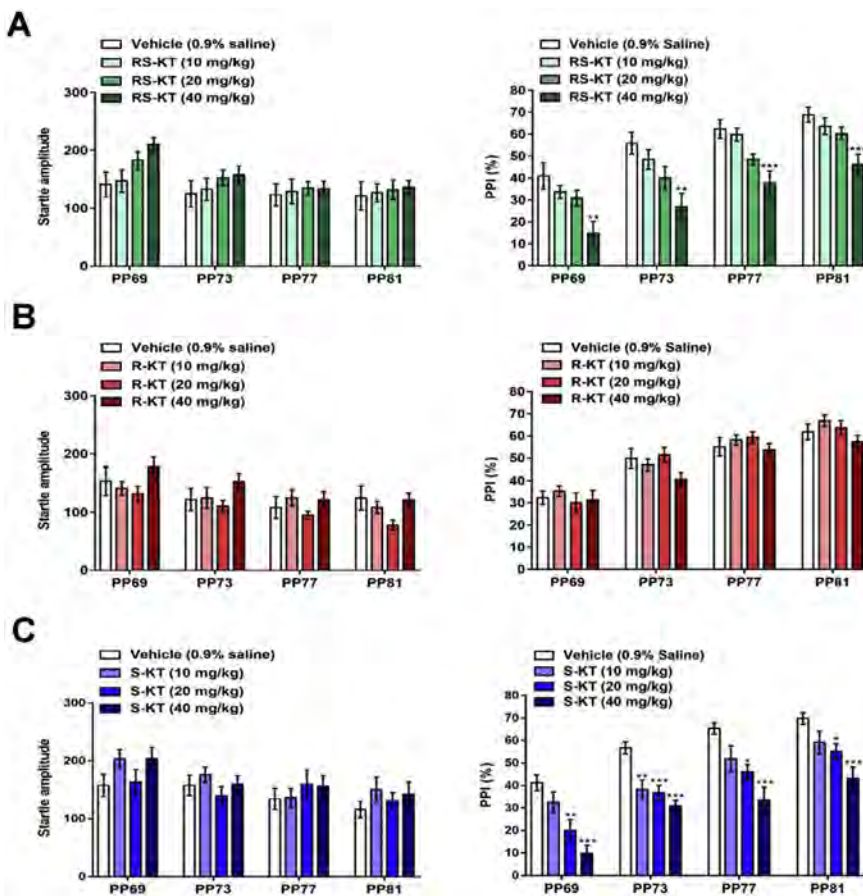


Fig. 3. Effects of (*R,S*)-ketamine, (*R*)-ketamine, and (*S*)-ketamine on PPI after a single intranasal administration. (A): Saline (0.5 ml/kg), or (*R,S*)-ketamine (10, 20, or 40 mg/kg) was administered intranasally into male mice. (B): Saline (0.5 ml/kg), or (*R*)-ketamine (10, 20, or 40 mg/kg) was administered intranasally into male mice. (C): Saline (0.5 ml/kg), or (*S*)-ketamine (10, 20, or 40 mg/kg) was administered intranasally into male mice. Startle response amplitude and PPI were measured as described in the [Method Section](#). The values represent the mean \pm S.E.M. ($n = 9$ or 10). * $P < 0.05$, ** $P < 0.01$, *** $P < 0.001$ compared with saline-treated mice. N.S.: not significant. R-KT: (*R*)-ketamine. RS-KT: (*R,S*)-ketamine. S-KT: (*S*)-ketamine.

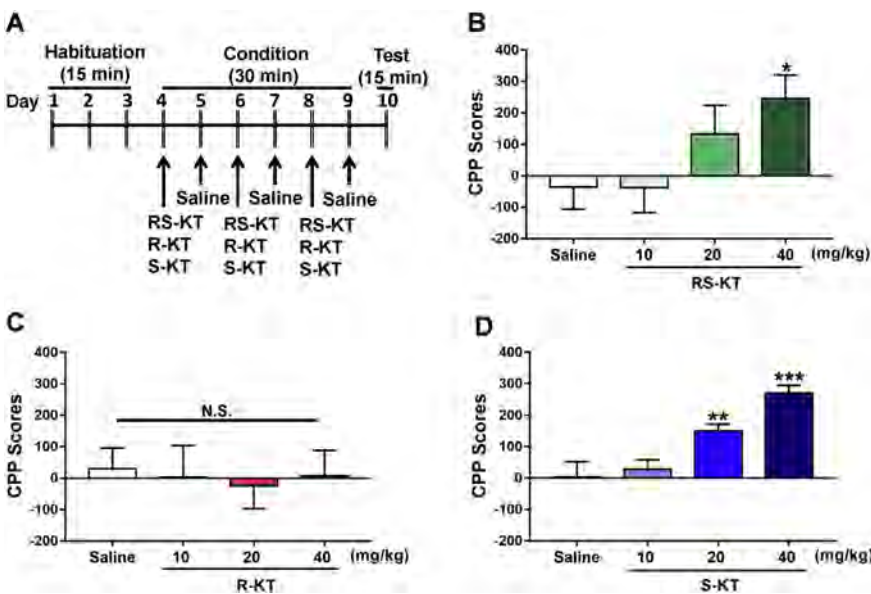


Fig. 4. Effects of (*R,S*)-ketamine, (*R*)-ketamine, and (*S*)-ketamine on CPP score after repeated intranasal administration. (A): Schedule of habituation, treatment, and behavioral test. (B): Saline (0.5 ml/kg), or (*R,S*)-ketamine (10, 20, or 40 mg/kg) was administered intranasally into male mice. (C): Saline (0.5 ml/kg), or (*R*)-ketamine (10, 20, or 40 mg/kg) was administered intranasally into male mice. (D): Saline (0.5 ml/kg), or (*S*)-ketamine (10, 20, or 40 mg/kg) was administered intranasally into male mice. CPP score was measured as described in the [Method Section](#). The values represent the mean \pm S.E.M. ($n = 8-10$). * $P < 0.05$, ** $P < 0.01$, *** $P < 0.001$ compared with saline-treated mice. N.S.: not significant. R-KT: (*R*)-ketamine. RS-KT: (*R,S*)-ketamine. S-KT: (*S*)-ketamine.

intranasal administration is (*S*)-ketamine > (*R,S*)-ketamine > (*R*)-ketamine. Collectively, it is likely that (*R*)-ketamine would be a rapid-acting and sustained antidepressant without side effects compared to (*R,S*)-ketamine and (*S*)-ketamine.

In this study, we found that antidepressant effects of (*R,S*)-ketamine and its two enantiomers in CSDS susceptible mice after a single intranasal administration may be less potent than those of a single i.p. administration (Dong et al., 2017; Yang et al., 2015, 2017a, 2017b, 2018a; Zhang et al., 2015; Zhang and Hashimoto, 2019b). Lower

bioavailability of intranasal administration of (*R,S*)-ketamine and its two enantiomers may contribute to lower efficacy of intranasal administration compared to i.p. administration. Interestingly, the potency of antidepressant effects of (*R,S*)-ketamine and its two enantiomers was not correlated with the potencies of these compounds at the NMDAR (Ebert et al., 1997), suggesting that NMDAR inhibition may not play a key role in the antidepressant effects of (*R,S*)-ketamine and its enantiomers. Previously, Fukumoto et al. (2017) reported that (*R,S*)-ketamine and (*R*)-ketamine, but not (*S*)-ketamine, show antidepressant

effects in rats with repeated corticosterone treatments after a single i.p. administration, consistent with our current data.

Due to its serious side effects, clinical use of ketamine has remained limited (Domino, 2010; Sanacora et al., 2017; Singh et al., 2017; Zhu et al., 2016), although it has been used as an off-label antidepressant in the USA (Reardon, 2018; Wilkinson et al., 2017). In this study, we found that locomotion after a single intranasal administration of (R)-ketamine is lower than those of (R,S)-ketamine and (S)-ketamine, consistent with the previous reports (Ryder et al., 1978; Yang et al., 2015) of subcutaneous or i.p. administration. Furthermore, we found that a single intranasal administration of (R)-ketamine did not cause PPI deficits in mice compared to (R,S)-ketamine and (S)-ketamine, consistent with the previous reports of i.p. administration (Yang et al., 2015). Interestingly, it was reported that the ED₅₀ of (R)-ketamine (6.33 mg/kg) for PPI deficits in rats was higher than that of (S)-ketamine (2.86 mg/kg), indicating that (S)-ketamine disrupts PPI with 2.5-fold higher potency than (R)-ketamine (Halberstadt et al., 2016). Finally, we found that repeated intranasal administration of (R)-ketamine did not increase CPP scores in mice although (R,S)-ketamine and (S)-ketamine increased CPP scores, in a dose dependent manner, consistent with the previous reports of i.p. administration (Yang et al., 2015, 2018b). A PET study showed that a single i.v. infusion of (S)-ketamine (0.5 mg/kg for 40-min), but not (R)-ketamine (0.5 mg/kg for 40-min), produced a marked reduction of dopamine D_{2/3} receptor binding in conscious monkey striatum, suggesting that (S)-ketamine-induced dopamine release might be associated with acute psychotomimetic and dissociative side effects in humans (Hashimoto et al., 2017). Unlike (R,S)-ketamine and (S)-ketamine, it seems that intranasal infusion of (R)-ketamine does not appear to cause psychotomimetic effects or have abuse potential in humans, based on the lack of behavioral abnormalities (e.g., PPI deficits, CPP) observed in mice after single or repeated intranasal administration (Hashimoto, 2016a, 2016b, 2016c).

Mathisen et al. (1995) reported that the incidence of side effects (i.e., blurred vision, altered hearing, dizziness, proprioceptive disturbances, illusions) of (S)-ketamine (0.45 mg/kg, i.m.) treated group in patients with oral pain was higher than (R)-ketamine (1.8 mg/kg, i.m.) treated group, although the dose of (S)-ketamine (0.45 mg/kg) is lower than (R)-ketamine (1.8 mg/kg). Furthermore, it is also reported that experiencing illusion and alterations in hearing, vision, and proprioception is attributable to (S)-ketamine's actions (Oye et al., 1992; Vollenweider et al., 1997), whereas the feelings of relaxation are associated with (R)-ketamine's actions (Vollenweider et al., 1997; Zanos et al., 2018). Taken all together, it seems likely that (S)-ketamine contributes to the acute psychotomimetic and dissociative effects of (R,S)-ketamine, whereas (R)-ketamine may not be associated with these side effects (Zanos et al., 2018).

On March 5, 2019, the US FDA approved nasal spray of (S)-ketamine for treatment-resistant depression (FDA, 2019). Due to the risk of serious adverse outcomes from sedation and dissociation caused by administration of (S)-ketamine, as well as the potential for abuse and misuse of the drug, FDA said that the drug will only be available through a restricted distribution system, under a Risk Evaluation and Mitigation Strategy (REMS). Patients will self-administer (S)-ketamine under the supervision of a health care provider in a certified doctor's office or clinic; the nasal spray cannot be taken home (FDA, 2019). Given the lack of adverse side effects of (R)-ketamine, it is possible that patients may take (R)-ketamine to their home.

In conclusion, this study suggests that the order of potency for antidepressant effects in a CSDS model after a single intranasal administration is (R)-ketamine > (R,S)-ketamine > (S)-ketamine. In contrast, the order of potency for side effects in mice after intranasal administration is (S)-ketamine > (R,S)-ketamine > (R)-ketamine. Therefore, it is likely that (R)-ketamine could be a safer antidepressant without side effects than (R,S)-ketamine and (S)-ketamine.

Acknowledgements

This study was supported by AMED, Japan (to K.H., JP19dm0107119). Dr. Lijia Chang was supported by the Japan China Sasakawa Medical Fellowship (Tokyo, Japan). Dr. Zhongwei Xiong (Wuhan University, China) was supported by the China Scholarship Council (China).

Conflict of interest

Dr. Hashimoto is an inventor on a filed patent application on "The use of (R)-ketamine in the treatment of psychiatric diseases" by Chiba University. Dr. Hashimoto has received research support from Daiinippon-Sumitomo, Otsuka, and Taisho. Other authors declare no conflict of interest.

References

- Abdallah, C.G., Sanacora, G., Duman, R.S., Krystal, J.H., 2018. The neurobiology of depression, ketamine and rapid-acting antidepressants: is it glutamate inhibition or activation? *Pharmacol. Ther.* 190, 148–158.
- Berman, R.M., Cappiello, A., Anand, A., Oren, D.A., Heninger, G.R., Charney, D.S., Krystal, J.H., 2000. Antidepressant effects of ketamine in depressed patients. *Biol. Psychiatry* 47, 351–354.
- Chaki, S., 2017a. Beyond ketamine: new approaches to the development of safer antidepressants. *Curr. Neuropharmacol.* 15, 963–976.
- Chaki, S., 2017b. mGlu_{2/3} receptor antagonists as novel antidepressants. *Trends Pharmacol. Sci.* 38, 569–580.
- Chang, L., Zhang, K., Pu, Y., Qu, Y., Wang, S.M., Xiong, Z., Shirayama, Y., Hashimoto, K., 2019. Lack of dopamine D₁ receptors in the antidepressant actions of (R)-ketamine in a chronic social defeat stress model. *Eur. Arch. Psychiatry Clin. Neurosci.* <https://doi.org/10.1007/s00406-019-01012-1>. 2019 Mar 29.
- Domino, E.F., 2010. Taming the ketamine tiger. 1965. *Anesthesiology* 113, 678–684.
- Dong, C., Zhang, J.C., Yao, W., Ren, Q., Ma, M., Yang, C., Chaki, S., Hashimoto, K., 2017. Rapid and sustained antidepressant action of the mGlu_{2/3} receptor antagonist MGS0039 in the social defeat stress model: comparison with ketamine. *Int. J. Neuropsychopharmacol.* 20, 228–236.
- Duman, R.S., 2018. Ketamine and rapid-acting antidepressants: a new era in the battle against depression and suicide. *F1000Res.* 7 (pii: F1000 Faculty Rev-659).
- Ebert, B., Mikkelsen, S., Thorkildsen, C., Borgbjerg, F.M., 1997. Norketamine, the main metabolite of ketamine, is a non-competitive NMDA receptor antagonist in the rat cortex and spinal cord. *Eur. J. Pharmacol.* 333, 99–104.
- FDA News Release on March 5, 2019. FDA Approves New Nasal Spray Medication for Treatment-resistant Depression; Available Only at a Certified Doctor's Office or Clinic. <https://www.fda.gov/NewsEvents/Newsroom/PressAnnouncements/ucm632761.htm>.
- Fukumoto, K., Toki, H., Iijima, M., Hashihayata, T., Yamaguchi, J.I., Hashimoto, K., Chaki, S., 2017. Antidepressant potential of (R)-ketamine in rodent models: comparison with (S)-ketamine. *J. Pharmacol. Exp. Ther.* 361, 9–16.
- Golden, S.A., Covington III, H.E., Berton, O., Russo, S.J., 2011. A standardized protocol for repeated social defeat stress in mice. *Nat. Protoc.* 6, 1183–1191.
- Gould, T.D., Zarate Jr., C.A., Thompson, S.M., 2019. Molecular pharmacology and neurobiology of rapid-acting antidepressants. *Annu. Rev. Pharmacol. Toxicol.* 59, 213–236.
- Grunebaum, M.F., Galfalvy, H.C., Choo, T.H., Keilp, J.G., Moitra, V.K., Parris, M.S., Marver, J.E., Burke, A.K., Milak, M.S., Sublette, M.E., Oquendo, M.A., Mann, J.J., 2018. Ketamine for rapid reduction of suicidal thoughts in major depression: a midazolam-controlled randomized clinical trial. *Am. J. Psychiatry* 175, 327–335.
- Halberstadt, A.L., Slepak, N., Hyun, J., Buell, M.R., Powell, S.B., 2016. The novel ketamine analog methoxetamine produces dissociative-like behavioral effects in rodents. *Psychopharmacology* 233, 1215–1225.
- Hashimoto, K., 2014. The R-stereoisomer of ketamine as an alternative for ketamine for treatment-resistant major depression. *Clin. Psychopharmacol. Neurosci.* 12, 72–73.
- Hashimoto, K., 2016a. R-ketamine: a rapid-onset and sustained antidepressant without risk of brain toxicity. *Psychol. Med.* 46, 2449–2451.
- Hashimoto, K., 2016b. Ketamine's antidepressant action: beyond NMDA receptor inhibition. *Expert Opin. Ther. Targets* 20, 1389–1392.
- Hashimoto, K., 2016c. Detrimental side effects of repeated ketamine infusions in the brain. *Am. J. Psychiatry* 173, 1044–1045.
- Hashimoto, K., Kakiuchi, T., Ohba, H., Nishiyama, S., Tsukada, H., 2017. Reduction of dopamine D_{2/3} receptor binding in the striatum after a single administration of es-ketamine, but not R-ketamine: a PET study in conscious monkeys. *Eur. Arch. Psychiatry Clin. Neurosci.* 267, 173–176.
- Kishimoto, T., Chawla, J.M., Hagi, K., Zarate, C.A., Kane, J.M., Bauer, M., Correll, C.U., 2016. Single-dose infusion ketamine and non-ketamine N-methyl-D-aspartate receptor antagonists for unipolar and bipolar depression: a meta-analysis of efficacy, safety and time trajectories. *Psychol. Med.* 46, 1459–1472.
- Krystal, J.H., Abdallah, C.G., Sanacora, G., Charney, D.S., Duman, R.S., 2019. Ketamine: a paradigm shift for depression research and treatment. *Neuron* 101, 774–778.
- Larkin, G.L., Beautrais, A.L., 2011. A preliminary naturalistic study of low-dose ketamine

- for depression and suicide ideation in the emergency department. *Int. J. Neuropsychopharmacol.* 14, 1127–1131.
- Li, L., Vlisides, P.E., 2016. Ketamine: 50 years of modulating the mind. *Front. Hum. Neurosci.* 10, 612.
- Mathisen, L.C., Skjelbred, P., Skoglund, L.A., Oye, I., 1995. Effect of ketamine, an NMDA receptor inhibitor, in acute and chronic orofacial pain. *Pain* 61, 215–220.
- Matsuura, A., Fujita, Y., Iyo, M., Hashimoto, K., 2015. Effects of sodium benzoate on pre-ulse inhibition deficits and hyperlocomotion in mice after administration of phen-cyclidine. *Acta. Neuropsychiatr.* 27, 159–167.
- Monteggia, L.M., Zarate Jr., C., 2015. Antidepressant actions of ketamine: from molecular mechanisms to clinical practice. *Curr. Opin. Neurobiol.* 30, 139–143.
- Murrough, J.W., Iosifescu, D.V., Chang, L.C., Al Jurdi, R.K., Green, C.E., Perez, A.M., Iqbal, S., Pillemer, S., Foulkes, A., Shah, A., Charney, D.S., Mathew, S.J., 2013. Antidepressant efficacy of ketamine in treatment-resistant major depression: a two-site randomized controlled trial. *Am. J. Psychiatry* 170, 1134–1142.
- Murrough, J.W., Soleimani, L., DeWilde, K.E., Collins, K.A., Lapidus, K.A., Iacoviello, B.M., Lener, M., Kautz, M., Kim, J., Stern, J.B., Price, R.B., Perez, A.M., Brallier, J.W., Rodriguez, G.J., Goodman, W.K., Iosifescu, D.V., Charney, D.S., 2015. Ketamine for rapid reduction of suicidal ideation: a randomized controlled trial. *Psychol. Med.* 45, 3571–3580.
- Murrough, J.W., Abdallah, C.G., Mathew, S.J., 2017. Targeting glutamate signalling in depression: progress and prospects. *Nat. Rev. Drug Discov.* 16, 472–486.
- Newport, D.J., Carpenter, L.L., McDonald, W.M., Potash, J.B., Tohen, M., Nemeroff, C.B., 2015. APA council of research task force on novel biomarkers and treatments. Ketamine and other NMDA antagonists: early clinical trials and possible mechanisms in depression. *Am. J. Psychiatry* 172, 950–966.
- Oye, I., Paulsen, O., Maurset, A., 1992. Effects of ketamine on sensory perception: evidence for a role of *N*-methyl-*D*-aspartate receptors. *J. Pharmacol. Exp. Ther.* 260, 1209–1213.
- Peltoniemi, M.A., Hagelberg, N.M., Olkkola, K.T., Saari, T., 2016. Ketamine: a review of clinical pharmacokinetics and pharmacodynamics in anesthesia and pain therapy. *Clin. Pharmacokinet.* 55, 1059–1077.
- Price, R.B., Nock, M.K., Charney, D.S., Mathew, S.J., 2009. Effects of intravenous ketamine on explicit and implicit measures of suicidality in treatment-resistant depression. *Biol. Psychiatry* 66, 522–526.
- Reardon, S., 2018. ‘Party drug’ turned antidepressant approaches approval. *Nat. Rev. Drug Discov.* 17, 773–775.
- Ryder, S., Way, W.L., Trevor, A.J., 1978. Comparative pharmacology of the optical isomers of ketamine in mice. *Eur. J. Pharmacol.* 49, 15–23.
- Sanacora, G., Frye, M.A., McDonald, W., Mathew, S.J., Turner, M.S., Schatzberg, A.F., Summergrad, P., Nemeroff, C.B., American Psychiatric Association (APA) Council of Research Task Force on Novel Biomarkers and Treatments, 2017. A consensus statement on the use of ketamine in the treatment of mood disorders. *JAMA Psychiatry* 74, 399–405.
- Singh, I., Morgan, C., Curran, V., Nutt, D., Schlag, A., McShane, R., 2017. Ketamine treatment for depression: opportunities for clinical innovation and ethical foresight. *Lancet Psychiatry* 4, 419–426.
- Su, T.P., Chen, M.H., Li, C.T., Lin, W.C., Hong, C.J., Gueorguieva, R., Tu, P.C., Bai, Y.M., Cheng, C.M., Krystal, J.H., 2017. Dose-related effects of adjunctive ketamine in Taiwanese patients with treatment-resistant depression. *Neuropsychopharmacology* 42, 2482–2492.
- Tian, Z., Dong, C., Fujita, A., Fujita, Y., Hashimoto, K., 2018. Expression of heat shock protein HSP-70 in the retrosplenial cortex of rat brain after administration of (*R,S*)-ketamine and (*S*)-ketamine, but not (*R*)-ketamine. *Pharmacol. Biochem. Behav.* 172, 17–21.
- Vollenweider, F.X., Leenders, K.L., Oye, I., Hell, D., Angst, J., 1997. Differential psychopathology and patterns of cerebral glucose utilisation produced by (*S*)- and (*R*)-ketamine in healthy volunteers using positron emission tomography (PET). *Eur. Neuropsychopharmacol.* 7, 25–38.
- Wilkinson, S.T., Toprak, M., Turner, M.S., Levine, S.P., Katz, R.B., Sanacora, G., 2017. A survey of the clinical, off-label use of ketamine as a treatment for psychiatric disorders. *Am. J. Psychiatry* 174, 695–696.
- Wilkinson, S.T., Ballard, E.D., Bloch, M.H., Mathew, S.J., Murrough, J.W., Feder, A., Sos, P., Wang, G., Zarate Jr., C.A., Sanacora, G., 2018. The effect of a single dose of intravenous ketamine on suicidal ideation: a systematic review and individual participant data meta-analysis. *Am. J. Psychiatry* 175, 150–158.
- Xiong, Z., Zhang, K., Ishima, T., Ren, Q., Chang, L., Chen, J., Hashimoto, K., 2018a. Comparison of rapid and long-lasting antidepressant effects of negative modulators of $\alpha 5$ -containing GABA_A receptors and (*R*)-ketamine in a chronic social defeat stress model. *Pharmacol. Biochem. Behav.* 175, 139–145.
- Xiong, Z., Zhang, K., Ishima, T., Ren, Q., Ma, M., Pu, Y., Chang, L., Chen, J., Hashimoto, K., 2018b. Lack of rapid antidepressant effects of Kir4.1 channel inhibitors in a chronic social defeat stress model: comparison with (*R*)-ketamine. *Pharmacol. Biochem. Behav.* 176, 57–62.
- Xu, Y., Hackett, M., Carter, G., Loo, C., Gálvez, V., Glozier, N., Glue, P., Lapidus, K., McGirr, A., Somogyi, A.A., Mitchell, P.B., Rodgers, A., 2016. Effects of low-dose and very low-dose ketamine among patients with major depression: a systematic review and meta-analysis. *Int. J. Neuropsychopharmacol.* 19 (pii: pyv124).
- Yang, C., Shirayama, Y., Zhang, J.C., Ren, Q., Yao, W., Ma, M., Dong, C., Hashimoto, K., 2015. *R*-ketamine: a rapid-onset and sustained antidepressant without psychotomimetic side effects. *Transl. Psychiatry* 5, e632.
- Yang, C., Han, M., Zhang, J.C., Ren, Q., Hashimoto, K., 2016. Loss of parvalbumin-immunoreactivity in mouse brain regions after repeated intermittent administration of esketamine, but not *R*-ketamine. *Psychiatric Res.* 239, 281–283.
- Yang, C., Qu, Y., Abe, M., Nozawa, D., Chaki, S., Hashimoto, K., 2017a. (*R*)-ketamine shows greater potency and longer lasting antidepressant effects than its metabolite (2*R,6R*)-hydroxynorketamine. *Biol. Psychiatry* 82, e43–e44.
- Yang, C., Qu, Y., Fujita, Y., Ren, Q., Ma, M., Dong, C., Hashimoto, K., 2017b. Possible role of the gut microbiota-brain axis in the antidepressant effects of (*R*)-ketamine in a social defeat stress model. *Transl. Psychiatry* 7, 1294.
- Yang, C., Ren, Q., Qu, Y., Zhang, J.C., Ma, M., Dong, C., Hashimoto, K., 2018a. Mechanistic target of rapamycin-independent antidepressant effects of (*R*)-ketamine in a social defeat stress model. *Biol. Psychiatry* 83, 18–28.
- Yang, C., Kobayashi, S., Nakao, K., Dong, C., Han, M., Qu, Y., Ren, Q., Zhang, J.C., Ma, M., Toki, H., Yamaguchi, J.I., Chaki, S., Shirayama, Y., Nakazawa, K., Manabe, T., Hashimoto, K., 2018b. AMPA receptor activation-independent antidepressant actions of ketamine metabolite (*S*)-norketamine. *Biol. Psychiatry* 84, 591–600.
- Zanos, P., Moaddel, R., Morris, P.J., Georgiou, P., Fischell, J., Elmer, G.I., Alkondon, M., Yuan, P., Pribut, H.J., Singh, N.S., Dossou, K.S., Fang, Y., Huang, X.P., Mayo, C.L., Wainer, I.W., Albuquerque, E.X., Thompson, S.M., Thomas, C.J., Zarate Jr., C.A., Gould, T.D., 2016. NMDAR inhibition-independent antidepressant actions of ketamine metabolites. *Nature* 533, 481–486.
- Zanos, P., Moaddel, R., Morris, P.J., Riggs, L.M., Highland, J.N., Georgiou, P., Pereira, E.F.R., Albuquerque, E.X., Thomas, C.J., Zarate Jr., C.A., Gould, T.D., 2018. Ketamine and ketamine metabolite pharmacology: insights into therapeutic mechanisms. *Pharmacol. Rev.* 70, 621–660.
- Zarate, C.A., Singh, J.B., Carlson, P.J., Brutsche, N.E., Ameli, R., Luckenbaugh, D.A., Charney, D.S., Manji, H.K., 2006. A randomized trial of an *N*-methyl-*D*-aspartate antagonist in treatment-resistant major depression. *Arch. Gen. Psychiatry* 63, 856–864.
- Zhang, J.C., Li, S.X., Hashimoto, K., 2014. *R*(–)-ketamine shows greater potency and longer lasting antidepressant effects than *S*(+)-ketamine. *Pharmacol. Biochem. Behav.* 116, 137–141.
- Zhang, J.C., Yao, W., Dong, C., Yang, C., Ren, Q., Ma, M., Han, M., Hashimoto, K., 2015. Comparison of ketamine, 7,8-dihydroxyflavone, and ANA-12 antidepressant effects in the social defeat stress model of depression. *Psychopharmacology* 232, 4325–4335.
- Zhang, K., Hashimoto, K., 2019a. An update on ketamine and its two enantiomers as rapid-acting antidepressants. *Expert Rev. Neurother.* 19, 83–92.
- Zhang, K., Hashimoto, K., 2019b. Lack of opioid system in the antidepressant actions of ketamine. *Biol. Psychiatry* 85, e25–e27.
- Zhang, K., Toki, H., Fujita, Y., Ma, M., Chang, L., Qu, Y., Harada, S., Nemoto, T., Mizuno-Yasuhira, A., Yamaguchi, J.I., Chaki, S., Hashimoto, K., 2018. Lack of deuterium isotope effects in the antidepressant effects of (*R*)-ketamine in a chronic social defeat stress model. *Psychopharmacology* 235, 3177–3185.
- Zhu, W., Ding, Z., Zhang, Y., Shi, J., Hashimoto, K., Lu, L., 2016. Risks associated with misuse of ketamine as a rapid-acting antidepressant. *Neurosci. Bull.* 32, 557–564.



Lack of dopamine D₁ receptors in the antidepressant actions of (*R*)-ketamine in a chronic social defeat stress model

Lijia Chang¹ · Kai Zhang¹ · Yaoyu Pu¹ · Youge Qu¹ · Si-ming Wang¹ · Zhongwei Xiong¹ · Yukihiko Shirayama^{1,2} · Kenji Hashimoto¹

Received: 17 February 2019 / Accepted: 26 March 2019 / Published online: 29 March 2019
© Springer-Verlag GmbH Germany, part of Springer Nature 2019

Abstract

It is reported that dopamine D₁ receptors in the medial prefrontal cortex play a role in the antidepressant actions of (*R,S*)-ketamine. However, its role in the antidepressant actions of (*R*)-ketamine, which is more potent than (*S*)-ketamine, is unknown. In the locomotion test, tail suspension test, forced swimming test and 1% sucrose preference test, pretreatment with dopamine D₁ receptor antagonist SCH-23390 did not block the antidepressant effects of (*R*)-ketamine in the susceptible mice after chronic social defeat stress. These findings suggest that dopamine D₁ receptors may not play a major role in the antidepressant actions of (*R*)-ketamine.

Keywords Antidepressant · (*R*)-ketamine · Dopamine D₁ receptor · Social defeat stress

Introduction

The *N*-methyl-D-aspartate receptor (NMDAR) antagonist (*R,S*)-ketamine exhibits rapid and sustained antidepressant effects in treatment-resistant patients with major depressive disorder [1–3]. (*R,S*)-ketamine is a racemic mixture containing equal parts of (*R*)-ketamine (or arketamine) and (*S*)-ketamine (or esketamine). (*R,S*)-ketamine (K_i = 0.53 μM for NMDAR) is a racemic mixture containing equal parts of (*R*)-ketamine (or arketamine) (K_i = 1.4 μM for NMDAR) and (*S*)-ketamine (or esketamine) (K_i = 0.30 μM for NMDAR) [4]. Interestingly, (*R*)-ketamine shows greater potency and longer-lasting antidepressant effects than (*S*)-ketamine in rodents with depression-like phenotype [5–11]. Thus, it is suggested that NMDAR may not play a major role in the antidepressant effects of (*R*)-ketamine [12]. Importantly, side effects of (*R*)-ketamine are less potent than (*S*)-ketamine [7, 13–15]. Collectively, (*R*)-ketamine may be a safer antidepressant in humans than (*R,S*)-ketamine and (*S*)-ketamine.

However, the precise mechanisms underlying the antidepressant actions of (*R*)-ketamine remain unknown.

Preclinical studies suggest that medial prefrontal cortex (mPFC) plays a role in the antidepressant effects of (*R,S*)-ketamine [or (*R*)-ketamine] in rats with or without depression-like phenotype [16, 17]. A recent study demonstrated that disruption of dopamine D₁ receptor encoded by the *Drd1* in the mPFC blocked the rapid antidepressant effects of (*R,S*)-ketamine in control mice [18], suggesting that *Drd1* cells, and activation of dopamine D₁ receptors in the mPFC, are necessary for the rapid antidepressant actions of (*R,S*)-ketamine. In contrast, Li et al. [19] reported that dopamine D₁ receptor antagonist SCH-23390 did not block the antidepressant-like effects of ketamine in control mice, inconsistent with the report from Hare et al. [18]. Importantly, these two reports did not use rodents with depression-like phenotype [20]. At present, the role of dopamine D₁ receptors in the antidepressant effects of (*R*)-ketamine in animal models of depression such as a chronic social defeat stress (CSDS) model has not been reported.

This study was undertaken to examine whether the pretreatment of dopamine D₁ receptor antagonist SCH-23390 could influence the antidepressant effects of (*R*)-ketamine in a CSDS model.

✉ Kenji Hashimoto
hashimoto@faculty.chiba-u.jp

¹ Division of Clinical Neuroscience, Chiba University Center for Forensic Mental Health, Chiba 260-8670, Japan

² Department of Psychiatry, Teikyo University Chiba Medical Center, Ichihara 299-0111, Japan

Methods and materials

Animals

Male adult C57BL/6 mice ($n = 60$), aged 8 weeks (body weight 20–25 g, Japan SLC, Inc., Hamamatsu, Japan) and male adult CD1 (ICR) mice ($n = 20$), aged 13–15 weeks (body weight > 40 g, Japan SLC, Inc., Hamamatsu, Japan) were used. Animals were housed under controlled temperatures and 12 h light/dark cycles (lights on between 07:00 and 19:00 h), with ad libitum food (CE-2; CLEA Japan, Inc., Tokyo, Japan) and water. The protocol was approved by the Chiba University Institutional Animal Care and Use Committee (Permission number: 30-385). This study was carried out in strict accordance with the recommendations in the Guide for the Care and Use of Laboratory Animals of the National Institutes of Health, USA. Animals were deeply anaesthetized with isoflurane before being killed by cervical dislocation. All efforts were made to minimize suffering.

Materials

(*R*)-ketamine hydrochloride was prepared as described previously [6]. The dose (10 mg/kg as hydrochloride) of (*R*)-ketamine dissolved in the saline was used as previously reported [7–11, 21]. The dose of SCH-23390 hydrochloride (0.1 mg/kg, Sigma-Aldrich Co., St Louis, MO, USA) was used as previously reported [19].

Chronic social defeat stress (CSDS) model, treatment and behavioral tests

The procedure of CSDS and behavioral tests were performed as previously reported [7–11, 21]. The CSDS susceptible mice were divided to four groups; saline + saline group,

saline + (*R*)-ketamine group, SCH-23390 + (*R*)-ketamine group, SCH-23390 + saline group. Saline or SCH-23390 was administered intraperitoneally (i.p.) into the susceptible mice 30 min before single i.p. administration of saline or (*R*)-ketamine (day 12). Control (no CSDS) mice received saline + saline. Behavioral tests, including locomotion test (LMT), tail suspension test (TST), forced swimming test (FST) and 1% sucrose preference test (SPT), were performed. LMT and TST were performed 2 and 4 h after a single injection of (*R*)-ketamine or saline, respectively. FST was performed 24 h after a single injection of (*R*)-ketamine or saline. SPT was performed 2 and 4 days after a single injection of (*R*)-ketamine or saline (Fig. 1).

Statistical analysis

The data show as the mean \pm standard error of mean (S.E.M.). Analysis was performed using PASW Statistics 20 (Tokyo, Japan). The behavioral data were analyzed using the one-way analysis of variance (ANOVA), followed by post hoc Tukey test. The *P* values of less than 0.05 were considered statistically significant.

Results

Effects of SCH-23390 in the antidepressant effect of (*R*)-ketamine in a CSDS model

Locomotion showed no difference ($F_{4,44} = 1.094$, $P = 0.371$) among the five groups (Fig. 2a). One-way ANOVA of TST and FST data showed a statistical significance (TST: $F_{4,44} = 12.08$, $P < 0.001$, FST: $F_{4,44} = 22.58$, $P < 0.001$) among the five groups (Fig. 2b, c). Post-hoc tests showed that (*R*)-ketamine (10 mg/kg) significantly

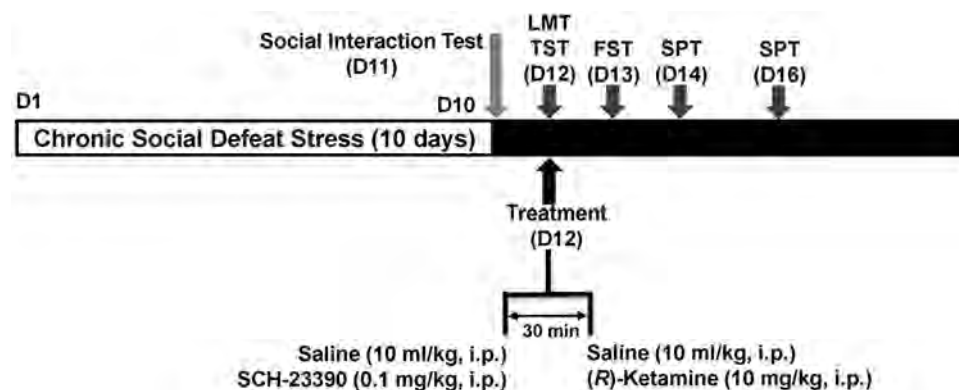


Fig. 1 Schedule of CSDS, treatment, and behavioral tests. CSDS was performed from day 1 to day 10, and the social interaction test (SIT) was performed on day 11. Saline (10 ml/kg) or SCH-23390 (0.1 mg/kg) was administered i.p. in the susceptible mice on day 12. Saline (10 ml/kg) or (*R*)-ketamine (10 mg/kg) was administered i.p. into

mice 30 min after administration of saline or SCH-23390. LMT and TST were performed 2 and 4 h after a single injection of (*R*)-ketamine or saline, respectively. SPT was performed 2 and 4 days after a single injection of (*R*)-ketamine or saline

attenuated the increased immobility times of TST and FST in susceptible mice after CSDS (Fig. 2b, c). However, there were no differences between saline + (*R*)-ketamine group and SCH-23390 + (*R*)-ketamine group in the immobility times of TST and FST (Fig. 2b, c). Furthermore, there were no differences between saline + saline group and SCH-23390 + saline group in the immobility times of TST and FST in the susceptible mice (Fig. 2b, c).

One-way ANOVA of SPT data showed statistical significances (2 days after a single injection: $F_{4,44} = 7.561$, $P < 0.001$, 4 days after a single injection: $F_{4,44} = 20.36$, $P < 0.001$) among five groups (Fig. 2d, e). Post-hoc tests showed that sucrose preference of saline + (*R*)-ketamine group was significantly higher from saline + saline group (Fig. 2d, e). Furthermore, sucrose preference of saline + (*R*)-ketamine group was not different from SCH-23390 + (*R*)-ketamine group (Fig. 2d, e). Moreover, sucrose preference of saline + saline group was not different from SCH-23390 + saline group (Fig. 2d, e).

Discussion

We demonstrated that pretreatment with SCH-23390 did not block the antidepressant effects of (*R*)-ketamine in the susceptible mice after CSDS, suggesting that dopamine D_1 receptors do not play a major role in the antidepressant actions of (*R*)-ketamine.

It is reported that pretreatment with haloperidol (0.15 mg/kg, a nonselective dopamine $D_{2/3}$ receptor antagonist), but not SCH-23390 (0.04 and 0.1 mg/kg, a selective dopamine D_1 receptor antagonist), significantly prevented the antidepressant-like effects of (*R,S*)-ketamine (20 mg/kg) in control mice [19]. Moreover, administration of (*R,S*)-ketamine (10 mg/kg) in combination with pramipexole (0.3 mg/kg, a dopamine $D_{2/3}$ receptor agonist) exerted antidepressant-like effects compared with each drug alone [19]. These results suggest that dopamine $D_{2/3}$ receptors, but not D_1 receptors, are involved in the antidepressant-like effects of ketamine in control mice [19]. In contrast, bilateral infusion (10 min before) of a selective dopamine D_1 receptor antagonist SCH-39166 into the mPFC completely

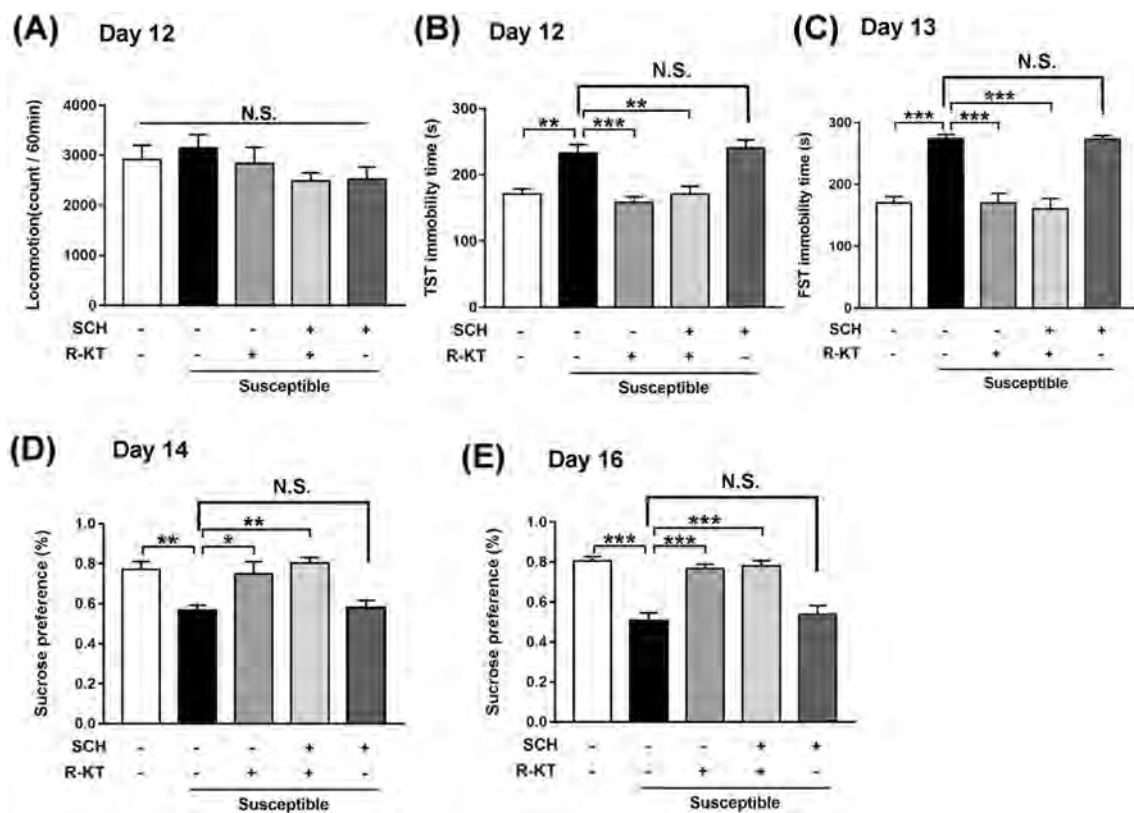


Fig. 2 Effects of SCH-23390 in the antidepressant effects of (*R*)-ketamine in a CSDS model. **a** LMT (day 12). **b** TST (day 12). **c** FST (day 13). **d** SPT (day 14) and **e** SPT (day 16). The values represent the mean \pm S.E.M. ($n = 9$ or 10). * $P < 0.05$, ** $P < 0.01$, *** $P < 0.001$.

N.S. not significance, LMT locomotion test, TST tail suspension test, FST forced swimming test, R-KT (*R*)-ketamine, SCH SCH-23390, SPT 1% sucrose preference test

blocked the antidepressant-like effects of (*R,S*)-ketamine in control mice [18]. In addition, infusion of a selective dopamine D₁ receptor agonist SKF-81297 into the mPFC decreased the immobility time of FST in the control mice 24 h after a single dose, suggesting antidepressant-like effects of SKF-81297 in mice [18]. This paper suggests that activation at dopamine D₁ receptors in the mPFC may contribute to ketamine's antidepressant-like effects [18]. Although the reasons underlying these discrepancies remain unclear, variations in the experimental conditions may contribute to these discrepancies. One possibility is the difference in the route of administration (systemic administration of (*R*)-ketamine vs. direct infusion of (*R,S*)-ketamine into the mPFC). Another possibility is the use of rodents with or without depression-like phenotype. Very interestingly, healthy control subjects exhibited modest, but significant, increases in depressive symptoms for up to 1 day after a single ketamine infusion [22], suggesting that ketamine does not induce antidepressant-like effects in healthy control subjects. Collectively, the use of rodents with or without depression-like phenotypes may contribute to these discrepancies [20]. Therefore, further detailed study using rodents with depression-like phenotype is needed to confirm the role of dopamine D₁ receptors in the antidepressant effects of ketamine and its enantiomers.

A high dose (30 mg/kg) of ketamine rapidly increases extracellular dopamine in the mPFC of rats [23], suggesting that ketamine-induced dopamine release may play a role in ketamine's actions such as antidepressant effects [18]. A recent study demonstrated that (*S*)-ketamine caused a robust increase in dopamine release in the PFC compared with (*R*)-ketamine [24]. If ketamine-induced dopamine release in the PFC plays a key role in the antidepressant effects of ketamine, (*S*)-ketamine must be more potent than (*R*)-ketamine in animal models of depression. Nonetheless, further detailed study underlying the role of dopamine D₁ receptors in the antidepressant effects of ketamine and its enantiomers is needed.

In conclusion, this study showed that pretreatment with SCH-23390 did not block the acute and long-lasting antidepressant effects of (*R*)-ketamine in a CSDS model. Therefore, it is unlikely that dopamine D₁ receptors play a major role in the antidepressant actions of (*R*)-ketamine although this may, in part, contribute to its other pharmacological actions.

Acknowledgements This study was supported by AMED (to K.H., JP18dm0107119). Dr. Hashimoto is an inventor on a filed patent application on "The use of (*R*)-ketamine in the treatment of psychiatric diseases" by Chiba University. Dr. Hashimoto has received research support from Dainippon-Sumitomo, Otsuka, and Taisho.

Compliance with ethical standards

Conflict of interest All authors declare that they have no conflict of interest.

References

- Newport DJ, Carpenter LL, McDonald WM, Potash JB, Tohen M, Nemeroff CB (2015) Ketamine and other NMDA antagonists: early clinical trials and possible mechanisms in depression. *Am J Psychiatry* 172(10):950–966
- Kishimoto T, Chawla JM, Hagi K, Zarate CA, Kane JM, Bauer M, Correll CU (2016) Single-dose infusion ketamine and non-ketamine *N*-methyl-*D*-aspartate receptor antagonists for unipolar and bipolar depression: a meta-analysis of efficacy, safety and time trajectories. *Psychol Med* 46(7):1459–1472
- Zhang K, Hashimoto K (2019) An update on ketamine and its two enantiomers as rapid-acting antidepressants. *Expert Rev Neurother* 19(1):83–92
- Ebert B, Mikkelsen S, Thorkildsen C, Borgbjerg FM (1997) Nor-ketamine, the main metabolite of ketamine, is a non-competitive NMDA receptor antagonist in the rat cortex and spinal cord. *Eur J Pharmacol* 333(1):99–104
- Fukumoto K, Toki H, Iijima M, Hashihayata T, J-i Yamaguchi, Hashimoto K, Chaki S (2017) Antidepressant potential of (*R*)-ketamine in rodent models: comparison with (*S*)-ketamine. *J Pharmacol Exp Ther* 36(1):9–16
- Zhang JC, Li SX, Hashimoto K (2014) *R*(-)-ketamine shows greater potency and longer lasting antidepressant effects than *S*(+)-ketamine. *Pharmacol Biochem Behav* 116:137–141
- Yang C, Shirayama Y, Jc Zhang, Ren Q, Yao W, Ma M, Dong C, Hashimoto K (2015) *R*-ketamine: a rapid-onset and sustained antidepressant without psychotomimetic side effects. *Transl Psychiatry* 5:e632
- Yang C, Qu Y, Abe M, Nozawa D, Chaki S, Hashimoto K (2017) (*R*)-ketamine shows greater potency and longer lasting antidepressant effects than its metabolite (2*R*,6*R*)-hydroxynorketamine. *Biol Psychiatry* 82(5):e43–e44
- Yang C, Qu Y, Fujita Y, Ren Q, Ma M, Dong C, Hashimoto K (2017) Possible role of the gut microbiota-brain axis in the antidepressant effects of (*R*)-ketamine in a social defeat stress model. *Transl Psychiatry* 7(12):1294
- Yang C, Ren Q, Qu Y, Zhang J-C, Ma M, Dong C, Hashimoto K (2018) Mechanistic target of rapamycin-independent antidepressant effects of (*R*)-ketamine in a social defeat stress model. *Biol Psychiatry* 83(1):18–28
- Zhang K, Ma M, Dong C, Hashimoto K (2018) Role of inflammatory bone markers in the antidepressant actions of (*R*)-ketamine in a chronic social defeat stress model. *Int J Neuropsychopharmacol* 21(11):1025–1030
- Hashimoto K (2016) Letter to the Editor: *R*-ketamine: a rapid-onset and sustained antidepressant without risk of brain toxicity. *Psychol Med* 46(11):2449–2451
- Yang C, Han M, J-c Zhang, Ren Q, Hashimoto K (2016) Loss of parvalbumin-immunoreactivity in mouse brain regions after repeated intermittent administration of esketamine, but not *R*-ketamine. *Psychiatry Res* 239:281–283
- Hashimoto K, Kakiuchi T, Ohba H, Nishiyama S, Tsukada H (2017) Reduction of dopamine D_{2/3} receptor binding in the striatum after a single administration of esketamine, but not *R*-ketamine: a PET study in conscious monkeys. *Eur Arch Psychiatry Clin Neurosci* 267(2):173–176

15. Tian Z, Dong C, Fujita A, Fujita Y, Hashimoto K (2018) Expression of heat shock protein HSP-70 in the retrosplenial cortex of rat brain after administration of (R, S)-ketamine and (S)-ketamine, but not (R)-ketamine. *Pharmacol Biochem Behav* 172:17–21
16. Fuchikami M, Thomas A, Liu R, Wohleb ES, Land BB, DiLeone RJ, Aghajanian GK, Duman RS (2015) Optogenetic stimulation of infralimbic PFC reproduces ketamine's rapid and sustained antidepressant actions. *Proc Natl Acad Sci USA* 112(26):8106–8111
17. Shirayama Y, Hashimoto K (2017) Effects of a single bilateral infusion of *R*-ketamine in the rat brain regions of a learned helplessness model of depression. *Eur Arch Psychiatry Clin Neurosci* 267(2):177–182
18. Hare BD, Shinohara R, Liu RJ, Pothula S, DiLeone RJ, Duman RS (2019) Optogenetic stimulation of medial prefrontal cortex *Drd1* neurons produces rapid and long-lasting antidepressant effects. *Nat Commun* 10(1):223
19. Li Y, Zhu ZR, Ou BC, Wang YQ, Tan ZB, Deng CM, Gao YY, Tang M, So JH, Mu YL, Zhang LQ (2015) Dopamine D₂/D₃ but not dopamine D₁ receptors are involved in the rapid antidepressant-like effects of ketamine in the forced swim test. *Behav Brain Res* 279:100–105
20. Hashimoto K, Shirayama Y (2018) What are the causes for discrepancies of antidepressant actions of (2*R*,6*R*)-hydroxynorketamine? *Biol Psychiatry* 84(1):e7–e8
21. Chang L, Toki H, Qu Y, Fujita Y, Mizuno-Yasuhira A, Yamaguchi JI, Chaki S, Hashimoto K (2018) No sex-specific differences in the acute antidepressant actions of (*R*)-ketamine in an inflammation model. *Int J Neuropsychopharmacol* 21(10):932–937
22. Nugent AC, Ballard ED, Gould TD, Park LT, Moaddel R, Brutsche NE, Zarate CA Jr (2018) Ketamine has distinct electrophysiological and behavioral effects in depressed and healthy subjects. *Mol Psychiatry*. <https://doi.org/10.1038/s41380-018-0028-2>
23. Moghaddam B, Adams B, Verma A, Daly D (1997) Activation of glutamatergic neurotransmission by ketamine: a novel step in the pathway from NMDA receptor blockade to dopaminergic and cognitive disruptions associated with the prefrontal cortex. *J Neurosci* 17(8):2921–2927
24. Ago Y, Tanabe W, Higuchi M, Tsukada S, Hashimoto K, Hashimoto H (2018) (*R*)-ketamine, (*S*)-ketamine and their metabolites affect differentially in vivo monoamine release in the prefrontal cortex of mice: different involvement of AMPA receptor. Poster W-131 at 57th annual meeting of The American College of Neuropsychopharmacology, Hollywood, FL, 12 Dec 2018

Metadata of the chapter that will be visualized online

Chapter Title	Antidepressant Actions of Ketamine and Its Two Enantiomers	
Copyright Year	2020	
Copyright Holder	Springer Nature Singapore Pte Ltd.	
Author	Family Name	Chang
	Particle	
	Given Name	Lijia
	Suffix	
	Division	Division of Clinical Neuroscience
	Organization/University	Chiba University Center for Forensic Mental Health
	Address	Chiba, Japan
Author	Family Name	Wei
	Particle	
	Given Name	Yan
	Suffix	
	Division	Division of Clinical Neuroscience
	Organization/University	Chiba University Center for Forensic Mental Health
	Address	Chiba, Japan
Corresponding Author	Family Name	Hashimoto
	Particle	
	Given Name	Kenji
	Suffix	
	Division	Division of Clinical Neuroscience
	Organization/University	Chiba University Center for Forensic Mental Health
	Address	Chiba, Japan
	Email	hashimoto@faculty.chiba-u.jp

Abstract

The *N*-methyl-D-aspartate receptor antagonist ketamine has been widely used as an off-label medication to treat depression because it elicits rapid and robust antidepressant effects in treatment-resistant patients with depression. (*R,S*)-ketamine is a racemic mixture containing equal amounts of (*R*)-ketamine (or arketamine) and (*S*)-ketamine (or esketamine). On March 5, 2019, the United States Food and Drug Administration approved an (*S*)-ketamine nasal spray for treatment-resistant depression. In contrast, (*R*)-ketamine has been reported to have a greater potency and longer-lasting antidepressant effects than (*S*)-ketamine in rodent models of depression. However, the precise mechanisms underlying the robust antidepressant effects of ketamine enantiomers remain unknown. In this chapter, we discuss recent findings on the antidepressant actions of two enantiomers of ketamine.

Keywords (separated
by “ - ”)

Arketamine - Ketamine - Esketamine

Antidepressant Actions of Ketamine and Its Two Enantiomers

Lijia Chang, Yan Wei, and Kenji Hashimoto

Abstract The *N*-methyl-D-aspartate receptor antagonist ketamine has been widely used as an off-label medication to treat depression because it elicits rapid and robust antidepressant effects in treatment-resistant patients with depression. (*R,S*)-ketamine is a racemic mixture containing equal amounts of (*R*)-ketamine (or arketamine) and (*S*)-ketamine (or esketamine). On March 5, 2019, the United States Food and Drug Administration approved an (*S*)-ketamine nasal spray for treatment-resistant depression. In contrast, (*R*)-ketamine has been reported to have a greater potency and longer-lasting antidepressant effects than (*S*)-ketamine in rodent models of depression. However, the precise mechanisms underlying the robust antidepressant effects of ketamine enantiomers remain unknown. In this chapter, we discuss recent findings on the antidepressant actions of two enantiomers of ketamine.

Keywords Arketamine · Ketamine · Esketamine

1 Introduction

Ketamine is a noncompetitive *N*-methyl-D-aspartate receptor (NMDAR) antagonist that has drawn significant attention in recent decades from scientists all over the world because of its robust antidepressant effects (Cusin 2019; Duman 2018; Hashimoto 2016b, 2017, 2019). Ketamine was first synthesized at Parke-Davis (Detroit, MI, USA) by Calvin Lee Stevens in 1962, with a study of ketamine's dissociative anesthetic effects in the prison population quickly following in 1964 (Cohen et al. 2018; Domino 2010; Li and Vlisides 2016). Afterward, ketamine's

L. Chang · K. Hashimoto (✉)

Division of Clinical Neuroscience, Chiba University Center for Forensic Mental Health,
Chiba, Japan

e-mail: hashimoto@faculty.chiba-u.jp

Y. Wei

Division of Clinical Neuroscience, Chiba University Center for Forensic Mental Health,
Chiba, Japan

Institute of Cardiovascular Research, Southwest Medical University, Luzhou, Sichuan, China

© Springer Nature Singapore Pte Ltd. 2020

K. Hashimoto et al. (eds.), *Ketamine*,

https://doi.org/10.1007/978-981-15-2902-3_7

anesthetic effects were subsequently confirmed by other investigators, and the drug began to be employed as an anesthetic in humans and animals in 1966 (Domino 2010; Stevenson 2005). In view of ketamine's unique pharmacological properties of pain relief and sedation (Gao et al. 2016), it was approved formally for use by the United States (US) Food and Drug Administration (FDA) in 1970 and was placed by the World Health Organization (WHO) in 1985 onto an essential medicines list as an intravenous anesthetic (Gowda et al. 2016; WHO 2011).

Berman et al. (2000) first conducted a placebo-controlled study of ketamine application in eight patients with major depressive disorder (MDD), who were given a dosage of 0.5 mg/kg over 40 min; their depressive symptoms significantly improved within 3 days, while feelings of perceptual disturbances or euphoria occurred in the same patients after treatment (Berman et al. 2000). More generally, in these individuals, the drug produced rapid-acting and sustained antidepressant effects although psychotomimetic effects were also reported after a single infusion of ketamine (Berman et al. 2000). Subsequent studies replicated the noted robust antidepressant effects of ketamine in treatment-resistant patients with MDD and bipolar disorder (BD) (Zarate et al. 2006; Newport et al. 2015; Kishimoto et al. 2016).

Despite ketamine's powerful antidepressant effects in humans, there are some potential drawbacks that cannot be neglected. When used as an anesthetic for anesthesia in surgical procedures, acute and chronic pain management, and critical care (Kurdi et al. 2014), side effects such as hallucinations, agitation, confusion, and psychotomimetic effects resembling schizophrenia can follow (Domino 2010; Gao et al. 2016; Krystal et al. 1994; Kurdi et al. 2014). For some patients, ketamine also brings about cognitive impairments (Molero et al. 2018; Szlachta et al. 2017), urinary tract inflammation (Sihra et al. 2018), liver enzyme abnormalities (Zhao et al. 2018), and other symptoms such as an increase in the heart rate or blood pressure (Sheth et al. 2018). Further, considering the effects reported during recreational usage or the euphoric "dissociated" state caused by higher doses, there exists a potential for abuse no matter what the drug's original intended purpose in a situation is (Heal et al. 2018; Ivan Ezquerra-Romano et al. 2018; Liao et al. 2017; Morgan and Curran 2012; Tracy et al. 2017). At present, however, there are no superior

AU4

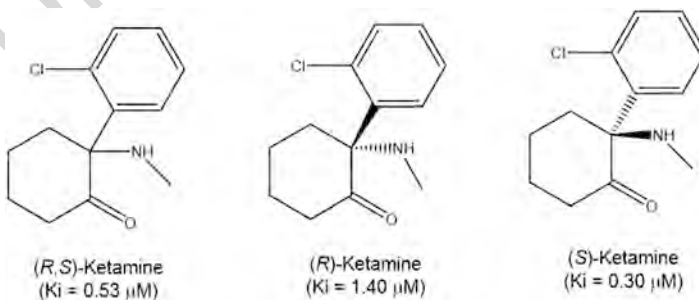


Fig. 1 Chemical structure of ketamine and its two enantiomers. The values in the parenthesis are the K_i value for the NMDAR (Hashimoto 2019)

antidepressants to ketamine that show robust antidepressant effects in patients with MDD (Duman 2018).

Ketamine is a racemic mixture containing equal amounts of (*R*)-ketamine (or arketamine) and (*S*)-ketamine (or esketamine) (Fig. 1) (Domino 2010). Different affinities and potencies of these two ketamine enantiomers exist. (*S*)-ketamine has about a three- to fourfold greater affinity for the NMDAR as compared with (*R*)-ketamine (Fig. 1). Conversely, (*S*)-ketamine holds approximately a three- to fourfold greater anesthetic potency and shows greater undesirable psychotomimetic side effects in comparison with (*R*)-ketamine (Domino 2010; Hashimoto 2016b, c). In prior research, (*R*)-ketamine showed a greater degree of potency and longer-lasting antidepressant effects than (*S*)-ketamine in several rodents model of depression (Fukumoto et al. 2017; Yang et al. 2015, 2018a; Zhang et al. 2014), and (*R*)-ketamine also did not present side effects on psychotomimetic actions or abuse liability in contrast with (*S*)-ketamine (Chang et al. 2019a; Yang et al. 2015). Third, (*R*)-ketamine is expected to constitute a safer choice than either (*R,S*)-ketamine or (*S*)-ketamine in consideration of its antidepressant actions (Chang et al. 2019a; Hashimoto 2016b, c). However, the precise molecular and cellular mechanisms underlying ketamine's antidepressant effects remain to be elucidated. To date, there is much debate ongoing about the molecular mechanisms underlying ketamine's antidepressant effects in humans and rodents alike. Therefore, it is necessary to summarize the current findings on ketamine's antidepressant effects to further the understanding of the neurobiology of ketamine's actions.

2 (*R,S*)-Ketamine's Antidepressant Effects

2.1 (*R,S*)-Ketamine's Antidepressant Effects

Data from the WHO indicate that more than 300 million people of all ages are suffering from depression, which is the leading cause of disability worldwide, leading to a great expenditure of medical and health resources (WHO 2017). Currently available antidepressants have a delay period of approximately 3–4 weeks before they begin working, and about 30% of patients with depression are resistant entirely to these antidepressants (Zhang and Hashimoto 2019). Moreover, other NMDAR antagonists except ketamine have failed in clinical trials (Hashimoto 2019). Therefore, it is unlikely that NMDAR inhibition plays a key role in the antidepressant actions of ketamine.

(*R,S*)-Ketamine's antidepressant effects have been studied for almost 20 years after Berman et al.'s seminal report (Berman et al. 2000). In the following decade, most studies on patients with MDD have revealed promising prospects for the use of (*R,S*)-ketamine's antidepressant effects. Furthermore, clinical trials conducted on the subjects of ketamine's administration dosage, timing, route, curative effect, tolerability, safety, and antisuicidal effects have also been investigated. Even its use in

different types of depression, including treatment-resistant depression, posttraumatic stress disorder (PTSD), and bipolar depression, has been explored in more recent studies (Bobo et al. 2016; Liriano et al. 2019; Schwartz et al. 2016; Zhang and Hashimoto 2019). Further, several rodent models of depression [i.e., the learned helplessness (LH) model, chronic unpredictable mild stress (CUMS) model, and chronic social defeat stress (CSDS) model] have been established for the purpose of testing (*R,S*)-ketamine's antidepressant effects (Krishnan and Nestler 2011). In short, an array of research modalities including original investigations, clinical trials, systematic reviews, and meta-analyses have been used to study (*R,S*)-ketamine's antidepressant effects (Krishnan and Nestler 2011; Sanacora et al. 2017; Short et al. 2018; Singh et al. 2017; Veraart et al. 2018).

2.2 (*R,S*)-Ketamine's Antidepressant Effects in Humans

In clinical trials, interventional studies have been adopted for evaluating the beneficial effects of (*R,S*)-ketamine. A number of randomized single-/double-blind placebo-/drug-controlled studies have been performed by many researchers to observe the antidepressant effects of (*R,S*)-ketamine in patients with MDD, who were often infused with only a single intravenous dose of 0.5 mg/kg. Berman et al. (2000) first reported the double-blinded and placebo-controlled study of (*R,S*)-ketamine. Then, Zarate et al. (2006) replicated that a high number (71%) of participants showed significant improvements in depressive symptoms within 24 h of drug administration, and 25% of the study subjects showed antidepressant effects for at least 1 week after a single dose of ketamine as part a randomized, placebo-controlled, double-blind crossover study.

A review of the [ClinicalTrials.gov](https://www.clinicaltrials.gov) database found that about 160 applications from around the world for studying (*R,S*)-ketamine's antidepressant effect on patients with depression existed by the end of June 2019. Study subjects mainly included those with MDD with or without suicide ideation, treatment-resistant depression, BD, and PTSD. Studies chiefly involved a randomized single-blind or double-blind design and were placebo-controlled or midazolam-controlled interventions. Collectively, it seems that (*R,S*)-ketamine is viewed as a promising antidepressant for the treatment of severe depression. Systematic reviews and meta-analyses have also been adopted as investigational means by scientists for evaluating the impact of the antidepressant effect of (*R,S*)-ketamine. Such meta-analyses often include treatment-resistant patients with MDD or BD, and their data are mainly a collection of those from randomized controlled trials (RCTs) (Coyle and Laws 2015; Kishimoto et al. 2016; Newport et al. 2015; Serafini et al. 2014; Wilkinson et al. 2018).

(*R,S*)-Ketamine appears to exhibit rapid antidepressant and antisuicidal ideation effects in treatment-resistant patients with depression. Two midazolam-controlled randomized clinical trials conducted in depressed patients with low levels of suicidal ideation (Grunebaum et al. 2018; Murrough et al. 2013a) demonstrated rapid

reductions in suicidal ideation and depressive symptoms within 24 h after treatment with (*R,S*)-ketamine as compared with in the midazolam treatment group (Grunebaum et al. 2018; Murrough et al. 2013a). (*R,S*)-Ketamine has similarly demonstrated early emerging evidence of having antisuicidal effects in depressed patients with suicidal ideation in other research that last from 1 day to 1 week (Bartoli et al. 2017; Reinstatler and Youssef 2015; Wilkinson et al. 2018).

In special studies on treatment-resistant depression, (*R,S*)-ketamine has been proposed as an effective antidepressant, but there is a lack of long-term data on sustained depression remission in patients (Serafini et al. 2014; Papadimitropoulou et al. 2017). When considering bipolar depression, (*R,S*)-ketamine was found to be an effective antidepressant (Parsaik et al. 2015), but there is also limited evidence to support the maintenance of a response for up to 24 h following a single intravenous dose of ketamine in bipolar depression, and (*R,S*)-ketamine did not show a statistical advantage in remission of bipolar depression (McCloud et al. 2015). Therefore, more RCT studies are needed to verify (*R,S*)-ketamine's antidepressant effect in different types of depression.

2.3 Routes of Administration of (*R,S*)-Ketamine

An understanding of the route of administration of (*R,S*)-ketamine is required to confirm its antidepressant effects. There exist a number of studies on routes of administration of (*R,S*)-ketamine, including intravenous, intramuscular, intranasal, subcutaneous, oral, sublingual, transmucosal, and intrarectal, and the bioavailability of these forms of administration varies widely as determined by the absorption of pharmacokinetics although the intravenous route is the most commonly used in patients with depression at this time (Andrade 2017; Hashimoto 2019; Zanos et al. 2018; Zhang and Hashimoto 2019). The bioavailability of intranasal administration of (*R,S*)-ketamine is lower than that of either intravenous or intramuscular administration (Hashimoto 2019; Zhang and Hashimoto 2019). In an effort to assess the safety and efficacy of (*R,S*)-ketamine, Andrade (2017) suggested that the infusion of ketamine by the subcutaneous, intranasal, and oral routes is worth further study based on their clinical practicability. Retrospective data from 22 patients given oral ketamine at a dose of 50 mg per 3 days, which was titrated up by 25 mg per 3 days, showed that 30% of patients with treatment-resistant depression responded to the oral (*R,S*)-ketamine and approximately 70% patients had no improvement in mood symptoms (Al Shirawi et al. 2017). Rosenblat et al. (2019) published a systematic review involving a small number of clinical studies that suggested that oral ketamine could produce significant antidepressant effects, but the drug's antisuicidal effects and efficacy remain undetermined in patients with treatment-resistant depression. Andrade (2019) suggested that oral ketamine should be evaluated by higher-quality studies in the future. Elsewhere, intranasal administration of a single dose of 50 mg of (*R,S*)-ketamine in a 2014 randomized, double-blind crossover study led to depressive symptoms being significantly improved in 44% of patients.

(8/18) after 24 h, with minimal psychosis and dissociation observed in the study (Lapidus et al. 2014). Thus, multiple routes other than the intravenous infusion of ketamine are under consideration in research.

2.4 *(R,S)-Ketamine's Antidepressant Effects*

Repeated ketamine infusion is very important for maintenance therapy of patients with treatment-resistant depression (Murrough et al. 2013b; Strong and Kabbaj 2018). In a randomized controlled trial, the infusion of ketamine with three methods, including single, repeated, and maintenance, was performed to observe *(R,S)*-ketamine's antidepressant effects in treatment-resistant patients; results suggested that a single intravenous dose (0.5 mg/kg) over 40 min significantly improved depressive symptoms after 24 h of infusion. Elsewhere, six repeated infusions worked for a time in 59% of participants whose response criteria met the clinical needs, while these participants had no further benefit from weekly maintenance infusions based on the Montgomery-Åsberg Depression Rating Scale (MADRS) scores (Phillips et al. 2019). In addition, the efficiency of *(R,S)*-ketamine's antidepressant effects were also investigated in patients with PTSD treated by eight repeated ketamine infusions done over 4 weeks (Abdallah et al. 2019) and in those with unipolar and bipolar depressive disorder with current suicidal ideation treated by six repeated ketamine infusions performed during a 12-day period (Zhan et al. 2019; Zheng et al. 2018); these studies supported that the rapid and robust antidepressant effects of *(R,S)*-ketamine can be cumulative and sustained following repeated infusion. Despite ketamine's potential for abuse and psychotomimetic effects, it represents a new drug option for antidepressant treatment. Thus, further investigation of *(R,S)*-ketamine's antidepressant effects is necessary.

2.5 *(R,S)-Ketamine's Antidepressant Effects in Rodents*

Animal models of depression were adopted by researchers to investigate *(R,S)*-ketamine's antidepressant effects. Animal models of depression have previously been used for the development of new antidepressants (Fernando and Robbins 2011; Pittenger et al. 2007). In a shock-induced depression model, Chaturvedi et al. (1999) reported that the antidepressant effects of *(R,S)*-ketamine at a dose range of 2.5–10 mg/kg significantly reduced ambulation and rearing in the open field test and increased the immobility time during the forced swimming test as compared with in control mice who received no shock. In a rat LH model, Koike et al. (2011) reported that *(R,S)*-ketamine (10 mg/kg) exerted rapid and sustained antidepressant effects for at least 72 h after treatment, in which the number of escape failures significantly decreased in the LH paradigm and the immobility time during the tail suspension test was significantly reduced in comparison with in the vehicle-treated group. In a

CUMS model of either mice or rats, (*R,S*)-ketamine at a single dose of 10 mg/kg elicited rapid-onset and long-lasting antidepressant effects as evaluated by the behavioral tests of forced swimming, tail suspension, and sucrose preference; even the ameliorated anhedonia lasted for 8 days in this model (Ma et al. 2013; Sun et al. 2016). Hollis and Kabbaj (2014) suggested in their research that CSDS model is a valuable research tool for investigating possible causes and treatments for human depression. In a CSDS model, as compared with the TrkB agonists 7,8-dihydroxyflavone and TrkB antagonist ANA-12, (*R,S*)-ketamine showed longer-lasting antidepressant effects for 7 days (Zhang et al. 2015). In contrast, however, Donahue et al. (2014) reported that a single administration of ketamine (10 mg/kg) showed a rapid antidepressant effect in a CSDS model, attenuating social avoidance in the social interaction test but having no effect on anhedonia in the intracranial self-stimulation test (Donahue et al. 2014).

In addition, inflammation-induced mice or rat depression models, such as those using lipopolysaccharides or complete Freund's adjuvant, can also be useful in observing (*R,S*)-ketamine's antidepressant effects, in that depression-like behaviors were often determined by forced swimming test; sucrose preference test; and the pro-inflammatory cytokine levels of interleukin (IL)-1 β , IL-6, and tumor necrosis factor- α (Ji et al. 2019; Remus and Dantzer 2016; Reus et al. 2017; Zhang et al. 2016). However, (*R,S*)-ketamine's potential psychotomimetic and other unwanted side effects have also been well-documented in these animal models, prompting behaviors such as hyperlocomotion, prepulse inhibition deficits, conditioned place preference, schizophrenia-like psychotic symptoms, and novel object recognition impairment (Becker et al. 2003; Chan et al. 2013; Chang et al. 2019a; Giorgetti et al. 2015; Imre et al. 2006; Lahti et al. 1995; Ma and Leung 2018; Yang et al. 2015; Zanos et al. 2017), which may pose a major barrier to further clinical study in patients with MDD.

3 (*S*)-Ketamine's Antidepressant Effects

3.1 (*S*)-Ketamine's Antidepressant Effects

(*S*)-Ketamine is an isomer of (*R,S*)-ketamine, which was introduced for medical use in analgesia and anesthesia in the early 1990s (Esketamine 2006; Trimmel et al. 2018). The US FDA originally stated that the stereoisomers of (*R,S*)-ketamine had not received enough attention for its commercial development in 1992 (Luft and Mendes 2005). Now, (*S*)-ketamine has been brought into greater focus over (*R,S*)-ketamine for its antidepressant effects in patients with treatment-resistant depression, due to its incorporation into a nasal spray approved by the US FDA on March 5, 2019 (Canady 2019; US Food and Drug Administration 2019). The evaluation of the (*S*)-ketamine nasal spray was conducted by way of four phase III RCTs, including three short-term (4-week) clinical trials and a withdrawal maintenance-of-effect

trial, where patients experienced many side effects including disassociation, dizziness, nausea, sedation, vertigo, anxiety, and lethargy (US Food and Drug Administration 2019). Therefore, there are many challenges in the study of (*S*)-ketamine, which cannot meet the needs of all patients with MDD, and even the antidepressant efficiency and the side effects of (*S*)-ketamine are still under discussion. On the other hand, the existing literature or studies concerning the use of (*S*)-ketamine in patients with MDD number far less than those on the topic of (*R,S*)-ketamine, but the latter is still not yet approved by FDA for treatment via any route of administration.

In a case report, Paslakis et al. (2010) reported their results obtained with using off-label oral (*S*)-ketamine (1.25 mg/kg) within 14 days: two patients with treatment-resistant depression showed rapid and sustained improvement in their psychopathology within the first week, while another two patients did not respond to the drug throughout the entire treatment period. In addition, several studies have concluded that (*S*)-ketamine produces similar antidepressant effects to those of (*R,S*)-ketamine (Paul et al. 2009) but is better-tolerated than (*R,S*)-ketamine, yet severe psychotomimetic effects with (*S*)-ketamine have also been reported (Correia-Melo et al. 2017; Paul et al. 2009). It is worth mentioning that a case series of repeated (*S*)-ketamine (0.25 mg/kg over 40 min) off-label use demonstrated an improvement in depressive symptoms in 50% of the patients following infusion within 1 or 2 weeks, although 25% of the patients suffered from dissociative symptoms (Segmiller et al. 2013). Another case series reported that the safety and efficacy of (*S*)-ketamine were well demonstrated in patients with treatment-resistant depression (TRD); still, the potential for associated psychotic symptoms can leave some patients out of consideration (Ajub and Lacerda 2018). Thus, additional case studies are needed to review the efficacy and psychosis effects of (*S*)-ketamine.

According to clinical trials records from [ClinicalTrials.gov](https://clinicaltrials.gov), about 18 applications for studying (*S*)-ketamine's antidepressant effect in patients with depression have been uploaded as of April 1, 2019. Some clinical trials have been completed, while others are currently recruiting patients. The route of administration in these clinical trials is mainly intranasal injection, for evaluating the efficacy and safety in patients with MDD or TRD. Therapeutic regimens in these clinical trials also include single and repeated administration. Singh et al. (2016) found in a double-blind, multicenter, randomized, placebo-controlled trial involving patients with TRD that 67% and 64% of the patients, respectively, responded to (*S*)-ketamine given at a single dose of 0.2 mg/kg or 0.4 mg/kg over 40 min within 1 day. Another clinical trial of a head-to-head study compared the antidepressant actions of (*S*)-ketamine and (*R,S*)-ketamine in 96 individuals with TRD given a single dose of (*S*)-ketamine (0.25 mg/kg) or (*R,S*)-ketamine (0.5 mg/kg) over 40 min (Correia-Melo et al. 2018). The authors considered their study as the best way to evaluate the efficacy and safety of (*S*)-ketamine and (*R,S*)-ketamine, as a diverse psychotomimetic effects between the two compounds may be different (Correia-Melo et al. 2018). Clinical trials still need to provide more powerful evidence to assist the clinical application of (*S*)-ketamine in depression or TRD.

Other research on (*S*)-ketamine's antidepressant effects mainly involves combination therapy. Bartova et al. (2015) investigated combined intravenous therapy of (*S*)-ketamine and oral tranylcypromine in two patients with multi-treatment-resistant depression, showing a confusing outcome of evident antisuicidal effects but no detailed improvement in antidepressant effectiveness. Electroconvulsive therapy (ECT) plus (*S*)-ketamine has also been applied in three patients with TRD. Kallmunzer et al. (2016) reported that all subjects showed remission in terms of suicidal ideation and no serious side effects during treatment. In contrast, another clinical trial suggested that (*S*)-ketamine (0.4 mg/kg in a bolus) as adjuvant therapy with propofol made no contribution to the enhanced role of ECT in patients with resistance to antidepressants, even going as far as to cause adverse effects like posttreatment disorientation and restlessness (Jarventausta et al. 2013). Although ECT can help to remedy depression, there is still a lack of clear evidence (Read et al. 2019). Therefore, there is no valid data to prove the combination of (*S*)-ketamine and ECT is beneficial, especially given that the antidepressant effects of (*R,S*)-ketamine are more potent than those of ECT (Muller et al. 2016).

In humans, the idea of using (*S*)-ketamine as an antidepressant is relatively new and its intranasal treatment modality has recently been receiving a lot of attention. However, many challenges need to be faced in future study. For instance, how about its optimal dose and route of administration? How to solve its side effects during treatment? How long does it sustain antidepressant effects? More importantly, how does it work as an antidepressant? These questions remain without an answer at this time.

3.2 (*S*)-Ketamine's Antidepressant Effects in Rodents

Animal experiments aimed at elucidating (*S*)-ketamine's antidepressant effect and its underlying mechanisms have also been conducted although no definitive answer was achieved. The current findings point out that (*S*)-ketamine works in a very complicated way, in that it can bind to multiple receptors in an organism, such as NMDAR, opioid receptors, monoamine receptors, adenosine receptors, α -amino-3-hydroxy-5-methyl-4-isoxazolepropionic acid (AMPA) receptors, metabotropic glutamate receptors, L-type calcium channels, and other purinergic receptors (Kohrs and Durieux 1998; Trimmel et al. 2018). The prevailing view is that (*S*)-ketamine's antidepressant effect is related with the noncompetitive inhibition of NMDAR through binding to the phencyclidine (PCP) sites (Sinner and Graf 2008), due to its three- to fourfold higher affinity in comparison with (*R*)-ketamine (Domino 2010; Kohrs and Durieux 1998). Yet, (*S*)-ketamine dominates in the areas of anesthetic potency and undesirable psychotomimetic side effects over (*R*)-ketamine, in that seeing illusions, hearing and vision changes, and proprioception are related to (*S*)-ketamine, while feelings of relaxation are connected with the actions of (*R*)-ketamine (Zanos et al. 2018).

Treccani et al. (2019) suggested that a single dose of (*S*)-ketamine (15 mg/kg) can induce acute antidepressant action in a rat model of depression, concluding first that dendritic spine density rapidly (<1 h) increases in brain structural changes and also that balancing the relationship between cofilin activity, homer3 levels, and the NMDAR subunits GluN2A and GluN2B plays a key role in the antidepressant effect. However, Ide et al. (2017), upon investigating the role of GluN2D in the antidepressant effects of ketamine enantiomers, suggested that such did not play a key role in the sustained antidepressant effects of (*R,S*)-ketamine and (*S*)-ketamine but rather in those of (*R*)-ketamine. Recent studies have indicated that (*S*)-ketamine elicits its acute and sustained antidepressant-like actions via a 5-hydroxytryptamine (5HT) receptor-dependent mechanism, which is confirmed via the forced swimming test by comparing the vortioxetine, fluoxetine, and (*S*)-ketamine in the serotonin system or by using the 5-HT_{1B} receptor agonist CP94253 in a genetic rat model (du Jardin et al. 2016, 2017).

Other studies of note regarding the mechanisms of (*S*)-ketamine's antidepressant actions are as follows. In a rat depression model of maternal deprivation, it was suggested that a single dose of (*S*)-ketamine showed long-term antidepressant effects through acting against neural damage induced by oxidative stress (Reus et al. 2015). In a long-term corticosterone infusion rat model of depression, it was suggested that (*S*)-ketamine decreased depressive-like behaviors for at least 4 weeks, but not in a manner related with rapid maturity of the new hippocampal neurons (Soumier et al. 2016). In a rat hippocampus study, Ardalan et al. (2017) put forward the notion that a single injection (15 mg/kg) of (*S*)-ketamine improved the immobility behavior during the modified forced swim test within 24 h after treatment, proving that astrocyte plasticity in the hippocampus has a bearing on the (*S*)-ketamine antidepressant effect in a rat genetic animal model of depression.

4 (*R*)-Ketamine's Antidepressant Effects

4.1 Summary of the Differences Between (*R*)-Ketamine and (*S*)-Ketamine

With the deepening and development of research, the focus on antidepressant effects will be quickly shifted toward (*R*)-ketamine, because its advantages are becoming more and more obvious. As compared with (*S*)-ketamine, (*R*)-ketamine has been proven to be more potent and have longer-lasting antidepressant effects and was deemed to be free of psychotomimetic side effects in many studies on rodent models of depression (Chang et al. 2019a; Fukumoto et al. 2017; Yang et al. 2015, 2016b; Zhang et al. 2014), signifying that (*R*)-ketamine will be one of the most promising antidepressants.

(*R*)-Ketamine is an isomer of (*R,S*)-ketamine. (*R*)-ketamine is a left-handed molecule, while (*S*)-ketamine is a right-handed molecule, per the carbon connections in

either one or the other direction of nonsuperimposable mirror images, prompting a difference in the body metabolism (Calvey 1995; Kharasch and Labroo 1992). As compared with (*S*)-ketamine, (*R*)-ketamine has a lower affinity to the PCP binding site of the NMDAR, with a lower anesthetic potency (Thomson et al. 1985; White et al. 1985; Zeilhofer et al. 1992). In addition, (*R*)-ketamine could also weakly bind to the sigma receptor sites, without (*S*)-ketamine binding to these sites (Vollenweider et al. 1997). Research on the side effects of the two isomers showed that (*R*)-ketamine produces a feeling of relaxation or “well-being,” while (*S*)-ketamine is mainly responsible for psychotomimetic effects, such as dissociations in hearing, vision, and proprioception (Hashimoto 2019; Vollenweider et al. 1997; Zanos et al. 2018). Moreover, Marietta et al. (1977) reported acute toxic effects of racemic ketamine and its two isomers at the dose of 40 mg/kg in male Sprague-Dawley rats based on median lethal dose values, indicating that (*R*)-ketamine is more secure than (*R,S*)-ketamine and (*S*)-ketamine, and its potential advantage is not a fatal drug according to the high dose and with less posthypnotic stimulation.

4.2 Different Antidepressant Effects Between (R)-Ketamine and (S)-Ketamine

Our group reported that (*R*)-ketamine has a greater potency and longer-lasting antidepressant roles than (*S*)-ketamine in rodent models of depression (Yang et al. 2015; Zhang et al. 2014). In addition, it was suggested that ketamine’s side effects (e.g., psychotomimetic behaviors, neurotoxicity, abuse potential) may be associated with (*S*)-ketamine but not (*R*)-ketamine (Chang et al. 2019a; Hashimoto 2016a, b, c). Subsequently, different kinds of depression models with comparative objects and their relevant behavioral tests were employed to evaluate and identify the advantages of (*R*)-ketamine’s antidepressant effects. Fukumoto et al. (2017) reported that (*R*)-ketamine can elicit longer-lasting antidepressant effects than (*S*)-ketamine in forced swimming and tail suspension tests, and (*R*)-ketamine showed a sustained antidepressant effect in a treatment-refractory model while (*S*)-ketamine did not. Moreover, Fukumoto et al. (2017) also suggested that (*R*)-ketamine’s antidepressant effects may be related with AMPAR by testing the rats of a repeated corticosterone treatment model with an AMPAR antagonist, NBQX (Fukumoto et al. 2017). In a conscious positron-emission tomography study, a single infusion of (*S*)-ketamine but not (*R*)-ketamine caused dopamine release, indicating that (*S*)-ketamine-induced dopamine release may be associated with acute psychotomimetic and dissociative effects in humans (Hashimoto et al. 2017).

In addition, further research on the molecular mechanisms revealed more data about the differences between (*R*)-ketamine and (*S*)-ketamine. Specifically, the extracellular-signal-regulated kinase signaling pathway may play a role in (*R*)-ketamine’s antidepressant effects, while the mammalian target of rapamycin signaling pathway plays a role in the antidepressant effects of (*S*)-ketamine (Yang et al.

2018a). Nevertheless, glutamate is the primary excitatory neurotransmitter in the human brain in physiology (Jewett and Thapa 2019) and its participation in the role of ketamine's antidepressant effects should not be neglected in the following study, although we still cannot explain the real difference between (*R,S*)-ketamine and its two isomers (Zanos and Gould 2018). Even more important, the causes for the differences in antidepressant effects between (*R*)-ketamine and (*S*)-ketamine may be related with the gut microbiota–brain axis (Qu et al. 2017; Yang et al. 2017). As compared with (*S*)-ketamine, (*R*)-ketamine significantly attenuated the decrease in the levels of *Mollicutes* of susceptible mice in a CSDS model, and (*R*)-ketamine presented a stronger advantage than (*S*)-ketamine in reducing the levels of *Butyrivimonas* (Yang et al. 2017).

4.3 (*R*)-Ketamine's Antidepressant Effects

(*R*)-ketamine has its own special features of antidepressant effects from the current study. As compared with the NMDAR partial agonist rapastinel, (*R*)-ketamine had longer-lasting antidepressant effects and significantly changed the brain-derived neurotrophic factor–TrkB signaling in a CSDS model (Yang et al. 2016a). Recent Ph3 data of rapastinel were negative (Hashimoto 2019).

In the light of the complex physiology and particularity that of NMDAR for regulating the electroneurographic signal in depression by voltage-gated ion channel influx, including calcium, sodium, and potassium (Cui et al. 2018; Yang et al. 2018b). Tian et al. (2018b) reported that the low-voltage-sensitive, T-type calcium channel blocker ethosuximide did not produce rapid or sustained antidepressant effects in a CSDS model, although (*R*)-ketamine showed rapid and sustained antidepressant effects in the same model (Tian et al. 2018b). Furthermore, Xiong et al. (2019) reported that the Kir4.1 inhibitors quinacrine and sertraline did not improve the depression-like behaviors during the tail suspension test and forced swimming test in a CSDS model, while (*R*)-ketamine produced rapid and sustained antidepressant effects in this model (Xiong et al. 2019).

Treatment with the 5-HT inhibitor para-chlorophenylalanine methyl ester hydrochloride also did not impact the antidepressant effects of (*R*)-ketamine in a CSDS model (Zhang et al. 2018). Furthermore, dopamine D₁ receptors may not play a major role in the antidepressant actions of (*R*)-ketamine, because pretreatment with the dopamine D₁ receptor antagonist SCH-23390 did not block the antidepressant effects of (*R*)-ketamine in the CSDS model (Chang et al. 2019b).

Given the role of gamma-aminobutyric acid receptors in depression (Zanos et al. 2017), both (*R*)-ketamine and MRK-016 (full inverse GABA_A agonist) displayed rapid antidepressant effects, while only (*R*)-ketamine produced a longer-lasting antidepressant effect in a CSDS model (Xiong et al. 2018).

In addition, (*R*)-ketamine's antidepressant effects had regional differences in rat brains. A single bilateral infusion of (*R*)-ketamine was injected into the brain in a rat LH model of depression, showing that the infralimbic cortex of the medial prefrontal

cortex (mPFC), dentate gyrus, and CA3 subregions of the hippocampus are related with (*R*)-ketamine's antidepressant effects as compared with other injection site areas including the mPFC subregion PrL, subregions of the shell and core in NAc, and BLA and CeA subregions of the amygdala, which had nothing to do with the antidepressant effects of (*R*)-ketamine (Shirayama and Hashimoto 2017). No toxicity was shown in the brain after repeated, intermittent administration with (*R*)-ketamine, with no loss in parvalbumin immunoreactivity in the brain region of mPFC and hippocampus observed, which was the opposite finding to those of (*S*)-ketamine (Yang et al. 2016b). Additionally, another interesting finding regarding neuropathological changes revealed that the neuronal injury marker heat shock protein HSP-70 was expressed in the rat retrosplenial cortex not because of (*R*)-ketamine but instead due to (*R,S*)-ketamine and (*S*)-ketamine (Tian et al. 2018a).

Based on the above findings, (*R*)-ketamine shows the rapid-acting and long-lasting antidepressant effects in rodents although its precise mechanism underlying these effects is still uncertain. A clinical trial of (*R*)-ketamine in humans is currently underway (Hashimoto 2019).

5 Conclusion

The discovery of the robust antidepressant actions of (*R,S*)-ketamine in depressed patients is serendipitous (Krystal et al. 2019). However, (*R,S*)-ketamine has not been approved by the US FDA for antidepressant treatment in clinical application because of a lack of patent. An (*S*)-ketamine nasal spray was approved by the FDA on March 5, 2019, although its side effects are known and it must be administered under supervision in a certified doctor's office or outpatient clinic after treatment. It seems that antidepressant effects of (*S*)-ketamine in patients with MDD are less potent than those related with (*R,S*)-ketamine in clinical studies. Although there is no clinical trial of (*R*)-ketamine in patients with MDD, many preclinical data show its more potent antidepressant effects without side effects, suggesting that (*R*)-ketamine could be a safer antidepressant alternative to (*R,S*)-ketamine and (*S*)-ketamine. Due to its lower adverse side effects, we are looking forward to seeing more data on (*R*)-ketamine's antidepressant effects in patients with MDD and other psychiatric disorders.

Acknowledgments This study was supported by grant from AMED, Japan (to K.H., JP19dm0107119). Dr. Lijia Chang was supported by the Japan China Sasakawa Medical Fellowship (Tokyo, Japan). Dr. Yan Wei (Southwest Medical University, China) was supported by the China Scholarship Council (China).

Disclosure Statement: Dr. Hashimoto is the inventor of filed patent applications on "The use of *R*-ketamine in the treatment of psychiatric diseases" by the Chiba University. Dr. Hashimoto also declares that he has received research support and consultant from Dainippon Sumitomo, Otsuka, and Taisho.

References

AU7

- Abdallah CG et al (2019) Repeated ketamine infusions for antidepressant-resistant PTSD: methods of a multicenter, randomized, placebo-controlled clinical trial. *Contemp Clin Trials* 81:11–18. <https://doi.org/10.1016/j.cct.2019.04.009>
- Ajub E, Lacerda ALT (2018) Efficacy of esketamine in the treatment of depression with psychotic features: a case series. *Biol Psychiatry* 83:e15–e16. <https://doi.org/10.1016/j.biopsych.2017.06.011>
- Al Shirawi MI, Kennedy SH, Ho KT, Byrne R, Downar J (2017) Oral ketamine in treatment-resistant depression: a clinical effectiveness case series. *J Clin Psychopharmacol* 37:464–467. <https://doi.org/10.1097/JCP.0000000000000717>
- Andrade C (2017) Ketamine for depression, 4: in what dose, at what rate, by what route, for how long, and at what frequency? *J Clin Psychiatry* 78:e852–e857. <https://doi.org/10.4088/JCP.17f11738>
- Andrade C (2019) Oral ketamine for depression, 2: practical considerations. *J Clin Psychiatry* 80. <https://doi.org/10.4088/JCP.19f12838>
- Ardalan M, Rafati AH, Nyengaard JR, Wegener G (2017) Rapid antidepressant effect of ketamine correlates with astroglial plasticity in the hippocampus. *Br J Pharmacol* 174:483–492. <https://doi.org/10.1111/bph.13714>
- Bartoli F, Riboldi I, Crocamo C, Di Brita C, Clerici M, Carra G (2017) Ketamine as a rapid-acting agent for suicidal ideation: a meta-analysis. *Neurosci Biobehav Rev* 77:232–236. <https://doi.org/10.1016/j.neubiorev.2017.03.010>
- Bartova L, Vogl SE, Stamenkovic M, Praschak-Rieder N, Naderi-Heiden A, Kasper S, Willeit M (2015) Combination of intravenous S-ketamine and oral tranylcypromine in treatment-resistant depression: a report of two cases. *Eur Neuropsychopharmacol* 25:2183–2184. <https://doi.org/10.1016/j.euroneuro.2015.07.021>
- Bartova L et al (2018) Rapid antidepressant effect of S-ketamine in schizophrenia. *Eur Neuropsychopharmacol* 28:980–982. <https://doi.org/10.1016/j.euroneuro.2018.05.007>
- Becker A, Peters B, Schroeder H, Mann T, Huether G, Grecksch G (2003) Ketamine-induced changes in rat behaviour: a possible animal model of schizophrenia. *Prog Neuropsychopharmacol Biol Psychiatry* 27:687–700. [https://doi.org/10.1016/S0278-5846\(03\)00080-0](https://doi.org/10.1016/S0278-5846(03)00080-0)
- Berman RM, Cappiello A, Anand A, Oren DA, Heninger GR, Charney DS, Krystal JH (2000) Antidepressant effects of ketamine in depressed patients. *Biol Psychiatry* 47:351–354
- Bobo WV, Vande Voort JL, Croarkin PE, Leung JG, Tye SJ, Frye MA (2016) Ketamine for treatment-resistant unipolar and bipolar major depression: critical review and implications for clinical practice. *Depress Anxiety* 33:698–710. <https://doi.org/10.1002/da.22505>
- Calvey TN (1995) Isomerism and anaesthetic drugs. *Acta Anaesthesiol Scand Suppl* 106:83–90
- Canady VA (2019) Nasal spray treatment for adults with TRD approved by FDA. *Mental Health Wkly* 29:4–5
- Chan KW, Lee TM, Siu AM, Wong DP, Kam CM, Tsang SK, Chan CC (2013) Effects of chronic ketamine use on frontal and medial temporal cognition. *Addict Behav* 38:2128–2132. <https://doi.org/10.1016/j.addbeh.2013.01.014>
- Chang L et al (2019a) Comparison of antidepressant and side effects in mice after intranasal administration of (R,S)-ketamine, (R)-ketamine, and (S)-ketamine. *Pharmacol Biochem Behav* 181:53–59. <https://doi.org/10.1016/j.pbb.2019.04.008>
- Chang L et al (2019b) Lack of dopamine D1 receptors in the antidepressant actions of (R)-ketamine in a chronic social defeat stress model. *Eur Arch Psychiatry Clin Neurosci*. <https://doi.org/10.1007/s00406-019-01012-1>
- Chaturvedi HK, Chandra D, Bapna JS (1999) Interaction between N-methyl-D-aspartate receptor antagonists and imipramine in shock-induced depression. *Indian J Exp Biol* 37:952–958
- Cohen SP et al (2018) Consensus guidelines on the use of intravenous ketamine infusions for chronic pain from the American Society of Regional Anesthesia and Pain Medicine, the

- American Academy of Pain Medicine, and the American Society of Anesthesiologists. *Reg Anesth Pain Med* 43:521–546. <https://doi.org/10.1097/AAP.0000000000000808>
- Correia-Melo FS, Silva SS, Araujo-de-Freitas L, Quarantini LC (2017) S-(+)-ketamine-induced dissociative symptoms as a traumatic experience in patients with treatment-resistant depression. *Braz J Psychiatry* 39:188–189. <https://doi.org/10.1590/1516-4446-2016-2070>
- Correia-Melo FS et al (2018) Comparative study of esketamine and racemic ketamine in treatment-resistant depression: Protocol for a non-inferiority clinical trial. *Medicine (Baltimore)* 97:e12414. <https://doi.org/10.1097/MD.00000000000012414>
- Coyle CM, Laws KR (2015) The use of ketamine as an antidepressant: a systematic review and meta-analysis. *Hum Psychopharmacol* 30:152–163. <https://doi.org/10.1002/hup.2475>
- Cui Y et al (2018) Astroglial Kir4.1 in the lateral habenula drives neuronal bursts in depression. *Nature* 554:323–327. <https://doi.org/10.1038/nature25752>
- Cusin C (2019) Ketamine as a rapid antidepressant. In: *The Massachusetts General Hospital guide to depression*. Springer, Berlin, pp 139–145
- Domino EF (2010) Taming the ketamine tiger. 1965. *Anesthesiology* 113:678–684. <https://doi.org/10.1097/ALN.0b013e3181ed09a2>
- Donahue RJ, Muschamp JW, Russo SJ, Nestler EJ, Carlezon WA Jr (2014) Effects of striatal DeltaFosB overexpression and ketamine on social defeat stress-induced anhedonia in mice. *Biol Psychiatry* 76:550–558. <https://doi.org/10.1016/j.biopsych.2013.12.014>
- du Jardin KG, Liebenberg N, Muller HK, Elfving B, Sanchez C, Wegener G (2016) Differential interaction with the serotonin system by S-ketamine, vortioxetine, and fluoxetine in a genetic rat model of depression. *Psychopharmacology (Berl)* 233:2813–2825. <https://doi.org/10.1007/s00213-016-4327-5>
- du Jardin KG, Liebenberg N, Cajina M, Muller HK, Elfving B, Sanchez C, Wegener G (2017) S-ketamine mediates its acute and sustained antidepressant-like activity through a 5-HT1B receptor dependent mechanism in a genetic rat model of depression. *Front Pharmacol* 8:978. <https://doi.org/10.3389/fphar.2017.00978>
- Duman RS (2018) Ketamine and rapid-acting antidepressants: a new era in the battle against depression and suicide. *F1000Res* 7. <https://doi.org/10.12688/f1000research.14344.1>
- Esketamine (2006) *Drugs and lactation database (LactMed)*. National Library of Medicine (US), Bethesda, MD
- Fernando AB, Robbins TW (2011) Animal models of neuropsychiatric disorders. *Annu Rev Clin Psychol* 7:39–61. <https://doi.org/10.1146/annurev-clinpsy-032210-104454>
- Fukumoto K, Toki H, Iijima M, Hashihayata T, Yamaguchi JI, Hashimoto K, Chaki S (2017) Antidepressant potential of (R)-ketamine in rodent models: comparison with (S)-ketamine. *J Pharmacol Exp Ther* 361:9–16. <https://doi.org/10.1124/jpet.116.239228>
- Gao M, Rejaei D, Liu H (2016) Ketamine use in current clinical practice. *Acta Pharmacol Sin* 37:865–872. <https://doi.org/10.1038/aps.2016.5>
- Giorgetti R, Marcotulli D, Tagliabracci A, Schifano F (2015) Effects of ketamine on psychomotor, sensory and cognitive functions relevant for driving ability. *Forensic Sci Int* 252:127–142. <https://doi.org/10.1016/j.forsciint.2015.04.024>
- Gowda MR, Srinivasa P, Kumbar PS, Ramalingaiah VH, Muthyalappa C, Durgoji S (2016) Rapid resolution of grief with IV infusion of ketamine: a unique phenomenological experience. *Indian J Psychol Med* 38:62–64. <https://doi.org/10.4103/0253-7176.175121>
- Grunebaum MF et al (2018) Ketamine for rapid reduction of suicidal thoughts in major depression: a midazolam-controlled randomized clinical trial. *Am J Psychiatry* 175:327–335. <https://doi.org/10.1176/appi.ajp.2017.17060647>
- Hashimoto K (2016a) Detrimental side effects of repeated ketamine infusions in the brain. *Am J Psychiatry* 173:1044–1045. <https://doi.org/10.1176/appi.ajp.2016.16040411>
- Hashimoto K (2016b) Ketamine's antidepressant action: beyond NMDA receptor inhibition. *Expert Opin Ther Targets* 20:1389–1392. <https://doi.org/10.1080/14728222.2016.1238899>

- Hashimoto K (2016c) Letter to the Editor: R-ketamine: a rapid-onset and sustained antidepressant without risk of brain toxicity. *Psychol Med* 46:2449–2451. <https://doi.org/10.1017/S0033291716000969>
- Hashimoto K (2017) Rapid antidepressant activity of ketamine beyond NMDA receptor. In: *The NMDA receptors*. Springer, Berlin, pp 69–81
- Hashimoto K (2019) Rapid-acting antidepressant ketamine, its metabolites and other candidates: A historical overview and future perspective. *Psychiatry Clin Neurosci* 73(10):613–627. <https://doi.org/10.1111/pcn.12902>
- Hashimoto K, Kakiuchi T, Ohba H, Nishiyama S, Tsukada H (2017) Reduction of dopamine D_{2/3} receptor binding in the striatum after a single administration of esketamine, but not R-ketamine: a PET study in conscious monkeys. *Eur Arch Psychiatry Clin Neurosci* 267:173–176
- Heal DJ, Gosden J, Smith SL (2018) Evaluating the abuse potential of psychedelic drugs as part of the safety pharmacology assessment for medical use in humans. *Neuropharmacology* 142:89–115. <https://doi.org/10.1016/j.neuropharm.2018.01.049>
- Hollis F, Kabbaj M (2014) Social defeat as an animal model for depression. *ILAR J* 55:221–232. <https://doi.org/10.1093/ilar/ilu002>
- Ide S, Ikeda K (2018) Mechanisms of the antidepressant effects of ketamine enantiomers and their metabolites. *Biol Psychiatry* 84:551–552. <https://doi.org/10.1016/j.biopsych.2018.07.018>
- Ide S, Ikekubo Y, Mishina M, Hashimoto K, Ikeda K (2017) Role of NMDA receptor GluN2D subunit in the antidepressant effects of enantiomers of ketamine. *J Pharmacol Sci* 135:138–140. <https://doi.org/10.1016/j.jphs.2017.11.001>
- Imre G, Salomons A, Jongsma M, Fokkema DS, Den Boer JA, Ter Horst GJ (2006) Effects of the mGluR2/3 agonist LY379268 on ketamine-evoked behaviours and neurochemical changes in the dentate gyrus of the rat. *Pharmacol Biochem Behav* 84:392–399. <https://doi.org/10.1016/j.pbb.2006.05.021>
- Ivan Ezquerra-Romano I, Lawn W, Krupitsky E, Morgan CJA (2018) Ketamine for the treatment of addiction: evidence and potential mechanisms. *Neuropharmacology* 142:72–82. <https://doi.org/10.1016/j.neuropharm.2018.01.017>
- Jarventausta K et al (2013) Effects of S-ketamine as an anesthetic adjuvant to propofol on treatment response to electroconvulsive therapy in treatment-resistant depression: a randomized pilot study. *J ECT* 29:158–161. <https://doi.org/10.1097/YCT.0b013e318283b7e9>
- Jewett BE, Thapa B (2019) Physiology, NMDA Receptor. In: *StatPearls*. StatPearls, Treasure Island, FL
- Ji M et al (2019) Acute ketamine administration attenuates lipopolysaccharide-induced depressive-like behavior by reversing abnormal regional homogeneity in the nucleus accumbens. *Neuroreport* 30:421–427. <https://doi.org/10.1097/WNR.0000000000001219>
- Kallmunzer B, Volbers B, Karthaus A, Tektas OY, Kornhuber J, Muller HH (2016) Treatment escalation in patients not responding to pharmacotherapy, psychotherapy, and electro-convulsive therapy: experiences from a novel regimen using intravenous S-ketamine as add-on therapy in treatment-resistant depression. *J Neural Transm (Vienna)* 123:549–552. <https://doi.org/10.1007/s00702-015-1500-7>
- Kharasch ED, Labroo R (1992) Metabolism of ketamine stereoisomers by human liver microsomes. *Anesthesiology* 77:1201–1207
- Kishimoto T, Chawla JM, Hagi K, Zarate CA, Kane JM, Bauer M, Correll CU (2016) Single-dose infusion ketamine and non-ketamine N-methyl-D-aspartate receptor antagonists for unipolar and bipolar depression: a meta-analysis of efficacy, safety and time trajectories. *Psychol Med* 46:1459–1472. <https://doi.org/10.1017/S0033291716000064>
- Kohrs R, Durieux ME (1998) Ketamine: teaching an old drug new tricks. *Anesth Analg* 87:1186–1193
- Koike H, Iijima M, Chaki S (2011) Involvement of AMPA receptor in both the rapid and sustained antidepressant-like effects of ketamine in animal models of depression. *Behav Brain Res* 224:107–111. <https://doi.org/10.1016/j.bbr.2011.05.035>

- Krishnan V, Nestler EJ (2011) Animal models of depression: molecular perspectives. *Curr Top Behav Neurosci* 7:121–147. https://doi.org/10.1007/7854_2010_108
- Krystal JH et al (1994) Subanesthetic effects of the noncompetitive NMDA antagonist, ketamine, in humans. Psychotomimetic, perceptual, cognitive, and neuroendocrine responses. *Arch Gen Psychiatry* 51:199–214. <https://doi.org/10.1001/archpsyc.1994.03950030035004>
- Krystal JH, Abdallah CG, Sanacora G, Charney DS, Duman RS (2019) Ketamine: a paradigm shift for depression research and treatment. *Neuron* 101:774–778. <https://doi.org/10.1016/j.neuron.2019.02.005>
- Kurdi MS, Theerth KA, Deva RS (2014) Ketamine: current applications in anesthesia, pain, and critical care. *Anesth Essays Res* 8:283–290. <https://doi.org/10.4103/0259-1162.143110>
- Lahti AC, Holcomb HH, Medoff DR, Tamminga CA (1995) Ketamine activates psychosis and alters limbic blood flow in schizophrenia. *Neuroreport* 6:869–872
- Lapidus KA et al (2014) A randomized controlled trial of intranasal ketamine in major depressive disorder. *Biol Psychiatry* 76:970–976. <https://doi.org/10.1016/j.biopsych.2014.03.026>
- Li L, Vlisides PE (2016) Ketamine: 50 years of modulating the mind. *Front Hum Neurosci* 10:612. <https://doi.org/10.3389/fnhum.2016.00612>
- Liao Y, Tang YI, Hao W (2017) Ketamine and international regulations. *Am J Drug Alcohol Abuse* 43:495–504
- Liriano F, Hatten C, Schwartz TL (2019) Ketamine as treatment for post-traumatic stress disorder: a review. *Drugs Context* 8:212305. <https://doi.org/10.7573/dic.212305>
- Luft A, Mendes FF (2005) Low S(+) ketamine doses: a review. *Rev Bras Anesthesiol* 55:460–469
- Ma J, Leung LS (2018) Involvement of posterior cingulate cortex in ketamine-induced psychosis relevant behaviors in rats. *Behav Brain Res* 338:17–27. <https://doi.org/10.1016/j.bbr.2017.09.051>
- Ma XC et al (2013) Long-lasting antidepressant action of ketamine, but not glycogen synthase kinase-3 inhibitor SB216763, in the chronic mild stress model of mice. *PLoS One* 8:e56053. <https://doi.org/10.1371/journal.pone.0056053>
- Marietta MP, Way WL, Castagnoli N Jr, Trevor AJ (1977) On the pharmacology of the ketamine enantiomorphs in the rat. *J Pharmacol Exp Ther* 202:157–165
- McCloud TL et al (2015) Ketamine and other glutamate receptor modulators for depression in bipolar disorder in adults. *Cochrane Database Syst Rev*:CD011611. <https://doi.org/10.1002/14651858.CD011611.pub2>
- Molero P, Ramos-Quiroga J, Martín-Santos R, Calvo-Sánchez E, Gutiérrez-Rojas L, Meana JJ (2018) Antidepressant efficacy and tolerability of ketamine and esketamine: a critical review. *CNS Drugs* 32:411–420
- Morgan CJA, Curran HV (2012) Ketamine use: a review. *Addiction* 107:27–38. <https://doi.org/10.1111/j.1360-0443.2011.03576.x>
- Muller J, Pentylala S, Dilger J, Pentylala S (2016) Ketamine enantiomers in the rapid and sustained antidepressant effects. *Ther Adv Psychopharmacol* 6:185–192. <https://doi.org/10.1177/2045125316631267>
- Murrough JW et al (2013a) Antidepressant efficacy of ketamine in treatment-resistant major depression: a two-site randomized controlled trial. *Am J Psychiatry* 170:1134–1142. <https://doi.org/10.1176/appi.ajp.2013.13030392>
- Murrough JW et al (2013b) Rapid and longer-term antidepressant effects of repeated ketamine infusions in treatment-resistant major depression. *Biol Psychiatry* 74:250–256. <https://doi.org/10.1016/j.biopsych.2012.06.022>
- Newport DJ et al (2015) Ketamine and other NMDA antagonists: early clinical trials and possible mechanisms in depression. *Am J Psychiatry* 172:950–966. <https://doi.org/10.1176/appi.ajp.2015.15040465>
- Palucha-Poniewiera A (2018) The role of glutamatergic modulation in the mechanism of action of ketamine, a prototype rapid-acting antidepressant drug. *Pharmacol Rep* 70:837–846. <https://doi.org/10.1016/j.pharep.2018.02.011>

- Papadimitropoulou K, Vossen C, Karabis A, Donatti C, Kubitz N (2017) Comparative efficacy and tolerability of pharmacological and somatic interventions in adult patients with treatment-resistant depression: a systematic review and network meta-analysis. *Curr Med Res Opin* 33:701–711. <https://doi.org/10.1080/03007995.2016.1277201>
- Parsaik AK, Singh B, Khosh-Chashm D, Mascarenhas SS (2015) Efficacy of ketamine in bipolar depression: systematic review and meta-analysis. *J Psychiatr Pract* 21:427–435. <https://doi.org/10.1097/PRA.0000000000000106>
- Paslakis G, Gilles M, Meyer-Lindenberg A, Deuschle M (2010) Oral administration of the NMDA receptor antagonist S-ketamine as add-on therapy of depression: a case series. *Pharmacopsychiatry* 43:33–35. <https://doi.org/10.1055/s-0029-1237375>
- Paul R, Schaaff N, Padberg F, Moller HJ, Frodl T (2009) Comparison of racemic ketamine and S-ketamine in treatment-resistant major depression: report of two cases. *World J Biol Psychiatry* 10:241–244. <https://doi.org/10.1080/15622970701714370>
- Phillips JL et al (2019) Single, repeated, and maintenance ketamine infusions for treatment-resistant depression: a randomized controlled trial. *Am J Psychiatry* 176:401–409. <https://doi.org/10.1176/appi.ajp.2018.18070834>
- Pittenger C, Sanacora G, Krystal JH (2007) The NMDA receptor as a therapeutic target in major depressive disorder. *CNS Neurol Disord Drug Targets* 6:101–115
- Qu Y, Yang C, Ren Q, Ma M, Dong C, Hashimoto K (2017) Comparison of (R)-ketamine and lanicemine on depression-like phenotype and abnormal composition of gut microbiota in a social defeat stress model. *Sci Rep* 7:15725. <https://doi.org/10.1038/s41598-017-16060-7>
- Read J, Cunliffe S, Jauhar S, McLoughlin DM (2019) Should we stop using electroconvulsive therapy? *BMJ* 364:k5233. <https://doi.org/10.1136/bmj.k5233>
- Reinstatler L, Youssef NA (2015) Ketamine as a potential treatment for suicidal ideation: a systematic review of the literature. *Drugs R D* 15:37–43. <https://doi.org/10.1007/s40268-015-0081-0>
- Remus JL, Dantzer R (2016) Inflammation models of depression in rodents: relevance to psychotropic drug discovery. *Int J Neuropsychopharmacol* 19:pyw028. <https://doi.org/10.1093/ijnp/pyw028>
- Reus GZ et al (2015) A single dose of S-ketamine induces long-term antidepressant effects and decreases oxidative stress in adulthood rats following maternal deprivation. *Dev Neurobiol* 75:1268–1281. <https://doi.org/10.1002/dneu.22283>
- Reus GZ et al (2017) Ketamine potentiates oxidative stress and influences behavior and inflammation in response to lipopolysaccharide (LPS) exposure in early life. *Neuroscience* 353:17–25. <https://doi.org/10.1016/j.neuroscience.2017.04.016>
- Rosenblat JD, Carvalho AF, Li M, Lee Y, Subramanieapillai M, McIntyre RS (2019) Oral ketamine for depression: a systematic review. *J Clin Psychiatry* 80. <https://doi.org/10.4088/JCP.18r12475>
- Ryder S, Way WL, Trevor AJ (1978) Comparative pharmacology of the optical isomers of ketamine in mice. *Eur J Pharmacol* 49:15–23
- Sanacora G et al (2017) A consensus statement on the use of ketamine in the treatment of mood disorders. *JAMA Psychiat* 74:399–405. <https://doi.org/10.1001/jamapsychiatry.2017.0080>
- Schwartz J, Murrough JW, Iosifescu DV (2016) Ketamine for treatment-resistant depression: recent developments and clinical applications. *Evid Based Ment Health* 19:35–38. <https://doi.org/10.1136/eb-2016-102355>
- Segmiller F et al (2013) Repeated S-ketamine infusions in therapy resistant depression: a case series. *J Clin Pharmacol* 53:996–998. <https://doi.org/10.1002/jcph.122>
- Serafini G, Howland RH, Rovedi F, Girardi P, Amore M (2014) The role of ketamine in treatment-resistant depression: a systematic review. *Curr Neuropharmacol* 12:444–461. <https://doi.org/10.2174/1570159x12666140619204251>
- Sheth MK, Brand A, Halterman J (2018) Ketamine-induced changes in blood pressure and heart rate in pre-hospital intubated patients. *Adv J Grad Res* 3:20–33
- Shirayama Y, Hashimoto K (2017) Effects of a single bilateral infusion of R-ketamine in the rat brain regions of a learned helplessness model of depression. *Eur Arch Psychiatry Clin Neurosci* 267:177–182. <https://doi.org/10.1007/s00406-016-0718-1>

- Short B, Fong J, Galvez V, Shelker W, Loo CK (2018) Side-effects associated with ketamine use in depression: a systematic review. *Lancet Psychiatry* 5:65–78. [https://doi.org/10.1016/S2215-0366\(17\)30272-9](https://doi.org/10.1016/S2215-0366(17)30272-9)
- Sihra N, Ockrim J, Wood D (2018) The effects of recreational ketamine cystitis on urinary tract reconstruction—a surgical challenge. *BJU Int* 121:458–465. <https://doi.org/10.1111/bju.14094>
- Singh JB et al (2016) Intravenous esketamine in adult treatment-resistant depression: a double-blind, double-randomization, placebo-controlled study. *Biol Psychiatry* 80:424–431. <https://doi.org/10.1016/j.biopsych.2015.10.018>
- Singh I, Morgan C, Curran V, Nutt D, Schlag A, McShane R (2017) Ketamine treatment for depression: opportunities for clinical innovation and ethical foresight. *Lancet Psychiatry* 4:419–426. [https://doi.org/10.1016/S2215-0366\(17\)30102-5](https://doi.org/10.1016/S2215-0366(17)30102-5)
- Sinner B, Graf BM (2008) Ketamine. *Handb Exp Pharmacol*:313–333. https://doi.org/10.1007/978-3-540-74806-9_15
- Soumier A, Carter RM, Schoenfeld TJ, Cameron HA (2016) New hippocampal neurons mature rapidly in response to ketamine but are not required for its acute antidepressant effects on neophagia in rats. *eNeuro* 3. <https://doi.org/10.1523/ENEURO.0116-15.2016>
- Stevenson C (2005) Ketamine: a review. *Update Anaesth* 20:25–29
- Strong CE, Kabbaj M (2018) On the safety of repeated ketamine infusions for the treatment of depression: effects of sex and developmental periods. *Neurobiol Stress* 9:166–175. <https://doi.org/10.1016/j.ynstr.2018.09.001>
- Sun HL et al (2016) Role of hippocampal p11 in the sustained antidepressant effect of ketamine in the chronic unpredictable mild stress model. *Transl Psychiatry* 6:e741. <https://doi.org/10.1038/tp.2016.21>
- Szlachta M et al (2017) Effect of clozapine on ketamine-induced deficits in attentional set shift task in mice. *Psychopharmacology (Berl)* 234:2103–2112. <https://doi.org/10.1007/s00213-017-4613-x>
- Thomson AM, West DC, Lodge D (1985) An N-methylaspartate receptor-mediated synapse in rat cerebral cortex: a site of action of ketamine? *Nature* 313:479–481
- Tian Z, Dong C, Fujita A, Fujita Y, Hashimoto K (2018a) Expression of heat shock protein HSP-70 in the retrosplenial cortex of rat brain after administration of (R,S)-ketamine and (S)-ketamine, but not (R)-ketamine. *Pharmacol Biochem Behav* 172:17–21. <https://doi.org/10.1016/j.pbb.2018.07.003>
- Tian Z, Dong C, Zhang K, Chang L, Hashimoto K (2018b) Lack of antidepressant effects of low-voltage-sensitive T-type calcium channel blocker ethosuximide in a chronic social defeat stress model: comparison with (R)-ketamine. *Int J Neuropsychopharmacol* 21:1031–1036. <https://doi.org/10.1093/ijnp/pyy072>
- Tracy DK, Wood DM, Baumeister D (2017) Novel psychoactive substances: types, mechanisms of action, and effects. *BMJ* 356:i6848. <https://doi.org/10.1136/bmj.i6848>
- Treccani G et al (2019) S-ketamine reverses hippocampal dendritic spine deficits in flinders sensitive line rats within 1 h of administration. *Mol Neurobiol* 56(11):7368–7379. <https://doi.org/10.1007/s12035-019-1613-3>
- Trimmel H, Helbok R, Staudinger T, Jaksch W, Messerer B, Schochl H, Likar R (2018) S(+)-ketamine: Current trends in emergency and intensive care medicine. *Wien Klin Wochenschr* 130:356–366. <https://doi.org/10.1007/s00508-017-1299-3>
- US Food and Drug Administration (2019) FDA approves new nasal spray medication for treatment-resistant depression; available only at a certified doctor's office or clinic. [PressAnnouncements/ucm632761.htm](https://www.fda.gov/pressannouncements/ucm632761.htm)
- Veraart JKE, Smith-Apeldoorn SY, Trueman H, de Boer MK, Schoevers RA, McShane R (2018) Characteristics of patients expressing an interest in ketamine treatment: results of an online survey. *BJPsych Open* 4:389–392. <https://doi.org/10.1192/bjo.2018.151>
- Vollenweider FX, Leenders KL, Oye I, Hell D, Angst J (1997) Differential psychopathology and patterns of cerebral glucose utilisation produced by (S)- and (R)-ketamine in healthy volunteers using positron emission tomography (PET). *Eur Neuropsychopharmacol* 7:25–38

- White PF, Schuttler J, Shafer A, Stanski DR, Horai Y, Trevor AJ (1985) Comparative pharmacology of the ketamine isomers. *Studies in volunteers*. *Br J Anaesth* 57:197–203. <https://doi.org/10.1093/bja/57.2.197>
- Wilkinson ST et al (2018) The effect of a single dose of intravenous ketamine on suicidal ideation: a systematic review and individual participant data meta-analysis. *Am J Psychiatry* 175:150–158. <https://doi.org/10.1176/appi.ajp.2017.17040472>
- World Health Organization (2011) WHO model list of essential medicines: 17th list, March 2011
- World Health Organization (2017) Depression and other common mental disorders: global health estimates (No. WHO/MSD/MER/2017.2). World Health Organization
- Xiong Z, Zhang K, Ishima T, Ren Q, Chang L, Chen J, Hashimoto K (2018) Comparison of rapid and long-lasting antidepressant effects of negative modulators of alpha5-containing GABA_A receptors and (R)-ketamine in a chronic social defeat stress model. *Pharmacol Biochem Behav* 175:139–145. <https://doi.org/10.1016/j.pbb.2018.10.005>
- Xiong Z et al (2019) Lack of rapid antidepressant effects of Kir4.1 channel inhibitors in a chronic social defeat stress model: Comparison with (R)-ketamine. *Pharmacol Biochem Behav* 176:57–62. <https://doi.org/10.1016/j.pbb.2018.11.010>
- Yang C et al (2015) R-ketamine: a rapid-onset and sustained antidepressant without psychotomimetic side effects. *Transl Psychiatry* 5:e632. <https://doi.org/10.1038/tp.2015.136>
- Yang B et al (2016a) Comparison of R-ketamine and rapastinel antidepressant effects in the social defeat stress model of depression. *Psychopharmacology (Berl)* 233:3647–3657. <https://doi.org/10.1007/s00213-016-4399-2>
- Yang C, Han M, Zhang JC, Ren Q, Hashimoto K (2016b) Loss of parvalbumin-immunoreactivity in mouse brain regions after repeated intermittent administration of esketamine, but not R-ketamine. *Psychiatry Res* 239:281–283. <https://doi.org/10.1016/j.psychres.2016.03.034>
- Yang C, Qu Y, Fujita Y, Ren Q, Ma M, Dong C, Hashimoto K (2017) Possible role of the gut microbiota-brain axis in the antidepressant effects of (R)-ketamine in a social defeat stress model. *Transl Psychiatry* 7:1294. <https://doi.org/10.1038/s41398-017-0031-4>
- Yang C, Ren Q, Qu Y, Zhang JC, Ma M, Dong C, Hashimoto K (2018a) Mechanistic target of rapamycin-independent antidepressant effects of (R)-ketamine in a social defeat stress model. *Biol Psychiatry* 83:18–28. <https://doi.org/10.1016/j.biopsych.2017.05.016>
- Yang Y, Cui Y, Sang K, Dong Y, Ni Z, Ma S, Hu H (2018b) Ketamine blocks bursting in the lateral habenula to rapidly relieve depression. *Nature* 554:317–322. <https://doi.org/10.1038/nature25509>
- Zanos P, Gould TD (2018) Intracellular signaling pathways involved in (s)- and (r)-ketamine antidepressant actions. *Biol Psychiatry* 83:2–4. <https://doi.org/10.1016/j.biopsych.2017.10.026>
- Zanos P, Nelson ME, Highland JN, Krimmel SR, Georgiou P, Gould TD, Thompson SM (2017) A negative allosteric modulator for alpha5 subunit-containing GABA receptors exerts a rapid and persistent antidepressant-like action without the side effects of the NMDA receptor antagonist ketamine in mice. *eNeuro* 4. <https://doi.org/10.1523/ENEURO.0285-16.2017>
- Zanos P et al (2018) Ketamine and ketamine metabolite pharmacology: insights into therapeutic mechanisms. *Pharmacol Rev* 70:621–660. <https://doi.org/10.1124/pr.117.015198>
- Zarate CA Jr et al (2006) A randomized trial of an N-methyl-D-aspartate antagonist in treatment-resistant major depression. *Arch Gen Psychiatry* 63:856–864. <https://doi.org/10.1001/archpsyc.63.8.856>
- Zeithofer HU, Swandulla D, Geisslinger G, Brune K (1992) Differential effects of ketamine enantiomers on NMDA receptor currents in cultured neurons. *Eur J Pharmacol* 213:155–158
- Zhan Y et al (2019) A preliminary study of anti-suicidal efficacy of repeated ketamine infusions in depression with suicidal ideation. *J Affect Disord* 251:205–212. <https://doi.org/10.1016/j.jad.2019.03.071>
- Zhang K, Hashimoto K (2019) An update on ketamine and its two enantiomers as rapid-acting antidepressants. *Expert Rev Neurother* 19:83–92. <https://doi.org/10.1080/14737175.2019.1554434>

- Zhang JC, Li SX, Hashimoto K (2014) R (-)-ketamine shows greater potency and longer lasting antidepressant effects than S (+)-ketamine. *Pharmacol Biochem Behav* 116:137–141. <https://doi.org/10.1016/j.pbb.2013.11.033>
- Zhang JC et al (2015) Comparison of ketamine, 7,8-dihydroxyflavone, and ANA-12 antidepressant effects in the social defeat stress model of depression. *Psychopharmacology (Berl)* 232:4325–4335. <https://doi.org/10.1007/s00213-015-4062-3>
- Zhang GF et al (2016) Acute single dose of ketamine relieves mechanical allodynia and consequent depression-like behaviors in a rat model. *Neurosci Lett* 631:7–12. <https://doi.org/10.1016/j.neulet.2016.08.006>
- Zhang K, Dong C, Fujita Y, Fujita A, Hashimoto K (2018) 5-hydroxytryptamine-independent antidepressant actions of (R)-ketamine in a chronic social defeat stress model. *Int J Neuropsychopharmacol* 21:157–163. <https://doi.org/10.1093/ijnp/pyx100>
- Zhao J, Wang Y, Wang D (2018) The effect of ketamine infusion in the treatment of complex regional pain syndrome: a systemic review and meta-analysis. *Curr Pain Headache Rep* 22:12. <https://doi.org/10.1007/s11916-018-0664-x>
- Zheng W et al (2018) Rapid and longer-term antidepressant effects of repeated-dose intravenous ketamine for patients with unipolar and bipolar depression. *J Psychiatr Res* 106:61–68. <https://doi.org/10.1016/j.jpsychires.2018.09.013>

ARTICLE

Open Access

Essential role of microglial transforming growth factor- β 1 in antidepressant actions of (*R*)-ketamine and the novel antidepressant TGF- β 1

Kai Zhang^{1,5}, Chun Yang^{1,6}, Lijia Chang¹, Akemi Sakamoto², Toru Suzuki³, Yuko Fujita¹, Youge Qu¹, Siming Wang¹, Yaoyu Pu¹, Yunfei Tan¹, Xingming Wang¹, Tamaki Ishima¹, Yukihiko Shirayama^{1,4}, Masahiko Hatano², Kenji F. Tanaka³ and Kenji Hashimoto¹

Abstract

In rodent models of depression, (*R*)-ketamine has greater potency and longer-lasting antidepressant effects than (*S*)-ketamine; however, the precise molecular mechanisms underlying the antidepressant actions of (*R*)-ketamine remain unknown. Using RNA-sequencing analysis, we identified novel molecular targets that contribute to the different antidepressant effects of the two enantiomers. Either (*R*)-ketamine (10 mg/kg) or (*S*)-ketamine (10 mg/kg) was administered to susceptible mice after chronic social defeat stress (CSDS). RNA-sequencing analysis of prefrontal cortex (PFC) and subsequent GSEA (gene set enrichment analysis) revealed that transforming growth factor (TGF)- β signaling might contribute to the different antidepressant effects of the two enantiomers. (*R*)-ketamine, but not (*S*)-ketamine, ameliorated the reduced expressions of *Tgfb1* and its receptors (*Tgfb1* and *Tgfb2*) in the PFC and hippocampus of CSDS susceptible mice. Either pharmacological inhibitors (i.e., RepSox and SB431542) or neutralizing antibody of TGF- β 1 blocked the antidepressant effects of (*R*)-ketamine in CSDS susceptible mice. Moreover, depletion of microglia by the colony-stimulating factor 1 receptor (CSF1R) inhibitor PLX3397 blocked the antidepressant effects of (*R*)-ketamine in CSDS susceptible mice. Similar to (*R*)-ketamine, the recombinant TGF- β 1 elicited rapid and long-lasting antidepressant effects in animal models of depression. Our data implicate a novel microglial TGF- β 1-dependent mechanism underlying the antidepressant effects of (*R*)-ketamine in rodents with depression-like phenotype. Moreover, TGF- β 1 and its receptor agonists would likely constitute a novel rapid-acting and sustained antidepressant in humans.

Introduction

In 1990, Trullas and Skolnick¹ demonstrated that *N*-methyl-D-aspartate receptor (NMDAR) antagonists such as (+)-MK-801 showed antidepressant-like effects in rodents. In 2000, Berman et al.² demonstrated the rapid-acting and sustained antidepressant effects of the NMDAR antagonist ketamine in patients with major

depressive disorder (MDD). Subsequently, several groups replicated the robust antidepressant effects of ketamine in treatment-resistant patients with either MDD or bipolar disorder^{3–10}. Interestingly, ketamine rapidly reduced suicidal thoughts in depressed patients with suicidal ideation within 1 day and for up to 1 week^{11,12}. In addition, it is suggested that suicidal thoughts may be related to symptoms of anhedonia independent of other depressive symptoms¹³. Meta-analyses revealed that ketamine has rapid-acting and sustained antidepressant effects and anti-suicidal ideation effects in treatment-resistant patients with depression^{14–16}. Importantly, meta-analyses showed that the effect sizes of ketamine are larger than those of

Correspondence: Kenji Hashimoto (hashimoto@faculty.chiba-u.jp)

¹Division of Clinical Neuroscience, Chiba University Center for Forensic Mental Health, Chiba 260-8670, Japan

²Department of Biomedical Science, Chiba University Graduate School of Medicine, Chiba 260-8670, Japan

Full list of author information is available at the end of the article.

© The Author(s) 2020



Open Access This article is licensed under a Creative Commons Attribution 4.0 International License, which permits use, sharing, adaptation, distribution and reproduction in any medium or format, as long as you give appropriate credit to the original author(s) and the source, provide a link to the Creative Commons license, and indicate if changes were made. The images or other third party material in this article are included in the article's Creative Commons license, unless indicated otherwise in a credit line to the material. If material is not included in the article's Creative Commons license and your intended use is not permitted by statutory regulation or exceeds the permitted use, you will need to obtain permission directly from the copyright holder. To view a copy of this license, visit <http://creativecommons.org/licenses/by/4.0/>.

other NMDAR antagonists^{14,15}, suggesting that NMDAR blockade is not a sole mechanism of antidepressant action for ketamine. The collective rapid-acting and sustained antidepressant actions of ketamine in depressed patients are serendipitous in the field of psychiatry;^{17–19} however, the precise molecular and cellular mechanisms underlying antidepressant effects of ketamine remain to be elucidated^{20–25}. Off-label use of ketamine is popular in the United States (US), although the adverse side-effects (i.e., psychotomimetic effects, dissociation, and abuse liability) of ketamine remain to be resolved^{26,27}.

Ketamine ($K_i = 0.53 \mu\text{M}$ for NMDAR), also known as (*R,S*)-ketamine, is a racemic mixture that contains equal amounts of (*R*)-ketamine (or arketamine) ($K_i = 1.4 \mu\text{M}$ for NMDAR) and (*S*)-ketamine (or esketamine) ($K_i = 0.30 \mu\text{M}$ for NMDAR)²⁴. Preclinical data have shown that (*R*)-ketamine displays greater potency and longer-lasting antidepressant effects than (*S*)-ketamine in rodent models of depression^{28–34}, suggesting that NMDARs do not play a major role in the robust antidepressant effects of ketamine²⁴. Importantly, in both rodents and monkey, the side-effects of (*R*)-ketamine were lower than were those of (*R,S*)-ketamine and (*S*)-ketamine^{29,35–38}. In addition, in humans, the incidence of psychotomimetic side-effects of (*S*)-ketamine (0.45 mg/kg) was higher than that of (*R*)-ketamine (1.8 mg/kg), although the dose of (*S*)-ketamine was lower than was that of (*R*)-ketamine³⁹. Though (*S*)-ketamine produced psychotic reactions, including depersonalization and hallucinations, the same dosage of (*R*)-ketamine did not induce psychotic symptoms in the healthy subjects, and most of them experienced a state of relaxation⁴⁰. These results indicate that (*S*)-ketamine contributes to the acute side-effects of ketamine, whereas (*R*)-ketamine may not be associated with these side-effects^{22,24}. On 5 March 2019, the US Food & Drug Administration approved (*S*)-ketamine nasal spray for treatment-resistant depressed patients. Due to the risk of serious adverse effects, (*S*)-ketamine nasal spray can be obtained only through a restricted distribution system under the Risk Evaluation and Mitigation Strategy. A clinical trial of (*R*)-ketamine in humans is underway²⁴. Meanwhile, little is known about the precise molecular mechanisms underlying the different antidepressant effects of the two enantiomers^{24,25,41,42}.

The aim of this study was to identify the novel molecular mechanisms underlying the antidepressant effects of (*R*)-ketamine in animal models of depression. First, we conducted RNA-sequencing analysis of the prefrontal cortex (PFC) of chronic social defeat stress (CSDS) susceptible mice treated with either (*R*)-ketamine or (*S*)-ketamine, as PFC contributes to the antidepressant actions of ketamine and its enantiomers^{29,43,44}. Second, we studied the effects of pharmacological inhibitors and a neutralizing antibody of the novel target in the antidepressant effects of (*R*)-ketamine. Finally, we investigated

whether the novel molecule (i.e., TGF- β) has rapid-acting and sustained antidepressant effects in rodent models of depression.

Materials and methods

Animals

Male adult C57BL/6 mice, aged 8 weeks (body weight 20–25 g, Japan SLC, Inc., Hamamatsu, Japan), male CD1 mice, aged 14 weeks (body weight 40–45 g, Japan SLC, Inc., Hamamatsu, Japan) were used in the experiments. Male Sprague-Dawley rats, aged 7 weeks (body weight 200–230 g, Charles-River Japan, Co., Tokyo, Japan) were used for learned helplessness (LH) model. No blinding for animal experiments was done. Animals were housed under controlled temperature and 12 h light/dark cycles (lights on between 07:00–19:00), with ad libitum food and water. The study was approved by the Chiba University Institutional Animal Care and Use Committee.

Compounds and treatment

(*R*)-ketamine hydrochloride and (*S*)-ketamine hydrochloride were prepared by recrystallization of (*R,S*)-ketamine (Ketalar[®], ketamine hydrochloride, Daiichi Sankyo Pharmaceutical Ltd., Tokyo, Japan) and D-(-)-tartaric acid (or L- (+)-tartaric acid), respectively²⁸. The purity of these enantiomers was determined by a high-performance liquid chromatography (CHIRALPAK[®] IA, Column size: 250 × 4.6 mm, Mobile phase: n-hexane/dichloromethane/diethylamine (75/25/0.1), Daicel Corporation, Tokyo, Japan)²⁸. The dose (10 mg/kg as hydrochloride salt) of (*R*)-ketamine and (*S*)-ketamine was selected as reported previously^{28,29,32–35}. RepSox (10 mg/kg, i.p., a TGF- β 1 receptor inhibitor; Selleck Chemicals, Co., Ltd, Houston, TX, USA), SB431542 (10 μM , 2 μl , i.c.v., a TGF- β 1 receptor inhibitor; Tocris Bioscience, Ltd., Bristol, UK), neutralized TGF- β antibody (Catalog #: MAB1835–500; R&D System, Inc. Minneapolis, MN), and mouse IgG1 control antibody (Catalog #: MAB002; R&D System, Inc. Minneapolis, MN) were used. Recombinant mouse TGF- β 1 (Catalog #: 7666-MB-005; R&D System, Inc. Minneapolis, MN) and recombinant mouse TGF- β 2 (Catalog #: 302-B2; R&D System, Inc. Minneapolis, MN) were used as previously reported^{45,46}. PLX3397 [Pexidartinib: a colony-stimulating factor 1 receptor (CSF1R) inhibitor, MedChemExpress Co., Ltd., Monmouth Junction, NJ] was used to decrease microglia in the brain. LPS (Catalog #: L-4130, serotype 0111:B4, Sigma-Aldrich, St Louis, MO, USA) was used for inflammation model of depression. Other reagents were purchased commercially.

CSDS model and LPS-induced model

The procedure of CSDS was performed as previously reported^{29,32–34,47}. Detailed methods were shown in the supplemental information.

RNA-sequencing analysis

(*R*)-Ketamine (10 mg/kg) or (*S*)-ketamine (10 mg/kg) was administered intraperitoneally (i.p.) to susceptible mice after CSDS (Fig. 1a). PFC was collected 3 days after a single administration. RNA-sequencing analysis of PFC samples was performed at Tataka Bio Inc. (Kusatsu, Shiga, Japan). Analysis of the biological functions was performed using gene set enrichment analysis (GSEA) (<http://software.broadinstitute.org/gsea/index.jsp>).

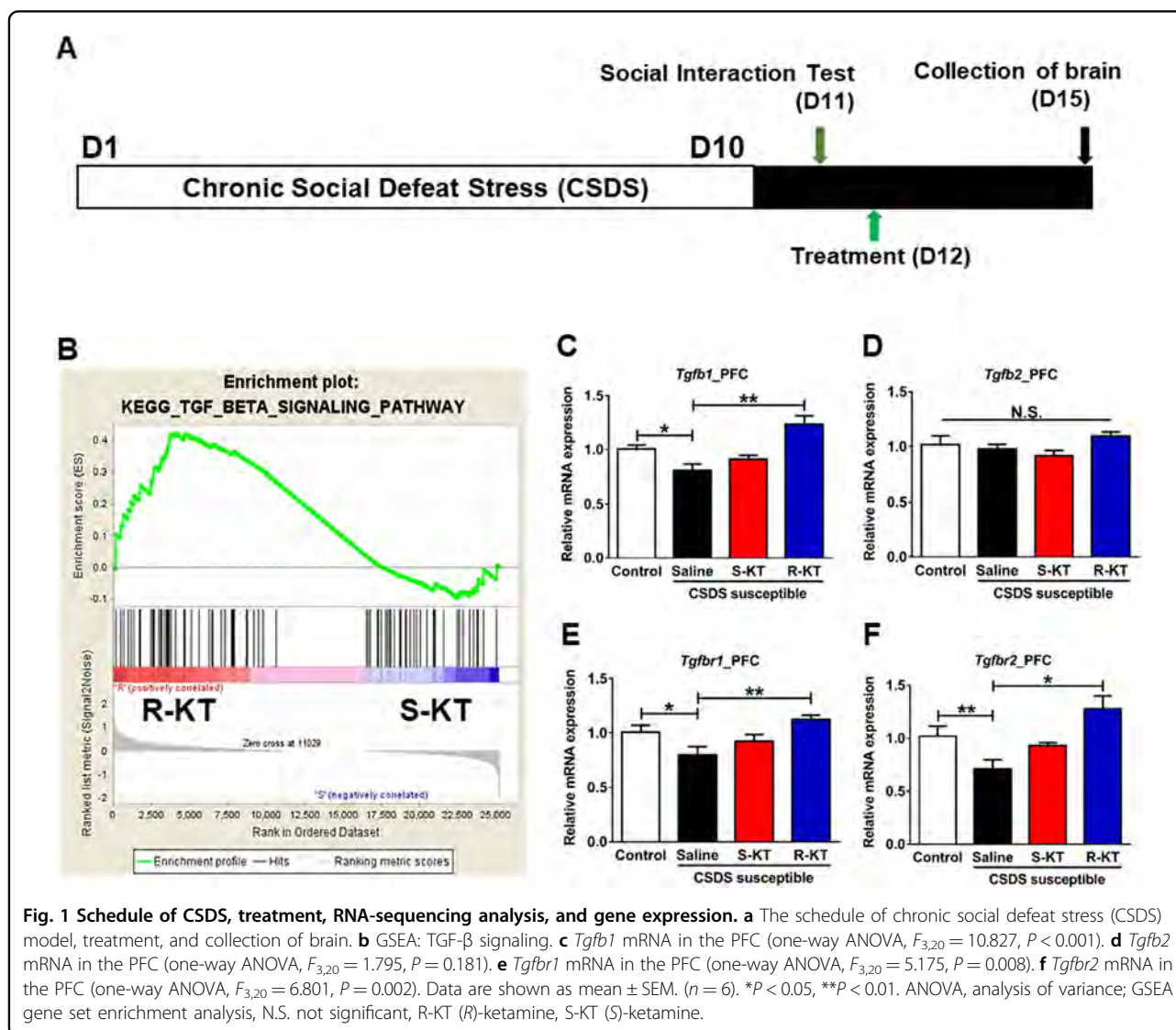
Gene expression analysis by quantitative real-time PCR

Control mice and CSDS susceptible mice were sacrificed 3 days after intraperitoneal (i.p.) administration of saline (10 ml/kg), (*R*)-ketamine (10 mg/kg), or (*S*)-ketamine (10 mg/kg). The PFC and hippocampus were quickly dissected on ice from whole brain since these brain regions play a key role in antidepressant effects of (*R*)-

ketamine⁴⁴. Detailed methods were shown in the supplemental information.

Inhibition of TGF- β 1 inhibitors and neutralizing antibody

To examine the role of TGF- β 1 in the antidepressant effects of (*R*)-ketamine, two inhibitors (RepSox and SB431542) of TGF- β receptor 1 were used. RepSox (10 mg/kg, i.p.) or vehicle (10 ml/kg, i.p.) was injected 30 min before i.p. administration of (*R*)-ketamine (10 mg/kg) in CSDS susceptible mice. SB431542 (10 μ M, 2 μ l, i.c.v.) or vehicle (2 μ l, i.c.v.) was injected 30 min before i.p. administration of (*R*)-ketamine (10 mg/kg) in CSDS susceptible mice. The neutralizing antibody of TGF- β 1 (1 μ g/ml, 2 μ l, i.c.v.) or control antibody (1 μ g/ml, 2 μ l, i.c.v.) was injected 30 min before i.p. administration of (*R*)-ketamine (10 mg/kg) in CSDS susceptible mice. Subsequently, behavioral tests were performed.



Depletion of microglia by PLX3397

PLX3397 was reported to eliminate microglia in the brain^{48–50}. For preliminary experiment, PLX3397 (10 μ M or 100 μ M, 2 μ l, i.c.v.) or vehicle [10% dimethyl sulfoxide (DMSO) and 90% (sulfobutylether- β -cyclodextrin)(SBE- β -CD)] was administered to mice under isoflurane anesthesia. The PFC was collected 6, 12, and 24 h after i.c.v. infusion, and Western blot analysis of Iba1 in the PFC was performed.

To examine the effects of microglia depletion, PLX3397 (100 μ M, 2 μ l, i.c.v.) or vehicle (10% DMSO and 90% SBE- β -CD) was administered to mice under isoflurane anesthesia. PFC was collected 24 h after injection. Right PFC and left PFC were used for FACS analysis and Western blot of Iba1, respectively.

To examine the effects of microglia depletion on antidepressant effects of (*R*)-ketamine, PLX3397 (100 μ M, 2 μ l, i.c.v.) or vehicle (10% DMSO and 90% SBE- β -CD) was administered to CSDS susceptible mice under isoflurane anesthesia. Saline (10 ml/kg) or (*R*)-ketamine (10 mg/kg) was administered i.p. 24 h after injection of PLX3397 or vehicle. Subsequently, behavioral tests were performed.

Antidepressant effects of TGF- β 1 in a CSDS model

Effects of recombinant TGF- β 1 in a CSDS model, LPS model, and LH model were examined. Saline (2 μ L, i.c.v.) or (*R*)-ketamine (1 mg/ml, 2 μ L, i.c.v.) was administered to CSDS susceptible mice. Saline (2 μ L, i.c.v.) was administered to control mice. Subsequently, behavioral tests were performed.

Antidepressant effects of TGF- β 1 in a LPS-induced inflammation model

Inflammation model by lipopolysaccharide (LPS) was performed as previously reported^{51–53}. Saline (10 ml/kg) or LPS (0.5 mg/kg) was administered i.p. to mice. Under isoflurane anesthesia, saline (2 μ l, i.c.v.) or TGF- β 1 (10 ng/ μ l, 2 μ l, i.c.v.) was administered to mice 23 hrs after LPS administration. The locomotion and FST were performed 1 and 3 h after injection, respectively.

For intranasal administration, saline (15 μ l) or TGF- β 1 (1.5 μ g, 15 μ l) was administered to mice 23 hrs after LPS administration, as previously reported³⁸. Mice were restrained by hand, and saline or TGF- β 1 was administered intranasally into awake mice using Eppendorf micropipette (Eppendorf Japan, Tokyo, Japan). The locomotion and FST were performed 1 and 3 h after injection, respectively.

Behavioral tests

Behavioral tests including locomotion, tail suspension test (TST), forced swimming test (FST), and one % sucrose preference test (SPT) were performed as

previously reported^{28,29,32–34}. Detailed methods were shown in the supplemental information.

Learned helplessness (LH) model

Rat LH paradigm was performed as previously reported^{44,54}. Detailed methods were shown in the supplemental information.

Western blot analysis of Iba1

Western blot analysis was performed as reported previously^{29,34,51,52}. Detailed methods were shown in the supplemental information.

Double staining by in situ hybridization and immunohistochemistry

Mice were deeply anesthetized with isoflurane and sodium pentobarbital, and transcardially perfused with 4% paraformaldehyde in 0.1 M phosphate buffer (pH 7.4). The brains were further immersed in the same fixative overnight, cryoprotected in 20% sucrose/phosphate-buffered saline (PBS), and frozen by liquid nitrogen. The brains were sectioned coronally on a cryostat (CM3050S; Leica Biosystems, Germany) at 25 μ m thickness. The cryosections were treated with proteinase K (40 μ g/ml; Merck). After they were washed and acetylated, sections were incubated with a digoxigenin (DIG)-labeled mouse *Tgfb1* (cat#: G430055L01), *Tgfb1* (cat#: F630025J19), or *Tgfb2* (cat#: I420016D17) cRNA probes (DNAFORM, Yokohama, Kanagawa, Japan). After the sections were washed in buffers with serial differences in stringency, they were incubated with an alkaline phosphatase-conjugated anti-DIG antibody (1:5000; Roche, Japan). The cRNA probes were visualized with freshly prepared colorimetric substrate (NBT/BCIP; Roche, Japan). After visualized, sections were incubated with primary antibodies overnight at RT. All antibodies were diluted in PBS with 0.1% Triton X-100. The following antibodies were used: anti-Iba1 (cat#: 019–19741, 1:1000, rabbit, polyclonal; Wako, Japan), and anti-S100b (cat#: ab52642, 1:200, rabbit, monoclonal; Abcam, Cambridge, UK). The sections were sequentially incubated with anti-rabbit IgG biotinylated secondary antibodies (1:250, goat, polyclonal; Vector Laboratories, USA) for 90 min at room temperature (RT), an avidin-biotin complex (Vector Laboratories, USA) for 30 min at RT, and then the colorimetric reactions were developed with DAB (3,3'-diaminobenzidine) (ImmPACT DAB; Vector Laboratories, USA). Images of the sections were captured using a light microscope (BZ-X710; Keyence, Japan).

FACS analysis

Mouse PFC tissues were mashed and passed through a 70 μ m mesh to prepare single cell suspension then subjected for FACS analysis. Cells were stained with

monoclonal antibodies against cell surface antigens at 4 °C for 30 min, then washed with PBS. In indicated cells, cells were fixed and permeabilized using FoxP3 staining buffer set (Invitrogen) according to the manufacturer instruction. Then intracellular antigens were stained with indicated antibodies at room temperature for 30 min. The following antibodies were used for staining; anti TMEM119-PE (Abcam, Cambridge, UK), allophycocyanin conjugated anti CD11b (BD Bioscience, Franklin Lakes, NJ), anti Iba1-FITC (Abcam), anti TGF- β -allophycocyanin (BioLegend, San Diego, CA). The stained cells were analyzed using FACSCantII and FlowJo software (BD).

Statistical analysis

The data show as the mean \pm standard error of the mean (S.E.M.). Analysis was performed using PASW Statistics 20 (formerly SPSS Statistics; SPSS). The data were analyzed using Student *t*-test or the one-way analysis of

variance (ANOVA), followed by post hoc Tukey test. The *P*-values < 0.05 were considered statistically significant.

Results

RNA-sequencing analysis of PFC samples

To identify the novel molecular targets for the antidepressant effects of (*R*)-ketamine, we collected PFC samples 3 days after either (*R*)-ketamine (10 mg/kg) or (*S*)-ketamine (10 mg/kg) were administered to CSDS susceptible mice. We performed RNA-sequencing analysis of PFC samples from animals treated with either (*R*)-ketamine or (*S*)-ketamine (Fig. 1a). GSEA revealed that TGF- β signaling might be involved in the differential antidepressant effects of the two enantiomers (Fig. 1b). We found reduced expression of *Tgfb1* and its receptors (*Tgfr1* and *Tgfr2*) in the PFC and hippocampus from CSDS susceptible mice (Fig. 1c–f and Fig. S1). Conversely, the expression of *Tgfb2* in the PFC and the hippocampus did not differ in the four groups (Fig. 1c–f and Fig. S1).

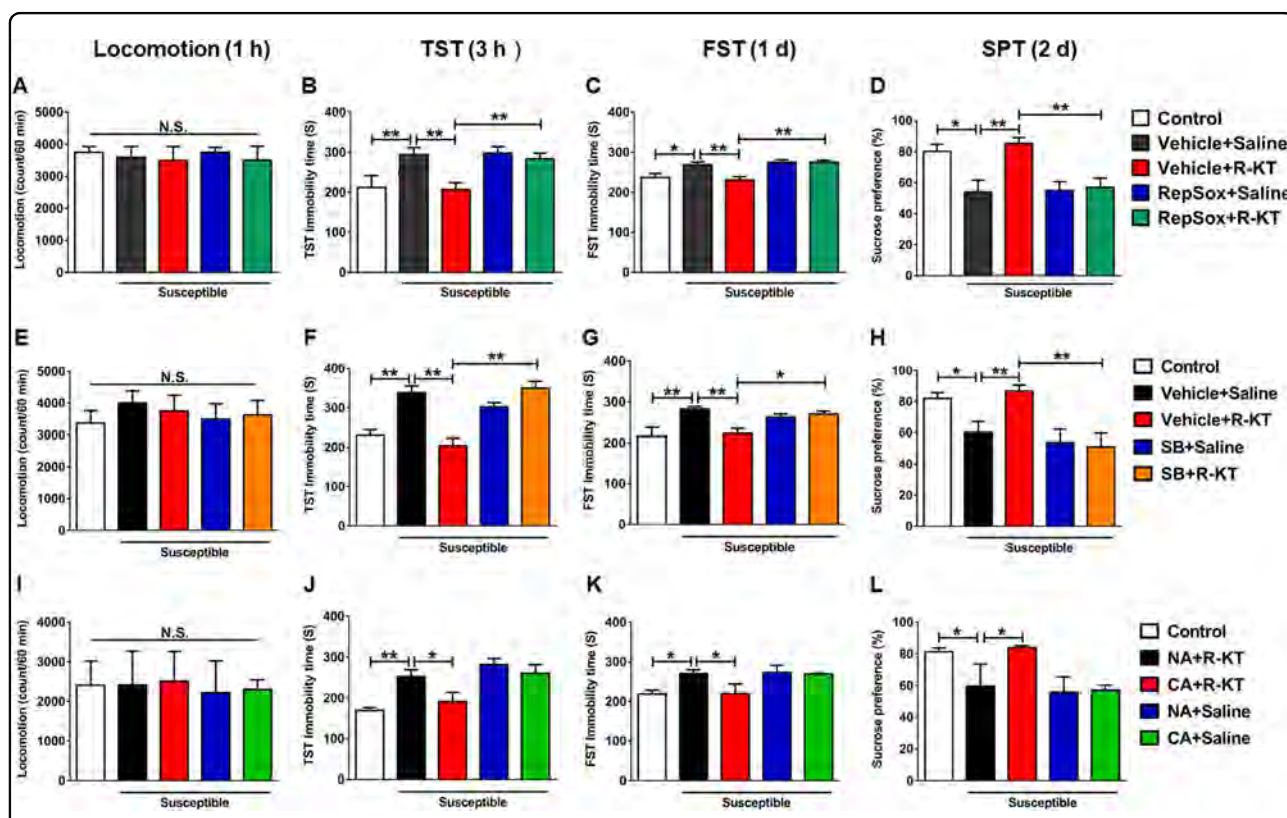


Fig. 2 Effects of TGF- β 1 inhibitors (RepSox and SB431542) and neutralizing TGF- β 1 antibody on antidepressant effects of (*R*)-ketamine in CSDS model. **a** Locomotion (1 h, one-way ANOVA, $F_{4,35} = 0.146$, $P = 0.964$). **b** TST (3 h, one-way ANOVA, $F_{4,35} = 5.439$, $P = 0.002$). **c** FST (1 day, one-way ANOVA, $F_{4,35} = 2.919$, $P = 0.035$). **d** SPT (2 days, one-way ANOVA, $F_{4,35} = 7.011$, $P < 0.001$). Data are shown as mean \pm SEM. ($n = 8$). * $P < 0.05$, ** $P < 0.01$. **e** Locomotion (1 h, one-way ANOVA, $F_{4,35} = 0.299$, $P = 0.877$). **f** TST (3 h, one-way ANOVA, $F_{4,35} = 16.586$, $P < 0.001$). **g** FST (1 day, one-way ANOVA, $F_{4,35} = 4.686$, $P = 0.004$). **h** SPT (2 day, one-way ANOVA, $F_{4,35} = 6.161$, $P = 0.001$). **i** Locomotion (1 h, one-way ANOVA, $F_{4,25} = 0.020$, $P = 0.999$). **j** TST (3 h, one-way ANOVA, $F_{4,35} = 8.165$, $P < 0.001$). **k** FST (1 day, one-way ANOVA, $F_{4,35} = 4.012$, $P = 0.015$). **l** SPT (2 day, one-way ANOVA, $F_{4,35} = 3.872$, $P = 0.021$). Data are shown as mean \pm SEM. ($n = 8$). * $P < 0.05$, ** $P < 0.01$. ANOVA analysis of variance, CA control antibody, FST forced swimming test, NA neutralizing antibody, N.S. not significant, R-KT (*R*)-ketamine, SB SB431542, SPT sucrose preference test, TST tail suspension test.

Interestingly, (*R*)-ketamine (10 mg/kg), but not (*S*)-ketamine (10 mg/kg), significantly ameliorated the reduced expression of these genes (Fig. 1c–f and Fig. S1).

Effects of TGF- β 1 inhibitors and neutralizing antibody in the antidepressant effects of (*R*)-ketamine

To study the role of TGF- β 1 in the antidepressant effects of (*R*)-ketamine, we used two TGF- β receptor 1 inhibitors: RepSox and SB431542. Pretreatment with RepSox (10 mg/kg, i.p., 30 min) significantly blocked the antidepressant effects of (*R*)-ketamine in CSDS susceptible mice (Fig. 2a–d). Likewise, pretreatment with SB431542 (10 μ M, 2 μ l, i.c.v., 30 min) significantly blocked the antidepressant effects of (*R*)-ketamine in CSDS susceptible mice (Fig. 2e–h). Moreover, pretreatment with neutralizing antibody of TGF- β 1 (1 μ g/ml, 2 μ l, i.c.v., 30 min) significantly blocked the antidepressant effects of (*R*)-ketamine in CSDS susceptible mice (Fig. 2i–l). These findings indicate that TGF- β 1 might contribute to the antidepressant effects of (*R*)-ketamine in CSDS susceptible mice.

Role of microglial TGF- β 1

TGF- β 1 is constitutively expressed in microglia into adulthood⁵⁵. An earlier study demonstrated that TGF- β 1 was necessary for the *in vitro* development of microglia and that microglia were absent in the brain of TGF- β 1-deficient mice⁵⁶, suggesting that TGF- β 1 plays a key role in microglia. Microglia rely on cytokine signaling, such as activation of CSF1R and TGF- β 1, for their survival⁵⁷. *In situ* hybridization with cell-type marker immunostaining revealed high expression of *Tgfb1* and its receptors (*Tgfb1* and *Tgfb2*) in microglia, but not in astrocytes, in mouse brain PFC (Fig. 3).

To examine whether microglia TGF- β 1 contributes to the antidepressant effects of (*R*)-ketamine, we studied the impact of microglial depletion on the antidepressant effects of (*R*)-ketamine. Preliminary experimentation revealed that i.c.v. injection of PLX3397, a potent CSF1R inhibitor, reduced the Iba1 protein in the mouse PFC (Fig. S2). In this study, we used the time (24 h) of PLX3397 (100 μ M, 2 μ l, i.c.v.). Using FACS analysis, we analyzed the expression of both Iba1 and TGF- β 1 in TMEM119⁺CD11b⁺ microglia in the PFC. Pretreatment with PLX3397 significantly reduced the expression of both TGF- β 1 and Iba1 in TMEM119⁺CD11b⁺ microglia (Fig. 4a–c). Furthermore, Western blot analysis revealed that PLX3397 injection reduced Iba1 protein in the PFC (Fig. 4d). These findings indicate partial depletion of microglia by PLX3397 in the PFC.

Next, we studied the impact of PLX3397 on the antidepressant effects of (*R*)-ketamine in CSDS susceptible mice (Fig. 5a). There were no changes in locomotion among the five groups (Fig. 5b). Findings from the TST and the forced

swim test (FST), showed that PLX3397 significantly blocked the antidepressant effects of (*R*)-ketamine for increased immobility time of both TST and FST (Fig. 5c, d). In the SPT, PLX3397 significantly blocked the effects of (*R*)-ketamine for reduced sucrose preference in CSDS susceptible mice (Fig. 5e). Collectively, partial depletion of microglia by PLX3397 significantly blocked the antidepressant effects of (*R*)-ketamine in CSDS susceptible mice (Fig. 5). These findings indicate that microglia-expressing molecules, including TGF- β 1 and its receptors, contribute to the antidepressant effects of (*R*)-ketamine in a CSDS model.

Antidepressant effects of TGF- β 1 in rodent models of depression

Finally, we studied whether mouse recombinant TGF- β 1 has antidepressant effects in three animal models of depression. First, we studied the effects of TGF- β 1 and TGF- β 2 in the CSDS model (Fig. 6a). There were no changes in locomotion in the four groups (Fig. 6b, h). A single i.c.v. injection of (*R*)-ketamine (1 mg/ml, 2 μ l) produced rapid and sustained antidepressant effects in CSDS susceptible mice, consistent with the previous report⁵⁸. Similar to (*R*)-ketamine, i.c.v. infusion of TGF- β 1 (10 ng/ml, 2 μ l) significantly the increased

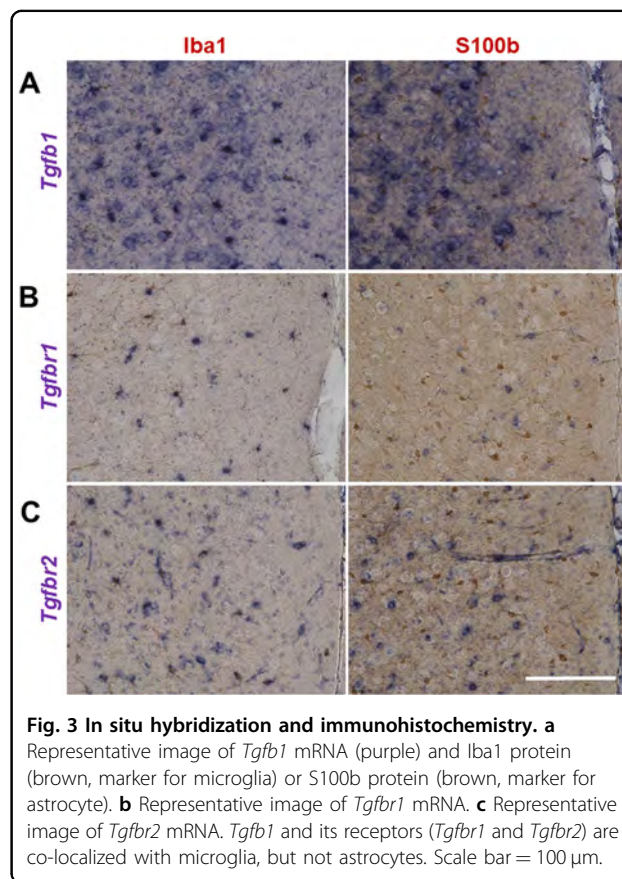
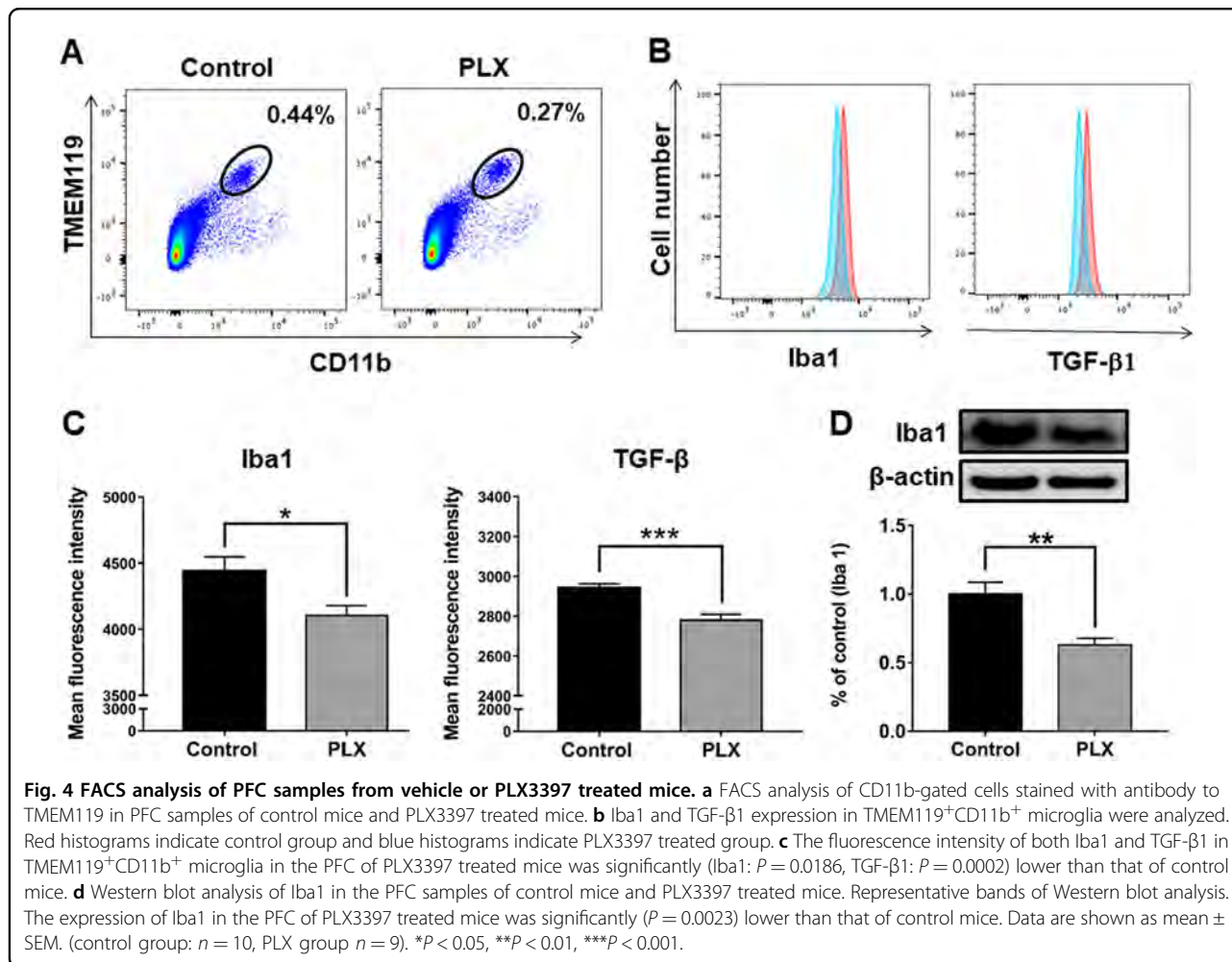


Fig. 3 *In situ* hybridization and immunohistochemistry. **a** Representative image of *Tgfb1* mRNA (purple) and Iba1 protein (brown, marker for microglia) or S100b protein (brown, marker for astrocyte). **b** Representative image of *Tgfb1* mRNA. **c** Representative image of *Tgfb2* mRNA. *Tgfb1* and its receptors (*Tgfb1* and *Tgfb2*) are co-localized with microglia, but not astrocytes. Scale bar = 100 μ m.



immobility time of both TST and FST in CSDS susceptible mice (Fig. 6c, d). In the SPT, i.c.v. infusion of TGF- β 1 significantly reduced sucrose preference in CSDS susceptible mice (Fig. 6e-g). Interestingly, we detected the beneficial effects of TGF- β 1 seven days after a single injection (Fig. 6g), indicating long-lasting antidepressant effects of TGF- β 1. Conversely, TGF- β 2 (10 ng/ml, 2 μ l) did not produce antidepressant effects in CSDS susceptible mice, though (*R*)-ketamine (1 mg/ml, 2 μ l) produced rapid and sustained antidepressant effects in the same model (Fig. 6h-l).

Moreover, a single i.c.v. infusion of TGF- β 1 (10 ng/ml, 2 μ l) significantly attenuated the increased immobility time of FST in LPS (0.5 mg/kg)-treated mice (Fig. 7a-c). In addition, a single intranasal administration of TGF- β 1 (1.5 μ g, 15 μ l) significantly attenuated the increased immobility time of FST in LPS-treated mice (Fig. 7d-f). In a rat LH model, bilateral i.c.v. infusion of TGF- β 1 (250 ng/side) significantly reduced the failure number and latency of LH rats 4 days after i.c.v. injection (Fig. 7g-i). These findings indicate that

recombinant TGF- β 1 has ketamine-like robust antidepressant effects in rodent models of depression.

Discussion

The main findings of this study are as follows: First, RNA-sequencing and GSEA revealed the role of TGF- β signaling in the beneficial antidepressant effects of (*R*)-ketamine compared with (*S*)-ketamine. RT-PCR revealed reduced expression of *Tgfb1* and its receptors (*Tgfb1* and *Tgfb2*) in the PFC and the hippocampus from CSDS susceptible mice. Furthermore, (*R*)-ketamine, but not (*S*)-ketamine, attenuated the reduced expression of these genes in the PFC and the hippocampus of CSDS susceptible mice. Second, pharmacological inhibitors and neutralizing antibody of TGF- β 1 blocked the antidepressant effects of (*R*)-ketamine in CSDS susceptible mice, indicating a role of TGF- β 1 signaling in the antidepressant effects of (*R*)-ketamine. Third, partial depletion of microglia by PLX3397 blocked antidepressant effects of (*R*)-ketamine in CSDS susceptible mice, indicating a role of microglia in the antidepressant

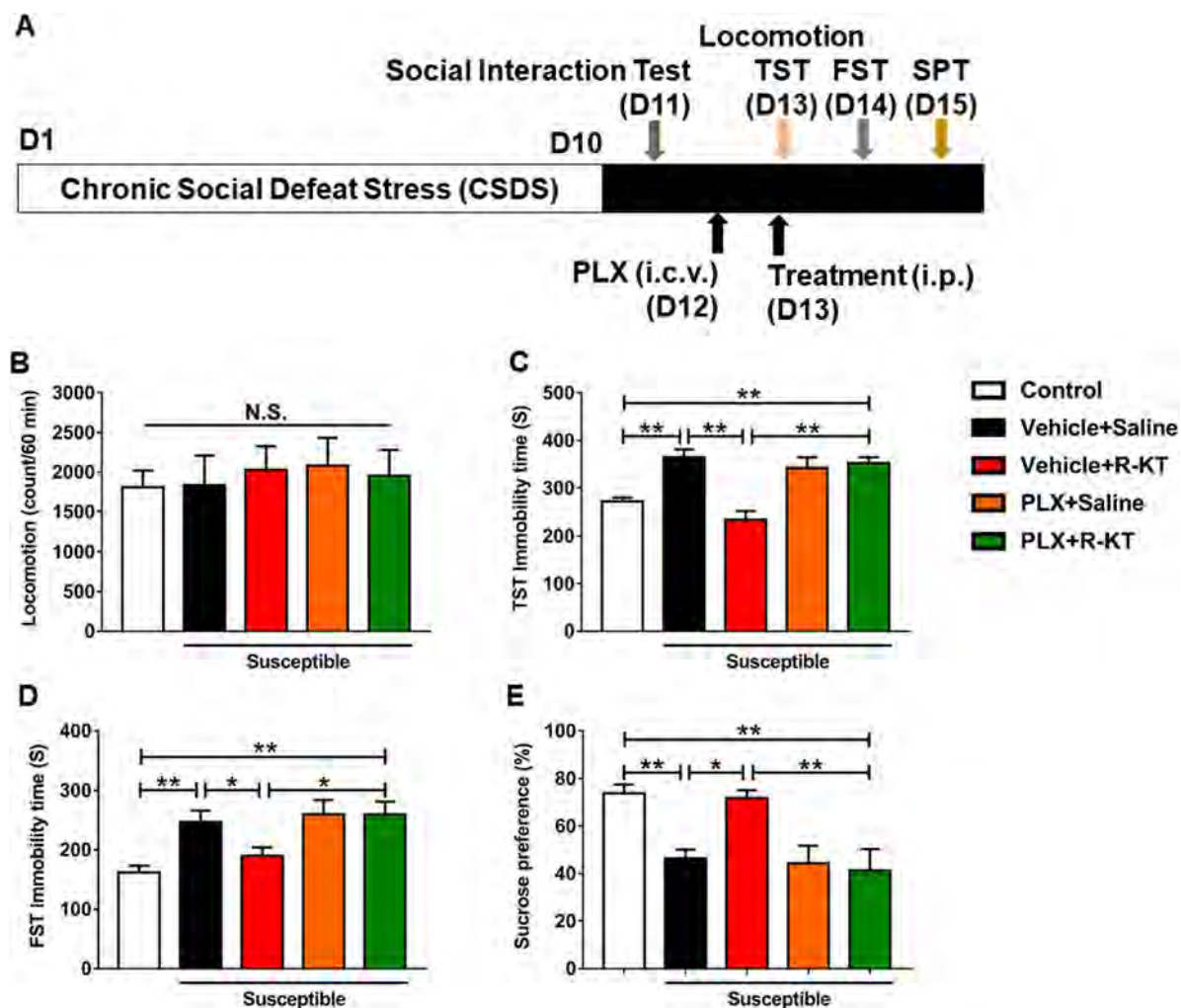


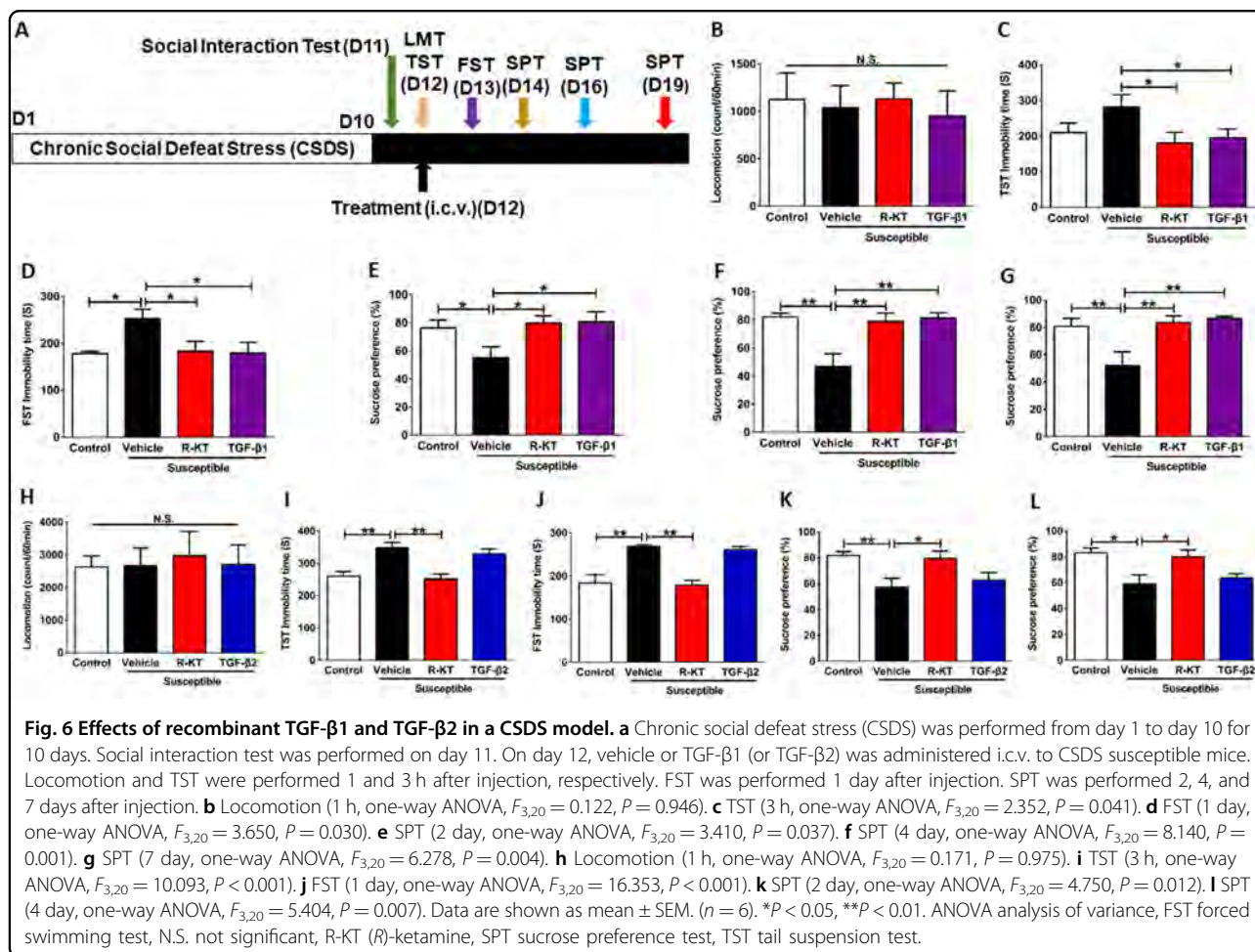
Fig. 5 Effects of PLX3397 on antidepressant effects of (*R*)-ketamine in a CSDS model. **a** Chronic social defeat stress (CSDS) was performed from day 1 to day 10 for 10 days. Social interaction test was performed on day 11. On day 12, vehicle or PLX3397 was administered i.c.v. to CSDS susceptible mice. On day 13, saline or (*R*)-ketamine (10 mg/kg) was administered i.p. 24 h after injection of PLX3397. Locomotion and FST were performed 1 and 3 h after injection, respectively. FST and SPT were performed 1 and 2 days after injection, respectively. **b** Locomotion (1 h, one-way ANOVA, $F_{4,35} = 0.226$, $P = 0.921$). **c** TST (3 h, one-way ANOVA, $F_{4,35} = 13.706$, $P < 0.001$). **d** FST (1 day, one-way ANOVA, $F_{4,35} = 5.362$, $P = 0.005$). **e** SPT (2 day, one-way ANOVA, $F_{4,35} = 6.045$, $P = 0.003$). Data are shown as mean \pm SEM. ($n = 8$). * $P < 0.05$, ** $P < 0.01$. ANOVA analysis of variance, FST forced swimming test, N.S. not significant, PLX PLX3397, R-KT (*R*)-ketamine, SPT sucrose preference test, TST tail suspension test.

effects of (*R*)-ketamine. Lastly, recombinant TGF- β 1 elicited rapid-acting and long-lasting antidepressant effects in CSDS, LPS, and LH models of depression. Overall, it appears likely that (*R*)-ketamine can exert antidepressant effects by normalizing microglial TGF- β 1 signaling in the PFC and the hippocampus of CSDS susceptible mice. Furthermore, TGF- β 1 has ketamine-like antidepressant effects in rodent models.

Microglia are the only cell type that express CSF1R. CSF1R knockout mice are devoid of microglia⁵⁹. Moreover, it has been reported that repeated treatment with CSF1R inhibitors, such as PLX3397, cause a dramatic reduction in the number of microglia within the adult brain^{48–50}.

Interestingly, microglia are absent in the brains of central nervous system TGF- β 1 knockout mice⁵⁶. Thus, microglia in the adult brain are physiologically dependent upon CSF1R and TGF- β 1 signaling⁵⁷. In this study, a single i.c.v. injection of PLX3397 produced significant reduction of Iba1 and TGF- β 1 in the PFC, suggesting partial depletion of microglia in the PFC. Interestingly, pretreatment of PLX3397 significantly blocked the antidepressant effects of (*R*)-ketamine in CSDS susceptible mice. Overall, it appears likely that microglial TGF- β 1 in the PFC might contribute to the antidepressant effects of (*R*)-ketamine.

In this study, i.c.v. infusion of TGF- β 1 produced rapid-acting and long-lasting antidepressant effects in a CSDS

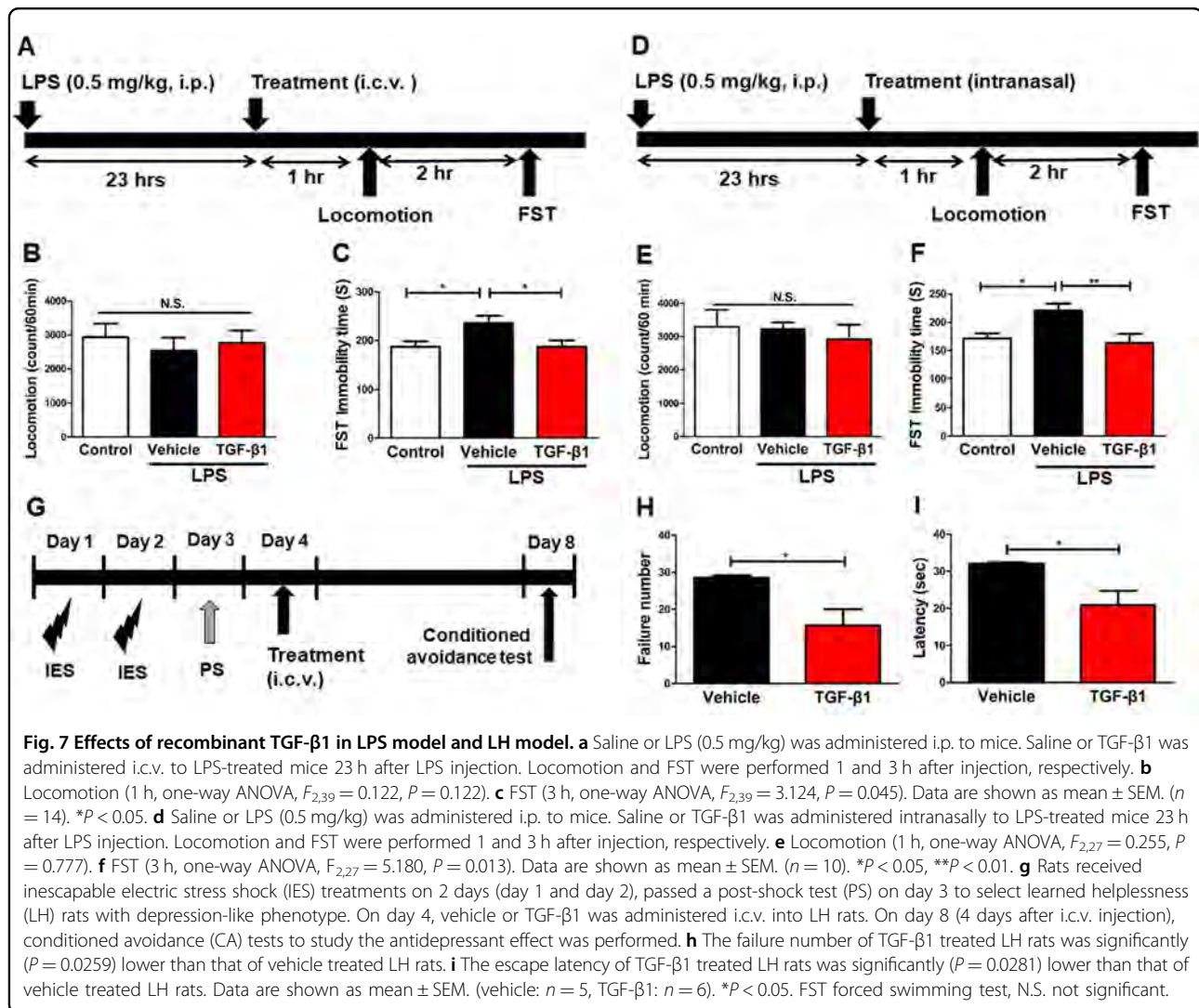


model, an LPS-induced model, and an LH model. Notably, we detected the antidepressant effects of TGF- β 1 in a CSDS model and an LH model 7 days and 4 days after a single dose, respectively. Collectively, the antidepressant effects of TGF- β 1 in these models are similar to those of (R)-ketamine, suggesting that TGF- β 1 has (R)-ketamine-like long-lasting antidepressant effects. Taylor et al⁶⁰ showed that a single i.c.v. injection of TGF- β 1 4 h after intracerebral hemorrhage (ICH) produced complete recovery of motor function at 24 h, and that this recovery persisted for at least one week. Furthermore, i.c.v. injection of TGF- β 1 alleviated N-methyl-4-phenylpyridinium ion (MPP⁺)-induced microglial inflammatory response and dopaminergic neuronal loss in the substantia nigra, indicating that TGF- β 1 plays a role in the pathology of Parkinson's disease (PD). Collectively, it is possible that TGF- β 1 can produce rapid and long-lasting beneficial effects in several models, such as depression, ICH, and PD.

Notably, intranasal administration of TGF- β 1 has rapid-acting antidepressant effects in LPS-treated mice. A previous study showed that intranasal administration of TGF- β 1 ameliorated neurodegeneration in the mouse

brain after β -amyloid₁₋₄₂ injection⁴⁴. It has also been reported that TGF- β 1 administered intranasally entered several brain regions, such as the PFC and the hippocampus, of control adult mice, whereas no increase was observed in the blood and peripheral organs⁶¹, indicating good permeability of the blood brain barrier for TGF- β 1. It is also reported that CSDS alters blood brain barrier integrity through loss of tight junction protein Cldn5⁶². In addition, TGF- β 1 might be free of the psychotomimetic side-effects of ketamine and its potential for abuse in humans, as TGF- β 1 does not interact with NMDAR in the brain. Therefore, it is likely that intranasal administration of TGF- β 1 would be a novel potential therapeutic approach for depression.

This study has some limitations. In this study, we used the CSF1R inhibitor to delete microglia in the brain although the partial depletion of microglia was detected. It is of great interest to investigate the role of microglia in the antidepressant effects of (R)-ketamine using CSF1R knockout mice since CSF1R knockout mice are devoid of microglia⁵⁹. Furthermore, it is also of interest to investigate the role of microglial TGF- β 1 in the antidepressant



effects of (*R*)-ketamine using TGF-β1 knockout mice since microglia were absent in the brain of TGF-β1 knockout mice⁵⁶.

In conclusion, this study shows that TGF-β1 in the microglia might contribute to the antidepressant effects of (*R*)-ketamine in animal models of depression. Furthermore, similar to (*R*)-ketamine, TGF-β1 seems to rapid-acting and long-lasting antidepressant effects. Therefore, it is likely that TGF-β1 would be a new rapid-acting and sustained antidepressant.

Acknowledgements

This study was supported by JSPS KAKENHI (to K.Z., 19K17054), AMED (to K.H., JP19dm0107119).

Author details

¹Division of Clinical Neuroscience, Chiba University Center for Forensic Mental Health, Chiba 260-8670, Japan. ²Department of Biomedical Science, Chiba University Graduate School of Medicine, Chiba 260-8670, Japan. ³Department of Neuropsychiatry, Keio University School of Medicine, Tokyo 160-8585, Japan.

⁴Department of Psychiatry, Teikyo University Chiba Medical Center, Chiba 299-0111, Japan. ⁵Present address: Department of Psychiatry, Chaohu Hospital of Anhui Medical University, Hefei 238000, China. ⁶Present address: Department of Anesthesiology and Perioperative Medicine, The First Affiliated Hospital of Nanjing Medical University, Nanjing 210029, China

Conflict of interest

K. H. is an inventor on the filed patent on "The use of (*R*)-ketamine in the treatment of psychiatric diseases" and "Transforming growth factor β1 in the treatment of depression". Other authors declare no conflict of interest.

Publisher's note

Springer Nature remains neutral with regard to jurisdictional claims in published maps and institutional affiliations.

Supplementary Information accompanies this paper at (<https://doi.org/10.1038/s41398-020-0733-x>).

Received: 13 November 2019 Revised: 2 January 2020 Accepted: 13 January 2020

Published online: 27 January 2020

References

- Trullas, R. & Skolnick, P. Functional antagonists at the NMDA receptor complex exhibit antidepressant actions. *Eur. J. Pharm.* **185**, 1–10 (1990).
- Berman, R. M. et al. Antidepressant effects of ketamine in depressed patients. *Biol. Psychiatry* **47**, 351–354 (2000).
- Zarate, C. A. Jr et al. A randomized trial of an N-methyl-D-aspartate antagonist in treatment-resistant major depression. *Arch. Gen. Psychiatry* **63**, 856–864 (2006).
- Murrough, J. W. et al. Antidepressant efficacy of ketamine in treatment-resistant major depression: a two-site randomized controlled trial. *Am. J. Psychiatry* **170**, 1134–1142 (2013).
- Diazgranados, N. et al. A randomized add-on trial of an N-methyl-D-aspartate antagonist in treatment-resistant bipolar depression. *Arch. Gen. Psychiatry* **67**, 793–802 (2010).
- Zarate, C. A. Jr et al. Replication of ketamine's antidepressant efficacy in bipolar depression: a randomized controlled add-on trial. *Biol. Psychiatry* **71**, 939–946 (2012).
- Singh, J. B. et al. A double-blind, randomized, placebo-controlled, dose-frequency study of intravenous ketamine in patients with treatment-resistant depression. *Am. J. Psychiatry* **173**, 816–826 (2016).
- Su, T. P. et al. Dose-related effects of adjunctive ketamine in Taiwanese patients with treatment-resistant depression. *Neuropsychopharmacology* **42**, 2482–2492 (2017).
- Phillips, J. L. et al. Single, repeated, and maintenance ketamine infusions for treatment-resistant depression: a randomized controlled trial. *Am. J. Psychiatry* **176**, 401–409 (2019).
- Fava, M. et al. Double-blind, placebo-controlled, dose-ranging trial of intravenous ketamine as adjunctive therapy in treatment-resistant depression (TRD). *Mol. Psychiatry* <https://doi.org/10.1038/s41380-018-0256-5> (2018).
- Murrough, J. W. et al. Ketamine for rapid reduction of suicidal ideation: a randomized controlled trial. *Psychol. Med.* **45**, 3571–3580 (2015).
- Grunebaum, M. F. et al. Ketamine for rapid reduction of suicidal thoughts in major depression: A midazolam-controlled randomized clinical trial. *Am. J. Psychiatry* **175**, 327–335 (2018).
- Ballard, E. D. et al. Anhedonia as a clinical correlate of suicidal thoughts in clinical ketamine trials. *J. Affect. Disord.* **218**, 195–200 (2017).
- Newport, D. J. et al. Ketamine and other NMDA antagonists: early clinical trials and possible mechanisms in depression. *Am. J. Psychiatry* **172**, 950–966 (2015).
- Kishimoto, T. et al. Single-dose infusion ketamine and non-ketamine N-methyl-D-aspartate receptor antagonists for unipolar and bipolar depression: a meta-analysis of efficacy, safety and time trajectories. *Psychol. Med.* **46**, 1459–1472 (2016).
- Wilkinson, S. T. et al. The effect of a single dose of intravenous ketamine on suicidal ideation: a systematic review and individual participant data meta-analysis. *Am. J. Psychiatry* **175**, 150–158 (2018).
- Duman, R. S. Ketamine and rapid-acting antidepressants: a new era in the battle against depression and suicide. *F1000Res* **7**, F1000 (2018).
- Krystal, J. H., Abdallah, C. G., Sanacora, G., Charney, D. & Duman, R. S. Ketamine: a paradigm shift for depression research and treatment. *Neuron* **101**, 774–778 (2019).
- Zhang, K. & Hashimoto, K. An update on ketamine and its two enantiomers as rapid-acting antidepressants. *Expert Rev. Neurother.* **19**, 83–92 (2019).
- Monteggia, L. M. & Zarate, C. A. Jr Antidepressant actions of ketamine: from molecular mechanisms to clinical practice. *Curr. Opin. Neurobiol.* **30**, 139–143 (2015).
- Murrough, J. W., Abdallah, C. G. & Mathew, S. J. Targeting glutamate signaling in depression: progress and prospects. *Nat. Rev. Drug Discov.* **16**, 472–486 (2017).
- Zanos, P. et al. Ketamine and ketamine metabolites pharmacology: Insights into therapeutic mechanisms. *Pharm. Rev.* **70**, 621–660 (2018).
- Gould, T. D., Zarate, C. A. Jr & Thompson, S. M. Molecular pharmacology and neurobiology of rapid-acting antidepressants. *Annu. Rev. Pharm. Toxicol.* **59**, 213–236 (2019).
- Hashimoto, K. Rapid-acting antidepressant ketamine, its metabolites and other candidates: a historical overview and future perspective. *Psychiatry Clin. Neurosci.* **73**, 613–627 (2019).
- Yang, C., Yang, J., Luo, A. & Hashimoto, K. Molecular and cellular mechanisms underlying the antidepressant effects of ketamine enantiomers and its metabolites. *Transl. Psychiatry* **9**, 280 (2019).
- Sanacora, G. et al. A consensus statement on the use of ketamine in the treatment of mood disorders. *JAMA Psychiatry* **74**, 399–405 (2017).
- Reardon, S. "Party drug" turned antidepressant approaches approval. *Nat. Rev. Drug Discov.* **17**, 773–775 (2018).
- Zhang, J. C., Li, S. X. & Hashimoto, K. R(-)-ketamine shows greater potency and longer lasting antidepressant effects than S(+)-ketamine. *Pharm. Biochem. Behav.* **116**, 137–141 (2014).
- Yang, C. et al. R-ketamine: a rapid-onset and sustained antidepressant without psychotomimetic side effects. *Transl. Psychiatry* **5**, e632 (2015).
- Zanos, P. et al. NMDAR inhibition-independent antidepressant actions of ketamine metabolites. *Nature* **533**, 481–486 (2016).
- Fukamoto, K. et al. Antidepressant potential of (R)-ketamine in rodent models: Comparison with (S)-ketamine. *J. Pharm. Exp. Ther.* **361**, 9–16 (2017).
- Yang, C. et al. (R)-Ketamine shows greater potency and longer lasting antidepressant effects than its metabolite (2R,6R)-hydroxynorketamine. *Biol. Psychiatry* **82**, e43–e44 (2017).
- Yang, C. et al. Possible role of the gut microbiota-brain axis in the antidepressant effects of (R)-ketamine in a social defeat stress model. *Transl. Psychiatry* **7**, 1294 (2017).
- Yang, C. et al. Mechanistic target of rapamycin-independent antidepressant effects of (R)-ketamine in a social defeat stress model. *Biol. Psychiatry* **83**, 18–28 (2018).
- Yang, C., Han, M., Zhang, J. C., Ren, Q. & Hashimoto, K. Loss of parvalbumin-immunoreactivity in mouse brain regions after repeated intermittent administration of esketamine, but not R-ketamine. *Psychiatry Res.* **239**, 281–283 (2016).
- Hashimoto, K., Kakiuchi, T., Ohba, H., Nishiyama, S. & Tsukada, H. Reduction of dopamine D_{2/3} receptor binding in the striatum after a single administration of esketamine, but not R-ketamine: a PET study in conscious monkeys. *Eur. Arch. Psychiatry Clin. Neurosci.* **267**, 173–176 (2017).
- Tian, Z., Dong, C., Fujita, A., Fujita, Y. & Hashimoto, K. Expression of heat shock protein HSP-70 in the retrosplenial cortex of rat brain after administration of (R,S)-ketamine and (S)-ketamine, but not (R)-ketamine. *Pharm. Biochem. Behav.* **172**, 17–21 (2018).
- Chang, L. et al. Comparison of antidepressant and side effects in mice after intranasal administration of (R,S)-ketamine, (R)-ketamine, and (S)-ketamine. *Pharm. Biochem. Behav.* **181**, 53–59 (2019).
- Mathisen, L. C., Skjelbred, P., Skoglund, L. A. & Oye, I. Effect of ketamine, an NMDA receptor inhibitor, in acute and chronic orofacial pain. *Pain* **61**, 215–220 (1995).
- Vollenweider, F. X., Leenders, K. L., Oye, I., Hell, D. & Angst, J. Differential psychopathology and patterns of cerebral glucose utilisation produced by (S)- and (R)-ketamine in healthy volunteers using positron emission tomography (PET). *Eur. Neuropsychopharmacol.* **7**, 25–38 (1997).
- Hashimoto, K. R-ketamine: a rapid-onset and sustained antidepressant without risk of brain toxicity. *Psychol. Med.* **46**, 2449–2451 (2016).
- Hashimoto, K. Ketamine's antidepressant action: beyond NMDA receptor inhibition. *Expert Opin. Ther. Targets* **20**, 1389–1392 (2016).
- Fuchikami, M. et al. Optogenetic stimulation of infralimbic PFC reproduces ketamine's rapid and sustained antidepressant actions. *Proc. Natl Acad. Sci. USA* **112**, 8106–8111 (2015).
- Shirayama, Y. & Hashimoto, K. Effects of a single bilateral infusion of R-ketamine in the rat brain regions of a learned helplessness model of depression. *Eur. Arch. Psychiatry Clin. Neurosci.* **267**, 177–182 (2017).
- Chen, J. H., Ke, K. F., Lu, J. H., Qiu, Y. H. & Peng, Y. P. Protection of TGF- β 1 against neuroinflammation and neurodegeneration in A β ₁₋₄₂-induced Alzheimer's disease model rats. *PLoS ONE* **10**, e0116549 (2015).
- Chen, X., Liu, Z., Cao, B. B., Qiu, Y. H. & Peng, Y. P. TGF- β 1 neuroprotection via inhibition of microglial activation in a rat model of Parkinson's disease. *J. Neuroimmune Pharm.* **12**, 433–446 (2017).
- Golden, S. A., Covington, H. E. R. 3rd, Berton, O. & Russo, S. J. A standardized protocol for repeated social defeat stress in mice. *Nat. Protoc.* **6**, 1183–1191 (2011).
- Elmore, M. R. et al. Colony-stimulating factor 1 receptor signaling is necessary for microglia viability, unmasking a microglia progenitor cell in the adult brain. *Neuron* **82**, 380–397 (2014).
- Tang, Y. et al. Interaction between astrocytic colony stimulating factor and its receptor on microglia mediates central sensitization and behavioral hypersensitivity in chronic post ischemic pain model. *Brain Behav. Immun.* **68**, 248–260 (2018).
- Liang, Y. J. et al. Contribution of microglial reaction to increased nociceptive responses in high-fat-diet (HFD)-induced obesity in male mice. *Brain Behav. Immun.* **80**, 777–792 (2019).

51. Zhang, J. C. et al. Antidepressant effects of TrkB ligands on depression-like behavior and dendritic changes in mice after inflammation. *Int. J. Neuropsychopharmacol.* **18**, pyu077 (2014).
52. Ma, M. et al. Antidepressant effects of combination of brexpiprazole and fluoxetine on depression-like behavior and dendritic changes in mice after inflammation. *Psychopharmacology* **234**, 525–533 (2017).
53. Zhang, K. & Hashimoto, K. Lack of opioid system in the antidepressant actions of ketamine. *Biol. Psychiatry* **85**, e25–e27 (2019).
54. Shirayama, Y. & Hashimoto, K. Lack of antidepressant effects of (2*R*,6*R*)-hydroxynorketamine in a rat learned helplessness model: comparison with (*R*)-ketamine. *Int. J. Neuropsychopharmacol.* **21**, 84–88 (2018).
55. Kiefer, R., Streit, W. J., Toyka, K. V., Kreutzberg, G. W. & Hartung, H. P. Transforming growth factor- β 1: a lesion-associated cytokine of the nervous system. *Int. J. Dev. Neurosci.* **13**, 331–339 (1995).
56. Butovsky, O. et al. Identification of a unique TGF- β -dependent molecular and functional signature in microglia. *Nat. Neurosci.* **17**, 131–143 (2014).
57. Priller, J. & Prinz, M. Targeting microglia in brain disorders. *Science* **365**, 32–33 (2019).
58. Zhang, K., Fujita, Y. & Hashimoto, K. Lack of metabolism in (*R*)-ketamine's antidepressant actions in a chronic social defeat stress model. *Sci. Rep.* **8**, 4007 (2018).
59. Erbilich, B., Zhu, L., Etgen, A. M., Dobrenis, K. & Pollard, J. W. Absence of colony stimulation factor-1 receptor results in loss of microglia, disrupted brain development and olfactory deficits. *PLoS ONE* **6**, e26317 (2011).
60. Taylor, R. A. et al. TGF- β 1 modulates microglial phenotype and promotes recovery after intracerebral hemorrhage. *J. Clin. Invest.* **127**, 280–292 (2017).
61. Ma, Y. P. et al. Intranasally delivered TGF- β 1 enters brain and regulates gene expressions of its receptors in rats. *Brain Res. Bull.* **74**, 271–277 (2007).
62. Menard, C. et al. Social defeat induces neurovascular pathology promoting depression. *Nat. Neurosci.* **20**, 1752–1760 (2017).



Research paper

Antibiotic-induced microbiome depletion is associated with resilience in mice after chronic social defeat stress



Siming Wang, Youge Qu, Lijia Chang, Yaoyu Pu, Kai Zhang, Kenji Hashimoto*

Division of Clinical Neuroscience, Chiba University Center for Forensic Mental Health, Chiba 260-8670, Japan

ARTICLE INFO

Keywords:

Anhedonia
Antibiotic
Chronic social defeat stress
Gut microbiota
Resilience
Susceptibility

ABSTRACT

Background: The brain–gut axis plays a role in the pathogenesis of stress-related disorders such as depression. However, the role of brain–gut axis in the resilience versus susceptibility after stress remains unclear. Here, we examined the effects of antibiotic-induced microbiome depletion on an anhedonia-like phenotype in adult mice subjected to chronic social defeat stress (CSDS).

Methods: Using CSDS paradigm, we investigated the effects of antibiotic-induced microbiome depletion on the resilience versus susceptibility in mice.

Results: Treatment with an antibiotic cocktail for 14 days significantly decreased the diversity and composition of the microbiota in the host gut. *Proteobacteria* were markedly increased after treatment with the antibiotic cocktail. At the genus and species levels, the antibiotic-treated group exhibited marked alterations in the microbiota compared with a control group. CSDS was shown to significantly improve the abnormal composition of gut microbiota in the antibiotic-treated group. CSDS did not produce an anhedonia-like phenotype in the antibiotic-treated mice, but did induce an anhedonia-like phenotype in control mice, suggesting that gut bacteria are essential for the development of CSDS-induced anhedonia. CSDS treatment did not alter the plasma levels of interleukin-6 or the expression of synaptic proteins, such as PSD-95 and GluA1, in the prefrontal cortex of antibiotic-treated mice.

Limitations: Specific microbiome were not determined.

Conclusions: These findings suggest that antibiotic-induced microbiome depletion contributed to resilience to anhedonia in mice subjected to CSDS. Therefore, it is likely that the brain–gut axis plays a role in resilience versus susceptibility to stress.

1. Introduction

In the past two decades, the gut microbiota has been recognized as a fundamental player in host physiology and pathology. The gut microbiota is prominently involved in the development and education of the immune system (Becattini et al., 2016; Cerf-Bensussan and Gaboriau-Routhiau, 2010; Round and Mazmanian, 2009). The brain–gut axis is a complex multi-organ bidirectional signaling system involving the gut microbiota and the brain, and plays a fundamental role in host physiology, homeostasis, development, and metabolism (Cusotto et al., 2018, 2019; Dinan and Cryan, 2017; Forsythe et al., 2016; Fung et al., 2017; Kelly et al., 2016; Ma et al., 2019; Molina-Torres et al., 2019; Zhu et al., 2019). Multiple lines of evidence suggest that an abnormal composition of microbiota in the host gut may contribute to the pathogenesis of stress-related diseases such as depression (Huang et al., 2019b; Jiang et al., 2015; Wong et al., 2016; Yang et al., 2019;

Zheng et al., 2016) and may affect the antidepressant actions of certain compounds (Burokas et al., 2017; Ho and Ross, 2017; Huang et al., 2019a; Lukic et al., 2019; Qu et al., 2017; Yang et al., 2017b; Zhang et al., 2017). Gut microbiota may also contribute to resilience versus susceptibility to anhedonia in rodents after repeated stress (Bailey et al., 2011; Hao et al., 2019; Szyszkowicz et al., 2017; Yang et al., 2017a). We found higher levels of *Bifidobacterium* in resilient mice compared with susceptible mice after chronic social defeat stress (CSDS), and supplementation with *Bifidobacterium* produced resilience in mice after CSDS, suggesting a role for *Bifidobacterium* in stress resilience (Yang et al., 2017a). It has also been reported that specific clusters of bacterial communities in the cecum may be linked to vulnerability to CSDS (Szyszkowicz et al., 2017).

Antibiotics are often beneficial, but can also be potentially harmful drugs. The abuse of antibiotics plays a role in the pathogenesis of several diseases associated with the impairment of microbiota

* Corresponding author.

E-mail address: hashimoto@faculty.chiba-u.jp (K. Hashimoto).<https://doi.org/10.1016/j.jad.2019.09.064>

Received 15 August 2019; Received in revised form 4 September 2019; Accepted 13 September 2019

Available online 13 September 2019

0165-0327/ © 2019 Elsevier B.V. All rights reserved.

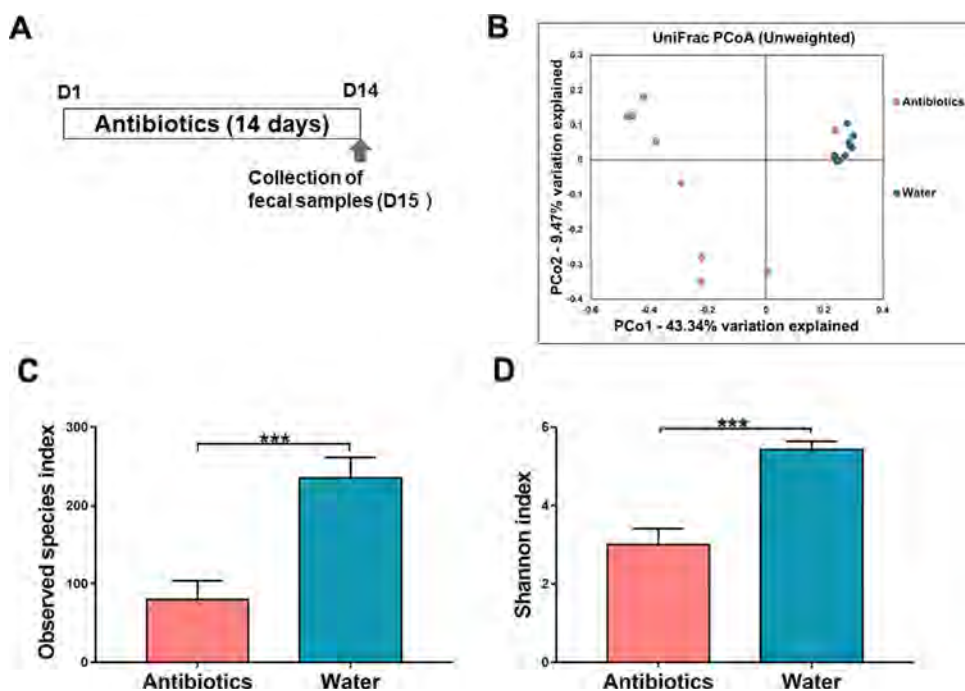


Fig. 1. Effects of antibiotic cocktail in the diversity of gut microbiota.

(A): The schedule of drinking water in antibiotic cocktail and feces collection. Drinking water including antibiotic cocktail or water was given to adult mice from day 1 to day 14. On day 15, feces were collected. (B): UniFrac PCoA of gut bacteria data. (C): Observed species index. (D): Shannon index. Data are shown as mean \pm S.E.M. ($n = 10$). $***P < 0.001$. NS: not significant.

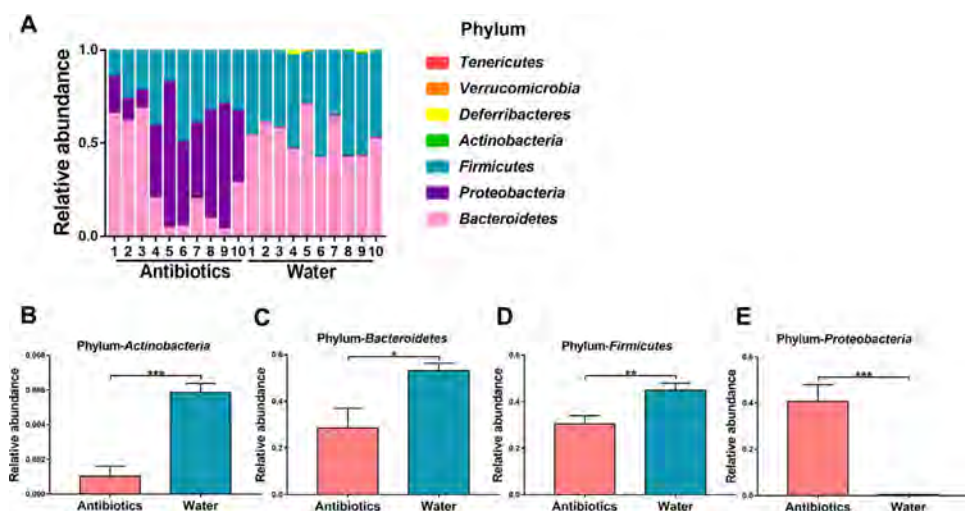


Fig. 2. Altered composition in the gut bacteria at the phylum level.

(A): The relative abundances of microbiome at phylum level in fecal samples of the two groups after repeated treatment with antibiotics for 14 days. (B): *Actinobacteria*. (C): *Bacteroidetes*. (D): *Firmicutes*. (E): *Proteobacteria*. Data are shown as mean \pm S.E.M. ($n = 10$). $*P < 0.05$, $**P < 0.01$, $***P < 0.001$. NS: not significant.

(Champagne-Jorgensen et al., 2019; Ianiro et al., 2016). Instead of germ-free mice, antibiotic cocktail-induced microbiome depletion has been used to investigate the role of gut microbiota in some pathological conditions (Hernandez-Chirlaque et al., 2016; Pu et al., 2019; Sampson et al., 2016; Zhan et al., 2018; Zhang et al., 2019). For example, dextran sulfate sodium (DSS) has been shown to cause colitis in mice, although mice treated with an antibiotic cocktail did not show DSS-induced colitis, suggesting that enteric bacteria are essential for the development of DSS-induced colitis (Hernandez-Chirlaque et al., 2016). Yang et al. (2019) reported that transplantation of fecal microbiota from rats with an anhedonia-like phenotype aggravated depression-like and anhedonia-like phenotypes in mice treated with an antibiotic cocktail. It appears likely that gut microbiota play a key role in the pathology of inflammation-related diseases such as colitis and depression. However, the effects of antibiotic-induced microbiome depletion on inflammation and anhedonia-like phenotype in rodents subjected to CSDS are unknown.

Anhedonia (loss of pleasure) is a core symptom of major depressive disorder. The neurobiological mechanisms of anhedonia remain poorly understood (Treadway and Zald, 2011). Therefore, we hypothesized

that antibiotic-induced microbiome depletion may affect the resilience of mice to anhedonia after CSDS. The purpose of this study was, therefore, to investigate the role of gut microbiota in anhedonia-like phenotypes in mice after CSDS. First, we examined whether repeated administration of an antibiotic cocktail for 14 days affected the diversity and composition of gut microbiota in mouse feces. Then, we examined whether antibiotic-induced microbiome depletion could affect the anhedonia-like phenotype, inflammation, and synaptic proteins in mice after CSDS, since CSDS causes an anhedonia-like phenotype through inflammation in the periphery (Zhang et al., 2017).

2. Materials and methods

2.1. Animals

Male adult C57BL/6 mice ($n = 40$), aged 8 weeks with a body weight of 20–25 g and male adult CD1 (ICR) mice ($n = 20$), aged 13–15 weeks with a body weight > 40 g (Japan SLC, Inc., Hamamatsu, Japan) were used. Animals were housed under controlled temperatures with 12 h light/dark cycles (lights on between 07:00 and 19:00), with ad

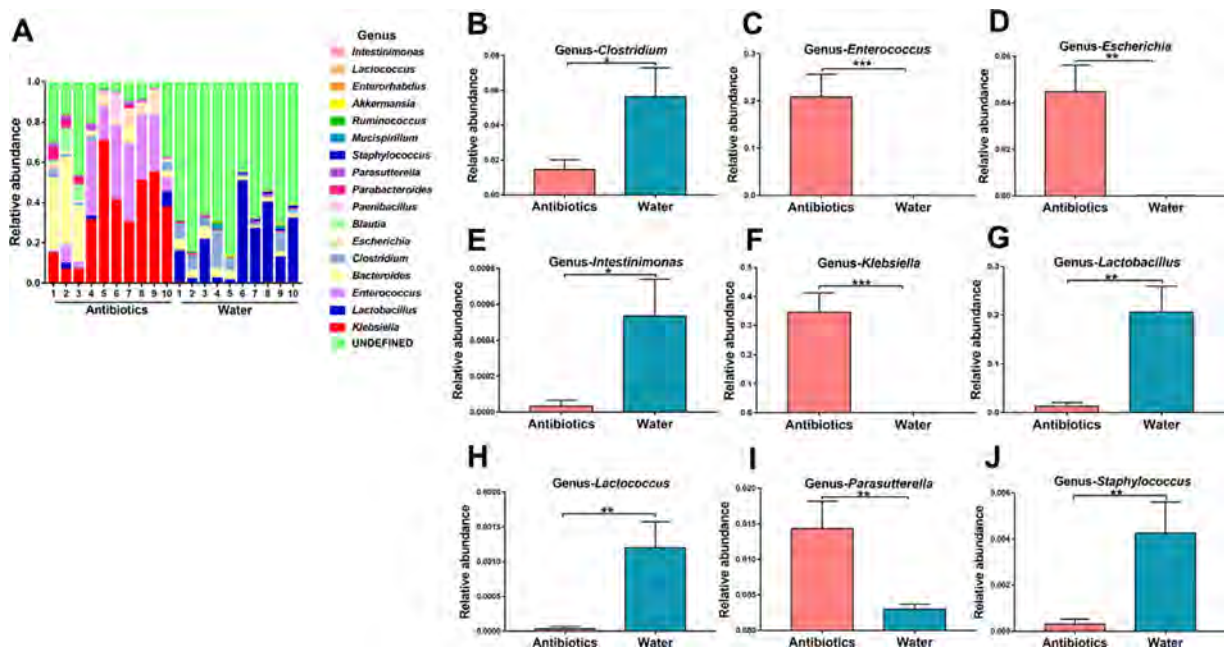


Fig. 3. Altered composition in the gut bacteria at the genus level. (A): The relative abundances of microbiome at genus level in fecal samples of the two groups after repeated treatment with antibiotics for 14 days. (B): *Clostridium*. (C): *Enterococcus*. (D): *Escherichia*. (E): *Intestinimonas*. (F): *Klebsiella*. (G): *Lactobacillus*. (H): *Lactococcus*. (I): *Parasutterella*. (J): *Staphylococcus*. Data are shown as mean ± S.E.M. (n = 10). **P* < 0.05, ***P* < 0.01, ****P* < 0.001. NS: not significant.

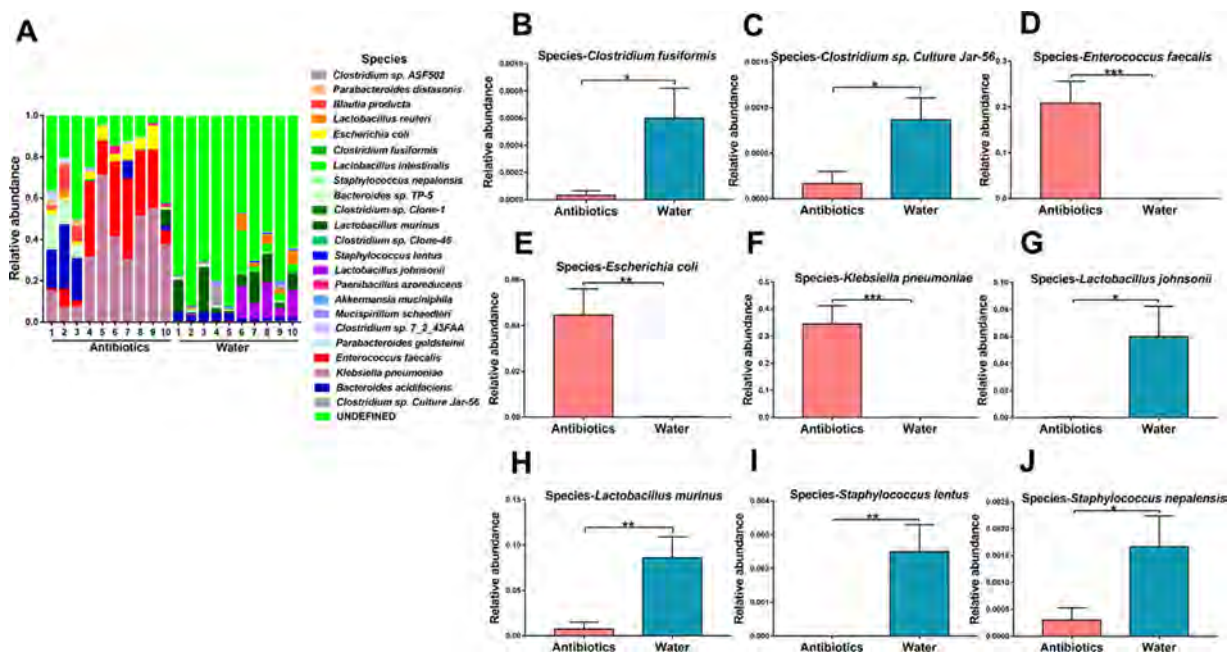


Fig. 4. Altered composition in the gut bacteria at the species level. (A): The relative abundances of microbiome at species level in fecal samples of the two groups after repeated treatment with antibiotics for 14 days. (B): *Clostridium fusiformis*. (C): *Clostridium sp. Culture Jar-56*. (D): *Enterococcus faecalis*. (E): *Escherichia coli*. (F): *Klebsiella pneumoniae*. (G): *Lactobacillus johnsonii*. (H): *Lactobacillus murinus*. (I): *Staphylococcus nepalensis*. Data are shown as mean ± S.E.M. (n = 10). **P* < 0.05, ***P* < 0.01, ****P* < 0.001. NS: not significant.

libitum access to food (CE-2; CLEA Japan, Inc., Tokyo, Japan) and water. The protocol was approved by the Chiba University Institutional Animal Care and Use Committee (Permission number: 30–399). This study was carried out in strict accordance with the recommendations in the Guide for the Care and Use of Laboratory Animals of the National Institutes of Health, USA. Animals were deeply anesthetized with isoflurane before being killed by cervical dislocation. All efforts were made to minimize suffering. CSDS was performed from 13:00 to 17:00,

and one percent sucrose preference tests (SPT) were performed from 17:00 to 18:00.

2.2. Treatment with antibiotic cocktail, CSDS and behavioral tests

Based upon previous reports (Pu et al., 2019; Yang et al., 2019; Zhan et al., 2018; Zhang et al., 2019b), broad-spectrum antibiotics (ampicillin 1 g/L, neomycin sulfate 1 g/L, and metronidazole 1 g/L,

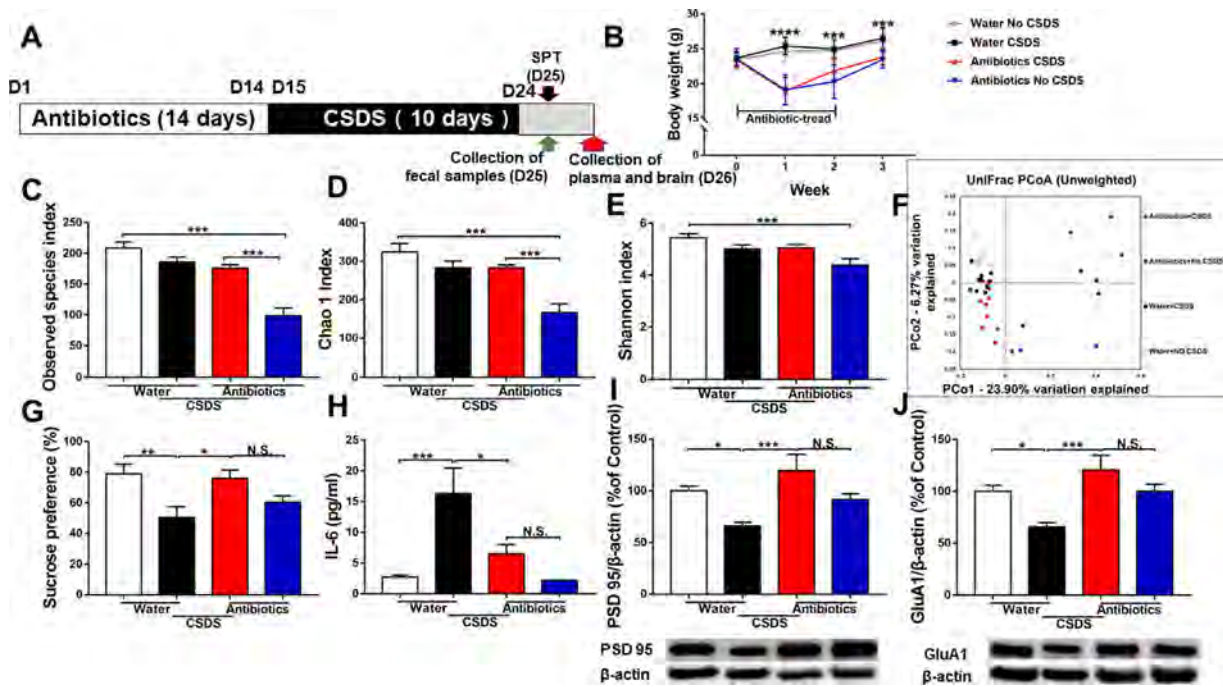


Fig. 5. Effects of antibiotics in the anhedonia-like phenotype in mice after CSDS.

(A): The schedule of antibiotics treatment, CSDS model, sucrose preference test and feces collection. Antibiotic cocktail or water in drinking water was given to mice for 14 days. Subsequently, CSDS was performed for 10 days from day 14 to day 24, and 1% sucrose preference test (SPT) was performed on day 25. On day 25, fresh feces were collected. On day 26, plasma and PFC were collected. (B): Body weight (repeated two-way ANOVA, antibiotics: $F_{1,36} = 52.436$, $P < 0.001$, CSDS: $F_{1,36} = 1.267$, $P = 0.268$, interaction: $F_{1,36} = 0.21$, $P = 0.885$). (C): Observed species index (two-way ANOVA, antibiotics: $F_{1,36} = 41.206$, $P < 0.001$, CSDS: $F_{1,36} = 8.378$, $P = 0.006$, interaction: $F_{1,36} = 28.863$, $P < 0.001$). (D): Chao 1 index (two-way ANOVA, antibiotics: $F_{1,36} = 18.192$, $P < 0.001$, CSDS: $F_{1,36} = 4.302$, $P = 0.045$, interaction: $F_{1,36} = 183.528$, $P < 0.001$). (E): Shannon index (two-way ANOVA, antibiotics: $F_{1,36} = 8.111$, $P = 0.007$, CSDS: $F_{1,36} = 0.448$, $P = 0.508$, interaction: $F_{1,36} = 9.493$, $P = 0.004$). (F): PCoA analysis of gut bacteria data. (G) Sucrose preference test (two-way ANOVA, antibiotics: $F_{1,36} = 0.357$, $P = 0.554$, CSDS: $F_{1,36} = 1.157$, $P = 0.289$, interaction: $F_{1,36} = 14.108$, $P = 0.001$). (H): Plasma IL-6 (two-way ANOVA, antibiotics: $F_{1,36} = 5.072$, $P = 0.031$, CSDS: $F_{1,36} = 16.133$, $P < 0.001$, interaction: $F_{1,36} = 4.322$, $P = 0.045$). (I): PSD 95 (two-way ANOVA, antibiotics: $F_{1,36} = 6.613$, $P = 0.014$, CSDS: $F_{1,36} = 0.114$, $P = 0.737$, interaction: $F_{1,36} = 12.465$, $P = 0.001$). (J): GluA1 (two-way ANOVA, antibiotics: $F_{1,36} = 10.163$, $P = 0.003$, CSDS: $F_{1,36} = 0.604$, $P = 0.442$, interaction: $F_{1,36} = 10.267$, $P = 0.003$). Data are shown as mean \pm S.E.M. ($n = 10$). * $P < 0.05$, ** $P < 0.01$, *** $P < 0.001$. NS: not significant.

Sigma-Aldrich Co. Ltd, MO, USA) dissolved in drinking water were provided ad libitum to male C57BL/6 mice for 14 consecutive days, as reported previously (Pu et al., 2019; Yang et al., 2019; Zhan et al., 2018; Zhang et al., 2019b). The drinking solution was renewed every 2 days. Fresh fecal samples were collected on day 15 before CSDS. We collected fresh fecal samples from each mouse at around 10:00 in order to avoid circadian effects on the microbiome. We also collected fecal samples when each mouse was placed in a new, clean cage. The fecal samples were put into a sterilized screw cap microtube immediately after defecation, and these samples were stored at -80°C until use.

Mice were divided into four groups: water + no CSDS; water + CSDS; antibiotics + no CSDS; and antibiotics + CSDS. The CSDS procedure was performed as previously reported (Golden et al., 2011; Qu et al., 2017; Yang et al., 2016, 2017b, 2015; Zhang et al., 2015, 2017). The C57BL/6 mice were exposed to a different CD1 aggressor mouse for 10 min per day for 10 consecutive days (day 15 to day 24). When the social defeat session ended, the resident CD1 mouse and the intruder mouse were housed in opposite sides of the cage, separated by a perforated Plexiglas divider to allow visual, olfactory, and auditory contact for the remainder of the 24-h period. At 24 h after the last session, all mice were housed individually. Control C57BL/6 mice without exposure to CSDS were housed in the cage before the behavioral tests.

On day 25, 1% SPTs were performed from 17:00 to 18:00, to identify anhedonia-like phenotypes. Mice were exposed to water and 1% sucrose solution for 48 h, followed by 4 h of water and food deprivation and a 1-h exposure to two identical bottles containing either water or a 1% sucrose solution. The bottles containing water and

sucrose were weighed before and at the end of this period. The sucrose preference was calculated as the ratio of sucrose solution consumption to total liquid consumption.

On day 25 (before SPT), fresh fecal samples were collected as described above, and stored at -80°C until use. On day 26, plasma and brain samples from the prefrontal cortex (PFC) were collected after anesthesia with 5% isoflurane. Tissues from the PFC were dissected from the brains on ice using a Leica microscope S9E (Leica Microsystems, Tokyo, Japan). We selected the PFC because the expression of synaptic proteins such as PSD-95 and GluA1 was significantly reduced in the PFC of CSDS-susceptible mice (Yang et al., 2016, 2015; Zhang et al., 2015). Plasma and PFC were stored at -80°C until use.

2.3. ELISA measurement of pro-inflammatory cytokine IL-6

Plasma levels of interleukin-6 (IL-6) were measured, because we previously found an increase in blood IL-6 in the CSDS model (Zhang et al., 2017). The plasma IL-6 levels were measured using the ELISA kit (Invitrogen, cat#: 88-7064-22) according to the manufacturer's instructions.

2.4. Western blot analysis

The PFC tissues were homogenized in Laemmli lysis buffer. The protein levels of 10 μg aliquots were measured using DC protein assay kits (Bio-Rad, Hercules, CA, USA) and incubated for 5 min at 95°C , with an equal volume of 125 mM Tris/HCl (pH 6.8), 20% glycerol, 0.1%

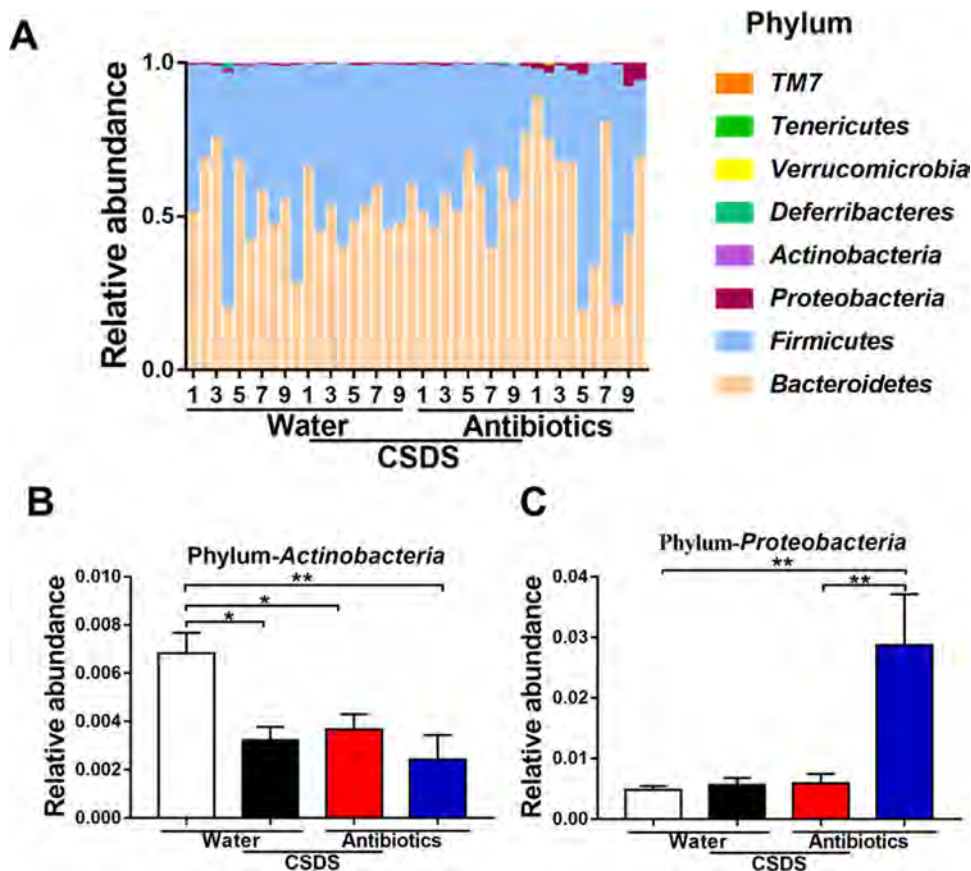


Fig. 6. Altered composition in the gut bacteria at the phylum level.

(A): The relative abundances of phylum in fecal samples of the four groups 24 hrs after CSDS. (B): *Actinobacteria* (two-way ANOVA, antibiotics: $F_{1,36} = 6.560$, $P = 0.015$, CSDS: $F_{1,36} = 2.335$, $P = 0.135$, interaction: $F_{1,36} = 9.740$, $P = 0.004$). (C): *Proteobacteria* (two-way ANOVA, antibiotics: $F_{1,36} = 7.943$, $P = 0.008$, CSDS: $F_{1,36} = 6.646$, $P = 0.014$, interaction: $F_{1,36} = 7.555$, $P = 0.009$). Data are shown as mean \pm S.E.M. ($n = 10$). * $P < 0.05$, ** $P < 0.01$, *** $P < 0.001$. NS: not significant.

bromophenol blue, 10% β -mercaptoethanol, and 4% sodium dodecyl sulfate, and subjected to sodium dodecyl sulfate polyacrylamide gel electrophoresis using 10% mini-gels (Mini-PROTEAN TGX™ Precast Gel; Bio-Rad). Proteins were transferred onto polyvinylidene difluoride membranes using a Trans Blot Mini Cell (Bio-Rad). For immunodetection, the blots were blocked with 2% bovine serum albumin in TBST (TBS + 0.1% Tween-20) for 1 h at room temperature and incubated with primary antibodies overnight at 4 °C. The primary antibody used was postsynaptic density protein 95 (PSD-95; 1 μ g/ml Invitrogen, Carlsbad, CA, USA). The next day, blots were washed thrice in TBST and incubated with horseradish peroxidase conjugated anti-rabbit antibody (1:5000) for 1 h at room temperature. After three final washes with TBST, bands were detected using enhanced chemiluminescence plus the Western Blotting Detection system (GE Healthcare Bioscience). The blots then were incubated in stripping buffer (2% sodium dodecyl sulfate, 100 mM β -mercaptoethanol, and 62.5 mM Tris-HCl, pH 6.8) for 30 min at 60 °C and then washed thrice with TBST. The stripped blots were kept in blocking solution for 1 h and incubated with a primary antibody directed against α -amino-3-hydroxy-5-methyl-4-isoxazolepropionic acid receptor (AMPA) 1 (GluA1; 1 μ g/ml Abcam, Cambridge, MA) and β -actin. Images were captured with a Fuji LAS3000-mini imaging system (Fujifilm, Tokyo, Japan), and immunoreactive bands were quantified.

2.5. 16S rRNA analysis

DNA extraction from mouse feces and 16S rRNA analysis of fecal samples were performed by MyMetagenome Co, Ltd. (Tokyo, Japan). The analysis of 16S rRNA from fecal samples was performed as previously described (Kim et al., 2013). Briefly, PCR was performed using 27Fmod 5'-AGRGTTTGATYMTGGCTCAG-3' and 338R 5'-TGCTGCCTCCGTAGGAGT-3' to amplify the V1–V2 region of the bacterial 16S rRNA gene. The amplified DNA (~330 bp) was purified using AMPure

XP (Beckman Coulter), and quantified using a Quant-iT Picogreen dsDNA assay kit (Invitrogen) and a TBS-380 Mini-Fluorometer (Turner Biosystems). The 16S amplicons were then sequenced using MiSeq according to the Illumina protocol. The paired-end reads were merged using the fastq-join program based on overlapping sequences. Reads with an average quality value of <25 and inexact matches to both universal primers were filtered out. Filter-passed reads were used for further analysis after trimming off both primer sequences. For each sample, 3000 high-quality filter-passed reads were rearranged in descending order according to the quality value and then clustered into operational taxonomic units (OTUs) with a 97% pairwise-identity cutoff, using the UCLUST program version 5.2.32 (<https://www.drive5.com>). Taxonomic assignment of OTUs was made by similarity searches against the Ribosomal Database Project and the National Center for Biotechnology Information genome database using the GLSEARCH program (Tanoue et al., 2019).

2.6. Statistical analysis

The data are shown as the mean \pm standard error of the mean (S.E.M.). Analysis was carried out using PASW Statistics 20 (now SPSS statistics; SPSS, Tokyo, Japan). Comparisons between groups were performed using Student t-tests and two-way analysis of variance (ANOVA), followed by *post hoc* Tukey test. The data of body weight were analyzed using repeated two-way ANOVA, followed by *post hoc* Tukey test. P values of less than 0.05 were considered to be statistically significant.

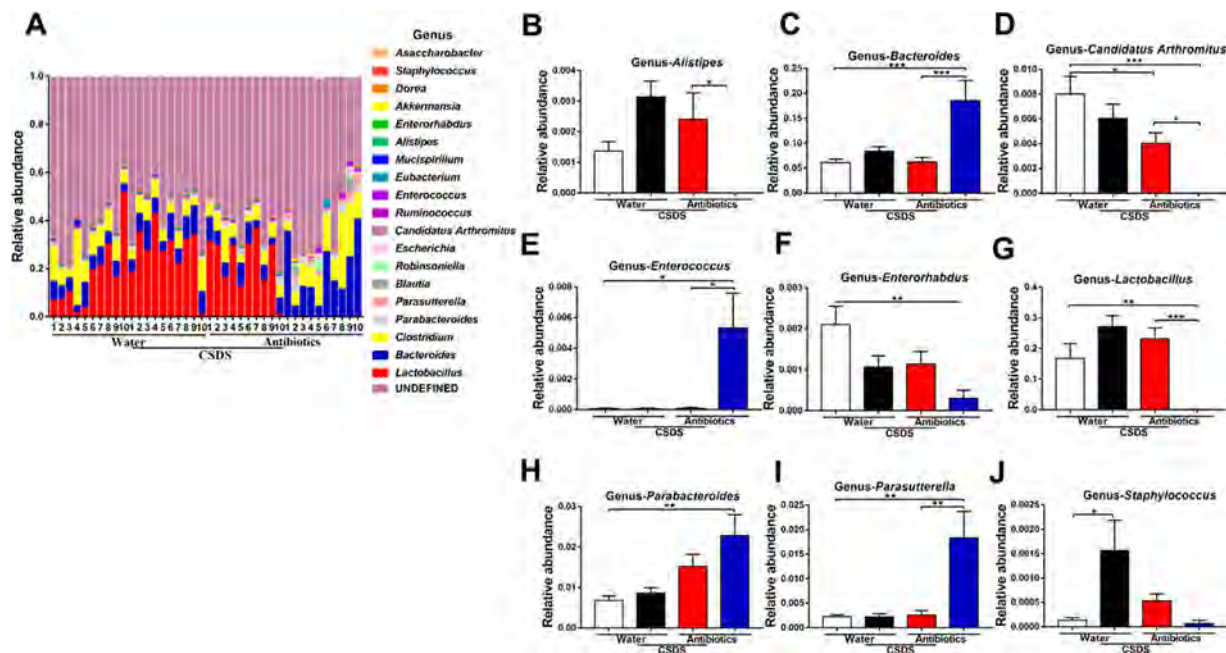


Fig. 7. Altered composition in the gut bacteria at the genus level.

(A): The relative abundances of genus in fecal samples of the four groups 24 days after drink antibiotics and CSDS. (B): *Alistipes* (two-way ANOVA, antibiotics: $F_{1,36} = 3.922$, $P = 0.055$, CSDS: $F_{1,36} = 15.438$, $P < 0.001$, interaction: $F_{1,36} = 0.357$, $P = 0.554$). (C): *Bacteroides* (two-way ANOVA, antibiotics: $F_{1,36} = 5.959$, $P = 0.020$, CSDS: $F_{1,36} = 5.567$, $P = 0.024$, interaction: $F_{1,36} = 11.801$, $P = 0.002$). (D): *Candidatus Arthromitus* (two-way ANOVA, antibiotics: $F_{1,36} = 24.682$, $P < 0.001$, CSDS: $F_{1,36} = 1.054$, $P = 0.311$, interaction: $F_{1,36} = 5.321$, $P = 0.027$). (E): *Enterococcus* (two-way ANOVA, antibiotics: $F_{1,36} = 5.457$, $P = 0.025$, CSDS: $F_{1,36} = 5.321$, $P = 0.027$, interaction: $F_{1,36} = 5.321$, $P = 0.027$). (F): *Enterorhabdus* (two-way ANOVA, antibiotics: $F_{1,36} = 7.308$, $P = 0.010$, CSDS: $F_{1,36} = 0.097$, $P = 0.757$, interaction: $F_{1,36} = 8.476$, $P = 0.006$). (G): *Lactobacillus* (two-way ANOVA, antibiotics: $F_{1,36} = 8.701$, $P = 0.006$, CSDS: $F_{1,36} = 22.717$, $P < 0.001$, interaction: $F_{1,36} = 3.312$, $P = 0.077$). (H): *Parabacteroides* (two-way ANOVA, antibiotics: $F_{1,36} = 13.509$, $P = 0.001$, CSDS: $F_{1,36} = 0.926$, $P = 0.342$, interaction: $F_{1,36} = 2.323$, $P = 0.136$). (I): *Parasutterella* (two-way ANOVA, antibiotics: $F_{1,36} = 8.645$, $P = 0.006$, CSDS: $F_{1,36} = 8.092$, $P = 0.007$, interaction: $F_{1,36} = 7.889$, $P = 0.008$). (J): *Staphylococcus* (two-way ANOVA, antibiotics: $F_{1,36} = 2.948$, $P = 0.095$, CSDS: $F_{1,36} = 8.794$, $P = 0.005$, interaction: $F_{1,36} = 2.276$, $P = 0.140$). Data are shown as mean \pm S.E.M. (n = 10). * $P < 0.05$, ** $P < 0.01$, *** $P < 0.001$. NS: not significant.

3. Results

3.1. Treatment with antibiotics caused significant differences in the diversity of gut microbiota

An antibiotic cocktail or water was given to mice for 14 days (Fig. 1A). Un-weighted UniFrac-based principal coordinate analysis (PCoA), based on the relative abundance of taxa in the gut microbiota of mice showed a significant difference between the two groups (Fig. 1B). There was a significant decrease in the observed species index in the antibiotic-treated group compared with the water-treated group (Fig. 1C). Shannon indices are commonly used to evaluate the α -diversity of gut microbiota. There was a significant decrease in the Shannon index of the antibiotic-treated group compared with that of the water-treated group (Fig. 1D).

3.2. Altered composition in gut bacteria at the phylum level

Analysis of 16S rRNA was used to identify differences in the composition of gut microbiota between the antibiotic-treated mice and the water-treated mice. The phylum level composition of gut bacterium was identified (Fig. 2A). *Bacteroidetes* and *Firmicutes* were the most abundant phyla in the water-treated group (Fig. 2A). At the phylum level, *Actinobacteria*, *Bacteroidetes*, and *Firmicutes* were present at significantly lower levels in the antibiotic-treated group than in the water-treated group (Fig. 2B–D). In contrast, *Proteobacteria* levels were markedly increased after treatment with the antibiotic cocktail (Fig. 2E).

3.3. Altered composition in gut bacteria at the genus level

The genus levels of gut bacteria were investigated (Fig. 3A). Five

genera of bacteria (*Clostridium*, *Intestinimonas*, *Lactobacillus*, *Lactococcus*, and *Staphylococcus*) were present at significantly lower levels in the antibiotic-treated group compared with the water-treated group (Figs. 3B, E, G, H, J). In contrast, four bacteria (*Enterococcus*, *Escherichia*, *Klebsiella*, and *Parasutterella*) were present at significantly higher levels in the antibiotic-treated group than those in the water-treated group (Figs. 3B, D, F, I).

3.4. Altered composition of gut bacteria at the species level

The genus levels of gut bacterium were identified (Fig. 4A). Three bacteria (*Enterococcus faecalis*, *Escherichia coli*, and *Klebsiella pneumoniae*) were present at significantly higher levels in the antibiotic-treated group than those in the water-treated group (Figs. 4D, E, F). In contrast, six bacteria (*Clostridium fusiformis*, *Clostridium* sp. *Culture Ja-56*, *Lactobacillus johnsonii*, *Lactobacillus murinus*, *Staphylococcus lentus*, and *Staphylococcus nepaiensis*) was present at significantly lower levels in the antibiotic-treated group than those in the water-treated group (Figs. 4B, C, G, H, I, J).

3.5. An antibiotic cocktail produced resilience in mice after csds

An antibiotic cocktail or water was provided as drinking water for 14 days, then CSDS was performed for 10 days (D15–D24) (Fig. 5A). The time course of the body weight of the mice was recorded (Fig. 5B). Treatment with an antibiotic cocktail significantly decreased body weight in the mice. CSDS did not alter body weight in the mice (Fig. 5B). There were significant differences in the α -diversity of microbiota among the four groups. CSDS significantly improved the reduced diversity of microbiota in the antibiotic-treated group (Figs. 5C, D, E). Un-weighted UniFrac-based PCoA showed significant differences

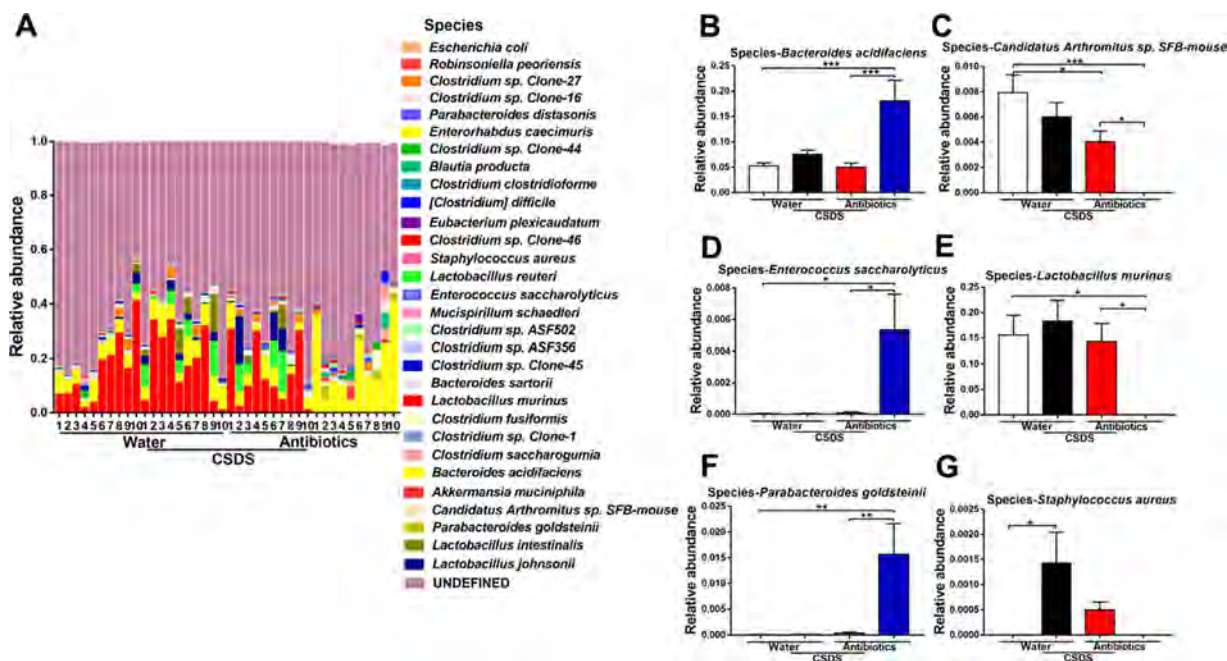


Fig. 8. Altered composition in the gut bacteria at the species level.

(A): The relative abundances of species in fecal samples of the four groups 24 days after drink antibiotics and CSDS. (B): *Bacteroides acidifaciens* (two-way ANOVA, antibiotics: $F_{1,36} = 5.757, P = 0.022$, CSDS: $F_{1,36} = 6.434, P = 0.016$, interaction: $F_{1,36} = 12.957, P = 0.001$). (C): *Candidatus Arthromitus sp. SFB-mouse* (two-way ANOVA, antibiotics: $F_{1,36} = 24.529, P < 0.001$, CSDS: $F_{1,36} = 1.104, P = 0.300$, interaction: $F_{1,36} = 8.910, P = 0.005$). (D): *Enterococcus saccharolyticus* (two-way ANOVA, antibiotics: $F_{1,36} = 5.597, P = 0.023$, CSDS: $F_{1,36} = 5.323, P = 0.027$, interaction: $F_{1,36} = 5.323, P = 0.027$). (E): *Lactobacillus murinus* (two-way ANOVA, antibiotics: $F_{1,36} = 8.450, P = 0.006$, CSDS: $F_{1,36} = 6.335, P = 0.016$, interaction: $F_{1,36} = 2.860, P = 0.099$). (F): *Parabacteroides goldsteinii* (two-way ANOVA, antibiotics: $F_{1,36} = 6.997, P = 0.012$, CSDS: $F_{1,36} = 6.422, P = 0.016$, interaction: $F_{1,36} = 6.478, P = 0.015$). (G): *Staphylococcus aureus* (two-way ANOVA, antibiotics: $F_{1,36} = 2.215, P = 0.145$, CSDS: $F_{1,36} = 9.503, P = 0.004$, interaction: $F_{1,36} = 2.215, P = 0.145$). Data are shown as mean \pm S.E.M. (n = 10). * $P < 0.05$, ** $P < 0.01$, *** $P < 0.001$. NS: not significant.

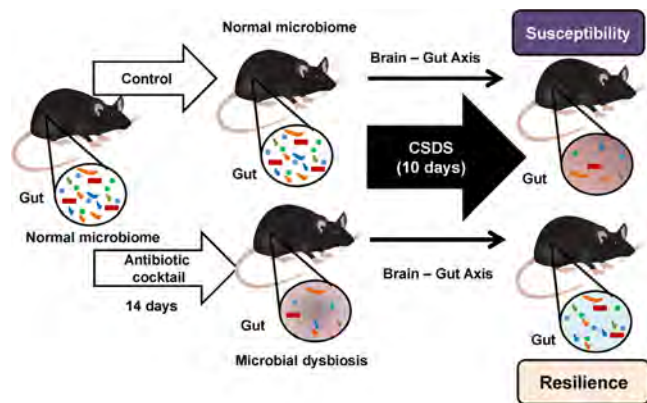


Fig. 9. Proposed scheme of brain-gut axis in resilience and susceptibility after repeated stress.

Treatment of an antibiotic cocktail for 14 days caused microbial dysbiosis in mice by microbiome depletion. Subsequently, chronic social defeat stress was performed 10 days. Water-treated control mice showed the susceptibility after CSDS. In contrast, antibiotic cocktail treated mice showed the resilience after CSDS. Brain-gut axis may play a role in the susceptibility versus resilience in mice after CSDS.

among the four groups (Fig. 5F).

In SPT, CSDS caused significant reduction in sucrose preference in the water-treated group, but not in the antibiotic-treated group (Fig. 5G). There was no significant difference between the antibiotic-treated non-CSDS group and the water-treated non-CSDS group (Fig. 5G). CSDS treatment significantly increased plasma levels of IL-6 in the water-treated group, whereas CSDS treatment did not alter plasma IL-6 levels in the antibiotic-treated group (Fig. 5H). CSDS significantly decreased the expression of PSD-95 and GluA1 in the PFC of

water-treated group, but not in the antibiotic-treated group (Figs. 5I, J).

Overall, the antibiotic-treated group appeared to be protected against the CSDS-induced anhedonia-like phenotype, inflammation, and decreased synaptogenesis in the PFC.

3.6. Effects of CSDS on altered composition in the gut bacteria

The effects of CSDS on the composition of the microbiome of antibiotic-treated mice were investigated. The phyla of gut bacteria were identified (Fig. 6A). At the phylum level, the antibiotic-treated group showed significant reduction in *Actinobacteria* compared with the water-treated group (Fig. 6B). CSDS significantly decreased *Actinobacteria* in the water-treated group, but not in the antibiotic-treated group (Fig. 6B). The antibiotic-treated group showed significantly higher levels of *Proteobacteria* compared with the water-treated group (Fig. 6C). CSDS also significantly decreased the levels of *Proteobacteria* in the antibiotic-treated group, but not in the water-treated group (Fig. 6C).

The genus levels of gut bacterium were also identified (Fig. 7A). CSDS significantly altered the levels of six genera (*Alistipes*, *Bacteroides*, *Candidatus Arthromitus*, *Enterococcus*, *Lactobacillus*, and *Parasutterella*) in the antibiotic-treated group, but not in the water-treated group (Figs. 7B–I). In contrast, CSDS significantly increased levels of *Staphylococcus* in the water-treated group, but not in the antibiotic-treated group (Fig. 7J).

The species of gut bacterium were identified (Fig. 8A). CSDS significantly altered the levels of five microbes (*Bacteroides acidifaciens*, *Candidatus Arthromitus sp. SFB-mouse*, *Enterococcus saccharolyticus*, *Lactobacillus murinus*, and *Parabacteroides goldsteinii*) in the antibiotic-treated group, but not in the water-treated group (Figs. 8B–F). In contrast, CSDS significantly increased levels of *Staphylococcus aureus* in the water-treated group, but not in the antibiotic-treated group (Fig. 8G).

4. Discussion

The major findings of this study are as follows. Treatment with an antibiotic cocktail in drinking water for 14 days caused marked reduction in the α -diversity of microbiota in the host gut compared with the water-treated group. At the phylum level, the antibiotic-treated group showed a marked increase in *Proteobacteria* in the host gut, whereas the levels of three bacteria (*Actinobacteria*, *Bacteroidetes*, and *Firmicutes*) were decreased after treatment with the antibiotic cocktail. At the genus and species levels, the antibiotic-treated group showed marked alterations in several bacteria. Overall, treatment with an antibiotic cocktail for 14 days caused significant changes in the diversity and composition of microbiota in the host gut, consistent with previous reports (Hernandez-Chirlaque et al., 2016; Sampson et al., 2016; Zarrinpar et al., 2018; Zhan et al., 2018; Zhang et al., 2019a).

We performed CSDS for 10 days after treatment with an antibiotic cocktail for 14 days. The UniFrac-based PCoA showed significant differences among the four groups. CSDS significantly improved the abnormal diversity of microbiota in the antibiotic-treated group. In particular, CSDS significantly decreased levels of bacteria from the phylum *Proteobacteria*, genus *Bacteroides*, genus *Enterococcus*, genus *Parasutterella*, species *Bacteroides acidifaciens*, species *Enterococcus saccharolyticus*, and species *Parabacteroides goldsteinii* in the antibiotic-treated mice. A study reported that supplementation with rhubarb extract changed the microbial ecosystem in favor of *Parabacteroides goldsteinii* (Neyrinck et al., 2017). It seems that *Parabacteroides goldsteinii* may contribute to resilience to stress although a further study is needed.

In contrast, CSDS significantly increased the levels of genus *Alistipes*, genus *Candidatus Arthromitus*, genus *Lactobacillus*, species *Candidatus Arthromitus* sp. *SFB-mouse*, species *Lactobacillus murinus*. A recent study showed that CSDS-induced depression-like phenotypes were correlated with *Candidatus Arthromitus* sp. *SFB-mouse* (Tian et al., 2019). The mechanisms underlying CSDS-induced recovery of the composition of the microbiota in the host gut of antibiotic-treated mice are currently unknown. Previously, Bailey et al. (2011) reported that the exposure to a social stressor called social disruption failed to increase blood IL-6 in antibiotic-treated mice, although the same stress caused increases in levels of IL-6 in the blood of control mice, suggesting that the microbiota are necessary for stress-induced increases in circulating cytokines. Furthermore, the restraint stress was able to disrupt both the mucosa-associated and lumenally-associated colonic microbiota by causing changes in the relative abundances of multiple groups of bacteria, suggesting that stress can have distinct effects upon the colonic microbiota of the mucosal epithelium as compared with the luminal-associated microbiota (Galley et al., 2014). Given the role of immune system in resilience (Cathomas et al., 2019; Dantzer et al., 2008), it is likely that modulation of the bidirectional relationship between resilience and immunity by the gut microbiota plays a role in the recovery from CSDS. In addition, we reported the role of the brain–gut axis in the resilience versus susceptibility in rats exposed to inescapable electric stress (Zhang et al., 2019b). Further detailed study on the relationship between resilience and immunity via the brain–gut axis is needed.

In this study, we found marked increases in organisms from the phylum *Proteobacteria* after antibiotic treatment, whereas levels of bacteria from two major phyla (*Bacteroidetes* and *Firmicutes*) were decreased after antibiotic treatment (Fig. 2). Previous studies (Antonopoulos et al., 2009; Young and Schmidt, 2004; Zarrinpar et al., 2018) have shown that the microbiome of antibiotic-treated mice had a compositional shift to *Proteobacteria* from the major microbiota (*Bacteroidetes*, *Firmicutes*), consistent with our current data. Although *Proteobacteria* are natural inhabitants of the intestine, they normally comprise a minority of the healthy homeostatic microbiota. It has been suggested that an increased prevalence of *Proteobacteria* in the microbial community can serve as a potential diagnostic signature of dysbiosis and risk of disease (Kim et al., 2017; Shin et al., 2015). It is also

well known that treatment with a broad antibiotic cocktail causes a dramatic loss in diversity, as well as in representation of specific taxa, insurgence of antibiotic resistant strains, and up-regulation of antibiotic resistance genes (Becattini et al., 2016; Jernberg et al., 2007). In this study, we found an increase in the relative abundance of *Proteobacteria* in the antibiotic-treated group compared with the water-only group. However, the precise mechanisms underlying the increase in the relative abundance of *Proteobacteria* after treatment of antibiotic cocktail is currently unknown. The proportions of several genera and species were altered after repeated treatment with the antibiotic cocktail. Thus, antibiotic-induced microbiome depletion could be useful to study the role of the gut microbiota in pathological conditions.

We also found that CSDS decreased the sucrose preference of SPT in the water-treated group, although CSDS did not decrease the sucrose preference of SPT in the antibiotic-treated group. CSDS also significantly increased the plasma levels of IL-6 in the water-treated group, but not in the antibiotic-treated group, suggesting anti-inflammatory effects in antibiotic-treated mice. It has been reported that CSDS resilient mice had lower blood levels of IL-6 than susceptible mice in response to acute stress (Hodes et al., 2014). CSDS significantly decreased the expression of the synaptic proteins PSD-95 and GluA1 in the PFC from the water-treated group, but not the antibiotic-treated group. These findings suggest that antibiotic-induced microbiome depletion may contribute to stress resilience in mice after CSDS via the brain–gut–microbiome axis. It has also been reported that treatment with DSS caused colitis in control mice, although antibiotic-induced microbiome depletion did not produce DSS-induced colitis in the mice, suggesting that enteric bacteria are essential for the development of DSS-induced colitis (Hernandez-Chirlaque et al., 2016). These data suggest that microbiome reduction by antibiotic cocktail treatment may play a role in the development of susceptibility in mice after CSDS, although the specific microbes were not identified in this study. It is also possible that a complex interaction of these manipulations—the antibiotic cocktail treatment and CSDS—may contribute to the current data. Further detailed study is needed to confirm the relationship between stress resilience and the microbiome.

The crosstalk between brain and gut is predominately influenced by the gut bacteria (Kelly et al., 2016). Imbalance of gut microbiota is well established as causing abnormal brain–gut axes in several neurological and psychiatric diseases (Fung et al., 2017; Kelly et al., 2016). Accumulating evidence suggests that an abnormal composition of gut microbiota may contribute to resilience versus susceptibility in rodents after repeated stress (Bailey et al., 2011; Hao et al., 2019; Szyzkowicz et al., 2017; Yang et al., 2017a) (Fig. 9). It is likely that an altered composition of gut microbiota may play a role in stress-induced disorders. In contrast, it is reported that antibiotic cocktail treatment for 14 days caused depression-like phenotype in mice, and subsequent administration of *Lactobacillus casei* DG for 7 days countered most of these gut inflammatory, behavioral and functional alterations (Guida et al., 2018). Therefore, further detailed study on relationship between antibiotic-induced microbiome depletion and behavioral abnormalities are needed.

This study has some limitations. In this study, we did not identify the specific microbiota, which plays a role in resilience after CSDS. We do not know whether the microbiome in the fecal samples reflects the microbiome in the gut. Additionally, we did not produce conclusive evidence that the improvement in the density of the microbiota is mainly due to CSDS. The control mice that did not receive CSDS were not exposed to a non-aggressive resident CD1 mouse. It is possible that exposure to an aggressive CD1 mouse may be the cause of the improvement in the abnormal composition of microbiota in the antibiotic-treated mice, although further study is needed. Furthermore, we did not measure short-chain fatty acids (SCFAs) in the fecal samples although the microbiome can produce SCFAs which play a role in the several pathological conditions (Sudo, 2019; Tan et al., 2014; Zaiss et al., 2019). Finally, treatment with the antibiotic cocktail significantly

decreased the body weight, which may affect the susceptibility and reaction to CSDS. Further detailed study is needed to resolve the above limitations.

In conclusion, the present study suggests that antibiotic-induced microbiome depletion may contribute to resilience versus susceptibility in mice subjected to CSDS, and that CSDS may improve the diversity and composition of gut microbiota in mice treated with an antibiotic cocktail. It is likely that the brain–gut axis plays a role in susceptibility to stress-related disorders.

CRedit authorship contribution statement

Siming Wang: Conceptualization, Data curation, Methodology, Formal analysis, Writing - original draft, Writing - review & editing. **Younge Qu:** Data curation, Methodology, Writing - review & editing. **Lijia Chang:** Data curation, Methodology, Writing - review & editing. **Yaoyu Pu:** Data curation, Methodology, Writing - review & editing. **Kai Zhang:** Data curation, Methodology, Writing - review & editing. **Kenji Hashimoto:** Conceptualization, Funding acquisition, Supervision, Writing - original draft, Writing - review & editing.

Declaration of Competing Interest

All authors report no biomedical financial interests or potential conflicts of interest.

Acknowledgements

This study was supported by Smoking Research Foundation, Japan (to K.H.), and AMED, Japan (to K.H., JP19dm0107119). Dr. Lijia Chang was supported by Japan China Sasakawa Medical Fellowship (Tokyo, Japan). Ms. Siming Wang was supported by TAKASE Scholarship Foundation (Tokyo, Japan).

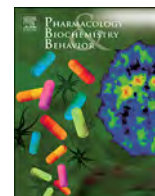
Supplementary materials

Supplementary material associated with this article can be found, in the online version, at [doi:10.1016/j.jad.2019.09.064](https://doi.org/10.1016/j.jad.2019.09.064).

References

- Antonopoulos, D.A., Huse, S.M., Morrison, H.G., Schmidt, T.M., Sogin, M.L., Young, V.B., 2009. Reproducible community dynamics of the gastrointestinal microbiota following antibiotic perturbation. *Infect. Immun.* 77, 2367–2375.
- Bailey, M.T., Dowd, S.E., Galley, J.D., Hufnagle, A.R., Allen, R.G., Lyte, M., 2011. Exposure to a social stressor alters the structure of the intestinal microbiota: implications for stressor-induced immunomodulation. *Brain Behav. Immun.* 25, 397–407.
- Becattini, S., Taur, Y., Pamer, E.G., 2016. Antibiotic-induced changes in the intestinal microbiota and disease. *Trends Mol. Med.* 22, 458–478.
- Burokas, A., Arboleya, S., Moloney, R.D., Peterson, V.L., Murphy, K., Clarke, G., Stanton, C., Dinan, T.G., Cryan, J.F., 2017. Targeting the microbiota-gut-brain axis: prebiotics have anxiolytic and antidepressant-like effects and reverse the impact of chronic stress in mice. *Biol. Psychiatry* 82, 472–487.
- Cathomas, F., Murrrough, J.W., Nestler, E.J., Han, M.H., Russo, S.J., 2019. Neurobiology of resilience: interface between mind and body. *Biol. Psychiatry*.
- Cerf-Bennussan, N., Gaboriau-Routhiau, V., 2010. The immune system and the gut microbiota: friends or foes? *Nat. Rev. Immunol.* 10, 735–744.
- Champagne-Jorgensen, K., Kunze, W.A., Forsythe, P., Bienenstock, J., Neufeld, K.A.M., 2019. Antibiotics and the nervous system: more than just the microbes? *Brain Behav. Immun.* 77, 7–15.
- Cusotto, S., Sandhu, K.V., Dinan, T.G., Cryan, J.F., 2018. The neuroendocrinology of the microbiota-gut-brain axis: a behavioural perspective. *Front Neuroendocrinol.* 51, 80–101.
- Cusotto, S., Strain, C.R., Fouhy, F., Strain, R.G., Peterson, V.L., Clarke, G., Stanton, C., Dinan, T.G., Cryan, J.F., 2019. Differential effects of psychotropic drugs on microbiome composition and gastrointestinal function. *Psychopharmacology (Berl)* 236, 1671–1685.
- Dantzer, R., Cohen, S., Russo, S.J., Dinan, T.G., 2008. Resilience and immunity. *Brain Behav. Immun.* 74, 28–42.
- Dinan, T.G., Cryan, J.F., 2017. Brain-gut-microbiota axis and mental health. *Psychosom. Med.* 79, 920–926.
- Forsythe, P., Kunze, W., Bienenstock, J., 2016. Moody microbes or fecal phrenology: what do we know about the microbiota-gut-brain axis? *BMC Med.* 14, 58.
- Fung, T.C., Olson, C.A., Hsiao, E.Y., 2017. Interactions between the microbiota, immune and nervous systems in health and disease. *Nat. Neurosci.* 20, 145–155.
- Galley, J.D., Yu, Z.T., Kumar, P., Dowd, S.E., Lyte, M., Bailey, M.T., 2014. The structures of the colonic mucosa-associated and luminal microbial communities are distinct and differentially affected by a prolonged murine stressor. *Gut Microbes* 5, 748–760.
- Golden, S.A., Covington 3rd, H.E., Berton, O., Russo, S.J., 2011. A standardized protocol for repeated social defeat stress in mice. *Nat. Protoc.* 6, 1183–1191.
- Guida, F., Turco, F., Iannotta, M., De Gregorio, D., Palumbo, I., Sarnelli, G., Furiano, A., Napolitano, F., Boccella, S., Luongo, L., Mazzitelli, M., Usiello, A., De Filippis, F., Iannotti, F.A., Piscitelli, F., Ercolini, D., de Novellis, V., Di Marzo, V., Cuomo, R., Maione, S., 2018. Antibiotic-induced microbiota perturbation causes gut endocannabinoidome changes, hippocampal neuroglial reorganization and depression in mice. *Brain Behav. Immun.* 67, 230–245.
- Hao, Z.K., Wang, W., Guo, R., Liu, H., 2019. *Faecalibacterium prausnitzii* (ATCC 27766) has preventive and therapeutic effects on chronic unpredictable mild stress-induced depression-like and anxiety-like behavior in rats. *Psychoneuroendocrinol.* 104, 132–142.
- Hernandez-Chirlaque, C., Aranda, C.J., Ocon, B., Capitan-Canadas, F., Ortega-Gonzalez, M., Carrero, J.J., Suarez, M.D., Zarzuelo, A., de Medina, F.S., Martinez-Augustin, O., 2016. Germ-free and antibiotic-treated mice are highly susceptible to epithelial injury in dss colitis. *J. Crohns. Colitis* 10, 1324–1335.
- Ho, P., Ross, D.A., 2017. More than a gut feeling: the implications of the gut microbiota in psychiatry. *Biol. Psychiatry* 81, E35–E37.
- Hodes, G.E., Pfau, M.L., Leboeuf, M., Golden, S.A., Christoffel, D.J., Bregman, D., Rebusi, N., Heshmati, M., Aleyasin, H., Warren, B.L., Lebonite, B., Horn, S., Lapidus, K.A., Stelzhammer, V., Wong, E.H.F., Bahn, S., Krishnan, V., Bolanos-Guzman, C.A., Murrrough, J.W., Merad, M., Russo, S.J., 2014. Individual differences in the peripheral immune system promote resilience versus susceptibility to social stress. *Proc. Natl. Acad. Sci. USA* 111, 16136–16141.
- Huang, N.N., Hua, D.Y., Zhan, G.F., Li, S., Zhu, B., Jiang, R.Y., Yang, L., Bi, J.J., Xu, H., Hashimoto, K., Luo, A.L., Yang, C., 2019a. Role of actinobacteria and coriobacteria in the antidepressant effects of ketamine in an inflammation model of depression. *Pharmacol. Biochem. Behav.* 176, 93–100.
- Huang, T.T., Lai, J.B., Du, Y.L., Xu, Y., Ruan, L.M., Hu, S.H., 2019b. Current understanding of gut microbiota in mood disorders: an update of human studies. *Front Genet.* 10, 98.
- Ianiro, G., Tilg, H., Gasbarrini, A., 2016. Antibiotics as deep modulators of gut microbiota: between good and evil. *Gut* 65, 1906–1915.
- Jernberg, C., Lofmark, S., Edlund, C., Jansson, J.K., 2007. Long-term ecological impacts of antibiotic administration on the human intestinal microbiota. *ISME J.* 1, 56–66.
- Jiang, H.Y., Ling, Z.X., Zhang, Y.H., Mao, H.J., Ma, Z.P., Yin, Y., Wang, W.H., Tang, W.X., Tan, Z.L., Shi, J.F., Li, L.J., Ruan, B., 2015. Altered fecal microbiota composition in patients with major depressive disorder. *Brain Behav. Immun.* 48, 186–194.
- Kelly, J.R., Clarke, G., Cryan, J.F., Dinan, T.G., 2016. Brain-gut-microbiota axis: challenges for translation in psychiatry. *Ann. Epidemiol.* 26, 366–372.
- Kim, S., Covington, A., Pamer, E.G., 2017. The intestinal microbiota: antibiotics, colonization resistance, and enteric pathogens. *Immunol. Rev.* 279, 90–105.
- Kim, S.W., Suda, W., Kim, S., Oshima, K., Fukuda, S., Ohno, H., Morita, H., Hattori, M., 2013. Robustness of gut microbiota of healthy adults in response to probiotic intervention revealed by high-throughput pyrosequencing. *DNA Res.* 20, 241–253.
- Lukic, I., Getselter, D., Ziv, O., Oron, O., Reuveni, E., Koren, O., Elliott, E., 2019. Antidepressants affect gut microbiota and *ruminococcus flavefaciens* is able to abolish their effects on depressive-like behavior. *Transl. Psychiatry* 9, 133.
- Ma, Q.Q., Xing, C.S., Long, W.Y., Wang, H.Y., Liu, Q., Wang, R.F., 2019. Impact of microbiota on central nervous system and neurological diseases: the gut-brain axis. *J. Neuroinflammation* 16, 53.
- Molina-Torres, G., Rodriguez-Arrastia, M., Roman, P., Sanchez-Labraca, N., Cardona, D., 2019. Stress and the gut microbiota-brain axis. *Behav. Pharmacol.* 30, 187–200.
- Neyrinck, A.M., Etxeberria, U., Taminiua, B., Daube, G., Van Hul, M., Everard, A., Cani, P.D., Bindels, L.B., Delzenne, N.M., 2017. Rhubarb extract prevents hepatic inflammation induced by acute alcohol intake, an effect related to the modulation of the gut microbiota. *Mol. Nutr. Food Res.* 61, 150899.
- Pu, Y., Chang, L., Qu, Y., Wang, S., Zhang, K., Hashimoto, K., 2019. Antibiotic-induced microbiome depletion protects against MPTP-induced dopaminergic neurotoxicity in the brain. *Aging* 11, 6915–6929. <https://doi.org/10.18632/aging.102221>.
- Qu, Y.G., Yang, C., Ren, Q., Ma, M., Dong, C., Hashimoto, K., 2017. Comparison of (R)-ketamine and lanicemine on depression-like phenotype and abnormal composition of gut microbiota in a social defeat stress model. *Sci. Rep.* 7, 15725.
- Round, J.L., Mazmanian, S.K., 2009. The gut microbiota shapes intestinal immune responses during health and disease. *Nat. Rev. Immunol.* 9, 313–323.
- Sampson, T.R., Debelius, J.W., Thron, T., Janssen, S., Shastri, G.G., Ilhan, Z.E., Challis, C., Schretter, C.E., Rocha, S., Gradinaru, V., Chesslet, M.F., Keshavarzian, A., Shannon, K.M., Krajmalnik-Brown, R., Wittung-Stafshede, P., Knight, R., Mazmanian, S.K., 2016. Gut microbiota regulate motor deficits and neuroinflammation in a model of Parkinson's disease. *Cell* 167, 1469–1480.
- Shin, N.R., Whon, T.W., Bae, J.W., 2015. Proteobacteria: microbial signature of dysbiosis in gut microbiota. *Trends Biotechnol.* 33, 496–503.
- Sudo, N., 2019. Role of gut microbiota in brain function and stress-related pathology. *Biosci. Microbiota Food Health* 38, 75–80.
- Szyszkowicz, J.K., Wong, A., Anisman, H., Merali, Z., Audet, M.C., 2017. Implications of the gut microbiota in vulnerability to the social avoidance effects of chronic social defeat in male mice. *Brain Behav. Immun.* 66, 45–55.
- Tan, J., McKenzie, C., Potamitis, M., Thorburn, A.N., MacKay, C.R., Macia, L., 2014. The role of short-chain fatty acids in health and disease. *Adv. Immunol.* 121, 91–119.
- Tian, T., Xu, B., Qin, Y., Fan, L., Chen, J., Zheng, P., Gong, X., Wang, H., Bai, M., Pu, J., Lu, J., Zhou, W., Zhao, L., Yang, D., Xie, P., 2019. *Clostridium butyricum* miyairi 588

- has preventive effects on chronic social defeat stress-induced depressive-like behaviour and modulates microglial activation in mice. *Brain Behav. Immun.* 516, 430–436.
- Tanoue, T., Morita, S., Plichta, D.R., Skelly, A.N., Suda, W., Sugiura, Y., Narushima, S., Vlamakis, H., Motoo, I., Sugita, K., Shiota, A., Takeshita, K., Yasuma-Mitobe, K., Riethmacher, D., Kaisho, T., Norman, J.M., Mucida, D., Suematsu, M., Yaguchi, T., Bucci, V., Inoue, T., Kawakami, Y., Olle, B., Roberts, B., Hattori, M., Xavier, R.J., Atarashi, K., Honda, K., 2019. A defined commensal consortium elicits CD8 t cells and anti-cancer immunity. *Nature* 565, 600–605.
- Treadway, M.T., Zald, D.H., 2011. Reconsidering anhedonia in depression: lessons from translational neuroscience. *Neurosci. Biobehav. Rev.* 35, 537–555.
- Wong, M.L., Inerra, A., Lewis, M.D., Mastronardi, C.A., Leong, L., Choo, J., Kentish, S., Xie, P., Morrison, M., Wesselingh, S.L., Rogers, G.B., Licinio, J., 2016. Inflammasome signaling affects anxiety- and depressive-like behavior and gut microbiome composition. *Mol. Psychiatry* 21, 797–805.
- Yang, B., Zhang, J.C., Han, M., Yao, W., Yang, C., Ren, Q., Ma, M., Chen, Q.X., Hashimoto, K., 2016. Comparison of R-ketamine and rapastinel antidepressant effects in the social defeat stress model of depression. *Psychopharmacology (Berl.)* 233, 3647–3657.
- Yang, C., Fang, X., Zhan, G.F., Huang, N.N., Li, S., Bi, J.J., Jiang, R.Y., Yang, L., Miao, L.Y., Zhu, B., Luo, A.L., Hashimoto, K., 2019. Key role of gut microbiota in anhedonia-like phenotype in rodents with neuropathic pain. *Transl. Psychiatry* 9, 57.
- Yang, C., Fujita, Y., Ren, Q., Ma, M., Dong, C., Hashimoto, K., 2017a. *Bifidobacterium* in the gut microbiota confer resilience to chronic social defeat stress in mice. *Sci. Rep.* 7, 45942.
- Yang, C., Qu, Y.G., Fujita, Y., Ren, Q., Ma, M., Dong, C., Hashimoto, K., 2017b. Possible role of the gut microbiota-brain axis in the antidepressant effects of (R)-ketamine in a social defeat stress model. *Transl. Psychiatry* 7, 15725.
- Yang, C., Shirayama, Y., Zhang, J.C., Ren, Q., Yao, W., Ma, M., Dong, C., Hashimoto, K., 2015. R-ketamine: a rapid-onset and sustained antidepressant without psychotomimetic side effects. *Transl. Psychiatry* 5, e632.
- Young, V.B., Schmidt, T.M., 2004. Antibiotic-associated diarrhea accompanied by large-scale alterations in the composition of the fecal microbiota. *J. Clin. Microbiol.* 42, 1203–1206.
- Zaiss, M.M., Jones, R.M., Schett, G., Pacifici, R., 2019. The gut-bone axis: how bacterial metabolites bridge the distance. *J. Clin. Invest.* 129, 3018–3028.
- Zarrinpar, A., Chaix, A., Xu, Z.J.Z., Chang, M.W., Marotz, C.A., Saghatelian, A., Knight, R., Panda, S., 2018. Antibiotic-induced microbiome depletion alters metabolic homeostasis by affecting gut signaling and colonic metabolism. *Nat. Commun.* 9, 2872.
- Zhan, G.F., Yang, N., Li, S., Huang, N.N., Fang, X., Zhang, J., Zhu, B., Yang, L., Yang, C., Luo, A.L., 2018. Abnormal gut microbiota composition contributes to cognitive dysfunction in SAMP8 mice. *Aging* 10, 1257–1267.
- Zhang, J., Bi, J.J., Guo, G.J., Yang, L., Zhu, B., Zhan, G.F., Li, S., Huang, N.N., Hashimoto, K., Yang, C., Luo, A.L., 2019a. Abnormal composition of gut microbiota contributes to delirium-like behaviors after abdominal surgery in mice. *CNS Neurosci. Ther.* 25, 685–696.
- Zhang, J.C., Yao, W., Dong, C., Yang, C., Ren, Q., Ma, M., Han, M., Hashimoto, K., 2015. Comparison of ketamine, 7,8-dihydroxyflavone, and ANA-12 antidepressant effects in the social defeat stress model of depression. *Psychopharmacology (Berl.)* 232, 4325–4335.
- Zhang, J.C., Yao, W., Dong, C., Yang, C., Ren, Q., Ma, M., Hashimoto, K., 2017. Blockade of interleukin-6 receptor in the periphery promotes rapid and sustained antidepressant actions: a possible role of gut-microbiota-brain axis. *Transl. Psychiatry* 7, e1138.
- Zhang, K., Fujita, Y., Chang, J., Qu, Y., Pu, Y., Wang, S., Shirayama, Y., Hashimoto, K., 2019b. Abnormal composition of gut microbiota is associated with resilience versus susceptibility to inescapable electric stress. *Transl. Psychiatry*. <https://doi.org/10.1038/s41398-019-0571-x>. In press.
- Zheng, P., Zeng, B., Zhou, C., Liu, M., Fang, Z., Xu, X., Zeng, L., Chen, J., Fan, S., Du, X., Zhang, X., Yang, D., Yang, Y., Meng, H., Li, W., Melgiri, N.D., Licinio, J., Wei, H., Xie, P., 2016. Gut microbiome remodeling induces depressive-like behaviors through a pathway mediated by the host's metabolism. *Mol. Psychiatry* 21, 786–796.
- Zhu, F., Guo, R., Wang, W., Ju, Y., Wang, Q., Ma, Q., Sun, Q., Fan, Y., Xie, Y., Yang, Z., Jie, Z., Zhao, B., Xiao, L., Yang, L., Zhang, T., Liu, B., Guo, L., He, X., Chen, Y., Chen, C., Gao, C., Xu, X., Yang, H., Wang, J., Dang, Y., Madsen, L., Brix, S., Kristiansen, K., Jia, H., Ma, X., 2019. Transplantation of microbiota from drug-free patients with schizophrenia causes schizophrenia-like abnormal behaviors and dysregulated kynurenine metabolism in mice. *Mol. Psychiatry*. <https://doi.org/10.1038/s41380-019-0475-4>. 2019 Aug 7.



Review

A historical review of antidepressant effects of ketamine and its enantiomers

Yan Wei^{a,b}, Lijia Chang^a, Kenji Hashimoto^{a,*}^a Division of Clinical Neuroscience, Chiba University Center for Forensic Mental Health, Chiba 260-8670, Japan^b Key Laboratory of Medical Electrophysiology of Ministry of Education and Medical Electrophysiological Key Laboratory of Sichuan Province, Collaborative Innovation Center for Prevention and Treatment of Cardiovascular Disease, Institute of Cardiovascular Research, Southwest Medical University, Luzhou 646000, Sichuan, China.

ARTICLE INFO

Keywords:

Antidepressant
Arketamine
Enantiomer
Esketamine
Ketamine

ABSTRACT

The robust antidepressant effects of (*R,S*)-ketamine are among the most important discoveries in mood research over the last half century. Off-label use of (*R,S*)-ketamine, which is an equal mixture of (*R*)-ketamine and (*S*)-ketamine, has become especially popular in the United States (US) for treatment-resistant depression. On March 5, 2019, the US Food and Drug Administration approved an (*S*)-ketamine nasal spray for use in treatment-resistant depression, though its use has been limited to certified medical offices or clinics. On December 19, 2019, (*S*)-ketamine nasal spray was approved for the same indication in Europe. However, despite its potential for benefit, there are several concerns about the efficacy of (*S*)-ketamine nasal spray. Accumulating evidence from preclinical studies show that (*R*)-ketamine has greater potency and longer lasting antidepressant effects than (*S*)-ketamine in animal models of depression, and that (*R*)-ketamine has fewer detrimental side effects than either (*R,S*)-ketamine or (*S*)-ketamine. As such, clinical studies of (*R*)-ketamine in humans are now underway by Perception Neuroscience Ltd. In this article, we review the brief history of (*R,S*)-ketamine and its two enantiomers as novel antidepressants. We also discuss the mechanisms of ketamine's antidepressant actions.

1. Introduction

More than 300 million people of all ages suffer from depression, which is a major contributor to the overall global burden of disease (WHO, 2017). Approximately one-third of depressed patients have a treatment-resistant form of depression after trialing typical antidepressants such as selective serotonin reuptake inhibitors (SSRIs) and serotonin and norepinephrine reuptake inhibitors (SNRIs). Moreover, these antidepressants have proven ineffective in the treatment of suicide ideation in patients with severe depression. Novel therapeutic agents are therefore required to meet these unmet needs. In recent decades, (*R,S*)-ketamine (Fig. 1) has come to the attention of neuroscientists and psychiatrists worldwide because it produces robust antidepressant effects in patients with treatment-resistant depression (Duman, 2018; Gould et al., 2019; Hashimoto, 2016a; Hashimoto, 2016b; Hashimoto, 2017; Hashimoto, 2019a; Krystal et al., 2019; Murrough et al., 2017; Witkin et al., 2018; Zhang and Hashimoto, 2019b).

In this article, we offer a review of the brief history of (*R,S*)-ketamine and its two enantiomers as novel antidepressants. Furthermore, we discuss the mechanisms of action for ketamine's antidepressant effects.

2. Brief history of ketamine

The discovery of ketamine's antidepressant effects is among the most important discoveries of the last half century. Not originally developed as an antidepressant, it took a long and fascinating journey for clinicians and researchers to discover its rapid-acting antidepressant effects (Fig. 2). The history of ketamine can be traced back to 1956 when phencyclidine (PCP) was first synthesized as a general anesthetic by the pharmaceutical company Parke-Davis (Maddox et al., 1965). It had an inhibitory constant (*K_i*) of 0.06 μM at the *N*-methyl-D-aspartate receptor (NMDAR) (Fig. 1) (Domino and Luby, 2012; Mion, 2017). However, subsequent studies in humans revealed that PCP could cause a high rate of side effects, including hallucinations, postoperative delirium, and confusion (Bush, 2013; Domino and Luby, 2012; Hoiseth et al., 2005), resulting in its medical use in humans being terminated in 1965 (Morris and Wallach, 2014).

In efforts to identify an alternative to PCP without the serious psychotomimetic side effects, but that retained the excellent anesthetic effects (Mion, 2017), the original form of ketamine (CI-581) was synthesized as short half-life derivative of PCP by Parke-Davis (Fig. 2) (Domino, 2010). In 1964, Dr., Edward Domino and Dr. Guenter Corsen performed the first study of the anesthetic effects of CI-581 in healthy prisoners (Domino, 2010). Shortly thereafter, in 1965, ketamine was

* Corresponding author.

E-mail address: hashimoto@faculty.chiba-u.jp (K. Hashimoto).<https://doi.org/10.1016/j.pbb.2020.172870>

Received 15 January 2020; Received in revised form 30 January 2020; Accepted 4 February 2020

Available online 05 February 2020

0091-3057/© 2020 The Authors. Published by Elsevier Inc. This is an open access article under the CC BY license

(http://creativecommons.org/licenses/by/4.0/).

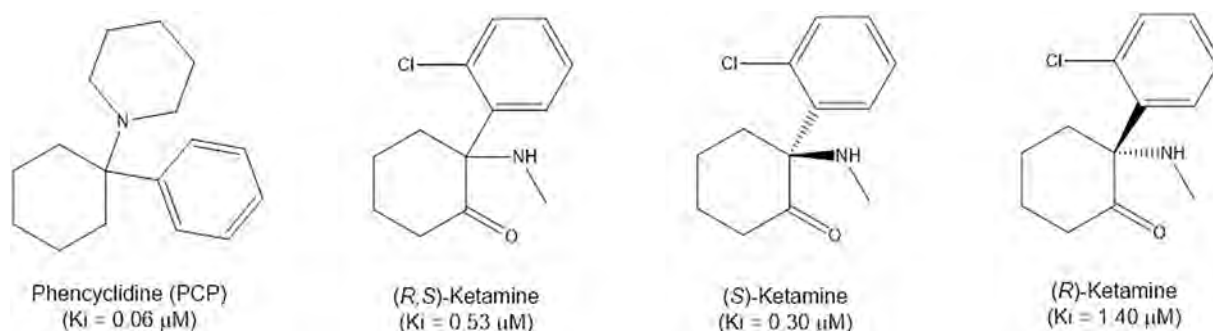


Fig. 1. Chemical structure of phencyclidine (PCP), (*R,S*)-ketamine and its enantiomers. K_i values for NMDAR are presented in parenthesis (Ebert et al., 1997).

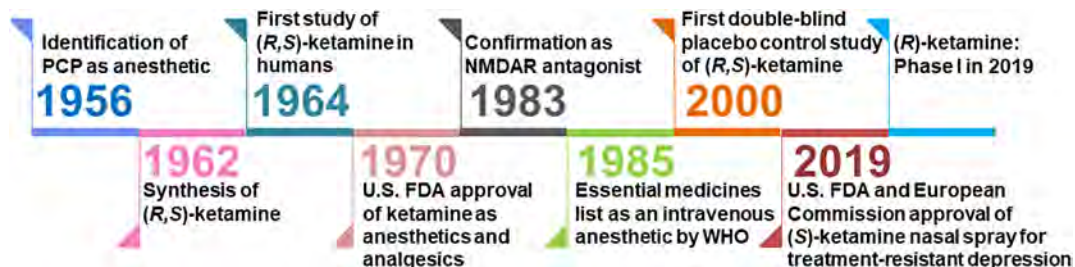


Fig. 2. Brief history of (*R,S*)-ketamine and two enantiomers from anesthetic to antidepressant.

confirmed to be an effective analgesic and anesthetic (Domino et al., 1965). In the first clinical study of ketamine among 130 patients who underwent surgical procedures it was reported to induce a unique state of altered consciousness, described as being disconnected (Corssen and Domino, 1966). Ketamine was later approved in 1970 for anesthetic use by the US Food Drug Administration (FDA) (Fig. 2) (Dong et al., 2015; Mion, 2017; Stevenson, 2005). However, due to its euphoric effects, ketamine became a popular recreational drug in the US and Europe in subsequent decades (Lankenau, 2016; Wolff, 2016). Ketamine remains a commonly abused illicit drug worldwide (Y. Liu et al., 2016).

Contemporaneous reports since the 1970s have shown that ketamine hydrochloride (Ketalar[®]) received much attention, with researchers exploring its pharmacokinetics and mechanism of anesthetic and analgesic action for therapeutic purposes (Li and Vlissides, 2016; Lodge and Mercier, 2015; Tyler et al., 2017). As part of this history, it is worth noting that ketamine was shown to be an NMDAR antagonist in 1983 (Fig. 2) (Anis et al., 1983). Given ketamine's unique properties in pain relief and sedation (Gao et al., 2016), ketamine was added to the WHO's essential medicines list as an intravenous anesthetic in 1985 (Fig. 2) (Gowda et al., 2016; WHO, 2011). Although it has now been used for more than 50 years, not only as an anesthetic and analgesic agent but also as a drug of abuse, its use remains limited due to its undesirable psychotomimetic effects.

3. Antidepressant-like effects of (*R,S*)-ketamine and NMDAR antagonists in rodents

In 1975, (*R,S*)-ketamine was reported to show antidepressant-like effects in animal models. For example, it was associated with the reversal of tetrabenazine-induced ptosis in mice, reversal of reserpine-induced hypothermia in rats, enhancement of yohimbine toxicity in mice, and inhibition of oxotremorine-induced tremors in mice (Sofia and Harakal, 1975). In these models, however, the antidepressant-like activity of ketamine was substantially less than that of imipramine (Sofia and Harakal, 1975).

As already mentioned, ketamine was identified to be an NMDAR antagonist in 1983 (Fig. 2) (Anis et al., 1983). In 1990 it was reported that NMDAR antagonists like AP-7 and (+)-MK-801 had

antidepressant-like effects in rodents (Trullas and Skolnick, 1990). In a chronic mild stress model, (+)-MK-801 showed anti-anhedonia-like effects in rats (Papp and Moryl, 1993). Several animal studies soon documented that NMDAR antagonists, such as MK-801, CGP 37849, and eliprodil, may have the antidepressant-like effects in animal model of depression (Autry et al., 2011; Leyer et al., 1995; Maj et al., 1992; Meloni et al., 1993; Papp and Moryl, 1994; Petrie et al., 2000; Skolnick et al., 1996; Wedzony et al., 1995; B. Yang et al., 2016). Importantly, (+)-MK-801 did not show ketamine-like long-lasting antidepressant effects in susceptible mice after chronic social defeat stress (CSDS), but it did produce rapid-acting antidepressant effects in CSDS-susceptible mice (B. Yang et al., 2016). Thus, available evidence indicated that NMDAR antagonists could alleviate depression-like behaviors in rodents, which led to several pharmaceutical companies developing NMDAR antagonists as novel antidepressants (Hashimoto, 2019a).

In a shock-induced depression model, Chaturvedi et al. (1999) reported that the antidepressant effects of (*R,S*)-ketamine at the dose of 5 and 10 mg/kg respectively significantly increased ambulation and rearing in the open field test and attenuated the increased immobility time in forced swimming test. In a rat learned helplessness (LH) model, Koike et al. (2011) reported that (*R,S*)-ketamine (10 mg/kg) exerted rapid antidepressant-like effects that were sustained for at least 72 h after a single dose. In a model of chronic unpredictable mild stress (CUMS), a single dose of (*R,S*)-ketamine (10 mg/kg) elicited rapid-onset persistent antidepressant effects in rodents (W.X. Liu et al., 2016; Ma et al., 2013; Sun et al., 2016). Comparable to tropomyosin receptor kinase B (TrkB) agonists and antagonists (7,8-dihydroxyflavone and ANA-12, respectively), it was reported that (*R,S*)-ketamine showed rapid-acting and longer lasting antidepressant effects in CSDS-susceptible mice (Zhang et al., 2015). It also showed antidepressant-like effects of (*R,S*)-ketamine in inflammation-induced depression models (Huang et al., 2019; Lindqvist et al., 2017; Remus and Dantzer, 2016; Yamaguchi et al., 2018; Zhang et al., 2016; Zhang and Hashimoto, 2019b).

Unfortunately, the potential psychotomimetic and other unwanted side effects of (*R,S*)-ketamine have also been well-documented in rodents. These include hyperlocomotion, prepulse inhibition (PPI) deficits, conditioned place preference, schizophrenia-like psychotic

symptoms, and cognitive deficits (Becker and Grecksch, 2004; Chan et al., 2013; Chang et al., 2019; Giorgetti et al., 2015; Imre et al., 2006; Lahti et al., 1995; Yang et al., 2015). These have limited interest in its use in humans.

4. Brief history of (R,S)-ketamine's antidepressant effects in humans

The discovery of (R,S)-ketamine's antidepressant effects in humans began in the 1970s (Fig. 2). As described in Edward Domino's review article, some PCP (or ketamine) abusers had used (R,S)-ketamine to improve depressive symptoms rapidly when usual antidepressants were not effective (Domino, 2010). However, he conducted no further study because of concerns that PCP and (R,S)-ketamine were illicit drugs (Domino, 2010). It was therefore a major advancement when (R,S)-ketamine's antidepressant effects were later acknowledged and the agent was introduced for the treatment of severe depression. Berman et al. (2000) had already demonstrated the rapid-acting and sustained antidepressant effects of (R,S)-ketamine in patients with depression, and these findings were replicated by Zarate Jr. et al. (2006) in treatment-resistant patients with major depressive disorder (MDD). Since then, many studies have confirmed the antidepressant effects of (R,S)-ketamine for treatment-resistant patients with MDD, bipolar disorder, and suicidal ideation (Bobo et al., 2016; Grunebaum et al., 2018; Kishimoto et al., 2016; Murrugh et al., 2013; Newport et al., 2015; Singh et al., 2016b).

In clinical trials, interventional studies have sought to evaluate the beneficial effects of (R,S)-ketamine. Several randomized single- and double-blind placebo- or drug-controlled studies have replicated the antidepressant effects of (R,S)-ketamine in both MDD and bipolar disorder, even after a single intravenous dose of 0.5 mg/kg (Berman et al., 2000; Zarate Jr. et al., 2006). Another cross-over double-blind study indicated that many patients with treatment-resistant bipolar disorder (71%) showed significant improvements (Diazgranados et al., 2010). Zarate Jr. et al. (2012) also evidenced that depressive symptoms and suicidal ideation improved within 40 min of patients with bipolar disorder receiving a single infusion of (R,S)-ketamine. Furthermore, in a dose-ranging trial of intravenous (R,S)-ketamine, Fava et al. (2018) suggested that there was evidence to support the validity of single dose therapy at either 0.5 mg/kg or 1.0 mg/kg in patients with treatment-resistant depression.

In two midazolam-controlled randomized clinical trials, (R,S)-ketamine caused rapid reductions in suicidal ideation and depressive symptoms within 24 h (Grunebaum et al., 2018; Murrugh et al., 2013). Moreover, (R,S)-ketamine was shown to have potent anti-suicidal effects in depressed patients with suicidal ideation (Bartoli et al., 2017; Reinstatler and Youssef, 2015; Wilkinson et al., 2018). These studies indicate that (R,S)-ketamine is a promising antidepressant for the treatment of severe depressed patients with suicide ideation.

Repeated ketamine infusion is important for maintenance therapy in patients with treatment-resistant depression (Phillips et al., 2019; Strong and Kabbaj, 2018). In a double-blind, randomized, placebo-controlled study, Singh et al., 2016b suggested that twice- or thrice-weekly administration of (R,S)-ketamine (0.5 mg/kg) was sufficient to maintain antidepressant efficacy over 15 days in patients with treatment-resistant depression. At present, there is a lack of long-term data on the long-term safety and efficacy of (R,S)-ketamine for patients with treatment-resistant depression. This is important given the potential for severe side effects.

5. Antidepressant-like effects of ketamine enantiomers in rodents

(R,S)-ketamine ($K_i = 0.53 \mu\text{M}$ for NMDAR) comprises a racemic mixture of (R)-ketamine ($K_i = 1.4 \mu\text{M}$ for NMDAR) and (S)-ketamine ($K_i = 0.30 \mu\text{M}$ for NMDAR) in equal measure (Fig. 1) (Ebert et al., 1997). In 2014, Zhang et al. (2014) first reported that (R)-ketamine had

greater potency and longer lasting antidepressant effects than (S)-ketamine in a neonatal dexamethasone-treated model of depression. In 2015, they further reported that (R)-ketamine had greater potency and longer lasting antidepressant effects than (S)-ketamine in CSDS and LH models of depression (Yang et al., 2015). Subsequently, the superiority of (R)-ketamine over (S)-ketamine was reported in rodents (Chang et al., 2019; Fukumoto et al., 2017; Zanos et al., 2016). Importantly, (R)-ketamine also has fewer detrimental side effects than either (R,S)-ketamine or (S)-ketamine in rodents and monkey (Chang et al., 2019; Fukumoto et al., 2017; Hashimoto, 2017; Hashimoto et al., 2017; Tian et al., 2018a; Yang et al., 2015; B. Yang et al., 2016a; C. Yang et al., 2016). However, in 2019, Masaki et al. (2019) demonstrated that the functional MRI (fMRI) responses in the brains of conscious rats after a single injection of (S)-ketamine, (R,S)-ketamine, or (+)-MK-801 were different from the fMRI responses after a single injection of (R)-ketamine. Their results indicated that NMDAR inhibition was unlikely to play a role in the pharmacological effects of (R)-ketamine in rat brains (Masaki et al., 2019).

6. Antidepressant-like effects of ketamine metabolites in rodents

In 2016, a group led by Dr. Todd Gould (University of Maryland) reported that the metabolism of (R,S)-ketamine to (2R,6R)-hydroxynorketamine (HNK) (Fig. 3) was essential for the antidepressant-like effects of the parent compound in rodents (Zanos et al., 2016). Although (2R,6R)-HNK is a minor metabolite of (R)-ketamine, the dose necessary to achieve antidepressant-like effects was similar to that for (R,S)-ketamine (Zanos et al., 2016). Unfortunately, our group was unable to replicate the antidepressant-like effects of (2R,6R)-HNK in rodents with depression-like phenotypes (Chaki, 2018; Chang et al., 2018; Hashimoto and Shirayama, 2018; Shirayama and Hashimoto, 2018; Xiong et al., 2019; Yamaguchi et al., 2018; Zhang et al., 2018b; Zhang et al., 2018c).

In a study using cytochrome P450 inhibitors, it was shown that metabolism to (2R,6R)-HNK was unnecessary for the antidepressant-like effects of (R)-ketamine, and that (R)-ketamine itself may be responsible for the observed antidepressant-like actions (Yamaguchi et al., 2018). Clinical study of (2R,6R)-HNK in humans is to be started by the US National Institute of Mental Health. A double-blind randomized study of (R)-ketamine versus (2R,6R)-HNK would be of great interest in depressed patients.

Finally, (S)-ketamine is metabolized to (S)-norketamine (Fig. 3). In 2018, Yang et al. (2018a) reported that (S)-norketamine produced rapid and sustained antidepressant-like effects in a CSDS model. Importantly, unlike to (S)-ketamine, (S)-norketamine did not produce the expected side effects in rodents (Yang et al., 2018a). Therefore, (S)-norketamine could be an alternative to (S)-ketamine, potentially offering antidepressant efficacy with fewer side effects (Hashimoto, 2019a; Hashimoto, 2019b; Hashimoto and Yang, 2018).

7. Effects of ketamine enantiomers in humans

Vollenweider et al. (1997) reported on the psychological state and cerebral glucose metabolism produced after injecting either (S)-ketamine or (R)-ketamine. Although (S)-ketamine produced psychotic reactions, including depersonalization and hallucinations, (R)-ketamine did not produce any psychotic symptoms in the same subjects at the same dose (Vollenweider et al., 1997). Positron emission tomography showed that (S)-ketamine led to markedly increased glucose utilization in the frontal cortex and thalamus, whereas (R)-ketamine suppressed glucose metabolism in several brain areas (Vollenweider et al., 1997). Collectively, these results suggested that (S)-ketamine contributed to the acute side effects of ketamine, whereas (R)-ketamine may be free of these side effects (Hashimoto, 2019a; Zanos et al., 2018).

In the US, Janssen Pharmaceutical developed (S)-ketamine nasal spray for use in treatment-resistant depression. This was based on the

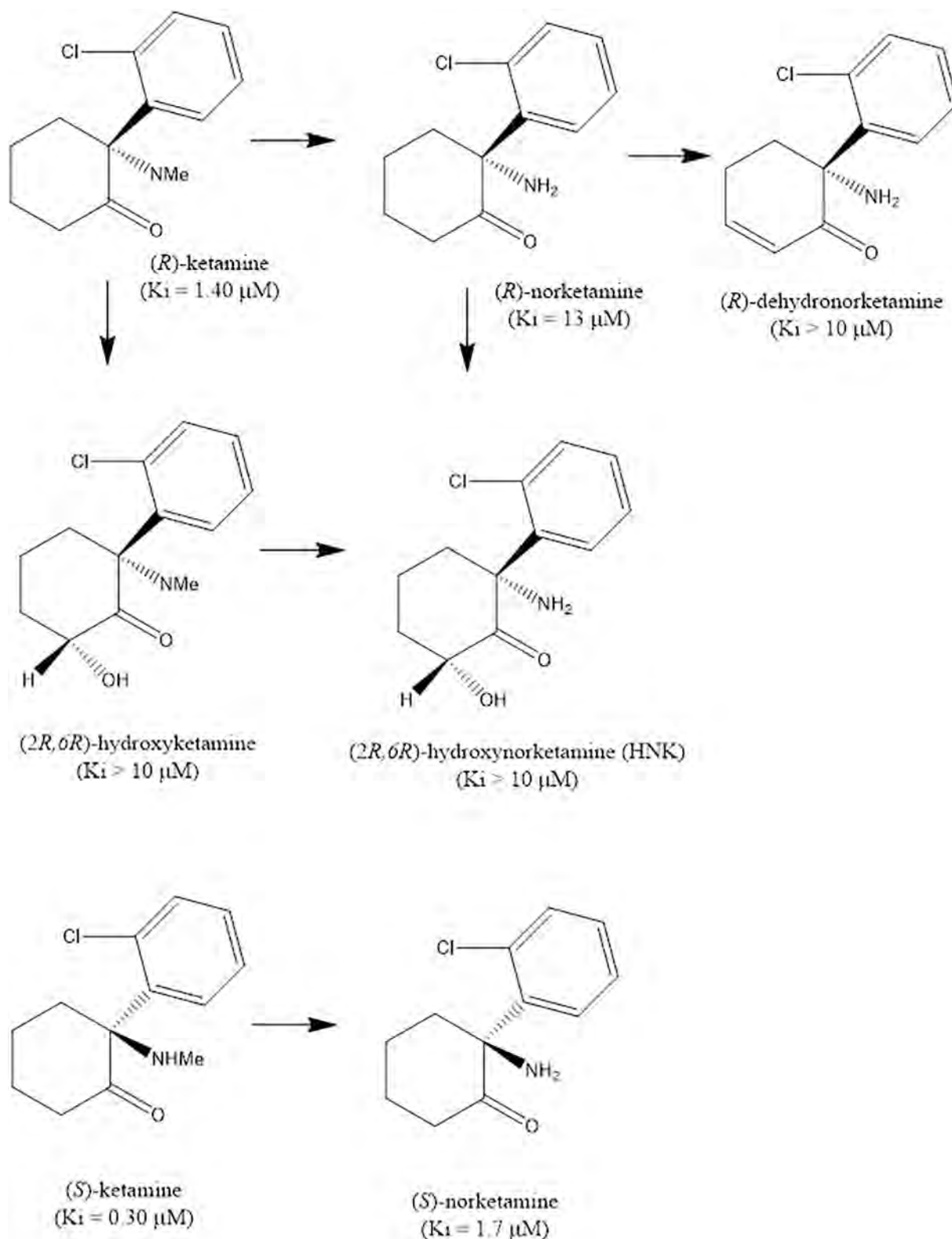


Fig. 3. Chemical structure of metabolites $(2R,6R)$ -HNK and (S) -norketamine of (R) -ketamine and (S) -ketamine. K_i values for NMDAR are presented in parenthesis (Ebert et al., 1997; Zanos et al., 2016).

results of a double-blind, multicenter, randomized, placebo-controlled trial (Singh et al., 2016a) in which it was reported that (S) -ketamine (0.2 and 0.40 mg/kg by intravenous infusion) showed a rapid and robust antidepressant effect (within 2 h) in patients with treatment-resistant depression. The most common treatment-emergent adverse

events were headache, nausea, and dissociation (Singh et al., 2016a). A recent head-to-head study of (S) -ketamine (0.25 mg/kg by intravenous infusion) and (R,S) -ketamine (0.5 mg/kg by intravenous infusion) demonstrated that (S) -ketamine produced similar antidepressant effects to those of (R,S) -ketamine in treatment-resistant patients with depression

(Correia-Melo et al., 2019), indicating the non-inferiority of (S)-ketamine (0.25 mg/kg) to (R,S)-ketamine (0.5 mg/kg) 24 h after a single infusion. Interestingly, however, the antidepressant effects of (R,S)-ketamine (0.5 mg/kg) by 7 days after a single injection were more potent than for (S)-ketamine, albeit without statistical significance ($P = 0.08$) (Correia-Melo et al., 2019). In contrast, based on the pre-clinical findings (Yang et al., 2015; Yang et al., 2018a; Zhang et al., 2014), it is likely that (R)-ketamine plays a role in the long-lasting antidepressant effects of (R,S)-ketamine. Double-blind, randomized trials of (R)-ketamine versus (S)-ketamine are therefore urgently needed to assess their relative efficacies in patients with depression.

Only two of the five phase III trials performed by Janssen Pharmaceutical showed positive results for (S)-ketamine. Nevertheless, on March 5, 2019, the US FDA approved the use of (S)-ketamine nasal spray (esketamine) for treatment-resistant depression in conjunction with an oral antidepressant (Fig. 2). Because of the risk of serious adverse effects, it is only available through a restricted distribution system, under the Risk Evaluation and Mitigation Strategy. On December 19, 2019, (S)-ketamine nasal spray was approved for use in treatment-resistant depression in Europe (Fig. 2) (Mahase, 2019). However, there are many concerns about the efficacy of esketamine nasal spray (Kaur et al., 2019; Turner, 2019; Zimmermann et al., 2020).

A recent pilot study in Brazil demonstrated that intravenous infusion of (R)-ketamine (0.5 mg/kg for 40-min) elicited rapid-acting and sustained antidepressant actions in treatment-resistant patients with MDD, and that side effects such as dissociation were low (Leal et al., 2020). At present, a clinical trial of (R)-ketamine by Perception Neuroscience Ltd. is underway for use in depressed patients (Hashimoto, 2019a).

8. Mechanisms of ketamine's antidepressant actions

8.1. NMDAR inhibition and AMPAR activation

It is widely acknowledged that the rapid antidepressant actions of ketamine occur via blockade of NMDARs located at inhibitory interneurons. This blockade causes the disinhibition of pyramidal cells that result in a burst of glutamatergic transmission (Duman, 2018; Krystal et al., 2019). Subsequently, activation of the AMPAR (α -amino-3-hydroxy-5-methyl-4-isoxazolepropionic acid receptor) is required for ketamine's antidepressant effects. This was demonstrated by research showing that pretreatment with an AMPAR antagonist blocked ketamine's antidepressant effects in rodents (Maeng et al., 2008). In addition, the role of AMPAR activation in the antidepressant effects of ketamine and its two enantiomers has been replicated (Autry et al., 2011; Yang et al., 2015).

Unfortunately, other NMDAR antagonists (e.g., memantine, lanicemine, rapastinel, and AV-101) do not show ketamine-like robust antidepressant actions in patients with depression (Hashimoto, 2019a; Kishimoto et al., 2016; Newport et al., 2015; Sanacora et al., 2017; Yang et al., 2019b; Zarate Jr. et al., 2006). Preclinical data using the two ketamine enantiomers has indicated that NMDAR inhibition may not be central to the antidepressant effects of ketamine in rodents (Hashimoto, 2019a; Yang et al., 2015, 2019b). Therefore, we must now reconsider the role of NMDAR inhibition in the antidepressant effects of ketamine and its enantiomers (Yang et al., 2019b). In addition, there are some questions that remain to be explored although role of NMDAR in ketamine's antidepressant effects is supported by convergent pre-clinical data. Nonetheless, a full picture of the multiple mechanistic pieces linking ketamine to antidepressant actions is still under experimental scrutiny.

8.2. Monoaminergic system

It has long been established that 5-hydroxytryptamine (5-HT) plays a key role in the mechanisms of action of SSRIs and SNRIs. Research also

indicates that AMPAR-dependent 5-HT release in the medial prefrontal cortex may be involved in the antidepressant effects of (R,S)-ketamine in rodents without depression-like phenotypes (Chaki and Fukumoto, 2019; Fukumoto et al., 2016), though it is considered unlikely that 5-HT plays a role in the antidepressant effects of either (R,S)-ketamine or (R)-ketamine in rodents with a depression-like phenotype (Gigliucci et al., 2013; Zhang et al., 2018a). Therefore, further detailed studies are needed on the role of 5-HT in the antidepressant effects of (R,S)-ketamine and its enantiomers in animals with depression-like phenotypes.

It has also been suggested that the dopamine system plays a role in depression. A recent study demonstrated that disruption of the dopamine D₁ receptor encoded by the *Drd1* in the medial prefrontal cortex blocked the rapid antidepressant effects of (R,S)-ketamine in control mice (Hare et al., 2019). This finding suggested that activation of dopamine D₁ receptors in the medial prefrontal cortex was necessary for the rapid antidepressant actions of (R,S)-ketamine. By contrast, Li et al. (2015) reported that the dopamine D₁ receptor antagonist SCH-23390 did not block the antidepressant-like effects of (R,S)-ketamine in control mice. It has also been shown that pretreatment with SCH-23390 failed to block the antidepressant effects of (R)-ketamine in CSDS-susceptible mice (Chang et al., 2020). A recent study also demonstrated that (S)-ketamine caused a robust increase in dopamine release in the prefrontal cortex compared with (R)-ketamine (Ago et al., 2019), but that its antidepressant effects were less potent than those of (R)-ketamine in animal models of depression. Therefore, although it is unlikely that dopamine D₁ receptors play a major role in the antidepressant actions of (R,S)-ketamine or (R)-ketamine, the dopamine system may contribute to some of the observed pharmacological actions (Chang et al., 2020).

8.3. BDNF-TrkB system

In 2011, Autry et al. (2011) demonstrated that the rapid-acting antidepressant effects of (R,S)-ketamine were dependent on the rapid synthesis of brain-derived neurotrophic factor (BDNF); this was based on the finding that (R,S)-ketamine did not cause antidepressant-like effects in inducible *Bdnf*-knockout mice. Subsequent studies have replicated the role of the BDNF-TrkB cascade in the antidepressant effects of (R,S)-ketamine (Yang et al., 2013; Zhou et al., 2014). The TrkB inhibitor ANA-12 has also been shown to block the rapid and long-lasting antidepressant effects of (R)-ketamine and (S)-ketamine in CSDS-susceptible mice (Yang et al., 2015). Regulation of glutamate transporter 1 on astrocytes, through the activation of TrkB, also appears to play a role in the beneficial effects of (R,S)-ketamine on behavioral abnormalities and in the morphological changes seen in the hippocampi of rats exposed to CUMS (W.X. Liu et al., 2016a). Collectively, it is likely that prolonged activation of the BDNF-TrkB cascade in the prefrontal cortex and hippocampus is responsible for the long-lasting antidepressant effects of (R,S)-ketamine and its enantiomers.

8.4. mTORC1 and ERK

In 2010, Dr. Ronald Duman (Yale University) and colleagues demonstrated that rapamycin, an mTOR inhibitor, blocked the antidepressant-like effects of (R,S)-ketamine in rodents (Li et al., 2010). By contrast, Autry et al. (2011) later showed that the level of phosphorylated mTOR was not altered in the hippocampi of control and *Bdnf*-knockout mice after injecting (R,S)-ketamine. The antidepressant-like effects of (R,S)-ketamine were not affected by rapamycin in wild-type mice. Furthermore, it was shown that (R,S)-ketamine did not alter the levels of phosphorylated mTOR in the hippocampi and prefrontal cortexes of mice, but that the levels of phosphorylated eukaryotic elongation factor 2 and BDNF were significantly increased in the hippocampi (Zanos et al., 2016). Interestingly, a CSDS model indicated that mTORC1 plays a major role in the antidepressant effects of (S)-ketamine, but not in those of (R)-ketamine, (Yang et al., 2018b). Instead, the antidepressant effects of (R)-ketamine may be mediated by ERK

activation, based on evidence that pretreatment with SL327 (an ERK inhibitor) inhibited its antidepressant effects (Yang et al., 2018b).

A recent randomized, placebo-controlled clinical study demonstrated that rapamycin did not alter the acute effects of (*R,S*)-ketamine in treatment-resistant patients with depression, but that combination therapy led to prolonged antidepressant effects (Abdallah et al., 2018). As such, the role of mTORC1 in the antidepressant effect of (*R,S*)-ketamine has not been confirmed in treatment-resistant patients with depression. Further investigation using a larger sample should help to confirm the role of mTORC1 in the antidepressant effects of (*R,S*)-ketamine and its enantiomers in clinically depressed patients.

8.5. Low-voltage-sensitive T-type calcium channel

In 2018, a group of Dr. Hailan Hu (Zhejiang University) demonstrated that blockade of NMDAR-dependent bursting activity in the lateral habenula was induced by (*R,S*)-ketamine. Further, they showed that this lateral habenula bursting promoted rapid-acting antidepressant effects in rodents and that it required both NMDARs and low-voltage-sensitive T-type calcium channels (Y. Yang et al., 2018). Giving ethosuximide (200 mg/kg), a T-type calcium channel inhibitor, resulted in rapid antidepressant effects in rodents (Y. Yang et al., 2018). However, giving ethosuximide (100, 200, 400 mg/kg) did not produce any antidepressant actions in CSDS-susceptible mice, whereas (*R*)-ketamine did, in the same model (Tian et al., 2018b). A recent double-blind, placebo-controlled study demonstrated that ethosuximide did not produce antidepressant actions in medication-free patients with depression (Zhang et al., 2020b).

Overall, existing research indicates that T-type calcium channel inhibitors are unlikely to might exert ketamine-like robust antidepressant actions in depressed patients. Further study is needed to confirm the antidepressant action of ethosuximide. At present, a randomized clinical trial is underway at Zhejiang University in China to assess the effects of ethosuximide in treatment-resistant patients with depression (Jiang et al., 2019).

8.6. Opioid system

It is well known that ketamine interacts with opioid receptors, with (*S*)-ketamine binding to mu and kappa receptors being 2- to 4-fold stronger than that of (*R*)-ketamine (Domino, 2010; Hirota and Lambert, 1996). Pretreatment with the opiate receptor antagonist naltrexone (50 mg) significantly blocked the antidepressant and anti-suicidal effects of (*R,S*)-ketamine in treatment-resistant patients with depression, suggesting that activation of the opioid system was necessary to produce the rapid-acting antidepressant effects of (*R,S*)-ketamine (Williams et al., 2019; Williams et al., 2018). Other research has shown that pretreatment with naltrexone did not alter the antidepressant effects of (*R,S*)-ketamine in depressed patients with alcohol use disorder (Yoon et al., 2019). Furthermore, (*R,S*)-ketamine still produced antidepressant effects in patients concurrently receiving a high-affinity mu opioid receptor agonists (i.e., buprenorphine, methadone, or naltrexone) (Marton et al., 2019). Thus, the role of the opioid system in the antidepressant effects of (*R,S*)-ketamine remains controversial in humans.

In CSDS and inflammation-induced models of depression, naltrexone pretreatment did not block the antidepressant-like effects of (*R,S*)-ketamine, suggesting that the opioid system may not facilitate the antidepressant-like effects of (*R,S*)-ketamine (Zhang and Hashimoto, 2019a). However, a recent study showed that NMDAR and opioid receptors were required for (*R,S*)-ketamine to reduce the depression-like and lateral habenula hyperactive cellular phenotypes in congenital LH rats (Klein et al., 2020). Both the behavioral and cellular effects of (*R,S*)-ketamine were blocked by naltrexone in congenital LH rats (Klein et al., 2020). The authors concluded that (*R,S*)-ketamine likely does not act as an opiate at antidepressant doses, with its cellular and behavioral effects instead primarily mediated through the NMDAR (Klein et al.,

2020). Further study with each ketamine enantiomer is needed to confirm the role of the opioid system in the antidepressant actions of (*R,S*)-ketamine.

8.7. Transforming growth factor β 1 system

The molecular mechanisms underpinning (*R*)-ketamine's antidepressant effects remain unclear, especially compared with our understanding of (*S*)-ketamine. However, based on RNA sequencing analysis, we demonstrated that transforming growth factor (TGF)- β 1 in the microglia plays a role in the antidepressant effects of (*R*)-ketamine (Zhang et al., 2020a). Of even greater interest, TGF- β 1 was shown to elicit rapid-acting and long-lasting antidepressant effects in CSDS, LH, and inflammation models (Zhang et al., 2020a). As such, it is likely that TGF- β 1 could be a novel therapeutic target for depression.

8.8. Brain-gut-microbiota axis

Multiple lines of evidence suggest a possible role of the brain-gut-microbiota axis in the stress-induced depression-like phenotype and in the antidepressant-like effects of certain compounds (Carlessi et al., 2019; Wang et al., 2020; Yang et al., 2017a; Yang et al., 2019a; Zhang et al., 2017; Zhang et al., 2019). (*R,S*)-ketamine is shown to improve abnormal composition of gut microbiota in rodents with depression-like phenotype (Huang et al., 2019). Furthermore, (*R*)-ketamine ameliorated abnormal composition of gut microbiota in the CSDS susceptible mice (Yang et al., 2017b; Qu et al., 2017). Taken together, the brain-gut-microbiota axis may, in part, play a role in the antidepressant actions of (*R*)-ketamine [or (*R,S*)-ketamine], although further studies are needed.

9. Concluding remarks

The discovery that (*R,S*)-ketamine had robust antidepressant actions in depressed patients was certainly serendipitous (Krystal et al., 2019), and has so far led to the esketamine nasal spray being approved for use in treatment-resistant depression in both the US and Europe, despite several concerns about its efficacy and side effects. By contrast, there are no therapeutic options for (*R*)-ketamine, although clinical research is underway in humans. From the preclinical and clinical findings, it seems that safety profile of (*R*)-ketamine in humans is better than (*R,S*)-ketamine and (*S*)-ketamine (Hashimoto, 2019a, 2019b, 2020). This is of great importance because there is accumulating preclinical data to show that (*R*)-ketamine has greater antidepressant potency and elicits longer lasting effects than either (*R,S*)-ketamine or (*S*)-ketamine. Collectively, existing data indicate that (*R*)-ketamine could be a safer antidepressant, necessitating that the research community conduct double-blind randomized study comparing (*R*)-ketamine with (*S*)-ketamine in depressed patients. As mentioned, non-ketamine NMDAR antagonists fail to produce robust ketamine-like antidepressant effects in patients with depression (Hashimoto, 2019a), suggesting that mechanisms other than NMDAR inhibition play a role in the antidepressant effects of (*R,S*)-ketamine (Hashimoto, 2019a; Yang et al., 2019b). Further detailed study is therefore needed to identify the primary target of (*R,S*)-ketamine's antidepressant actions.

Acknowledgements

This study was supported by Japan Agency for Medical Research and Development, AMED (to K.H., JP19dm0107119). Dr. Yan Wei (Southwest Medical University, China) was supported by the China Scholarship Council (China). Dr. Lijia Chang was supported by the Japan China Sasakawa Medical Fellowship (Tokyo, Japan).

Declaration of competing interest

Dr. Hashimoto is an inventor on a filed patent application on “The use of (R)-ketamine in the treatment of psychiatric diseases”, “(S)-norketamine and salt thereof as pharmaceutical”, and “transforming growth factor- β 1 in the treatment of depression” by Chiba University. Dr. Hashimoto has received research support from Dainippon-Sumitomo, Otsuka, and Taisho (Japan). Other authors declare no conflict of interest.

References

- Abdallah, C.G., Averill, L.A., Gueorguieva, R., Goktas, S., Purohit, P., Ranganathan, M., D'Souza, D.C., Formica, R., Southwick, S.M., Duman, R.S., Sanacora, G., Krystal, J.H., 2018. Rapamycin, an immunosuppressant and mTORC1 inhibitor, triples the antidepressant response rate of ketamine at 2 weeks following treatment: A double-blind, placebo-controlled, cross-over, randomized clinical trial. *bioRxiv*, 500959.
- Ago, Y., Tanabe, W., Higuchi, M., Tsukada, S., Tanaka, T., Yamaguchi, T., Igarashi, H., Yokoyama, R., Seiriki, K., Kasai, A., Nakazawa, T., Nakagawa, S., Hashimoto, K., Hashimoto, H., 2019. (R)-ketamine induces a greater increase in prefrontal 5-HT release than (S)-ketamine and ketamine metabolites via an AMPA receptor-independent mechanism. *Int. J. Neuropsychopharmacol.* 22 (10), 665–674.
- Anis, N.A., Berry, S.C., Burton, N.R., Lodge, D., 1983. The dissociative anaesthetics, ketamine and phencyclidine, selectively reduce excitation of central mammalian neurones by *N*-methyl-aspartate. *Br. J. Pharmacol.* 79 (2), 565–575.
- Autry, A.E., Adachi, M., Nosyreva, E., Na, E.S., Los, M.F., Cheng, P.-f., Kavalali, E.T., Monteggia, L.M., 2011. NMDA receptor blockade at rest triggers rapid behavioural antidepressant responses. *Nature* 475 (7354), 91–95.
- Bartoli, F., Riboldi, I., Crocama, C., Di Brita, C., Clerici, M., Carra, G., 2017. Ketamine as a rapid-acting agent for suicidal ideation: a meta-analysis. *Neurosci. Biobehav. Rev.* 77, 232–236.
- Becker, A., Grecksch, G., 2004. Ketamine-induced changes in rat behaviour: a possible animal model of schizophrenia. Test of predictive validity. *Prog. Neuro-Psychopharmacol. Biol. Psychiatry* 28 (8), 1267–1277.
- Berman, R.M., Cappiello, A., Anand, A., Oren, D.A., Heninger, G.R., Charney, D.S., Krystal, J.H., 2000. Antidepressant effects of ketamine in depressed patients. *Biol. Psychiatry* 47 (4), 351–354.
- Bobo, W.V., Vande Voort, J.L., Croarkin, P.E., Leung, J.G., Tye, S.J., Frye, M.A., 2016. Ketamine for treatment-resistant unipolar and bipolar major depression: critical review and implications for clinical practice. *Depress. Anxiety* 33 (8), 698–710.
- Bush, D.M., 2013. Emergency department visits involving phencyclidine (PCP). In: *The CBHSQ Report*, pp. 1–8 Rockville (MD).
- Carlessi, A.S., Borba, L.A., Zugno, A.L., Quevedo, J., Reus, G.Z., 2019. Gut microbiota-brain axis in depression: the role of neuroinflammation. *Eur. J. Neurosci.* <https://doi.org/10.1111/ejn.14631>. 2019 Nov. 30.
- Chaki, S., 2018. Is metabolism of (R)-ketamine essential for the antidepressant effects? *Int. J. Neuropsychopharmacol.* 21 (2), 154–156.
- Chaki, S., Fukumoto, K., 2019. Role of serotonergic system in the antidepressant actions of mGlu_{2/3} receptor antagonists: similarity to ketamine. *Int. J. Mol. Sci.* 20 (6), 1270.
- Chan, K.W., Lee, T.M., Siu, A.M., Wong, D.P., Kam, C.M., Tsang, S.K., Chan, C.C., 2013. Effects of chronic ketamine use on frontal and medial temporal cognition. *Addict. Behav.* 38 (5), 2128–2132.
- Chang, L., Toki, H., Qu, Y., Fujita, Y., Mizuno-Yasuhiro, A., Yamaguchi, J.I., Chaki, S., Hashimoto, K., 2018. No sex-specific differences in the acute antidepressant actions of (R)-ketamine in an inflammation model. *Int. J. Neuropsychopharmacol.* 21 (10), 932–937.
- Chang, L., Zhang, K., Pu, Y., Qu, Y., Wang, S.M., Xiong, Z., Ren, Q., Dong, C., Fujita, Y., Hashimoto, K., 2019. Comparison of antidepressant and side effects in mice after intranasal administration of (R,S)-ketamine, (R)-ketamine, and (S)-ketamine. *Pharmacol. Biochem. Behav.* 181, 53–59.
- Chang, L., Zhang, K., Pu, Y., Qu, Y., Wang, S.-m., Xiong, Z., Shirayama, Y., Hashimoto, K., 2020. Lack of dopamine D₁ receptors in the antidepressant actions of (R)-ketamine in a chronic social defeat stress model. *Eur. Arch. Psych. Clin. Neurosci.* <https://doi.org/10.1007/s00406-019-01012-1>. press.
- Chaturvedi, H.K., Chandra, D., Bapna, J.S., 1999. Interaction between *N*-methyl-D-aspartate receptor antagonists and imipramine in shock-induced depression. *Indian J. Exp. Biol.* 37 (10), 952–958.
- Correia-Melo, F.S., Leal, G.C., Vieira, F., Jesus-Nunes, A.P., Mello, R.P., Magnavita, G., Caliman-Fontes, A.T., Echegaray, M.V.F., Bandeira, I.D., Silva, S.S., Cavalcanti, D.E., Araújo-de-Freitas, L., Sarin, L.M., Tuena, M.A., Nakahira, C., Sampaio, A.S., Del-Porto, J.A., Turecki, G., Loo, C., Lacerda, A.L.T., Quarantini, L.C., 2019. Efficacy and safety of adjunctive therapy using esketamine or racemic ketamine for adult treatment-resistant depression: a randomized, double-blind, non-inferiority study. *J. Affect. Disord.* <https://doi.org/10.1016/j.jad.2019.11.086>.
- Corssen, G., Domino, E.F., 1966. Dissociative anesthesia: further pharmacologic studies and first clinical experience with the phencyclidine derivative CI-581. *Anesth. Analg.* 45 (1), 29–40.
- Diazgranados, N., Ibrahim, L., Brutsche, N.E., Newberg, A., Kronstein, P., Khalife, S., Kammerer, W.A., Quezado, Z., Luckenbaugh, D.A., Salvador, G., Machado-Vieira, R., Manji, H.K., Zarate Jr., C.A., 2010. A randomized add-on trial of an *N*-methyl-D-aspartate antagonist in treatment-resistant bipolar depression. *Arch. Gen. Psychiatry* 67 (8), 793–802.
- Domino, E.F., 2010. Taming the ketamine tiger. 1965. *Anesthesiology* 113 (3), 678–684.
- Domino, E.F., Luby, E.D., 2012. Phencyclidine/schizophrenia: one view toward the past, the other to the future. *Schizophr. Bull.* 38 (5), 914–919.
- Domino, E.F., Chodoff, P., Corssen, G., 1965. Pharmacologic effects of CI-581, a new dissociative anesthetic in man. *Clin. Pharmacol. Ther.* 6, 279–291.
- Dong, T.T., Mellin-Olsen, J., Gelb, A.W., 2015. Ketamine: a growing global health-care need. *Br. J. Anaesth.* 115 (4), 491–493.
- Duman, R.S., 2018. Ketamine and rapid-acting antidepressants: a new era in the battle against depression and suicide. *F1000Res* 7 (F1000 Faculty Rev), 659.
- Ebert, B., Mikkelsen, S., Thorkildsen, C., Borgbjerg, F.M., 1997. Norketamine, the main metabolite of ketamine, is a non-competitive NMDA receptor antagonist in the rat cortex and spinal cord. *Eur. J. Pharmacol.* 333 (1), 99–104.
- Fava, M., Freeman, M.P., Flynn, M., Judge, H., Hoepfner, B.B., Cusin, C., Ionescu, D.F., Mathew, S.J., Chang, L.C., Iosifescu, D.V., Murrrough, J., DeBattista, C., Schatzberg, A.F., Trivedi, M.H., Jha, M.K., Sanacora, G., Wilkinson, S.T., Papakostas, G.I., 2018. Double-blind, placebo-controlled, dose-ranging trial of intravenous ketamine as adjunctive therapy in treatment-resistant depression (TRD). *Mol. Psychiatry.* <https://doi.org/10.1038/s41380-018-0256-5>.
- Fukumoto, K., Iijima, M., Chaki, S., 2016. The antidepressant effects of an mGlu_{2/3} receptor antagonist and ketamine require AMPA receptor stimulation in the mPFC and subsequent activation of the 5-HT neurons in the DRN. *Neuropsychopharmacology* 41 (4), 1046–1056.
- Fukumoto, K., Toki, H., Iijima, M., Hashihayata, T., Yamaguchi, J.I., Hashimoto, K., Chaki, S., 2017. Antidepressant potential of (R)-ketamine in rodent models: comparison with (S)-ketamine. *J. Pharmacol. Exp. Ther.* 361 (1), 9–16.
- Gao, M., Rejaei, D., Liu, H., 2016. Ketamine use in current clinical practice. *Acta Pharmacol. Sin.* 37 (7), 865–872.
- Gigliucci, V., O'Dowd, G., Casey, S., Egan, D., Gibney, S., Harkin, A., 2013. Ketamine elicits sustained antidepressant-like activity via a serotonin-dependent mechanism. *Psychopharmacology* 228 (1), 157–166.
- Giorgetti, R., Marcotulli, D., Tagliabracchi, A., Schifano, F., 2015. Effects of ketamine on psychomotor, sensory and cognitive functions relevant for driving ability. *Forensic Sci. Int.* 252, 127–142.
- Gould, T.D., Z. Jr., C.A., Thompson, S.M., 2019. Molecular pharmacology and neurobiology of rapid-acting antidepressants. *Annu. Rev. Pharmacol. Toxicol.* 59 (1), 213–236.
- Gowda, M.R., Srinivasa, P., Kumbar, P.S., Ramalingaiah, V.H., Muthyalappa, C., Durgaji, S., 2016. Rapid resolution of grief with IV infusion of ketamine: a unique phenomenological experience. *Indian J. Psychol. Med.* 38 (1), 62–64.
- Grunebaum, M.F., Galfalvy, H.C., Choo, T.H., Keilp, J.G., Moitra, V.K., Parris, M.S., Marver, J.E., Burke, A.K., Milak, M.S., Sublette, M.E., Oquendo, M.A., Mann, J.J., 2018. Ketamine for rapid reduction of suicidal thoughts in major depression: a midazolam-controlled randomized clinical trial. *Am. J. Psychiatry* 175 (4), 327–335.
- Hare, B.D., Shinohara, R., Liu, R.J., Pothula, S., DiLeone, R.J., Duman, R.S., 2019. Optogenetic stimulation of medial prefrontal cortex Drd1 neurons produces rapid and long-lasting antidepressant effects. *Nat. Commun.* 10 (1), 223.
- Hashimoto, K., 2016a. Detrimental side effects of repeated ketamine infusions in the brain. *Am. J. Psychiatry* 173 (10), 1044–1045.
- Hashimoto, K., 2016b. Ketamine's antidepressant action: beyond NMDA receptor inhibition. *Expert Opin. Ther. Targets* 20 (11), 1389–1392.
- Hashimoto, K., 2017. Rapid Antidepressant Activity of Ketamine Beyond NMDA Receptor, the NMDA Receptors. *Humana Press*, Cham, pp. 69–81.
- Hashimoto, K., 2019a. Rapid-acting antidepressant ketamine, its metabolites and other candidates: a historical overview and future perspective. *Psychiatry Clin. Neurosci.* 73 (10), 613–627.
- Hashimoto, K., 2019b. Mood, psychomotor, and cognitive function in major depressive disorder: from biomarkers to rapid-acting antidepressants. *Eur. Arch. Psychiatry Clin. Neurosci.* 269, 759–760.
- Hashimoto, K., 2020. Impact of age on optimal dose of antidepressants. *EclinicalMedicine* 18, 100233.
- Hashimoto, K., Kakiuchi, T., Ohba, H., Nishiyama, S., Tsukada, H., 2017. Reduction of dopamine D_{2/3} receptor binding in the striatum after a single administration of esketamine, but not R-ketamine: a PET study in conscious monkeys. *Eur. Arch. Psychiatry Clin. Neurosci.* 267 (2), 173–176.
- Hashimoto, K., Shirayama, Y., 2018. What are the causes for discrepancies of antidepressant actions of (2R,6R)-hydroxynorketamine? *Biol. Psychiatry* 84 (1), e7–e8.
- Hashimoto, K., Yang, C., 2018. Is (S)-norketamine an alternative antidepressant for esketamine? *Eur. Arch. Psych. Clin. Neurosci.* 269 (7), 867–868.
- Hirota, K., Lambert, D.G., 1996. Ketamine: its mechanism(s) of action and unusual clinical uses. *Br. J. Anaesth.* 77 (4), 441–444.
- Hoiseth, G., Hjelmeland, K., Bachs, L., 2005. Phencyclidine-angel dust. *Tidsskr. Nor. Laegeforen.* 125 (20), 2775–2776.
- Huang, N., Hua, D., Zhan, G., Li, S., Zhu, B., Jiang, R., Yang, L., Bi, J., Xu, H., Hashimoto, K., Luo, A., Yang, C., 2019. Role of *Actinobacteria* and *Coriobacteriia* in the antidepressant effects of ketamine in an inflammation model of depression. *Pharmacol. Biochem. Behav.* 176, 93–100.
- Imre, G., Fokkema, D.S., Den Boer, J.A., Ter Horst, G.J., 2006. Dose-response characteristics of ketamine effect on locomotion, cognitive function and central neuronal activity. *Brain Res. Bull.* 69 (3), 338–345.
- Jiang, J., Wang, Z., Dong, Y., Yang, Y., Ng, C.H., Ma, S., Xu, Y., Hu, H., Hu, S., 2019. A statistical analysis plan for a randomized clinical trial to evaluate the efficacy and safety of ethosuximide in patients with treatment-resistant depression. *Medicine* 98 (31), e16674-e16674.
- Kaur, U., Pathak, B.K., Singh, A., Chakrabarti, S.S., 2019. Esketamine: a glimmer of hope in treatment-resistant depression. *Eur. Arch. Psych. Clin. Neurosci.* <https://doi.org/>

- 10.1007/s00406-019-01084-z.
- Kishimoto, T., Chawla, J.M., Hagi, K., Zarate, C.A., Kane, J.M., Bauer, M., Correll, C.U., 2016. Single-dose infusion ketamine and non-ketamine *N*-methyl-D-aspartate receptor antagonists for unipolar and bipolar depression: a meta-analysis of efficacy, safety and time trajectories. *Psychol. Med.* 46 (7), 1459–1472.
- Klein, M.E., Chandra, J., Sheriff, S., Malinow, R., 2020. Opioid system is necessary but not sufficient for antidepressive actions of ketamine in rodents. *Proc. Natl. Acad. Sci. U. S. A.* 117 (5), 2656–2662.
- Koike, H., Iijima, M., Chaki, S., 2011. Involvement of AMPA receptor in both the rapid and sustained antidepressant-like effects of ketamine in animal models of depression. *Behav. Brain Res.* 224 (1), 107–111.
- Krystal, J.H., Abdallah, C.G., Sanacora, G., Charney, D.S., Duman, R.S., 2019. Ketamine: a paradigm shift for depression research and treatment. *Neuron* 101 (5), 774–778.
- Lahti, A.C., Koffel, B., LaPorte, D., Tamminga, C.A., 1995. Subanesthetic doses of ketamine stimulate psychosis in schizophrenia. *Neuropsychopharmacology* 13 (1), 9–19.
- Lankenau, S.E., 2016. On ketamine: in and out of the K hole. In: *Drugs, Clubs and Young People*. Routledge, pp. 91–101.
- Layer, R.T., Popik, P., Olds, T., Skolnick, P., 1995. Antidepressant-like actions of the polyamine site NMDA antagonist, eliprodil (SL-82.0715). *Pharmacol. Biochem. Behav.* 52 (3), 621–627.
- Leal, G.C., Bandeira, I.D., Correia-Melo, F.S., Telles, M., Mello, R.P., Vieira, F., Lima, C.S., Jesus-Nunes, A.P., Guerreiro-Costa, L.N.F., Marback, R.F., Caliman-Fontes, A.T., Marques, B.L.S., Bezerra, M.L.O., Dias-Neto, A.L., Silva, S.S., Sampaio, A.S., Sanacora, G., Turecki, G., Loo, C., Lacerda, A.L.T., Quarantini, L.C., 2020. Intravenous esketamine for treatment-resistant depression: open-label pilot study. *Eur. Arch. Psych. Clin. Neurosci.* <https://doi.org/10.1007/s00406-020-01110-5>. In press.
- Li, L., Vlissides, P.E., 2016. Ketamine: 50 years of modulating the mind. *Front. Hum. Neurosci.* 10, 612.
- Li, N., Lee, B., Liu, R.J., Banasr, M., Dwyer, J.M., Iwata, M., Li, X.Y., Aghajanian, G., Duman, R.S., 2010. mTOR-dependent synapse formation underlies the rapid antidepressant effects of NMDA antagonists. *Science* 329 (5994), 959–964.
- Li, Y., Zhu, Z.R., Ou, B.C., Wang, Y.Q., Tan, Z.B., Deng, C.M., Gao, Y.Y., Tang, M., So, J.H., Mu, Y.L., Zhang, L.Q., 2015. Dopamine D_{2/3} but not dopamine D₁ receptors are involved in the rapid antidepressant-like effects of ketamine in the forced swim test. *Behav. Brain Res.* 279, 100–105.
- Lindqvist, D., Dhabhar, F.S., James, S.J., Hough, C.M., Jain, F.A., Bersani, F.S., Reus, V.I., Verhoeven, J.E., Epel, E.S., Mahan, L., Rosser, R., Wolkowitz, O.M., Mellon, S.H., 2017. Oxidative stress, inflammation and treatment response in major depression. *Psychoneuroendocrinology* 76, 197–205.
- Liu, W.X., Wang, J., Xie, Z.M., Xu, N., Zhang, G.F., Jia, M., Zhou, Z.Q., Hashimoto, K., Yang, J.J., 2016a. Regulation of glutamate transporter 1 via BDNF-TrkB signaling plays a role in the anti-apoptotic and antidepressant effects of ketamine in chronic unpredictable stress model of depression. *Psychopharmacology* 233 (3), 405–415.
- Liu, Y., Lin, D., Wu, B., Zhou, W., 2016b. Ketamine abuse potential and use disorder. *Brain Res. Bull.* 126 (Pt 1), 68–73.
- Lodge, D., Mercier, M.S., 2015. Ketamine and phencyclidine: the good, the bad and the unexpected. *Br. J. Pharmacol.* 172 (17), 4254–4276.
- Ma, X.C., Dang, Y.H., Jia, M., Ma, R., Wang, F., Wu, J., Gao, C.G., Hashimoto, K., 2013. Long-lasting antidepressant action of ketamine, but not glycogen synthase kinase-3 inhibitor SB216763, in the chronic mild stress model of mice. *PLoS One* 8 (2), e56503.
- Maddox, V.H., Godefroi, E.F., Parcell, R.F., 1965. The synthesis of phencyclidine and other 1-arylclohexylamines. *J. Med. Chem.* 8, 230–235.
- Maeng, S., Zarate, C.A., Du, J., Schloesser, R.J., McCammon, J., Chen, G., Manji, H.K., 2008. Cellular mechanisms underlying the antidepressant effects of ketamine: role of α -amino-3-hydroxy-5-methylisoxazole-4-propionic acid receptors. *Biol. Psychiatry* 63 (4), 349–352.
- Mahase, E., 2019. Measles cases rise 300% globally in first few months of 2019. *Br. Med. J.* 365, 11810.
- Maj, J., Rogoz, Z., Skuza, G., Sowinska, H., 1992. Effects of MK-801 and antidepressant drugs in the forced swimming test in rats. *Eur. Neuropsychopharmacol.* 2 (1), 37–41.
- Marton, T., Barnes, D.E., Wallace, A., Woolley, J.D., 2019. Concurrent use of buprenorphine, methadone, or naltrexone does not inhibit ketamine's antidepressant activity. *Biol. Psychiatry* 85 (12), e75–e76.
- Masaki, Y., Kashiwagi, Y., Watabe, H., Abe, K., 2019. (R)- and (S)-ketamine induce differential fMRI responses in conscious rats. *Synapse* 73 (12), e22126.
- Meloni, D., Gambarana, C., De Montis, M.G., Dal Pra, P., Taddei, I., Tagliamonte, A., 1993. Dizocilpine antagonizes the effect of chronic imipramine on learned helplessness in rats. *Pharmacol. Biochem. Behav.* 46 (2), 423–426.
- Mion, G., 2017. History of anaesthesia: the ketamine story - past, present and future. *Eur. J. Anaesthesiol.* 34 (9), 571–575.
- Morris, H., Wallach, J., 2014. From PCP to MXE: a comprehensive review of the non-medical use of dissociative drugs. *Drug Test. Anal.* 6 (7–8), 614–632.
- Murrough, J.W., Iosifescu, D.V., Chang, L.C., Al Jurdi, R.K., Green, C.E., Perez, A.M., Iqbal, S., Pillemer, S., Foulkes, A., Shah, A., Charney, D.S., Mathew, S.J., 2013. Antidepressant efficacy of ketamine in treatment-resistant major depression: a two-site randomized controlled trial. *Am. J. Psychiatry* 170 (10), 1134–1142.
- Murrough, J.W., Abdallah, C.G., Mathew, S.J., 2017. Targeting glutamate signalling in depression: progress and prospects. *Nat. Rev. Drug Discov.* 16 (7), 472–486.
- Newport, D.J., Carpenter, L.L., McDonald, W.M., Potash, J.B., Tohen, M., Nemeroff, C.B., Biomarkers, A.P.A.C.o.R.T.F.o.N., Treatments, 2015. Ketamine and other NMDA antagonists: early clinical trials and possible mechanisms in depression. *Am. J. Psychiatry* 172 (10), 950–966.
- Papp, M., Moryl, E., 1993. New evidence for the antidepressant activity of MK-801, a non-competitive antagonist of NMDA receptors. *Pol. J. Pharmacol.* 45 (5–6), 549–553.
- Papp, M., Moryl, E., 1994. Antidepressant activity of non-competitive and competitive NMDA receptor antagonists in a chronic mild stress model of depression. *Eur. J. Pharmacol.* 263 (1–2), 1–7.
- Petrie, R.X., Reid, I.C., Stewart, C.A., 2000. The *N*-methyl-D-aspartate receptor, synaptic plasticity, and depressive disorder. A critical review. *Pharmacol. Ther.* 87 (1), 11–25.
- Phillips, J.L., Norris, S., Talbot, J., Birmingham, M., Hatchard, T., Ortiz, A., Owoeye, O., Batten, L.A., Blier, P., 2019. Single, repeated, and maintenance ketamine infusions for treatment-resistant depression: a randomized controlled trial. *Am. J. Psychiatry* 176 (5), 401–409.
- Qu, Y., Yang, C., Ren, Q., Ma, M., Dong, C., Hashimoto, K., 2017. Comparison of (R)-ketamine and lanicemine on depression-like phenotype and abnormal composition of gut microbiota in a social defeat stress model. *Sci. Rep.* 7 (1), 15725.
- Reinstatler, L., Youssef, N.A., 2015. Ketamine as a potential treatment for suicidal ideation: a systematic review of the literature. *Drugs R&D* 15 (1), 37–43.
- Remus, J.L., Dantzer, R., 2016. Inflammation models of depression in rodents: relevance to psychotropic drug discovery. *Int. J. Neuropsychopharmacol.* 19 (9).
- Sanacora, G., Heimer, H., Hartman, D., Mathew, S.J., Frye, M., Nemeroff, C., Robinson Beale, R., 2017. Balancing the promise and risks of ketamine treatment for mood disorders. *Neuropsychopharmacology* 42 (6), 1179–1181.
- Shirayama, Y., Hashimoto, K., 2018. Lack of antidepressant effects of (2R,6R)-hydroxynorketamine in a rat learned helplessness model: comparison with (R)-ketamine. *Int. J. Neuropsychopharmacol.* 21 (1), 84–88.
- Singh, J.B., Fedgchin, M., Daly, E.J., De Boer, P., Cooper, K., Lim, P., Pinter, C., Murrough, J.W., Sanacora, G., Shelton, R.C., Kurian, B., Winokur, A., Fava, M., Manji, H., Drevets, W.C., Van Nueten, L., 2016b. A double-blind, randomized, placebo-controlled, dose-frequency study of intravenous ketamine in patients with treatment-resistant depression. *Am. J. Psychiatry* 173 (8), 816–826.
- Singh, J.B., Fedgchin, M., Daly, E., Xi, L., Melman, C., De Bruecker, G., Tadic, A., Sienaert, P., Wiegand, F., Manji, H., Drevets, W.C., Van Nueten, L., 2016a. Intravenous esketamine in adult treatment-resistant depression: a double-blind, double-randomization, placebo-controlled study. *Biol. Psychiatry* 80 (6), 424–431.
- Skolnick, P., Layer, R.T., Popik, P., Nowak, G., Paul, I.A., Trullas, R., 1996. Adaptation of *N*-methyl-D-aspartate (NMDA) receptors following antidepressant treatment: implications for the pharmacotherapy of depression. *Pharmacopsychiatry* 29 (1), 23–26.
- Sofia, R.D., Harakal, J.J., 1975. Evaluation of ketamine HCl for anti-depressant activity. *Arch. Int. Pharmacodyn. Ther.* 214 (1), 68–74.
- Stevenson, C., 2005. Ketamine: a review. *Update in Anaesthesia* 20 (20), 25–29.
- Strong, C.E., Kabbaj, M., 2018. On the safety of repeated ketamine infusions for the treatment of depression: effects of sex and developmental periods. *Neurobiol. Stress* 9, 166–175.
- Sun, H.L., Zhou, Z.Q., Zhang, G.F., Yang, C., Wang, X.M., Shen, J.C., Hashimoto, K., Yang, J.J., 2016. Role of hippocampal p11 in the sustained antidepressant effect of ketamine in the chronic unpredictable mild stress model. *Transl. Psychiatry* 6, e741.
- Tian, Z., Dong, C., Fujita, A., Fujita, Y., Hashimoto, K., 2018a. Expression of heat shock protein HSP-70 in the retrosplenial cortex of rat brain after administration of (R,S)-ketamine and (S)-ketamine, but not (R)-ketamine. *Pharmacol. Biochem. Behav.* 172, 17–21.
- Tian, Z., Dong, C., Zhang, K., Chang, L., Hashimoto, K., 2018b. Lack of antidepressant effects of low-voltage-sensitive T-type calcium channel blocker ethosuximide in a chronic social defeat stress model: comparison with (R)-ketamine. *Int. J. Neuropsychopharmacol.* 21 (11), 1031–1036.
- Trullas, R., Skolnick, P., 1990. Functional antagonists at the NMDA receptor complex exhibit antidepressant actions. *Eur. J. Pharmacol.* 185 (1), 1–10.
- Turner, E.H., 2019. Esketamine for treatment-resistant depression: seven concerns about efficacy and FDA approval. *Lancet Psychiatry* 6 (12), 977–979.
- Tyler, M.W., Yourish, H.B., Ionescu, D.F., Haggarty, S.J., 2017. Classics in chemical neuroscience: ketamine. *ACS Chem. Neurosci.* 8 (6), 1122–1134.
- Vollenweider, F.X., Leenders, K.L., Oye, I., Hell, D., Angst, J., 1997. Differential psychopathology and patterns of cerebral glucose utilisation produced by (S)- and (R)-ketamine in healthy volunteers using positron emission tomography (PET). *Eur. Neuropsychopharmacol.* 7 (1), 25–38.
- Wang, S., Qu, Y., Chang, L., Pu, Y., Zhang, K., Hashimoto, K., 2020. Antibiotic-induced microbiome depletion is associated with resilience in mice after chronic social defeat stress. *J. Affect. Disord.* 260, 448–457.
- Wedzony, K., Klimek, V., Nowak, G., 1995. Rapid down-regulation of beta-adrenergic receptors evoked by combined forced swimming test and CGP 37849—a competitive antagonist of NMDA receptors. *Pol. J. Pharmacol.* 47 (6), 537–540.
- WHO, 2011. WHO Model List of Essential Medicines: 17th List. (March 2011).
- WHO, 2017. Depression and Other Common Mental Disorders: Global Health Estimates. World Health Organization.
- Wilkinson, S.T., Ballard, E.D., Bloch, M.H., Mathew, S.J., Murrough, J.W., Feder, A., Sos, P., Wang, G., Zarate Jr., C.A., Sanacora, G., 2018. The effect of a single dose of intravenous ketamine on suicidal ideation: a systematic review and individual participant data meta-analysis. *Am. J. Psychiatry* 175 (2), 150–158.
- Williams, N.R., Heifets, B.D., Blasey, C., Sudheimer, K., Pannu, J., Pankow, H., Hawkins, J., Birnbaum, J., Lyons, D.M., Rodriguez, C.I., Schatzberg, A.F., 2018. Attenuation of antidepressant effects of ketamine by opioid receptor antagonism. *Am. J. Psychiatry* 175 (12), 1205–1215.
- Williams, N.R., Heifets, B.D., Bentzley, B.S., Blasey, C., Sudheimer, K.D., Hawkins, J., Lyons, D.M., Schatzberg, A.F., 2019. Attenuation of antidepressant and antisuicidal effects of ketamine by opioid receptor antagonism. *Mol. Psychiatry* 24 (12), 1779–1786.
- Witkin, J.M., Knutson, D.E., Rodriguez, G.J., Shi, S., 2018. Rapid-acting antidepressants. *Curr. Pharm. Des.* 24 (22), 2556–2563.
- Wolff, K., 2016. Ketamine: The pharmacokinetics and pharmacodynamics in misusing populations. In: *The SAGE Handbook of Drug & Alcohol Studies: Biological Approaches*, pp. 177.

- Xiong, Z., Fujita, Y., Zhang, K., Pu, Y., Chang, L., Ma, M., Chen, J., Hashimoto, K., 2019. Beneficial effects of (R)-ketamine, but not its metabolite (2R,6R)-hydroxynorketamine, in the depression-like phenotype, inflammatory bone markers, and bone mineral density in a chronic social defeat stress model. *Behav. Brain Res.* 368, 111904.
- Yamaguchi, J.I., Toki, H., Qu, Y., Yang, C., Koike, H., Hashimoto, K., Mizuno-Yasuhiro, A., Chaki, S., 2018. (2R,6R)-hydroxynorketamine is not essential for the antidepressant actions of (R)-ketamine in mice. *Neuropsychopharmacology* 43 (9), 1900–1907.
- Yang, C., Hu, Y.-M., Zhou, Z.-Q., Zhang, G.-F., Yang, J.-J., 2013. Acute administration of ketamine in rats increases hippocampal BDNF and mTOR levels during forced swimming test. *Ups. J. Med. Sci.* 118 (1), 3–8.
- Yang, C., Shirayama, Y., Zhang, J.C., Ren, Q., Yao, W., Ma, M., Dong, C., Hashimoto, K., 2015. R-ketamine: a rapid-onset and sustained antidepressant without psychotomimetic side effects. *Transl. Psychiatry* 5, e632.
- Yang, B., Ren, Q., Ma, M., Chen, Q.X., Hashimoto, K., 2016a. Antidepressant effects of (+)-MK-801 and (–)-MK-801 in the social defeat stress model. *Int. J. Neuropsychopharmacol.* 19 (12), pyw080.
- Yang, C., Han, M., Zhang, J.C., Ren, Q., Hashimoto, K., 2016b. Loss of parvalbumin-immunoreactivity in mouse brain regions after repeated intermittent administration of esketamine, but not R-ketamine. *Psychiatry Res.* 239, 281–283.
- Yang, C., Fujita, Y., Ren, Q., Ma, M., Dong, C., Hashimoto, K., 2017a. *Bifidobacterium* in the gut microbiota confer resilience to chronic social defeat stress in mice. *Sci. Rep.* 7, 45942.
- Yang, C., Qu, Y., Fujita, Y., Ren, Q., Ma, M., Dong, C., Hashimoto, K., 2017b. Possible role of gut-microbiota in the antidepressant effects of (R)-ketamine in a social defeat stress model. *Transl. Psychiatry* 7, 1294.
- Yang, C., Kobayashi, S., Nakao, K., Dong, C., Han, M., Qu, Y., Ren, Q., Zhang, J.C., Ma, M., Toki, H., Yamaguchi, J.I., Chaki, S., Shirayama, Y., Nakazawa, K., Manabe, T., Hashimoto, K., 2018a. AMPA receptor activation-independent antidepressant actions of ketamine metabolite (S)-norketamine. *Biol. Psychiatry* 84 (8), 591–600.
- Yang, C., Ren, Q., Qu, Y., Zhang, J.-C., Ma, M., Dong, C., Hashimoto, K., 2018b. Mechanistic target of rapamycin-independent antidepressant effects of (R)-ketamine in a social defeat stress model. *Biol. Psychiatry* 83 (1), 18–28.
- Yang, Y., Cui, Y., Sang, K., Dong, Y., Ni, Z., Ma, S., Hu, H., 2018c. Ketamine blocks bursting in the lateral habenula to rapidly relieve depression. *Nature* 554 (7692), 317–322.
- Yang, C., Fang, X., Zhan, G., Huang, N., Li, S., Bi, J., Jiang, R., Yang, L., Miao, L., Zhu, B., Luo, A., Hashimoto, K., 2019a. Key role of gut microbiota in anhedonia-like phenotype in rodents with neuropathic pain. *Transl. Psychiatry* 9, 57.
- Yang, C., Yang, J., Luo, A., Hashimoto, K., 2019b. Molecular and cellular mechanisms underlying the antidepressant effects of ketamine enantiomers and its metabolites. *Transl. Psychiatry* 9 (1), 280.
- Yoon, G., Petrakis, I.L., Krystal, J.H., 2019. Association of combined naltrexone and ketamine with depressive symptoms in a case series of patients with depression and alcohol use disorder. *JAMA Psychiatry* 76 (3), 337–338.
- Zanos, P., Moaddel, R., Morris, P.J., Georgiou, P., Fischell, J., Elmer, G.I., Alkondon, M., Yuan, P., Pribut, H.J., Singh, N.S., Dossou, K.S., Fang, Y., Huang, X.P., Mayo, C.L., Wainer, I.W., Albuquerque, E.X., Thompson, S.M., Thomas, C.J., Zarate Jr., C.A., Gould, T.D., 2016. NMDAR inhibition-independent antidepressant actions of ketamine metabolites. *Nature* 533 (7604), 481–486.
- Zanos, P., Moaddel, R., Morris, P.J., Riggs, L.M., Highland, J.N., Georgiou, P., Pereira, E.F.R., Albuquerque, E.X., Thomas, C.J., Zarate, C.A., Gould, T.D., 2018. Ketamine and ketamine metabolite pharmacology: insights into therapeutic mechanisms. *Pharmacol. Rev.* 70 (3), 621–660.
- Zarate Jr., C.A., Singh, J.B., Carlson, P.J., Brutsche, N.E., Ameli, R., Luckenbaugh, D.A., Charney, D.S., Manji, H.K., 2006. A randomized trial of an N-methyl-D-aspartate antagonist in treatment-resistant major depression. *Arch. Gen. Psychiatry* 63 (8), 856–864.
- Zarate Jr., C.A., Brutsche, N.E., Ibrahim, L., Franco-Chaves, J., Diazgranados, N., Cravchik, A., Selter, J., Marquardt, C.A., Liberty, V., Luckenbaugh, D.A., 2012. Replication of ketamine's antidepressant efficacy in bipolar depression: a randomized controlled add-on trial. *Biol. Psychiatry* 71 (11), 939–946.
- Zhang, K., Hashimoto, K., 2019a. Lack of opioid system in the antidepressant actions of ketamine. *Biol. Psychiatry* 85 (6), e25–e27.
- Zhang, K., Hashimoto, K., 2019b. An update on ketamine and its two enantiomers as rapid-acting antidepressants. *Expert. Rev. Neurother.* 19 (1), 83–92.
- Zhang, K., Jia, G., Xia, L., Du, J., Gai, G., Wang, Z., Cao, L., Zhang, F., Tao, R., Liu, H., Hashimoto, K., Wang, G., 2020b. Efficacy of anticonvulsant ethosuximide for major depressive disorder: a randomized, placebo-control clinical trial. *Eur. Arch. Psych. Clin. Neurosci.* <https://doi.org/10.1007/s00406-020-01103-4>.
- Zhang, J.C., Li, S.X., Hashimoto, K., 2014. R (–)-ketamine shows greater potency and longer lasting antidepressant effects than S (+)-ketamine. *Pharmacol. Biochem. Behav.* 116, 137–141.
- Zhang, K., Yang, C., Chang, L., Sakamoto, A., Suzuki, T., Fujita, Y., Qu, Y., Wang, S., Pu, Y., Tan, Y., Wang, X., Ishima, T., Shirayama, Y., Hatano, M., Tanaka, K.F., Hashimoto, K., 2020a. Essential role of microglial transforming growth factor- β 1 in antidepressant actions of (R)-ketamine and the novel antidepressant TGF- β 1. *Transl. Psychiatry* 10, 32.
- Zhang, J.C., Yao, W., Dong, C., Yang, C., Ren, Q., Ma, M., Han, M., Hashimoto, K., 2015. Comparison of ketamine, 7,8-dihydroxyflavone, and ANA-12 antidepressant effects in the social defeat stress model of depression. *Psychopharmacology* 232 (23), 4325–4335.
- Zhang, J.C., Yao, W., Hashimoto, K., 2016. Brain-derived neurotrophic factor (BDNF)-TrkB signaling in inflammation-related depression and potential therapeutic targets. *Curr. Neuropharmacol.* 14 (7), 721–731.
- Zhang, J.C., Yao, W., Dong, C., Yang, C., Ren, Q., Ma, M., Hashimoto, K., 2017. Blockade of interleukin-6 receptor in the periphery promotes rapid and sustained antidepressant actions: a possible role of gut-microbiota-brain axis. *Transl. Psychiatry* 7, e1138.
- Zhang, K., Dong, C., Fujita, Y., Fujita, A., Hashimoto, K., 2018a. 5-hydroxytryptamine-independent antidepressant actions of (R)-ketamine in a chronic social defeat stress model. *Int. J. Neuropsychopharmacol.* 21 (2), 157–163.
- Zhang, K., Fujita, Y., Hashimoto, K., 2018b. Lack of metabolism in (R)-ketamine's antidepressant actions in a chronic social defeat stress model. *Sci. Rep.* 8 (1), 4007.
- Zhang, K., Toki, H., Fujita, Y., Ma, M., Chang, L., Qu, Y., Harada, S., Nemoto, T., Mizuno-Yasuhiro, A., Yamaguchi, J.I., Chaki, S., Hashimoto, K., 2018c. Lack of deuterium isotope effects in the antidepressant effects of (R)-ketamine in a chronic social defeat stress model. *Psychopharmacology* 235 (11), 3177–3185.
- Zhang, K., Fujita, Y., Chang, L., Qu, Y., Pu, Y., Wang, S., Shirayama, Y., Hashimoto, K., 2019. Abnormal composition of gut microbiota is associated with resilience versus susceptibility to inescapable electric stress. *Transl. Psychiatry* 9, 231.
- Zhou, W., Wang, N., Yang, C., Li, X.M., Zhou, Z.Q., Yang, J.J., 2014. Ketamine-induced antidepressant effects are associated with AMPA receptors-mediated upregulation of mTOR and BDNF in rat hippocampus and prefrontal cortex. *Eur. Psychiatry* 29 (7), 419–423.
- Zimmermann, K.S., Ricvhardson, R., Baker, K.D., 2020. Esketamine as a treatment for paediatric depression: questions of safety and efficacy. *Lancet Psychiatry.* [https://doi.org/10.1016/S2215-0366\(19\)30521-8](https://doi.org/10.1016/S2215-0366(19)30521-8). 2020 Jan. 14.

Antibiotic-induced microbiome depletion protects against MPTP-induced dopaminergic neurotoxicity in the brain

Yaoyu Pu¹, Lijia Chang¹, Youge Qu¹, Siming Wang¹, Kai Zhang¹, Kenji Hashimoto¹

¹Division of Clinical Neuroscience, Chiba University Center for Forensic Mental Health, Chiba 260-8670, Japan

Correspondence to: Kenji Hashimoto; email: hashimoto@faculty.chiba-u.jp

Keywords: antibiotic, dopamine, gut microbiota, MPTP, neurotoxicity

Received: July 30, 2019

Accepted: August 13, 2019

Published: September 3, 2019

Copyright: Pu et al. This is an open-access article distributed under the terms of the Creative Commons Attribution License (CC BY 3.0), which permits unrestricted use, distribution, and reproduction in any medium, provided the original author and source are credited.

ABSTRACT

Although the brain–gut axis appears to play a role in the pathogenesis of Parkinson’s disease, the precise mechanisms underlying the actions of gut microbiota in this disease are unknown. This study was undertaken to investigate whether antibiotic-induced microbiome depletion affects dopaminergic neurotoxicity in the mouse brain after administration of 1-methyl-4-phenyl-1,2,3,6-tetrahydropyridine (MPTP). MPTP significantly decreased dopamine transporter (DAT) immunoreactivity in the striatum and tyrosine hydroxylase (TH) immunoreactivity in the substantia nigra of water-treated mice. However, MPTP did not decrease DAT or TH immunoreactivity in the brains of mice treated with an antibiotic cocktail. Furthermore, antibiotic treatment significantly decreased the diversity and altered the composition of the host gut microbiota at the genus and species levels. Interestingly, MPTP also altered microbiome composition in antibiotic-treated mice. These findings suggest that antibiotic-induced microbiome depletion might protect against MPTP-induced dopaminergic neurotoxicity in the brain via the brain–gut axis.

INTRODUCTION

Parkinson’s disease (PD) is a common and progressive neurodegenerative disease that predominately affects dopaminergic neurons in the striatum and substantia nigra (SNr) [1, 2]. There is also evidence that loss of dopamine at extrastriatal sites in the basal ganglia, thalamus, or cortex contributes to PD pathology [3]. Although the precise mechanisms underlying PD pathology remain largely unknown, evidence suggests that the brain–gut axis plays a crucial role [4–13]. For example, alterations in bowel function, mainly in the form of constipation, can precede the onset of the prototypical motor symptoms of PD [14].

Over the past two decades, it has become apparent that gut microbiota is a fundamental factor in host physiology and pathology. The brain–gut axis is a complex, multi–organ, bidirectional signaling system involving the gut microbiota and the brain [6, 15–23]. Moreover, although antibiotics are crucial, their overuse plays a role in the pathogenesis of several diseases

associated with microbiota impairment [24, 25]. Antibiotic cocktail-induced microbiome depletion has been used to investigate the role of gut microbiota in some pathological conditions [26–35]. In addition, Sampson et al. [36] reported that gut microbiota are necessary for motor deficits induced by α -synuclein overexpression in mice. Interestingly, antibiotic treatment ameliorated these deficits, while microbial re-colonization promoted PD pathology in mice. Remarkably, colonization of α -synuclein overexpressing mice with microbiota from PD patients enhanced physical impairments compared to microbiota transplants from healthy control subjects. Collectively, these findings suggest that the effects of the brain–gut axis in the pathology of PD are mediated at least in part by the gut microbiota. However, the effects of antibiotic-induced microbiome depletion on dopaminergic neurotoxicity in the brains of PD model mice are unknown.

In this study, we investigated whether antibiotic-induced microbiome depletion affects MPTP (1-methyl-4-

phenyl-1,2,3,6-tetrahydropyridine)-induced dopaminergic neurotoxicity, which is widely used as an animal model of PD [37], in the mouse brain.

RESULTS

Effects of the antibiotic cocktail on body weight

A repeated measures two-way ANOVA revealed that treatment with an antibiotic cocktail for 14 days reduced mouse body weights (antibiotic: $F_{1,36} = 20.549$, $P < 0.001$; MPTP: $F_{1,36} = 0.005$, $P = 0.994$; interaction (antibiotic \times MPTP): $F_{1,36} = 0.045$, $P = 0.833$; Figure 1B). On day 22, antibiotic + saline group body weights, but not antibiotic + MPTP group weights, remained lower than those of mice that did not receive antibiotics (Figure 1B). Thus, antibiotic + MPTP group body weights recovered gradually after treatment, while antibiotic + saline group weights did not.

Antibiotic treatment protected against MPTP-induced neurotoxicity in the mouse brain

DAT immunohistochemistry revealed that MPTP reduced DAT levels in the striatum of the water-treated group, but not the antibiotic-treated group (Figure 1C). A two-way ANOVA revealed significant differences in DAT immunoreactivity among the four groups (antibiotic: $F_{1,36} = 11.30$, $P = 0.002$; MPTP: $F_{1,36} = 20.46$, $P < 0.001$; interaction (antibiotic \times MPTP): $F_{1,36} = 15.32$, $P < 0.001$; Figure 1D). TH immunohistochemistry revealed that MPTP reduced TH immunoreactivity in the SNr of the water-treated group, but not the antibiotic-treated group (Figure 1E). A two-way ANOVA revealed significant differences in TH immunoreactivity among the four groups (antibiotic: $F_{1,36} = 11.48$, $P = 0.002$; MPTP: $F_{1,36} = 10.19$, $P = 0.003$; interaction (antibiotic \times MPTP): $F_{1,36} = 11.75$, $P = 0.002$; Figure 1F). Collectively, these results indicate that treatment with an antibiotic cocktail for 14 days protected against MPTP-induced dopaminergic neurotoxicity in the striatum and SNr.

Gut microbiota composition

Next, we investigated the composition of the gut microbiota, which can be altered by antibiotic cocktail treatment [33–35], in the four experimental groups. α -diversity is defined as the richness of gut microbiota and can be measured using different indices. Two-way ANOVAs revealed a significant difference in the Chao1 (antibiotic: $F_{1,36} = 15.928$, $P < 0.001$; MPTP: $F_{1,36} = 37.541$, $P < 0.001$; interaction (antibiotic \times MPTP): $F_{1,36} = 20.587$, $P < 0.001$; Figure 2A) and Ace (antibiotic: $F_{1,36} = 12.968$, $P < 0.001$; MPTP: $F_{1,36} = 43.032$, $P < 0.001$; interaction (antibiotic \times MPTP): $F_{1,36} = 22.827$, $P < 0.001$; Figure 2B) indices among the four groups.

Specifically, Chao 1 and Ace indices were higher in the water + MPTP group than in both the water + saline and antibiotic + MPTP groups ($P < 0.001$). Interestingly, antibiotic cocktail treatment attenuated the MPTP-induced increase in the Chao 1 and Ace indices. A two-way ANOVA also revealed significant differences in the Shannon index among the four groups (antibiotic: $F_{1,36} = 8.942$, $P = 0.005$; MPTP: $F_{1,36} = 0.593$, $P = 0.446$; interaction (antibiotic \times MPTP): $F_{1,36} = 3.427$, $P = 0.072$; Figure 2C). The Shannon index in the antibiotic + MPTP group was lower than that of the water + MPTP group. In an unweighted UniFrac PCoA dot map, dots representing the antibiotic-treated groups were far away from dots representing the water-treated groups (Figure 2D). Interestingly, dots representing the antibiotic + MPTP group were isolated from dots representing the other three groups (Figure 2D).

At the phylum level, *Firmicutes* were the most abundant phylum in the water + saline group microbiota (Figure 3A and 3B). The abundance of *Firmicutes* was lower in the antibiotic + MPTP group than in the water + MPTP and antibiotic + saline groups ($P < 0.001$, Figure 3B). In contrast, the most dominant phylum in the antibiotic + MPTP group, *Bacteroidetes*, was less abundant in the water + MPTP and antibiotic + saline groups ($P < 0.001$, Figure 3C). *Proteobacteria* levels were higher after treatment with the antibiotic cocktail compared to the two water-treated groups (Figure 3D), while *Deferribacteres* and *TM7* levels decreased after treatment with the antibiotic cocktail or with MPTP (Figure 3E, 3F).

Antibiotic and MPTP treatment also altered the composition of fecal microbiota at the genus level (Figure 4A). *Lactobacillus*, *Mucispirillum*, and *Candidatus Arthromitus* levels decreased after treatment with the antibiotic cocktail (Figure 4B–4D). In contrast, *Parasutterella*, *Blautia*, *Robinsoniella*, *Escherichia*, *Dorea*, and *Eubacterium* levels increased after treatment with antibiotic cocktail (Figure 4E–4J). Interestingly, *Asaccharobacter* levels increased in the antibiotic + MPTP group compared to the other three groups (Figure 4K). *Clostridium*, which was the most dominant genus in control mice, decreased after MPTP injections and antibiotic cocktail treatment (Figure 4L). Furthermore, the antibiotic + MPTP group had a higher abundance of *Parabacteroides* than the other three groups (Figure 4M). Finally, MPTP treatment attenuated the antibiotic-induced increase in the abundance of *Bacteroides* and *Enterococcus* (Figure 4N, 4O).

Gut microbiota composition at the species level in the four experimental groups is shown in Figure 5A. *Lactobacillus murinus*, *Lactobacillus johnsonii*, *Mucispirillum schaedleri*, and *Candidatus Arthromitus sp. SFB-mouse*

decreased after antibiotic cocktail treatment (Figure 5B–5E). In contrast, *Escherichia coli*, *Blautia sp. Ser8*, and *Robinsoniella peoriensis* increased after antibiotic treatment (Figure 5F–5H). *Clostridium sp. Clone-27*, the most abundant species in control water + saline group

mice, decreased in all other groups (Figure 5I). On the other hand, *Blautia sp. canine oral taxon 143*, *Parabacteroides distasonis*, *Blautia coccoides*, *Clostridium sp. HGF2*, and *Clostridium bolteae* increased in the antibiotic + MPTP group (Figure 5J–5N).

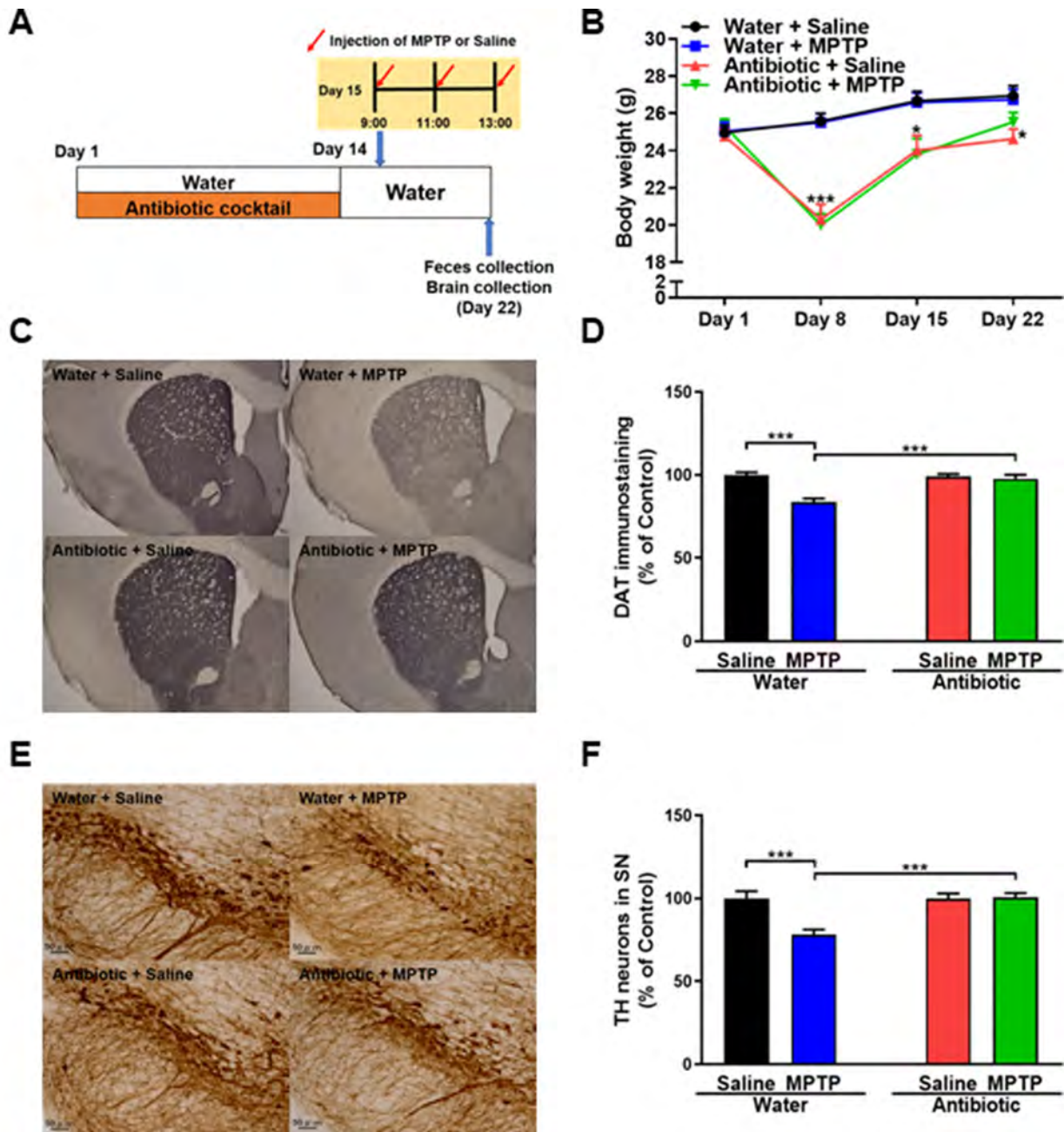


Figure 1. Effects of antibiotic treatment on gut microbiota diversity. (A) Treatment schedule. Adult mice received drinking water with or without antibiotic cocktail from day 1 to day 14. On day 15, MPTP or saline injections were administered. On day 22, fresh feces were collected. Mice were then perfused for immunohistochemistry. (B) Body weights in the different groups (repeated two-way ANOVA, antibiotic: $F_{1,36} = 20.549$, $P < 0.001$; MPTP: $F_{1,36} = 0.005$, $P = 0.994$; interaction (antibiotic \times MPTP): $F_{1,36} = 0.045$, $P = 0.833$). (C) Representative images of DAT immunohistochemistry in the water + saline, water + MPTP, antibiotic + saline, and antibiotic + MPTP groups. (D) Striatal DAT immunoreactivity data. (E) Representative images of TH immunohistochemistry in the water + saline, water + MPTP, antibiotic + saline, and antibiotic + MPTP groups. (F) SNr TH immunoreactivity data. Data are shown as mean \pm S.E.M. ($n = 10$). *** $P < 0.001$. Bar = 50 μ m.

In addition, *Lactobacillus intestinalis* and *Lactobacillus reuteri*, which increased in the water + MPTP group compared to the water + saline group, were markedly reduced after antibiotic treatment (Figure 5O and 5P). Interestingly, DAT immunoreactivity was negatively correlated with levels of *Lactobacillus intestinalis* ($r = -0.38$, $P = 0.01$) and *Lactobacillus reuteri* ($r = -0.39$, $P = 0.01$; Figure 5U and 5V). The antibiotic-induced increase in the abundance of *Bacteroides acidifaciens*, *[Clostridium] cocleatum*, and *Enterococcus casseliflavus* was largely reversed after MPTP administration (Figure 5Q–5S). In addition, MPTP restored *Bacteroides sp. TP-5* to control levels after it had been reduced by antibiotic treatment (Figure 5T).

DISCUSSION

In this study, we examined the effects of treatment with an antibiotic cocktail on gut microbiota in a mouse model of PD. We found that MPTP markedly reduced DAT immunoreactivity in the striatum and TH immunoreactivity in the SNr of the water-treated group,

but not the antibiotic-treated group. Second, antibiotic cocktail treatment caused substantial alterations in host gut microbiota composition compared to the water-treated group. In an unweighted UniFrac PCoA, dots representing the two unantibiotic-treated groups were located far away from dots representing the two water-treated groups. Interestingly, dots representing the antibiotic + MPTP group were also far from the dots of the other three groups. At the phylum level, *Proteobacteria* was markedly increased, while *Deferribacteres*, and *TM7* were markedly decreased, in the gut of antibiotic-treated mice. Antibiotic treatment was also associated with substantial microbiome alterations at the genus and species levels. Overall, 14 days of treatment with an antibiotic cocktail caused significant changes in the diversity and composition of the host gut microbiota, which is consistent with previous reports [33–35]. Taken together, these results suggest that antibiotic-induced microbiome depletion might protect against MPTP-induced dopaminergic neurotoxicity in the mouse brain via the brain–gut microbiota axis.

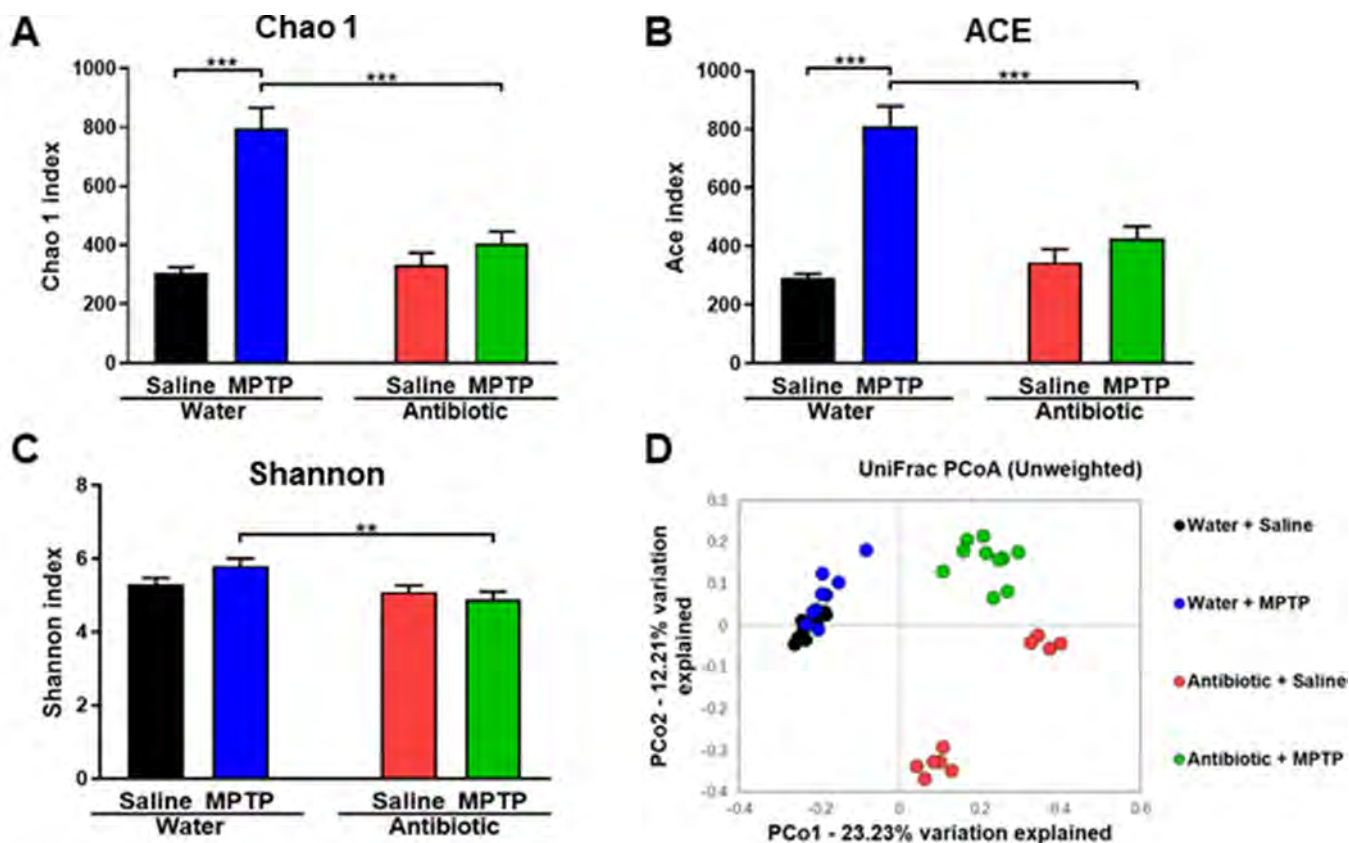


Figure 2. α -diversity and β -diversity in gut microbiota. Diversity index values for the four groups. (A) *Chao 1* index (two-way ANOVA, antibiotic: $F_{1,36} = 15.928$, $P < 0.001$; MPTP: $F_{1,36} = 37.541$, $P < 0.001$; interaction (antibiotic \times MPTP): $F_{1,36} = 20.587$, $P < 0.001$). (B) *ACE* index (two-way ANOVA, antibiotic: $F_{1,36} = 12.968$, $P < 0.001$; MPTP: $F_{1,36} = 43.032$, $P < 0.001$; interaction (antibiotic \times MPTP): $F_{1,36} = 22.827$, $P < 0.001$). (C) *Shannon* index (two-way ANOVA, antibiotic: $F_{1,36} = 8.942$, $P = 0.005$; MPTP: $F_{1,36} = 0.593$, $P = 0.446$; interaction (antibiotic \times MPTP): $F_{1,36} = 3.427$, $P = 0.072$). (D) PCoA analysis of gut bacteria data (Bray–Curtis dissimilarity).

In another recent study, we reported that 14 days of antibiotic treatment increases levels of bacteria from the phylum *Proteobacteria* and decreases levels of the major bacterial phyla *Bacteroidetes* and *Firmicutes* in the mouse gut microbiota (Wang et al., submitted); similar results have also been observed in other studies [26, 31, 32]. Here, we found that the relative abundance of *Proteobacteria* increased in the antibiotic-treated groups compared to the water-treated groups. In contrast, the relative abundance of *Firmicutes* and *Bacteroidetes* was

similar in the antibiotic + saline and water + saline groups, indicating that spontaneous recovery of these bacteria occurred. The mechanisms underlying the increased relative abundance of *Proteobacteria* after antibiotic cocktail treatment are currently unknown. Interestingly, MPTP significantly altered the relative abundance of *Firmicutes* and *Bacteroidetes* in the antibiotic-treated group, but not in the water-treated group. Thus, MPTP might further alter gut microbiome composition after antibiotic-induced microbiome depletion.

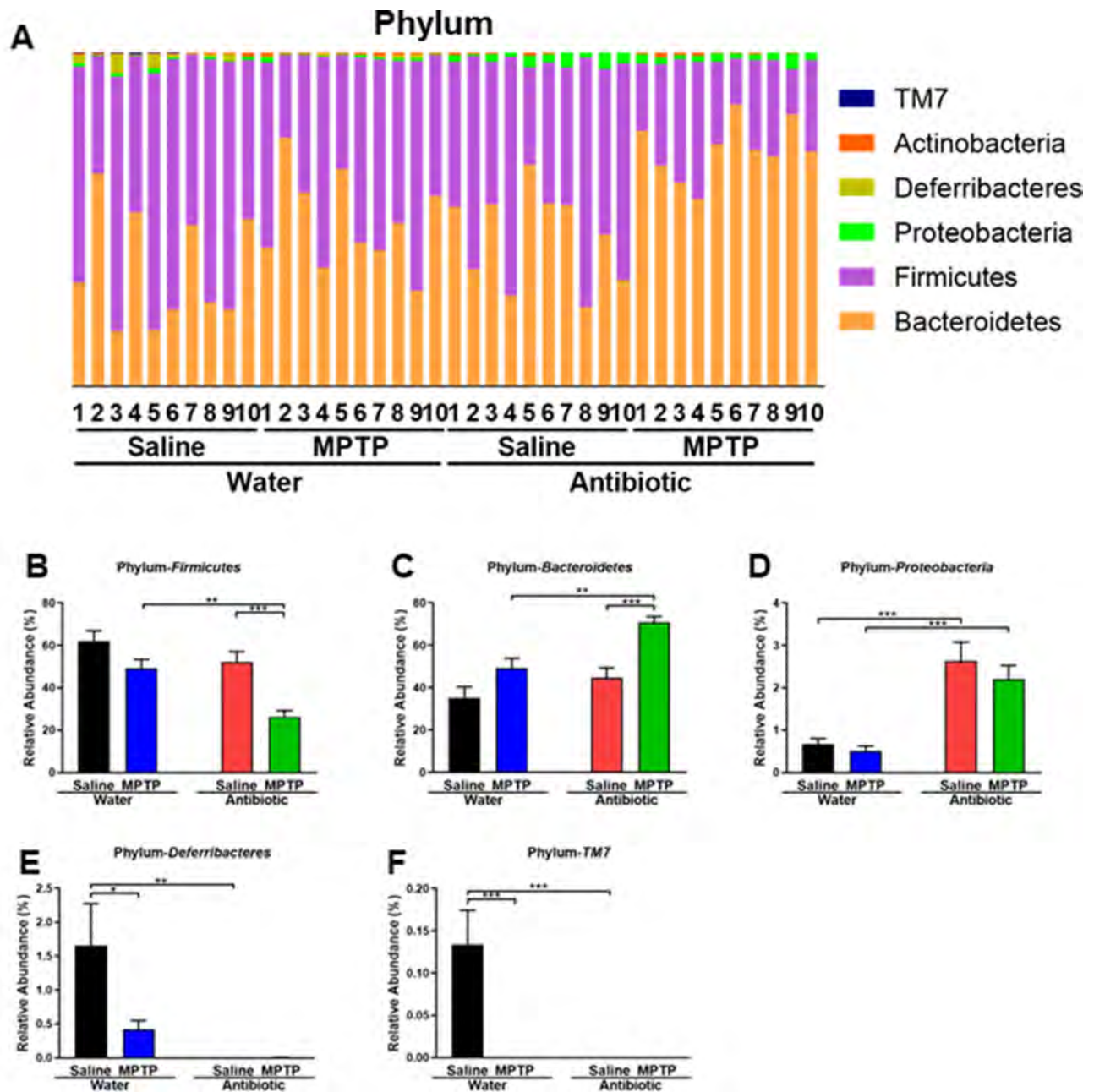


Figure 3. Altered gut bacteria composition at the phylum level. (A) Relative abundance at the phylum level. (B) *Bacteroidetes*. (C) *Firmicutes*. (D) *Proteobacteria*. (E) *Deferribacteres*. (F) *TM7*. Data are shown as mean \pm S.E.M. (n = 10). **P < 0.01, ***P < 0.001. See the Supplementary Table 1 for detailed statistical analysis.

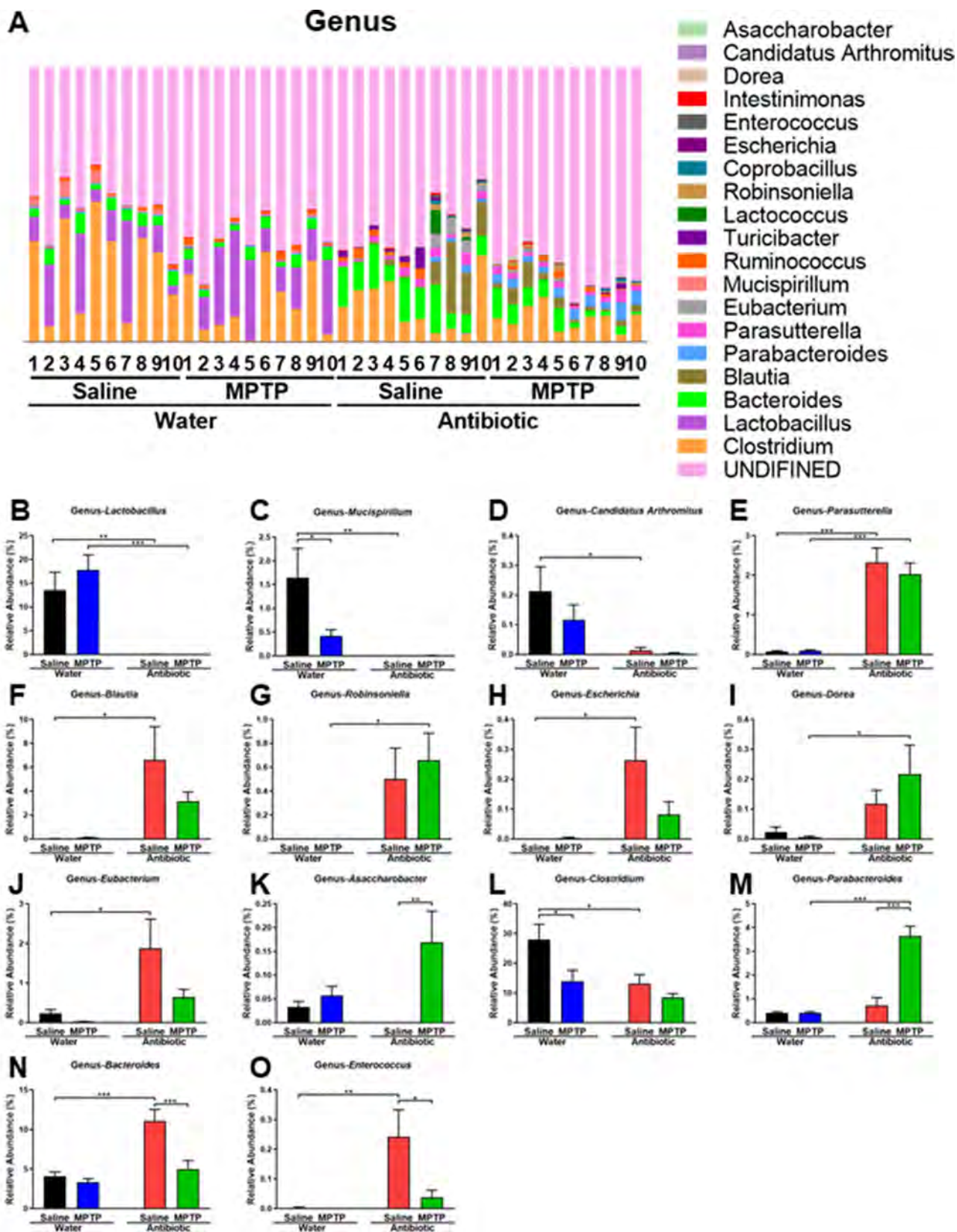


Figure 4. Altered gut bacteria composition at the genus level. (A) Relative abundance at the genus level. (B) *Lactobacillus*. (C) *Mucispirillum*. (D) *Candidatus Arthromitus*. (E) *Parasutterella*. (F) *Blautia*. (G) *Robinsoniella*. (H) *Escherichia*. (I) *Dorea*. (J) *Eubacterium*. (K) *Asaccharobacter*. (L) *Clostridium*. (M) *Parabacteroides*. (N) *Bacteroides*. (O) *Enterococcus*. Data are shown as mean \pm S.E.M. (n = 10). **P < 0.01, ***P < 0.001. See the Supplementary Table 2 for detailed statistical analysis.

MPTP specifically increased levels of the following bacterial species in the guts of antibiotic-treated mice: *Blautia sp. Canine oral taxon 143*, *Parabacteroides distasonis*, *Blautia coccoides*, *Clostridium sp. HGF2*, *Clostridium bolteae*, and *Bacteroides sp. TP-5*. A recent study demonstrated that *Parabacteroides distasonis* alleviated obesity and metabolic dysfunction via production of succinate and secondary bile acids [38]. In addition, *Parabacteroides distasonis* reduced the severity of intestinal inflammation in murine models of acute and chronic colitis induced by dextran sulphate sodium, suggesting that *Parabacteroides distasonis* may be useful for treating inflammatory bowel diseases [39]. *Blautia coccoides* produce hydrogen [13], which might have beneficial effects in the MPTP mouse model [40]. Interestingly, *Clostridium sp. HGF2* plays an important role in the metabolism of mannitol [41], which could attenuate behavioral abnormalities and aggregations of α -synuclein in the rodent brain [42, 43]. Among the bacteria increased by MPTP, *Bacteroides sp. TP-5* is particularly noteworthy due to its ability to modulate immune system function [44]. Furthermore, a recent study demonstrated that fecal microbiota transplantation protected against MPTP-induced neurotoxicity by suppressing neuroinflammation [45]. The effects of supplementation with *Bacteroides sp. TP-5* on dopaminergic neurotoxicity in mouse MPTP model should be investigated further.

MPTP treatment also decreased levels of the *Bacteroides acidifaciens*, *[Clostridium] cocleatum*, and *Enterococcus casseliflavus* bacterial species. *Bacteroides acidifaciens* are important for promoting IgA production in the large intestine [46]. Interestingly, *Bacteroides acidifaciens* levels were increased in the feces of *Atg7^{ACD11c}* mice with a lean phenotype compared to those of control *Atg7^{fl/fl}* mice, and wild-type C57BL/6 mice fed with a diet including *Bacteroides acidifaciens* gained less weight and fat mass than mice fed control food [47]. Those results suggest that *Bacteroides acidifaciens* might be a potential treatment for metabolic diseases such as obesity [47]. The functional roles of *[Clostridium] cocleatum* and *Enterococcus casseliflavus* are unclear, and the mechanisms underlying the recovery of the three bacterial species that increased in the gut microbiome of antibiotic-treated mice after MPTP administration in this study are currently unknown. Regardless, it is likely that interactions between the brain–gut axis and these microbiomes play a role in MPTP-induced neurotoxicity, and the relationship between neuroprotection, the immune system, and the brain–gut axis warrants further investigation.

In this study, we found that DAT immunoreactivity was negatively correlated with *Lactobacillus intestinalis* and *Lactobacillus reuteri* levels despite the marked decrease observed in these species after antibiotic treatment. Both

of these bacteria produce lactic acid, which was more abundant in the striatum of MPTP-treated mice [48]. Furthermore, treatment with *Lactobacillus reuteri* selectively rescues social deficits in genetic, environmental, and idiopathic autism spectrum disorder (ASD) models, suggesting that this species may be a promising non-invasive microbial-based therapy for ASD-related social dysfunctions [49]. Additionally, short-chain fatty acids promote proliferation of *Lactobacillus reuteri* [50]; this effect should be investigated further. It is possible that *Lactobacillus intestinalis*, *Lactobacillus reuteri*, and lactic acid might affect the dopaminergic neurotoxicity of MPTP in the brain. Furthermore, antibiotic-induced microbiome depletion might enhance or counteract MPTP-induced dopaminergic neurotoxicity in mouse brain, although the specific microbes that might be involved in these effects were not identified in this study. Additional studies are needed to confirm the relationship between MPTP-induced dopaminergic neurotoxicity and the gut microbiome.

Accumulating evidence suggests that abnormal gut microbiota composition might affect neuroprotection [8, 51, 52]. Choi et al. [53] identified dramatic and widespread increases in levels of *Enterobacteriaceae*, and particularly of *Proteus mirabilis*, in the mouse MPTP model. Administration of *Proteus mirabilis* isolated from MPTP-treated mice produced motor deficits, dopaminergic neuronal damage, and inflammation in the striatum and SNr, suggesting that *Proteus mirabilis* promotes PD pathology in the brain. Furthermore, Srivastav et al. [54] reported neuroprotective effects of a probiotic cocktail containing *Lactobacillus rhamnosus GG*, *Bifidobacterium animalis lactis*, and *Lactobacillus acidophilus* in MPTP-treated mice. Together, these results indicate that altered gut microbiota composition likely plays a role in dopaminergic neurotoxicity related to PD.

In conclusion, the present study suggests that antibiotic-induced microbiome depletion might protect against MPTP-induced dopaminergic neurotoxicity in the mouse brain, and that MPTP might improve the diversity and composition of gut microbiota in antibiotic-treated mice. These results indicate that the brain–gut axis plays a key role in the pathology of PD.

MATERIALS AND METHODS

Animals

Male adult C57BL/6 mice (8 weeks old) weighting 20–25 g were purchased from SLC (Inc., Hamamatsu, Japan). Animals were housed under controlled temperatures and 12-hour light/dark cycles (lights on between 07:00–19:00) with ad libitum food (CE-2; CLEA Japan, Inc., Tokyo,

Japan) and water. All experiments were carried out according to the Guide for Animal Experimentation of Chiba University. The experimental protocol was approved by the Chiba University Institutional Animal Care and Use Committee.

Preparation of antibiotics and MPTP

As described in previous reports [33–35], broad-spectrum antibiotics (ampicillin 1 g/L, neomycin sulfate 1 g/L, metronidazole 1 g/L, Sigma-Aldrich Co., Ltd, St Louis, MO, USA) were dissolved in drinking water. This antibiotic cocktail, which was prepared fresh every other day, was administered to adult C57BL/6 mice for 14 continuous days. 1-Methyl-4-phenyl-1,2,3,6-tetrahydropyridine (MPTP: Tokyo Chemical Industry CO., Ltd., Tokyo, Japan) was dissolved in saline. Other compounds were purchased commercially.

Schedule of treatment and collection of fecal and brain samples

The procedure for establishing MPTP-induced neurotoxicity was performed as previously reported [55, 56]. Forty mice (8 weeks old) were divided among the following four groups: water + saline; water + MPTP; antibiotic cocktail + saline; antibiotic cocktail + MPTP. Mice were given drinking water with or without the antibiotic cocktail from day 1 to day 14 (Figure 1A). All mice were given water without antibiotics from day 15 to day 22. On day 15, mice received intraperitoneal injections of MPTP (10 mg/kg x 3, 2-hr interval) or saline (5 mL/kg x 3, 2-hr interval; Figure 1A). One week after MPTP or saline injection, fresh fecal samples were collected and stored at -80°C until use. Subsequently, the mice were anesthetized with 5% isoflurane and sodium pentobarbital (50 mg/kg) for brain collection. Mice were perfused transcardially with 10 mL of isotonic saline followed by 30 mL of ice-cold 4% paraformaldehyde in 0.1 M phosphate buffer (pH 7.4). Brains were removed, post-fixed overnight at 4°C, and then used for immunohistochemical staining of dopamine transporter (DAT) and tyrosine hydroxylase (TH).

DAT and TH Immunohistochemistry

Immunohistochemical staining of DAT and TH was performed as reported previously [55, 56]. Consecutive 50 µm-thick coronal brain sections (bregma 0.86–1.54 mm and -2.92–3.88 mm) were cut in ice-cold 10 mM phosphate buffered saline (pH 7.5) using a vibrating blade microtome (VT1000s, Leica Microsystems AG, Wetzlar, Germany). Free-floating sections were treated with 0.3% H₂O₂ in 50 mM Tris-HCL saline (TBS) for 30 min and blocked in 0.2% Triton X-100 TBS (TBST) with 1.5% normal serum for 1 hour at room temperature.

Samples were then incubated for 36 hours at 4°C with rat anti-DAT antibody (1:10,000, Merck Millipore, Burlington, MA, USA) or rabbit anti-TH antibody (1:500, Sigma-Aldrich, St Louis, MO, USA). The sections were then washed three times in TBS and processed according to the avidin-biotin-peroxidase method (Vectastain Elite ABC, Vector Laboratories, Inc., Burlingame, CA, USA). Sections were then incubated with 0.15 mg/mL diaminobenzidine and 0.01% H₂O₂ for 5 minutes; the staining solution for DAT only also contained 0.06% NiCl₂. The sections were then mounted on gelatinized slides, dehydrated, cleared, and coverslipped with Permount® (Fisher Scientific, Fair Lawn, NJ, USA). Images were taken and DAT and TH immunoreactivity staining intensity in the anterior region (0.25 mm²) of the striatum as well as the number of TH-positive cells in SNr region (0.36 mm²) were analyzed using a Keyence BZ-9000 Generation microscope (Keyence Co., Ltd, Osaka, Japan). Eight data points (four brain slides) from each mouse were used for the quantitative analyses of DAT and TH immunoreactivity.

16S rRNA analysis

DNA was extracted from fecal samples and 16S rRNA analyses were performed as previously described [57] by MyMetagenome Co., Ltd. (Tokyo, Japan). Briefly, PCR was performed using 27Fmod 5'-AGRGTTTGATYMTGGCTCAG-3' and 338R 5'-TGCTGCCTCCCGTAGGAGT-3' primers to amplify the V1–V2 region of the bacterial 16S rRNA gene. The amplified DNA (~330bp) was purified using AMPure XP (Beckman Coulter) and quantified using a Quant-iT Picogreen dsDNA assay kit (Invitrogen) and a TBS-380 Mini-Fluorometer (Turner Biosystems). The 16S amplicons were then sequenced using a MiSeq according to the Illumina protocol. The paired-end reads were merged using the fastq-join program based on overlapping sequences. Reads with an average quality value of <25 and inexact matches to both universal primers were filtered out. Filter-passed reads were analyzed further after trimming off both primer sequences. For each sample, 3,000 high-quality filter-passed reads were rearranged in descending order according to quality value and then clustered into operational taxonomic units (OTUs) with a 97% pairwise-identity cutoff using the UCLUST program version 5.2.32 (<https://www.drive5.com>). Taxonomic assignments of OTUs were performed based on similarity searches against the Ribosomal Database Project and the National Center for Biotechnology Information genome database using the GLSEARCH program [58].

Statistical analysis

Animal experiment data are presented as the mean ± standard error of the mean (S.E.M.). Statistical analyses

were performed using SPSS Statistics 20 (SPSS, Tokyo, Japan). Body weight data were analyzed using repeated two-way analysis of variance (ANOVA) followed by *post-hoc* Tukey's multiple comparison tests. DAT and TH immunohistochemistry and 16S rDNA data were analyzed using two-way ANOVAs followed by *post-hoc* Tukey's multiple comparison tests. *P* values of less than 0.05 were considered statistically significant.

CONFLICTS OF INTEREST

The authors have no conflicts of interest to declare.

FUNDING

This study was supported by Smoking Research Foundation, Japan (to K.H.), and AMED, Japan (to K.H., JP19dm0107119). Ms. Siming Wang was supported by TAKASE Scholarship Foundation (Tokyo, Japan). Dr. Lijia Chang was supported by the Japan China Sasakawa Medical Fellowship (Tokyo, Japan).

REFERENCES

1. Ascherio A, Schwarzschild MA. The epidemiology of Parkinson's disease: risk factors and prevention. *Lancet Neurol.* 2016; 15:1257–72. [https://doi.org/10.1016/S1474-4422\(16\)30230-7](https://doi.org/10.1016/S1474-4422(16)30230-7) PMID:[27751556](https://pubmed.ncbi.nlm.nih.gov/27751556/)
2. Kalia LV, Lang AE. Parkinson's disease. *Lancet.* 2015; 386:896–912. [https://doi.org/10.1016/S0140-6736\(14\)61393-3](https://doi.org/10.1016/S0140-6736(14)61393-3) PMID:[25904081](https://pubmed.ncbi.nlm.nih.gov/25904081/)
3. Wichmann T. Changing views of the pathophysiology of Parkinsonism. *Mov Disord.* 2019; 34:1130–43. <https://doi.org/10.1002/mds.27741> PMID:[31216379](https://pubmed.ncbi.nlm.nih.gov/31216379/)
4. Aho VT, Pereira PA, Voutilainen S, Paulin L, Pekkonen E, Auvinen P, Scheperjans F. Gut microbiota in Parkinson's disease: temporal stability and relations to disease progression. *EBioMedicine.* 2019; 44:691–707. <https://doi.org/10.1016/j.ebiom.2019.05.064> PMID:[31221587](https://pubmed.ncbi.nlm.nih.gov/31221587/)
5. Chiang HL, Lin CH. Altered Gut Microbiome and Intestinal Pathology in Parkinson's Disease. *J Mov Disord.* 2019; 12:67–83. <https://doi.org/10.14802/jmd.18067> PMID:[31158941](https://pubmed.ncbi.nlm.nih.gov/31158941/)
6. Dinan TG, Cryan JF. Gut instincts: microbiota as a key regulator of brain development, ageing and neurodegeneration. *J Physiol.* 2017; 595:489–503. <https://doi.org/10.1113/JP273106> PMID:[27641441](https://pubmed.ncbi.nlm.nih.gov/27641441/)
7. Felice VD, Quigley EM, Sullivan AM, O'Keefe GW, O'Mahony SM. Microbiota-gut-brain signalling in Parkinson's disease: implications for non-motor symptoms. *Parkinsonism Relat Disord.* 2016; 27:1–8. <https://doi.org/10.1016/j.parkreldis.2016.03.012> PMID:[27013171](https://pubmed.ncbi.nlm.nih.gov/27013171/)
8. Girolamo F, Coppola C, Ribatti D. Immunoregulatory effect of mast cells influenced by microbes in neurodegenerative diseases. *Brain Behav Immun.* 2017; 65:68–89. <https://doi.org/10.1016/j.bbi.2017.06.017> PMID:[28676349](https://pubmed.ncbi.nlm.nih.gov/28676349/)
9. Mulak A, Bonaz B. Brain-gut-microbiota axis in Parkinson's disease. *World J Gastroenterol.* 2015; 21:10609–20. <https://doi.org/10.3748/wjg.v21.i37.10609> PMID:[26457021](https://pubmed.ncbi.nlm.nih.gov/26457021/)
10. Parashar A, Udayabanu M. Gut microbiota: implications in Parkinson's disease. *Parkinsonism Relat Disord.* 2017; 38:1–7. <https://doi.org/10.1016/j.parkreldis.2017.02.002> PMID:[28202372](https://pubmed.ncbi.nlm.nih.gov/28202372/)
11. Scheperjans F, Aho V, Pereira PA, Koskinen K, Paulin L, Pekkonen E, Haapaniemi E, Kaakkola S, Eerola-Rautio J, Pohja M, Kinnunen E, Murros K, Auvinen P. Gut microbiota are related to Parkinson's disease and clinical phenotype. *Mov Disord.* 2015; 30:350–58. <https://doi.org/10.1002/mds.26069> PMID:[25476529](https://pubmed.ncbi.nlm.nih.gov/25476529/)
12. Scheperjans F. Gut microbiota, 1013 new pieces in the Parkinson's disease puzzle. *Curr Opin Neurol.* 2016; 29:773–80. <https://doi.org/10.1097/WCO.0000000000000389> PMID:[27653288](https://pubmed.ncbi.nlm.nih.gov/27653288/)
13. Suzuki A, Ito M, Hamaguchi T, Mori H, Takeda Y, Baba R, Watanabe T, Kurokawa K, Asakawa S, Hirayama M, Ohno K. Quantification of hydrogen production by intestinal bacteria that are specifically dysregulated in Parkinson's disease. *PLoS One.* 2018; 13:e0208313. <https://doi.org/10.1371/journal.pone.0208313> PMID:[30586410](https://pubmed.ncbi.nlm.nih.gov/30586410/)
14. Adams-Carr KL, Bestwick JP, Shribman S, Lees A, Schrag A, Noyce AJ. Constipation preceding Parkinson's disease: a systematic review and meta-analysis. *J Neurol Neurosurg Psychiatry.* 2016; 87:710–16. <https://doi.org/10.1136/jnnp-2015-311680> PMID:[26345189](https://pubmed.ncbi.nlm.nih.gov/26345189/)
15. Cusotto S, Clarke G, Dinan TG, Cryan JF. Psychotropics and the Microbiome: a Chamber of Secrets... *Psychopharmacology (Berl).* 2019; 236:1411–32. <https://doi.org/10.1007/s00213-019-5185-8> PMID:[30806744](https://pubmed.ncbi.nlm.nih.gov/30806744/)
16. Cusotto S, Sandhu KV, Dinan TG, Cryan JF. The Neuroendocrinology of the Microbiota-Gut-Brain Axis: A Behavioural Perspective. *Front Neuroendocrinol.* 2018; 51:80–101.

- <https://doi.org/10.1016/j.yfrne.2018.04.002>
PMID:29753796
17. Cusotto S, Strain CR, Fouhy F, Strain RG, Peterson VL, Clarke G, Stanton C, Dinan TG, Cryan JF. Differential effects of psychotropic drugs on microbiome composition and gastrointestinal function. *Psychopharmacology (Berl)*. 2019; 236:1671–85.
<https://doi.org/10.1007/s00213-018-5006-5>
PMID:30155748
18. Forsythe P, Kunze W, Bienenstock J. Moody microbes or fecal phrenology: what do we know about the microbiota-gut-brain axis? *BMC Med*. 2016; 14:58.
<https://doi.org/10.1186/s12916-016-0604-8>
PMID:27090095
19. Fung TC, Olson CA, Hsiao EY. Interactions between the microbiota, immune and nervous systems in health and disease. *Nat Neurosci*. 2017; 20:145–55.
<https://doi.org/10.1038/nn.4476>
PMID:28092661
20. Kelly JR, Clarke G, Cryan JF, Dinan TG. Brain-gut-microbiota axis: challenges for translation in psychiatry. *Ann Epidemiol*. 2016; 26:366–72.
<https://doi.org/10.1016/j.annepidem.2016.02.008>
PMID:27005587
21. Ma Q, Xing C, Long W, Wang HY, Liu Q, Wang RF. Impact of microbiota on central nervous system and neurological diseases: the gut-brain axis. *J Neuroinflammation*. 2019; 16:53.
<https://doi.org/10.1186/s12974-019-1434-3>
PMID:30823925
22. Molina-Torres G, Rodriguez-Arrastia M, Roman P, Sanchez-Labraca N, Cardona D. Stress and the gut microbiota-brain axis. *Behav Pharmacol*. 2019; 30:187–200.
<https://doi.org/10.1097/FBP.0000000000000478>
PMID:30844962
23. Round JL, Mazmanian SK. The gut microbiota shapes intestinal immune responses during health and disease. *Nat Rev Immunol*. 2009; 9:313–23.
<https://doi.org/10.1038/nri2515>
PMID:19343057
24. Champagne-Jorgensen K, Kunze WA, Forsythe P, Bienenstock J, McVey Neufeld KA. Antibiotics and the nervous system: more than just the microbes? *Brain Behav Immun*. 2019; 77:7–15.
<https://doi.org/10.1016/j.bbi.2018.12.014>
PMID:30582961
25. Ianiro G, Tilg H, Gasbarrini A. Antibiotics as deep modulators of gut microbiota: between good and evil. *Gut*. 2016; 65:1906–15.
<https://doi.org/10.1136/gutjnl-2016-312297>
PMID:27531828
26. Antonopoulos DA, Huse SM, Morrison HG, Schmidt TM, Sogin ML, Young VB. Reproducible community dynamics of the gastrointestinal microbiota following antibiotic perturbation. *Infect Immun*. 2009; 77:2367–75.
<https://doi.org/10.1128/IAI.01520-08>
PMID:19307217
27. Becattini S, Taur Y, Pamer EG. Antibiotic-Induced Changes in the Intestinal Microbiota and Disease. *Trends Mol Med*. 2016; 22:458–78.
<https://doi.org/10.1016/j.molmed.2016.04.003>
PMID:27178527
28. Davey KJ, Cotter PD, O’Sullivan O, Crispie F, Dinan TG, Cryan JF, O’Mahony SM. Antipsychotics and the gut microbiome: olanzapine-induced metabolic dysfunction is attenuated by antibiotic administration in the rat. *Transl Psychiatry*. 2013; 3:e309.
<https://doi.org/10.1038/tp.2013.83>
PMID:24084940
29. Jernberg C, Löfmark S, Edlund C, Jansson JK. Long-term ecological impacts of antibiotic administration on the human intestinal microbiota. *ISME J*. 2007; 1:56–66.
<https://doi.org/10.1038/ismej.2007.3>
PMID:18043614
30. Kim S, Covington A, Pamer EG. The intestinal microbiota: Antibiotics, colonization resistance, and enteric pathogens. *Immunol Rev*. 2017; 279:90–105.
<https://doi.org/10.1111/imr.12563>
PMID:28856737
31. Young VB, Schmidt TM. Antibiotic-associated diarrhea accompanied by large-scale alterations in the composition of the fecal microbiota. *J Clin Microbiol*. 2004; 42:1203–06.
<https://doi.org/10.1128/JCM.42.3.1203-1206.2004>
PMID:15004076
32. Zarrinpar A, Chaix A, Xu ZZ, Chang MW, Marotz CA, Saghatelian A, Knight R, Panda S. Antibiotic-induced microbiome depletion alters metabolic homeostasis by affecting gut signaling and colonic metabolism. *Nat Commun*. 2018; 9:2872.
<https://doi.org/10.1038/s41467-018-05336-9>
PMID:30030441
33. Yang C, Fang X, Zhan G, Huang N, Li S, Bi J, Jiang R, Yang L, Miao L, Zhu B, Luo A, Hashimoto K. Key role of gut microbiota in anhedonia-like phenotype in rodents with neuropathic pain. *Transl Psychiatry*. 2019; 9:57.
<https://doi.org/10.1038/s41398-019-0379-8>
PMID:30705252
34. Zhan G, Yang N, Li S, Huang N, Fang X, Zhang J, Zhu B, Yang L, Yang C, Luo A. Abnormal gut microbiota composition contributes to cognitive dysfunction in

- SAMP8 mice. Aging (Albany NY). 2018; 10:1257–67.
<https://doi.org/10.18632/aging.101464>
PMID:29886457
35. Zhang J, Bi JJ, Guo GJ, Yang L, Zhu B, Zhan GF, Li S, Huang NN, Hashimoto K, Yang C, Luo AL. Abnormal composition of gut microbiota contributes to delirium-like behaviors after abdominal surgery in mice. *CNS Neurosci Ther*. 2019; 25:685–96.
<https://doi.org/10.1111/cns.13103> PMID:30680947
36. Sampson TR, Debelius JW, Thron T, Janssen S, Shastri GG, Ilhan ZE, Challis C, Schretter CE, Rocha S, Gradinaru V, Chesselet MF, Keshavarzian A, Shannon KM, et al. Gut Microbiota Regulate Motor Deficits and Neuroinflammation in a Model of Parkinson's Disease. *Cell*. 2016; 167:1469–1480.e12.
<https://doi.org/10.1016/j.cell.2016.11.018>
PMID:27912057
37. Jackson-Lewis V, Przedborski S. Protocol for the MPTP mouse model of Parkinson's disease. *Nat Protoc*. 2007; 2:141–51.
<https://doi.org/10.1038/nprot.2006.342>
PMID:17401348
38. Wang K, Liao M, Zhou N, Bao L, Ma K, Zheng Z, Wang Y, Liu C, Wang W, Wang J, Liu SJ, Liu H. Parabacteroides distasonis Alleviates Obesity and Metabolic Dysfunctions via Production of Succinate and Secondary Bile Acids. *Cell Rep*. 2019; 26:222–235.e5.
<https://doi.org/10.1016/j.celrep.2018.12.028>
PMID:30605678
39. Kverka M, Zakostelska Z, Klimesova K, Sokol D, Hudcovic T, Hrcir T, Rossmann P, Mrazek J, Kopečný J, Verdu EF, Tlaskalova-Hogenova H. Oral administration of Parabacteroides distasonis antigens attenuates experimental murine colitis through modulation of immunity and microbiota composition. *Clin Exp Immunol*. 2011; 163:250–59.
<https://doi.org/10.1111/j.1365-2249.2010.04286.x>
PMID:21087444
40. Fujita K, Seike T, Yutsudo N, Ohno M, Yamada H, Yamaguchi H, Sakumi K, Yamakawa Y, Kido MA, Takaki A, Katafuchi T, Tanaka Y, Nakabeppu Y, Noda M. Hydrogen in drinking water reduces dopaminergic neuronal loss in the 1-methyl-4-phenyl-1,2,3,6-tetrahydropyridine mouse model of Parkinson's disease. *PLoS One*. 2009; 4:e7247.
<https://doi.org/10.1371/journal.pone.0007247>
PMID:19789628
41. Feng Q, Liu Z, Zhong S, Li R, Xia H, Jie Z, Wen B, Chen X, Yan W, Fan Y, Guo Z, Meng N, Chen J, et al. Integrated metabolomics and metagenomics analysis of plasma and urine identified microbial metabolites associated with coronary heart disease. *Sci Rep*. 2016; 6:22525.
<https://doi.org/10.1038/srep22525>
PMID:26932197
42. Shaltiel-Karyo R, Frenkel-Pinter M, Rockenstein E, Patrick C, Levy-Sakin M, Schiller A, Egoz-Matia N, Masliah E, Segal D, Gazit E. A blood-brain barrier (BBB) disrupter is also a potent α -synuclein (α -syn) aggregation inhibitor: a novel dual mechanism of mannitol for the treatment of Parkinson disease (PD). *J Biol Chem*. 2013; 288:17579–88.
<https://doi.org/10.1074/jbc.M112.434787>
PMID:23637226
43. Paul A, Zhang BD, Mohapatra S, Li G, Li YM, Gazit E, Segal D. Novel Mannitol-Based Small Molecules for Inhibiting Aggregation of α -Synuclein Amyloids in Parkinson's Disease. *Front Mol Biosci*. 2019; 6:16.
<https://doi.org/10.3389/fmolb.2019.00016>
PMID:30968030
44. Lazar V, Ditu LM, Pircalabioru GG, Gheorghe I, Curutiu C, Holban AM, Picu A, Petcu L, Chifiriuc MC. Aspects of Gut Microbiota and Immune System Interactions in Infectious Diseases, Immunopathology, and Cancer. *Front Immunol*. 2018; 9:1830.
<https://doi.org/10.3389/fimmu.2018.01830>
PMID:30158926
45. Sun MF, Zhu YL, Zhou ZL, Jia XB, Xu YD, Yang Q, Cui C, Shen YQ. Neuroprotective effects of fecal microbiota transplantation on MPTP-induced Parkinson's disease mice: gut microbiota, glial reaction and TLR4/TNF- α signaling pathway. *Brain Behav Immun*. 2018; 70:48–60.
<https://doi.org/10.1016/j.bbi.2018.02.005>
PMID:29471030
46. Yanagibashi T, Hosono A, Oyama A, Tsuda M, Suzuki A, Hachimura S, Takahashi Y, Momose Y, Itoh K, Hirayama K, Takahashi K, Kaminogawa S. IgA production in the large intestine is modulated by a different mechanism than in the small intestine: bacteroides acidifaciens promotes IgA production in the large intestine by inducing germinal center formation and increasing the number of IgA+ B cells. *Immunobiology*. 2013; 218:645–51.
<https://doi.org/10.1016/j.imbio.2012.07.033>
PMID:22940255
47. Yang JY, Lee YS, Kim Y, Lee SH, Ryu S, Fukuda S, Hase K, Yang CS, Lim HS, Kim MS, Kim HM, Ahn SH, Kwon BE, et al. Gut commensal Bacteroides acidifaciens prevents obesity and improves insulin sensitivity in mice. *Mucosal Immunol*. 2017; 10:104–16.
<https://doi.org/10.1038/mi.2016.42>
PMID:27118489
48. Koga K, Mori A, Ohashi S, Kurihara N, Kitagawa H, Ishikawa M, Mitsumoto Y, Nakai M. H MRS identifies lactate rise in the striatum of MPTP-treated C57BL/6 mice. *Eur J Neurosci*. 2006; 23:1077–81.

- <https://doi.org/10.1111/j.1460-9568.2006.04610.x>
PMID:16519673
49. Sgritta M, Dooling SW, Buffington SA, Momin EN, Francis MB, Britton RA, Costa-Mattioli M. Mechanisms underlying microbial-mediated changes in social behavior in mouse models of autism spectrum disorder. *Neuron*. 2019; 101:246–259.e6.
<https://doi.org/10.1016/j.neuron.2018.11.018>
PMID:30522820
50. Oh JH, Alexander LM, Pan M, Schueler KL, Keller MP, Attie AD, Walter J, van Pijkeren JP. Dietary fructose and microbiota-derived short-chain fatty acids promote bacteriophage production in the gut symbiont *Lactobacillus reuteri*. *Cell Host Microbe*. 2019; 25:273–284.e6.
<https://doi.org/10.1016/j.chom.2018.11.016>
PMID:30658906
51. Kigerl KA, Hall JC, Wang L, Mo X, Yu Z, Popovich PG. Gut dysbiosis impairs recovery after spinal cord injury. *J Exp Med*. 2016; 213:2603–20.
<https://doi.org/10.1084/jem.20151345>
PMID:27810921
52. Zhu CS, Grandhi R, Patterson TT, Nicholson SE. A Review of Traumatic Brain Injury and the Gut Microbiome: Insights into Novel Mechanisms of Secondary Brain Injury and Promising Targets for Neuroprotection. *Brain Sci*. 2018; 8:E113.
<https://doi.org/10.3390/brainsci8060113>
PMID:29921825
53. Choi JG, Kim N, Ju IG, Eo H, Lim SM, Jang SE, Kim DH, Oh MS. Oral administration of *Proteus mirabilis* damages dopaminergic neurons and motor functions in mice. *Sci Rep*. 2018; 8:1275.
<https://doi.org/10.1038/s41598-018-19646-x>
PMID:29352191
54. Srivastav S, Neupane S, Bhurtel S, Katila N, Maharjan S, Choi H, Hong JT, Choi DY. Probiotics mixture increases butyrate, and subsequently rescues the nigral dopaminergic neurons from MPTP and rotenone-induced neurotoxicity. *J Nutr Biochem*. 2019; 69:73–86.
<https://doi.org/10.1016/j.jnutbio.2019.03.021>
PMID:31063918
55. Pu Y, Qu Y, Chang L, Wang SM, Zhang K, Ushida Y, Saganuma H, Hashimoto K. Dietary intake of glucoraphanin prevents the reduction of dopamine transporter in the mouse striatum after repeated administration of MPTP. *Neuropsychopharmacol Rep*. 2019. [Epub ahead of print].
<https://doi.org/10.1002/npr2.12060> PMID:31132231
56. Ren Q, Ma M, Yang J, Nonaka R, Yamaguchi A, Ishikawa KI, Kobayashi K, Murayama S, Hwang SH, Saiki S, Akamatsu W, Hattori N, Hammock BD, Hashimoto K. Soluble epoxide hydrolase plays a key role in the pathogenesis of Parkinson's disease. *Proc Natl Acad Sci USA*. 2018; 115:E5815–23.
<https://doi.org/10.1073/pnas.1802179115>
PMID:29735655
57. Kim SW, Suda W, Kim S, Oshima K, Fukuda S, Ohno H, Morita H, Hattori M. Robustness of gut microbiota of healthy adults in response to probiotic intervention revealed by high-throughput pyrosequencing. *DNA Res*. 2013; 20:241–53.
<https://doi.org/10.1093/dnares/dst006>
PMID:23571675
58. Tanoue T, Morita S, Plichta DR, Skelly AN, Suda W, Sugiura Y, Narushima S, Vlamakis H, Motoo I, Sugita K, Shiota A, Takeshita K, Yasuma-Mitobe K, et al. A defined commensal consortium elicits CD8 T cells and anti-cancer immunity. *Nature*. 2019; 565:600–05.
<https://doi.org/10.1038/s41586-019-0878-z>
PMID:30675064

SUPPLEMENTARY MATERIALS

Supplementary Tables

Supplementary Table 1. Statistical analysis data of gut microbiota data at phylum.

Graph	Factor effect (Antibiotic)	Factor effect (MPTP)	Interaction effect (Antibiotic × MPTP)
<i>Bacteroidetes</i>	$F_{(1,36)} = 12.695, P = 0.001$	$F_{(1,36)} = 21.180, P < 0.001$	$F_{(1,36)} = 1.806, P = 0.187$
<i>Firmicutes</i>	$F_{(1,36)} = 14.284, P = 0.001$	$F_{(1,36)} = 20.353, P < 0.001$	$F_{(1,36)} = 2.272, P = 0.140$
<i>Proteobacteria</i>	$F_{(1,36)} = 40.495, P < 0.001$	$F_{(1,36)} = 1.034, P = 0.316$	$F_{(1,36)} = 0.190, P = 0.665$
<i>Deferrribacteres</i>	$F_{(1,36)} = 10.911, P = 0.002$	$F_{(1,36)} = 3.872, P = 0.057$	$F_{(1,36)} = 3.948, P = 0.055$
<i>TM7</i>	$F_{(1,36)} = 10.916, P = 0.002$	$F_{(1,36)} = 10.916, P = 0.002$	$F_{(1,36)} = 10.916, P = 0.002$

Supplementary Table 2. Statistical analysis data of gut microbiota data at genus.

Graph	Factor effect (Antibiotic)	Factor effect (MPTP)	Interaction effect (Antibiotic × MPTP)
<i>lactobacillus</i>	$F_{(1,36)} = 40.826, P < 0.001$	$F_{(1,36)} = 0.743, P = 0.394$	$F_{(1,36)} = 0.744, P = 0.394$
<i>Mucispirillum</i>	$F_{(1,36)} = 10.835, P = 0.002$	$F_{(1,36)} = 3.818, P = 0.059$	$F_{(1,36)} = 3.893, P = 0.056$
<i>Candidatus Arthromitus</i>	$F_{(1,36)} = 10.302, P = 0.003$	$F_{(1,36)} = 1.204, P = 0.280$	$F_{(1,36)} = 0.796, P = 0.378$
<i>Parasutterella</i>	$F_{(1,36)} = 81.500, P < 0.001$	$F_{(1,36)} = 0.344, P = 0.561$	$F_{(1,36)} = 0.495, P = 0.486$
<i>Blautia</i>	$F_{(1,36)} = 11.239, P = 0.002$	$F_{(1,36)} = 1.430, P = 0.240$	$F_{(1,36)} = 1.542, P = 0.222$
<i>Robinsoniella</i>	$F_{(1,36)} = 11.589, P = 0.002$	$F_{(1,36)} = 0.211, P = 0.649$	$F_{(1,36)} = 0.211, P = 0.649$
<i>Escherichia</i>	$F_{(1,36)} = 8.289, P = 0.007$	$F_{(1,36)} = 2.245, P = 0.143$	$F_{(1,36)} = 2.399, P = 0.130$
<i>Dorea</i>	$F_{(1,36)} = 7.766, P = 0.008$	$F_{(1,36)} = 0.548, P = 0.464$	$F_{(1,36)} = 1.104, P = 0.300$
<i>Eubacterium</i>	$F_{(1,36)} = 8.529, P = 0.006$	$F_{(1,36)} = 3.508, P = 0.069$	$F_{(1,36)} = 1.747, P = 0.195$
<i>Asaccharobacter</i>	$F_{(1,36)} = 1.292, P = 0.263$	$F_{(1,36)} = 7.712, P = 0.009$	$F_{(1,36)} = 4.353, P = 0.044$
<i>Clostridium</i>	$F_{(1,36)} = 7.982, P = 0.008$	$F_{(1,36)} = 6.757, P = 0.013$	$F_{(1,36)} = 1.664, P = 0.205$
<i>Parabacteroides</i>	$F_{(1,36)} = 43.663, P < 0.001$	$F_{(1,36)} = 29.742, P < 0.001$	$F_{(1,36)} = 29.742, P < 0.001$
<i>Bacteroides</i>	$F_{(1,36)} = 19.018, P < 0.001$	$F_{(1,36)} = 12.176, P = 0.001$	$F_{(1,36)} = 7.447, P = 0.010$
<i>Enterococcus</i>	$F_{(1,36)} = 8.910, P = 0.005$	$F_{(1,36)} = 4.904, P = 0.033$	$F_{(1,36)} = 4.624, P = 0.038$


Supplementary Table 3. Statistical analysis data of gut microbiota data at species.

Graph	Factor effect (Antibiotic)	Factor effect (MPTP)	Interaction effect (Antibiotic × MPTP)
<i>Lactobacillus murinus</i>	F _(1,36) = 19.973, P < 0.001	F _(1,36) = 0.007, P = 0.935	F _(1,36) = 0.006, P = 0.936
<i>Lactobacillus johnsonii</i>	F _(1,36) = 21.666, P < 0.001	F _(1,36) = 1.126, P = 0.296	F _(1,36) = 1.126, P = 0.296
<i>Mucispirillum schaedleri</i>	F _(1,36) = 10.803, P = 0.002	F _(1,36) = 3.836, P = 0.058	F _(1,36) = 3.912, P = 0.056
<i>Candidatus Arthromitus sp. SFB-mouse</i>	F _(1,36) = 10.302, P = 0.003	F _(1,36) = 1.204, P = 0.280	F _(1,36) = 0.796, P = 0.378
<i>Escherichia coli</i>	F _(1,36) = 8.289, P = 0.007	F _(1,36) = 2.245, P = 0.143	F _(1,36) = 2.399, P = 0.130
<i>Blautia sp. Ser8</i>	F _(1,36) = 10.059, P = 0.003	F _(1,36) = 3.457, P = 0.071	F _(1,36) = 3.457, P = 0.071
<i>Robinsoniella peoriensis</i>	F _(1,36) = 11.921, P = 0.001	F _(1,36) = 0.239, P = 0.628	F _(1,36) = 0.239, P = 0.628
<i>Clostridium sp. Clone-27</i>	F _(1,36) = 6.957, P = 0.012	F _(1,36) = 9.366, P = 0.004	F _(1,36) = 6.036, P = 0.019
<i>Blautia sp. canine oral taxon 143</i>	F _(1,36) = 5.309, P = 0.027	F _(1,36) = 5.309, P = 0.027	F _(1,36) = 5.309, P = 0.027
<i>Parabacteroides distasonis</i>	F _(1,36) = 30.573, P < 0.001	F _(1,36) = 40.561, P < 0.001	F _(1,36) = 39.576, P < 0.001
<i>Blautia coccoides</i>	F _(1,36) = 26.794, P < 0.001	F _(1,36) = 6.406, P = 0.016	F _(1,36) = 6.406, P = 0.016
<i>Clostridium sp. HGF2</i>	F _(1,36) = 21.898, P < 0.001	F _(1,36) = 12.850, P = 0.001	F _(1,36) = 12.850, P = 0.001
<i>Clostridium bolteae</i>	F _(1,36) = 8.670, P = 0.006	F _(1,36) = 5.094, P = 0.030	F _(1,36) = 5.094, P = 0.030
<i>Lactobacillus intestinalis</i>	F _(1,36) = 23.328, P < 0.001	F _(1,36) = 8.172, P = 0.007	F _(1,36) = 8.105, P = 0.007
<i>Lactobacillus reuteri</i>	F _(1,36) = 23.676, P < 0.001	F _(1,36) = 8.288, P = 0.007	F _(1,36) = 8.214, P = 0.007
<i>Bacteroides acidifaciens</i>	F _(1,36) = 26.102, P < 0.001	F _(1,36) = 18.528, P < 0.001	F _(1,36) = 11.141, P = 0.002
<i>[Clostridium] cocleatum</i>	F _(1,36) = 14.097, P = 0.001	F _(1,36) = 9.975, P = 0.003	F _(1,36) = 9.975, P = 0.003
<i>Enterococcus casseliflavus</i>	F _(1,36) = 6.743, P = 0.014	F _(1,36) = 5.058, P = 0.031	F _(1,36) = 5.058, P = 0.031
<i>Bacteroides sp. TP-5</i>	F _(1,36) = 7.426, P = 0.010	F _(1,36) = 4.685, P = 0.037	F _(1,36) = 4.747, P = 0.036

ARTICLE

Open Access

Abnormal composition of gut microbiota is associated with resilience versus susceptibility to inescapable electric stress

Kai Zhang^{1,2}, Yuko Fujita¹, Lijia Chang¹, Youge Qu¹, Yaoyu Pu¹, Siming Wang¹, Yukihiko Shirayama^{1,3} and Kenji Hashimoto¹ 

Abstract

Increasing evidence indicates that abnormalities in the composition of gut microbiota might play a role in stress-related disorders. In the learned helplessness (LH) paradigm, ~60–70% rats are susceptible to LH in the face of inescapable electric stress. The role of gut microbiota in susceptibility in the LH paradigm is unknown. In this study, male rats were exposed to inescapable electric stress under the LH paradigm. The compositions of gut microbiota and short-chain fatty acids were assessed in fecal samples from control rats, non-LH (resilient) rats, and LH (susceptible) rats. Members of the order *Lactobacillales* were present at significantly higher levels in the susceptible rats than in control and resilient rats. At the family level, the number of *Lactobacillaceae* in the susceptible rats was significantly higher than in control and resilient rats. At the genus level, the numbers of *Lactobacillus*, *Clostridium* cluster III, and *Anaerofustis* in susceptible rats were significantly higher than in control and resilient rats. Levels of acetic acid and propionic acid in the feces of susceptible rats were lower than in those of control and resilient rats; however, the levels of lactic acid in the susceptible rats were higher than those of control and resilient rats. There was a positive correlation between lactic acid and *Lactobacillus* levels among these three groups. These findings suggest that abnormal composition of the gut microbiota, including organisms such as *Lactobacillus*, contributes to susceptibility versus resilience to LH in rats subjected to inescapable electric foot shock. Therefore, it appears likely that brain–gut axis plays a role in stress susceptibility in the LH paradigm.

Introduction

Resilience is adaptation in the face of stress and adversity. It is well known that humans display wide variability in their responses to stress. Increasing amounts of evidence show that resilience might be mediated by adaptive changes in several neural circuits, including numerous molecular and cellular pathways^{1–11}. An understanding of the molecular and cellular mechanisms underlying resilience will facilitate the discovery of new therapeutic drugs for stress-related psychiatric disorders,

but the detailed mechanisms underlying resilience and susceptibility remain unclear.

The brain–gut–microbiome axis is a complex, bidirectional signaling system between the brain and the gut microbiota^{12–16}. Accumulating studies suggest that an abnormal composition of the gut microbiota contributes to the pathophysiology of depression^{17–21} and the antidepressant effects of certain potential compounds^{22–29}. Previously, we reported that the presence of *Bifidobacterium* in the gut microbiome confers stress resilience in a chronic social defeat stress (CSDS) model³⁰. It has been shown that ~30–40% of rats are resilient to inescapable electric stress in the learned helplessness (LH) paradigm^{31–34}; however, the role of gut microbiota in the production of this resilience has not yet been investigated. Microbes in the gut can produce short-chain fatty acids.

Correspondence: Kenji Hashimoto (hashimoto@faculty.chiba-u.jp)

¹Division of Clinical Neuroscience, Chiba University Center for Forensic Mental Health, Chiba 260-8670, Japan

²Department of Psychiatry, Chaohu Hospital of Anhui Medical University, 238000 Hefei, China

Full list of author information is available at the end of the article.

© The Author(s) 2019



Open Access This article is licensed under a Creative Commons Attribution 4.0 International License, which permits use, sharing, adaptation, distribution and reproduction in any medium or format, as long as you give appropriate credit to the original author(s) and the source, provide a link to the Creative Commons license, and indicate if changes were made. The images or other third party material in this article are included in the article's Creative Commons license, unless indicated otherwise in a credit line to the material. If material is not included in the article's Creative Commons license and your intended use is not permitted by statutory regulation or exceeds the permitted use, you will need to obtain permission directly from the copyright holder. To view a copy of this license, visit <http://creativecommons.org/licenses/by/4.0/>.

The presence and abundance of such acids could possibly be used as an indicator of the types of bacteria present in the gut. However, it is also currently unknown how the altered composition of the gut microbiota affects the concentration of short-chain fatty acids in fecal samples.

The purpose of this study was to investigate the role of gut microbiota on stress resilience using a rat LH paradigm. First, we investigated whether the composition of the gut microbiota was altered in fecal samples from LH (susceptible) and non-LH (resilient) rats compared with control rats. Then we examined whether the levels of short-chain fatty acids—acetic acid, propionic acid, butyric acid, lactic acid, and succinic acid—in the fecal samples from susceptible and resilient rats were altered compared with control rats, since these short-chain fatty acids can be produced by the gut microbiota²³.

Materials and methods

Animals

Male Sprague-Dawley rats ($n = 25$, 200–230 g; 7 weeks, Charles River Japan, Co., Tokyo, Japan) were used. The animals were housed under a 12-h light/dark cycle with ad libitum access to food and water. The experimental procedures were approved by the Chiba University Institutional Animal Care and Use Committee (Permission number: 31-341).

Stress paradigm (LH model) and collection of fecal sample

The LH paradigm was performed as previously reported^{6–8,11,31–34}. Animals were initially exposed to uncontrollable stress to create LH rats. When the rats were later placed in a situation in which the shock is controllable; that is, the animal could escape it, an animal exhibiting LH not only fails to acquire an escape response but also often makes no effort to escape the shock at all.

We used the Gemini Avoidance System (San Diego Instruments, San Diego, CA) for LH paradigm. This apparatus has two compartments by a retractable door. On day 1 and day 2, rats were subjected to 30 inescapable electric foot shocks (0.65 mA, 30 s duration, at random intervals averaging 18–42 s). On day 3, a post-shock test using a two-way conditioned avoidance test was performed to determine whether the rats would exhibit the predicted escape deficits (Fig. 1a). This session consisted of 30 trials, in which electric foot shocks (0.65 mA, 6 s duration, at random intervals with a mean of 30 s) were preceded by a 3-s conditioned stimulus tone that remained on until the shock was terminated. The numbers of escape failures and the latency to escape in each of the 30 trials were counted. Animals with more than 25 escape failures in the 30 trials were regarded as having met the criterion for LH rats (susceptible). Animals with fewer than 24 failures were defined as non-LH rats

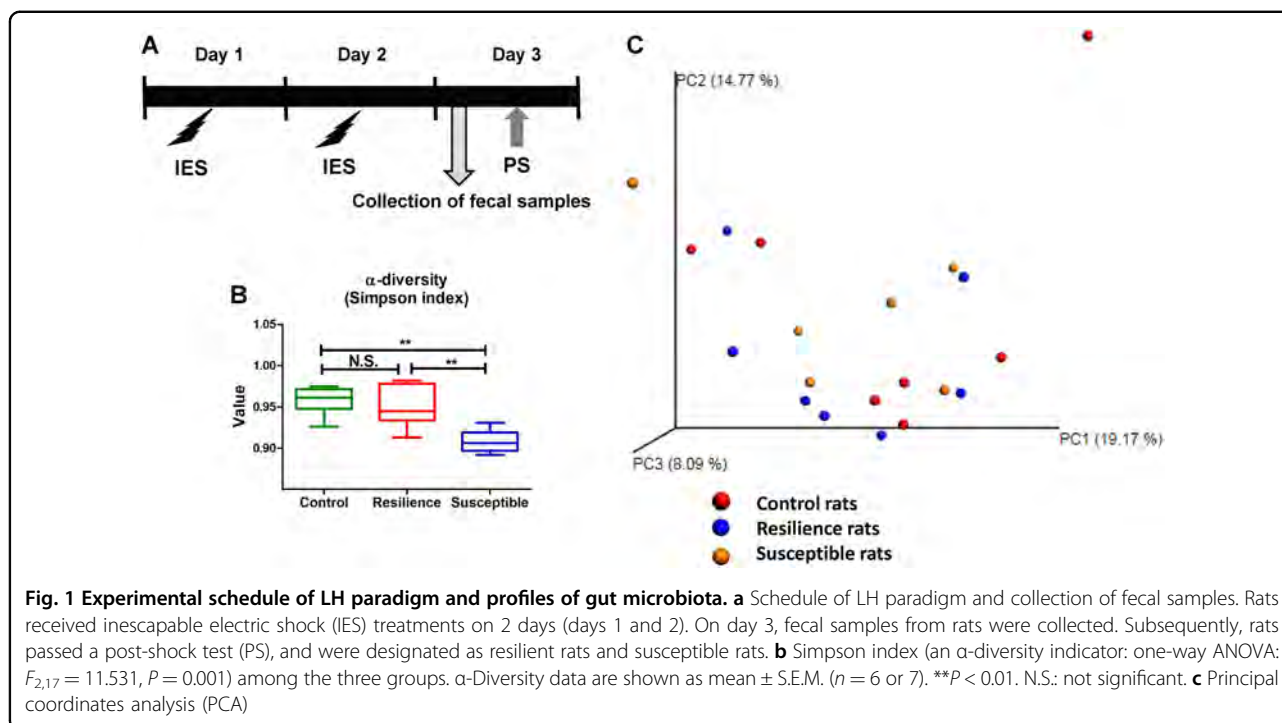
(resilient)^{31–34}. Fresh fecal samples were collected in a blind manner before post-shock stress on day 4, and stored at -80°C until use (Fig. 1A).

16S rDNA analysis

DNA extraction from fecal samples and the 16S rDNA analysis were performed at the TechnoSuruga Laboratory, Co., Ltd. (Shizuoka, Japan), as reported previously³⁵. Briefly, the samples were suspended in a buffer containing 4 M guanidium thiocyanate, 100 mM Tris-HCl (pH 9.0) and 40 mM EDTA and broken up in the presence of zirconia beads using the FastPrep-24 5G homogenizer (MP Biomedicals, Irvine, CA). Then, DNA was extracted using GENE PREP STAR PI-480 (KURABO, Japan). The final concentration (10 ng/ μL) of the DNA sample was used. Briefly, the V3-V4 hypervariable regions of the 16S rRNA were amplified from microbial genomic DNA using PCR with the bacterial universal primers (341F/R806)³⁵ and the dual-index method³⁶. For bioinformatics analysis, the overlapping paired-end reads were merged using the fastq-join program with default settings³⁷. The reads were processed for quality and chimera filtering as follows. Only reads with quality value scores of 20 for >99% of the sequence were extracted, and chimeric sequences were removed using the program usearch6.1³⁸. Non-chimeric reads were submitted for 16S rDNA-based taxonomic analysis using the Ribosomal Database Project (RDP) Multiclassifier tool³⁹. Reads obtained in the Multi-FASTA format were assigned to genus or phylum levels with an 80% confidence threshold. Principal component analysis (PCA) was performed using Metagenome@KIN software (World Fusion Co., Ltd., Tokyo, Japan) based on data obtained from the bacterial family using the RDP taxonomic analysis software.

Measurement of fecal short-chain fatty acids

Measurement of short-chain fatty acids—acetic acid, propionic acid, butyric acid, lactic acid, and succinic acid—in fecal samples was performed at the TechnoSuruga Laboratory, Co., Ltd. (Shizuoka, Japan). For the determination of these short-chain fatty acids, feces were suspended in distilled water, heated at 85°C for 15 min to inactivate viruses, and then centrifuged according to previously reported methods^{40,41}. The concentrations of these short-chain fatty acids in feces were measured using a high-performance liquid chromatography organic acid analysis system with a Prominence CDD-10A conductivity detector (Shimadzu, Kyoto, Japan), two tandemly arranged Shim-pack SCR-102(H) columns [300 mm \times 8 mm inner diameter (ID)], and a Shim-pack SCR-102(H) guard column (50 mm \times 6 mm ID)^{40,41}. The HPLC calibration curves for the measurement of the short-chain fatty acids were created using prepared standard solutions.



Statistical analysis

The data are presented as the mean \pm standard error of the mean (S.E.M.). Analysis was performed using the PASW Statistics 20 software (now SPSS statistics; SPSS, Tokyo, Japan). Comparisons between groups were performed using one-way analysis of variance, followed by post hoc Fisher's Least Significant Difference test. A P value < 0.05 was considered statistically significant.

Results

Composition of gut microbiota in control, resilient, and susceptible rats

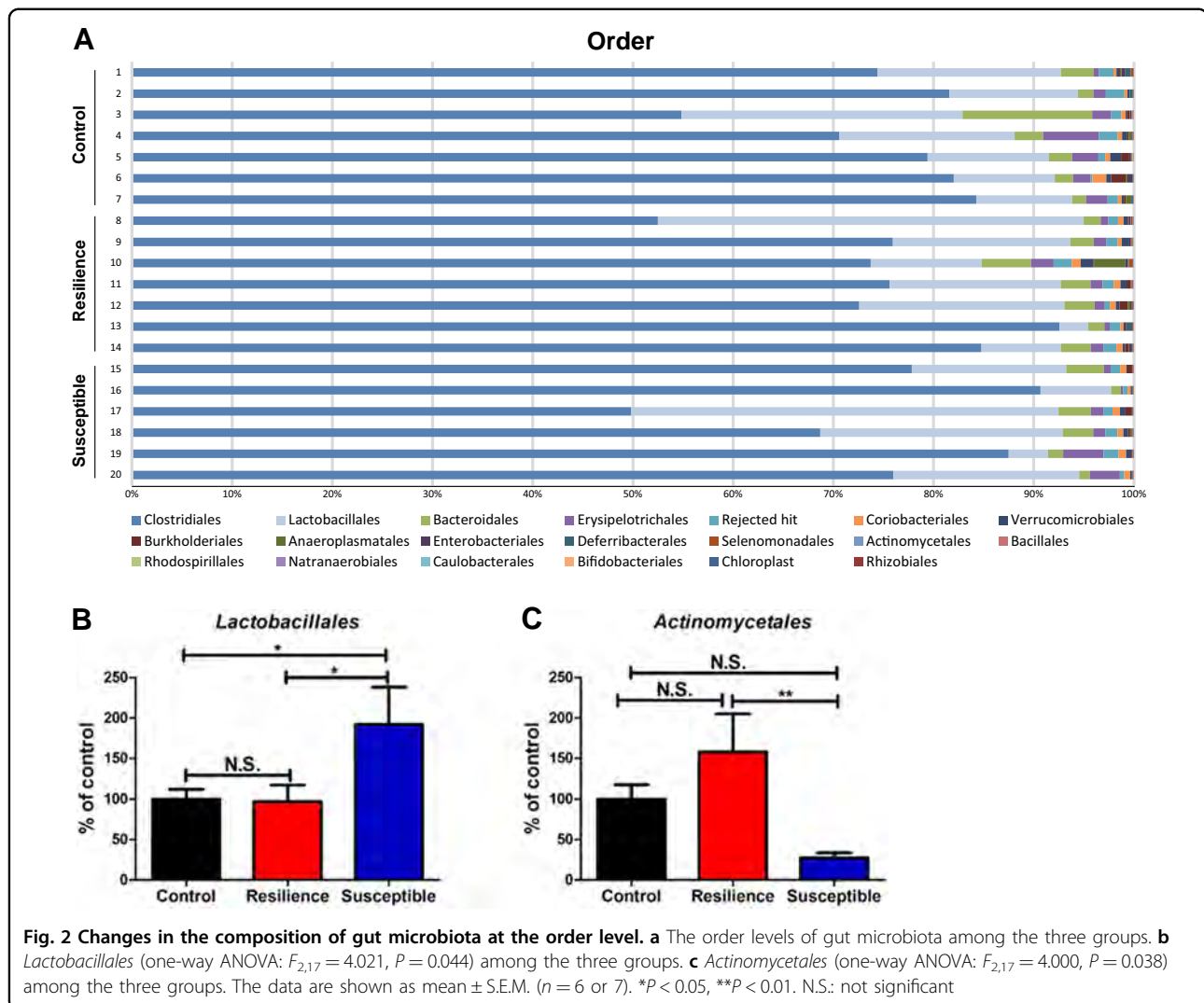
We used 16S rDNA gene sequencing to determine differences in the gut microbiota composition among the three groups of rats. α -diversity refers to the diversity of bacteria or species within a community or habitat. The susceptible rats showed a significant decrease in the α -diversity value compared with control rats or resilient rats (Fig. 1b). In the three-dimensional PCoA data, the measurements from susceptible rats were well separated from those of control rats and resilient rats. Four measurements from the susceptible group were close to those of the sham group, whereas the other three measurements were close to those of the resilient group (Fig. 1c).

Firmicutes were the most dominant phylum, comprising $>85\%$ of the total sequences. There were no significant differences in the levels of this phylum among the three groups. The order levels of gut bacterium in control rats, resilient rats, and susceptible rats were identified (Fig. 2a).

Clostridiales and *Lactobacillales* were the most dominant orders, with $>80\%$ of total sequences. The number of *Lactobacillales* was significantly increased in the susceptible rats compared with that in control and resilient rats (Fig. 2b). In contrast, the number of *Lactobacillales* in the resilient rats was similar to that in the control rats (Fig. 2b). The number of *Actinomycetales* in the susceptible rats was significantly lower than that in the resilient rats (Fig. 2c). Although the number of *Actinomycetales* in the resilient rats was higher than that in the control rats, the difference did not reach statistical significance.

The families of the gut bacteria in control, resilient, and susceptible rats are shown (Fig. 3a). *Lactobacillaceae* were significantly more highly represented in the susceptible rats than in the control and resilient rats, although the number of *Lactobacillaceae* in the resilient rats was similar to that in the control rats (Fig. 3b). In contrast, the number of *Corynebacteriaceae* was significantly lower in the susceptible rats than that in the resilient rats, although these two did not significantly differ from the control rats (Fig. 3c).

The genera of gut bacteria in the control, resilient, and susceptible rats are shown (Fig. 4a). *Lactobacillus*, *Clostridium* cluster III, and *Anaerofustis* numbers were significantly higher in the susceptible rats than in the control and resilient rats (Fig. 4b, c, e). *Corynebacterium* numbers were significantly lower in the susceptible rats than in the resilient rats, although these two groups were not significantly altered compared with the control rats (Fig. 4d).



Measurement of short-chain fatty acids in fecal samples

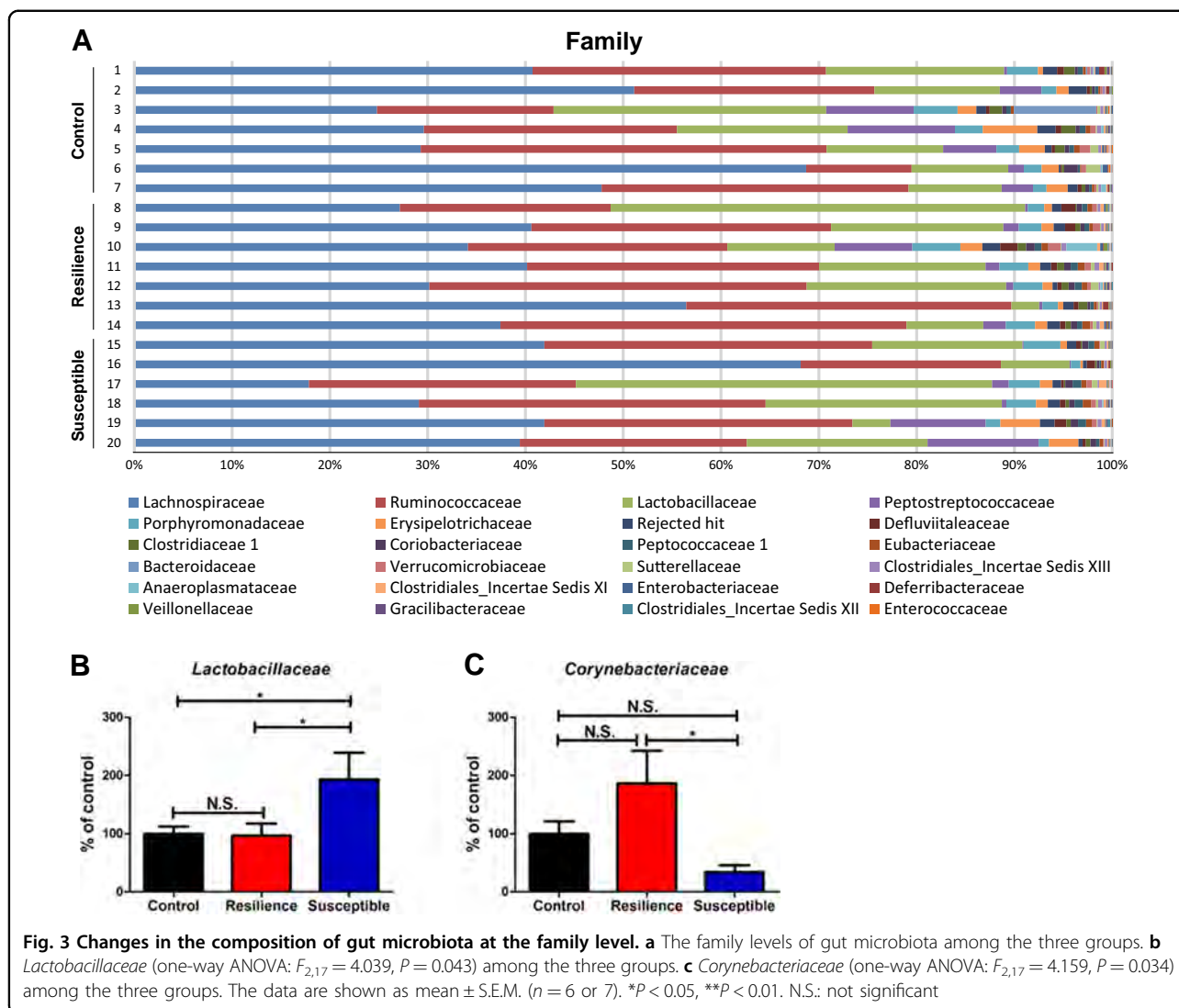
Levels of acetic acid and propionic acid in the susceptible rats were significantly lower than those in control rats and resilient rats, and there were no significant differences between control rats and resilient rats (Fig. 5a, b). There were no changes in butyric acid and succinic acid among the three groups (Fig. 5c, e). In contrast, levels of lactic acid in the susceptible rats were significantly higher than those of control rats and resilient rats, although there were no changes between control rats and resilient rats (Fig. 5d). There was a positive correlation ($r = 0.461$, $P = 0.041$) between lactic acid and *Lactobacillus* levels among three groups (Fig. 5f). There were no correlations between other short-chain fatty acids and the microbiome composition among the three experimental groups.

Discussion

The major findings of this study are as follows. At the order level, susceptibility to LH in rats exposed to

inescapable shock might be associated with an increase of *Lactobacillales* and a decrease of *Actinomycetales* in the host gut. At the family level, stress susceptibility might be associated with an increase in *Lactobacillaceae* and decrease of *Corynebacteriaceae* in the host gut. At the gene level, stress susceptibility might be associated with the increase of *Lactobacillus*, *Clostridium* cluster III and *Anaerofustis*, and the decrease of *Corynebacterium* in the host gut. Levels of acetic acid and propionic acid in the feces from susceptible rats were lower than those in the feces of control and resilient rats, whereas levels of lactic acid in the susceptible rats were higher than those of control and resilient rats. There was a positive correlation between lactic acid and *Lactobacillus* levels among these three groups. These findings suggest that alterations in the composition of these microbiota contribute to susceptibility versus resilience in rats in the LH situation.

In this study, we found an increase in the abundance of members of the order *Lactobacillales* and the family

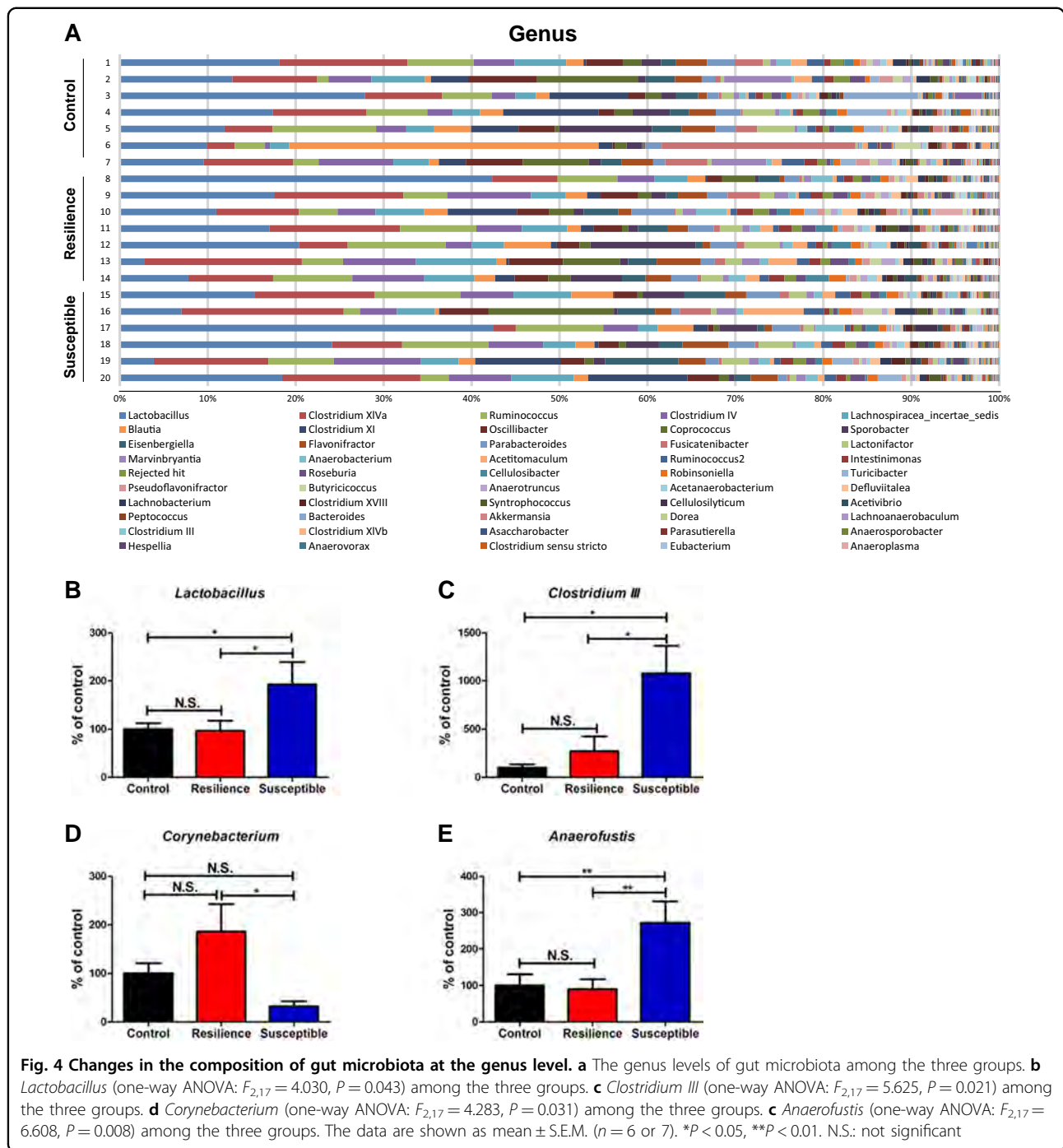


Lactobacillaceae in susceptible rats, in comparison with control and resilient rats. It is possible that increased abundance of members of the *Lactobacillales* order and *Lactobacillaceae* family might play a role in susceptibility versus resilience of rats to LH after inescapable electric stress.

At the genus level, susceptibility in rats exposed to inescapable shock might be associated with an increase in *Lactobacillus*, *Clostridium* cluster III, and *Anaerofustis* and a decrease of *Corynebacterium* in the host gut. *Clostridium*, a genus of Gram-positive bacteria, includes several significant human pathogens, such as the causative agent of botulism. High levels of members of the genus *Clostridium* have been reported in patients with major depressive disorder (MDD) compared with controls^{42,43}, suggesting that increased levels of *Clostridium* play a role in depression. We reported that susceptible mice after CSDS have higher levels of *Clostridium*, and that the

novel antidepressant candidate (*R*)-ketamine attenuated the increased levels of *Clostridium* in susceptible mice²⁵. This study shows that the antidepressant effects of (*R*)-ketamine might be partly mediated by the restoration of altered composition of the gut microbiota in the CSDS susceptible mice. Although the role of members of *Clostridium* cluster III in depression is currently unclear, it appears that *Clostridium* cluster III may contribute to susceptibility in rats subjected to inescapable electric stress.

Anaerofustis is a strictly anaerobic, Gram-positive, rod-shaped, non-spore-forming bacterial genus of the family *Eubacteriaceae*⁴⁴. In this study, we found decreased levels of *Anaerofustis* in the susceptible rats compared with the control and resilient rats. At present, there have been no reports showing alterations in *Anaerofustis* in patients with MDD, or in rodents with depression-like phenotypes. Therefore, it is unclear how decreased levels of

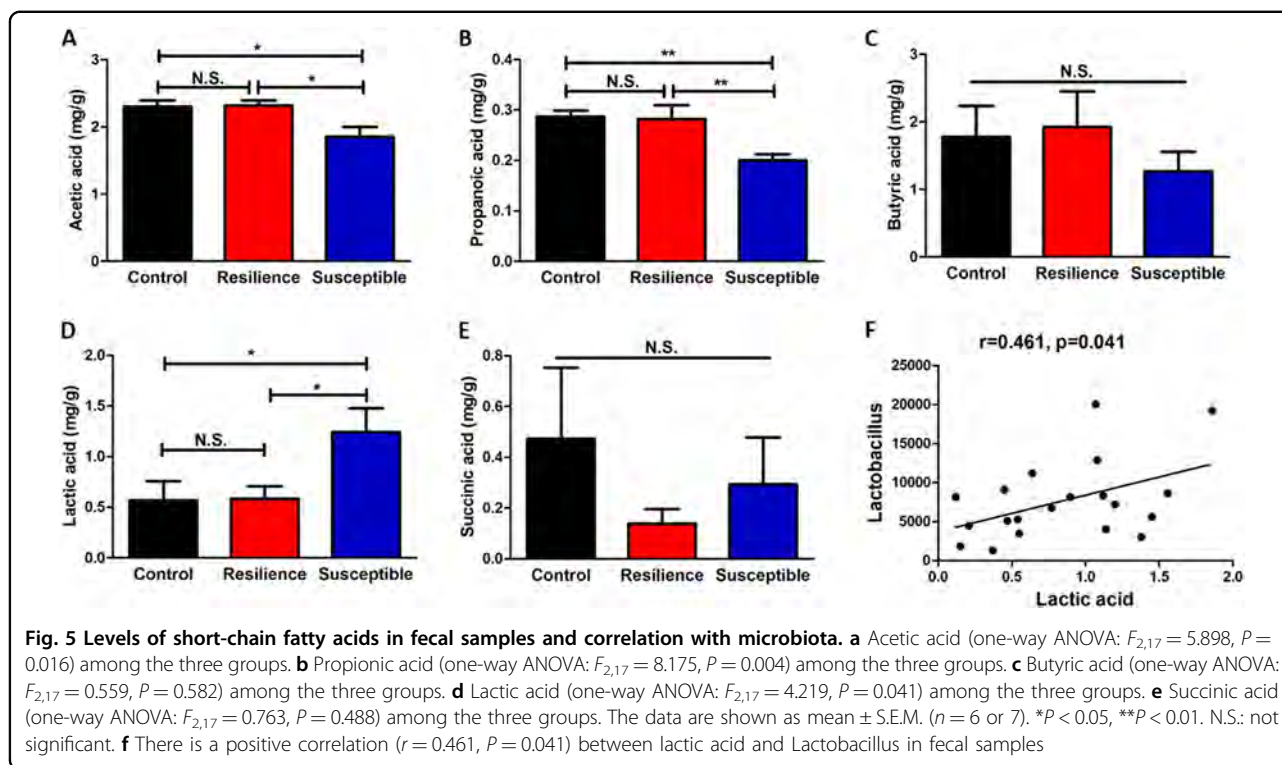


Anaerofustis play a role in susceptibility to LH. Further study into the role of *Anaerofustis* in depression is needed.

In this study, we found lower levels of *Corynebacterium* in the susceptible rats compared with control and resilient rats. It has been reported that sub-chronic and chronic exposure to glyphosate-based herbicides decreases the composition of microbiota, such as *Corynebacterium*, resulting in behavioral abnormalities including depression and anxiety⁴⁵. Low levels of *Corynebacterium* were also

reported in a chronic variable stress-induced rat model of depression⁴⁶. It appears likely that lowered levels of *Corynebacterium* might play a role in a depression-like phenotype in rodents, although further study into the role of *Corynebacterium* in depression is needed.

Short-chain fatty acids—acetic acid, propionic acid, butyric acid, lactic acid, and succinic acid—are generated as the end products of the degradation and fermentation of indigestible carbohydrates by the gut microbiota⁴⁷.



Measurement of these short-chain fatty acids could therefore serve as an indirect method for the analysis of microbiota composition. These organic acids have specific anti-microbial activities⁴⁸. It has been reported that levels of acetic acid and propionic acid in feces from women with depression are lower than those in control subjects, and that there are negative correlations between acetic acid or propionic acid and depression scores⁴⁹. In this study, we found decreased levels of acetic acid and propionic acid in rats susceptible to LH, compared with control and resilient rats, consistent with the results from a recent clinical study⁴⁹. We also found decreased levels of butyric acid in the susceptible rats, although the difference did not reach statistical significance. Three short-chain fatty acids containing C2–C4, acetic acid, propionic acid, and butyric acid, account for over 95% of the pool of short-chain fatty acids²³. It is likely that decreased levels of acetic acid and propionic acid in feces may be associated with susceptibility to LH, and with depression in patients with MDD.

Elevated levels of lactic acid in the blood, cerebrospinal fluid and brain have been reported in patients with MDD^{50–52}. Higher levels of lactic acid in rodents with depression-like behaviors have also been reported⁵³. In contrast, peripheral administration of lactic acid produced antidepressant-like effects in different models of depression⁵⁴. In this research we found higher levels of lactic acid in feces from susceptible rats compared with those from control and resilient rats. We found a positive

correlation between *Lactobacillus*, microbes which produce lactic acid, and the amounts of lactic acid in fecal samples. It appears likely that the increased levels of lactic acid produced by *Lactobacillus* might contribute to susceptibility to inescapable electric stress, although further study is needed.

The crosstalk between the brain and the gut is predominately influenced by the gut bacteria⁵⁵. Imbalance of gut microbiota has been found to cause abnormalities in the brain–gut axis in several neurological and psychiatric diseases^{13,55}. Multiple lines of evidence suggest that an abnormal composition of the gut microbiota contributes to the resilience or susceptibility to LH in rodents after repeated stress^{30,56–59}. It is well recognized that gut microbiota plays a role in animal behaviors^{14,60–62}, although the precise mechanisms underlying the microbiome-mediated behaviors are currently unknown. For example, it has been reported that the vagus nerve plays a major role in modulating the constitutive communication pathway between the brain and the bacteria in the gut^{63,64}. It is likely that altered composition of microbiota might play a key role in the stress-induced disorders although further study is needed.

This research has some limitations. In this study, we did not identify the specific microbiome which can affect susceptibility or resilience in the LH experiments. Therefore, from the present data, we do not know how the specific microbiome can affect behaviors under the LH paradigm. In the future, it will be necessary to identify

the specific microbiome, using approaches such as shotgun metagenomics sequencing. It will also be of interest to investigate the way in which specific microbiomes affect behaviors related to LH.

In conclusion, the present study suggests that an altered composition of the gut microbiota, including organisms, such as *Lactobacillus*, *Clostridium* cluster III, *Anaerofustis*, and *Corynebacterium*, contributes to resilience and susceptibility to learned helplessness in rats subjected to inescapable electric foot shock.

Acknowledgements

This study was supported by SENSHIN Medical Research Foundation, Japan (to K.Z.), Smoking Research Foundation, Japan (to K.H.), and AMED, Japan (to K.H., JP19dm0107119). L.C. was supported by Japan China Sasakawa Medical Fellowship (Tokyo, Japan). S.W. was supported by TAKASE Scholarship Foundation (Tokyo, Japan).

Author details

¹Division of Clinical Neuroscience, Chiba University Center for Forensic Mental Health, Chiba 260-8670, Japan. ²Department of Psychiatry, Chaohu Hospital of Anhui Medical University, 238000 Hefei, China. ³Department of Psychiatry, Teikyo University Chiba Medical Center, Ichihara, Chiba 299-0111, Japan

Conflict of interest

K.H. has received research support from Dainippon-Sumitomo, Otsuka, and Taisho. The remaining authors declare that they have no conflict of interest.

Publisher's note

Springer Nature remains neutral with regard to jurisdictional claims in published maps and institutional affiliations.

Received: 10 May 2019 Revised: 29 June 2019 Accepted: 30 July 2019

Published online: 17 September 2019

References

- Southwick, S. M., Vythilingam, M. & Charney, D. S. The psychobiology of depression and resilience to stress: implications for prevention and treatment. *Ann. Rev. Clin. Psychol.* **1**, 255–291 (2005).
- Feder, A., Nestler, E. J. & Charney, D. S. Psychobiology and molecular genetics of resilience. *Nat. Rev. Neurosci.* **10**, 446–457 (2009).
- Franklin, T. B., Saab, B. J. & Mansuy, I. M. Neural mechanisms of stress resilience and vulnerability. *Neuron* **75**, 747–761 (2012).
- Russo, S. J., Murrough, J. W., Han, M. H., Charney, D. S. & Nestler, E. J. Neurobiology of resilience. *Nat. Neurosci.* **15**, 1475–1484 (2012).
- Taliaz, D. et al. Resilience to chronic stress is mediated by hippocampal brain-derived neurotrophic factor. *J. Neurosci.* **31**, 4475–4483 (2012).
- Yang, C., Shirayama, Y., Zhang, J. C., Ren, Q. & Hashimoto, K. Regional differences in brain-derived neurotrophic factor levels and dendritic spine density confer resilience to inescapable stress. *Int. J. Neuropsychopharmacol.* **18**, pyu121 (2015).
- Yang, C., Shirayama, Y., Zhang, J. C., Ren, Q. & Hashimoto, K. Peripheral interleukin-6 promotes resilience versus susceptibility to inescapable electric stress. *Acta Neuropsychiatr.* **27**, 312–316 (2015).
- Yang, B. et al. Regional differences in the expression of brain-derived neurotrophic factor (BDNF) pro-peptide, proBDNF and preproBDNF in the brain confer stress resilience. *Eur. Arch. Psychiatry Clin. Neurosci.* **266**, 765–769 (2016).
- Dantzer, R., Cohen, S., Russo, S. J. & Dinan, T. G. Resilience and immunity. *Brain Behav. Immun.* **74**, 28–42 (2018).
- Qu, Y. et al. Regional differences in dendritic spine density confer resilience to chronic social defeat stress. *Acta Neuropsychiatr.* **30**, 117–122 (2018).
- Zhang, J. C. et al. Keap1-Nrf2 signaling pathway confers resilience versus susceptibility to inescapable electric stress. *Eur. Arch. Psychiatry Clin. Neurosci.* **268**, 865–870 (2018).
- Dinan, T. G. & Cryan, J. F. Brain-gut-microbiota axis and mental health. *Psychosom. Med.* **79**, 920–926 (2017).
- Fung, T. C., Olson, C. A. & Hsiao, E. Y. Interactions between the microbiota, immune and nervous systems in health and disease. *Nat. Neurosci.* **20**, 145–155 (2017).
- Cusotto, S., Sandhu, K. V., Dinan, T. G. & Cryan, J. F. The neuroendocrinology of the microbiota-gut-brain axis: a behavioural perspective. *Front. Neuroendocrinol.* **51**, 80–101 (2018).
- Molina-Torres, G., Rodriguez-Arrastia, M., Roman, P., Sanchez-Labraca, N. & Cardona, D. Stress and the gut microbiota-brain axis. *Behav. Pharmacol.* **30**(2 and 3 Special Issue), 187–202 (2019).
- Cusotto S., et al. Differential effects of psychotropic drugs on microbiome composition and gastrointestinal function. *Psychopharmacology (Berl.)*. <https://doi.org/10.1007/s00213-018-5006-5> (2018).
- Jiang, H. et al. Altered fecal microbiota composition in patients with major depressive disorder. *Brain Behav. Immun.* **48**, 186–194 (2015).
- Zheng, P. et al. Gut microbiome remodeling induces depressive-like behaviors through a pathway mediated by the host's metabolism. *Mol. Psychiatry* **21**, 786–796 (2016).
- Wong, M. L. et al. Inflammasome signaling affects anxiety- and depressive-like behavior and gut microbiome composition. *Mol. Psychiatry* **21**, 797–805 (2016).
- Huang, T. T. et al. Current understanding of gut microbiota in mood disorders: an update of human studies. *Front. Genet.* **10**, 98 (2019).
- Yang, C. et al. Key role of gut microbiota in anhedonia-like phenotype in rodents with neuropathic pain. *Transl. Psychiatry* **9**, 57 (2019).
- Burokas, A. et al. Targeting the microbiota-gut-brain axis: prebiotics have anxiolytic and antidepressant-like effects and reverse the impact of chronic stress in mice. *Biol. Psychiatry* **82**, 472–487 (2017).
- den Besten, G. et al. The role of short-chain fatty acids in the interplay between diet, gut microbiota, and host energy metabolism. *J. Lipid Res.* **54**, 2325–2340 (2013).
- Ho, P. & Ross, D. A. More than a gut feeling: the implications of the gut microbiota in psychiatry. *Biol. Psychiatry* **81**, e35–e37 (2017).
- Qu, Y. et al. Comparison of (R)-ketamine and lanicemine on depression-like phenotype and abnormal composition of gut microbiota in a social defeat stress model. *Sci. Rep.* **7**, 15725 (2017).
- Yang, C. et al. Possible role of the gut microbiota-brain axis in the antidepressant effects of (R)-ketamine in a social defeat stress model. *Transl. Psychiatry* **7**, 1294 (2017).
- Zhang, J. C. et al. Blockade of interleukin-6 receptor in the periphery promotes rapid and sustained antidepressant actions: a possible role of gut-microbiota-brain axis. *Transl. Psychiatry* **7**, e1138 (2017).
- Huang, N. et al. Role of *Actinobacteria* and *Coriobacteria* in the antidepressant effects of ketamine in an inflammation model of depression. *Pharmacol. Biochem. Behav.* **176**, 93–100 (2019).
- Lukić, I. et al. Antidepressants affect gut microbiota and *Ruminococcus flavefaciens* is able to abolish their effects on depressive-like behavior. *Transl. Psychiatry* **9**, 133 (2019).
- Yang, C. et al. *Bifidobacterium* in the gut microbiota confer resilience to chronic social defeat stress in mice. *Sci. Rep.* **7**, 45942 (2017).
- Muneoka, K., Shirayama, Y., Horio, M., Iyo, M. & Hashimoto, K. Differential levels of brain amino acids in rat models presenting learned helplessness or non-learned helplessness. *Psychopharmacol. (Berl.)* **226**, 63–71 (2013).
- Shirayama, Y. et al. Alterations in brain-derived neurotrophic factor (BDNF) and its precursor proBDNF in the brain regions of a learned helplessness rat model and the antidepressant effects of a TrkB agonist and antagonist. *Eur. Neuropsychopharmacol.* **25**, 2449–2458 (2015).
- Shirayama, Y. & Hashimoto, K. Effects of a single bilateral infusion of R-ketamine in the rat brain regions of a learned helplessness model of depression. *Eur. Arch. Psychiatry Clin. Neurosci.* **267**, 177–182 (2017).
- Shirayama, Y. & Hashimoto, K. Lack of antidepressant effects of (2R,6R)-hydroxynorketamine in a rat learned helplessness model: Comparison with (R)-ketamine. *Int. J. Neuropsychopharmacol.* **21**, 84–88 (2018).
- Takahashi, S., Tomita, J., Nishioka, K., Hisada, T. & Nishijima, M. Development of a prokaryotic universal primer for simultaneous analysis of *Bacteria* and *Archaea* using next-generation sequencing. *PLoS ONE* **9**, e105592 (2014).

36. Hisada, T., Endoh, K. & Kuriki, K. Inter- and intra-individual variations in seasonal and daily stabilities of the human gut microbiota in Japanese. *Arch. Microbiol.* **197**, 919–934 (2015).
37. Erik A. ea-utils "Command-line tools for processing biological sequencing data". <http://code.google.com/p/ea-utils> (2011).
38. Edgar, R. C., Haas, B. J., Clemente, J. C., Quince, C. & Knight, R. UCHIME improves sensitivity and speed of chimera detection. *Bioinformatics* **27**, 2194–2200 (2011).
39. Wang, Q., Garrity, G. M., Tiedje, J. M. & Cole, J. R. Naïve Bayesian classifier for rapid assignment of rRNA sequences into the new bacterial taxonomy. *Appl. Environ. Microbiol.* **72**, 5261–5267 (2007).
40. Higashimura, Y. et al. Protective effect of agaro-oligosaccharides on gut dysbiosis and colon tumorigenesis in high-fat diet-fed mice. *Am. J. Physiol. Gastrointest. Liver Physiol.* **310**, G367–G375 (2016).
41. Aoe, S., Nakamura, F. & Fujiwara, S. Effect of wheat bran on fecal butyrate-producing bacteria and wheat bran combined with barley on *Bacteroides* abundance in Japanese healthy adults. *Nutrients* **10**, 1980 (2018).
42. Lin, P. et al. *Prevotella* and *Klebsiella* proportions in fecal microbial communities are potential characteristic parameters for patients with major depressive disorder. *J. Affect. Disord.* **207**, 300–304 (2017).
43. Rong, H. et al. Similarly in depression, nuances of gut microbiota: Evidences from a shotgun metagenomics sequencing study on major depressive disorder versus bipolar disorder with current major depressive episode patients. *J. Psychiatr. Res.* **113**, 90–99 (2019).
44. Finegold, S. M. et al. *Anaerofustis stercorihominis* gen. nov., sp. nov., from human feces. *Anaerobe* **10**, 41–45 (2004).
45. Aitbali, Y. et al. Glyphosate based- herbicide exposure affects gut microbiota, anxiety and depression-like behaviors in mice. *Neurotoxicol. Teratol.* **67**, 44–49 (2018).
46. Yu, M. et al. Variations in gut microbiota and fecal metabolic phenotype associated with depression by 16S rRNA gene sequencing and LC/MS-based metabolomics. *J. Pharm. Biomed. Anal.* **138**, 231–239 (2017).
47. Koh, A., De Vadder, F., Kovatcheva-Datchary, P. & Backhed, F. From dietary fiber to host physiology: short-chain fatty acids as key bacterial metabolites. *Cell* **165**, 1332–1345 (2016).
48. Dibner, J. J. & Buttin, P. Use of organic acids as a model to study the impact of gut microflora on nutrition and metabolism. *J. Appl. Poult. Res.* **11**, 453–463 (2002).
49. Skonieczna-Żydecka, K. et al. Faecal short chain fatty acids profile is changed in Polish depressive women. *Nutrients* **10**, E1939 (2018).
50. Levine, J., Panchalingam, K., McClure, R. J., Gershon, S. & Pettegrew, J. W. Stability of CSF metabolites measured by proton NMR. *J. Neural Transm. (Vienna)*. **107**, 843–848 (2000).
51. Regenold, W. T. et al. Elevated cerebrospinal fluid lactate concentrations in patients with bipolar disorder and schizophrenia: implications for the mitochondrial dysfunction hypothesis. *Biol. Psychiatry* **65**, 489–494 (2009).
52. Ernst, J. et al. Increased pregenual anterior cingulate glucose and lactate concentrations in major depressive disorder. *Mol. Psychiatry* **22**, 113–119 (2017).
53. Shi, B. et al. A ¹H-NMR plasma metabolomic study of acute and chronic stress models of depression in rats. *Behav. Brain Res.* **241**, 86–91 (2013).
54. Carrard, A. et al. Peripheral administration of lactate produces antidepressant-like effects. *Mol. Psychiatry* **23**, 392–399 (2018).
55. Kelly, J. R., Clarke, G., Cryan, J. F. & Dinan, T. G. Brain-gut-microbiota axis: challenges for translation in psychiatry. *Ann. Epidemiol.* **26**, 366–372 (2016).
56. Szyzkowicz, J. K., Wong, A., Anisman, H., Merali, Z. & Audet, M. C. Implications of the gut microbiota in vulnerability to the social avoidance effects of chronic social defeat in male mice. *Brain Behav. Immun.* **66**, 45–55 (2017).
57. Hao, Z., Wang, W., Guo, R. & Liu, H. *Faecalibacterium prausnitzii* (ATCC 27766) has preventive and therapeutic effects on chronic unpredictable mild stress-induced depression-like and anxiety-like behavior in rats. *Psychoneuroendocrinology* **104**, 132–142 (2019).
58. Kentner, A. C., Cryan, J. F. & Brummelte, S. Resilience priming: Translational models for understanding resiliency and adaptation to early life adversity. *Dev. Psychobiol.* **61**, 350–375 (2019).
59. Gururajan, A. et al. Resilience to chronic stress is associated with specific neurobiological, neuroendocrine and immune responses. *Brain Behav. Immun.* <https://doi.org/10.1016/j.bbi.2019.05.004> (2019).
60. Ezewa, V. O., Gerardo, N. M., Inouye, D. W., Medina, M. & Xavier, J. B. Animal behavior and microbiome. *Science* **338**, 198–199 (2012).
61. Borre, Y. E., Moloney, R. D., Clarke, G., Dinan, T. G. & Cryan, J. F. The impact of microbiota on brain and behavior: mechanisms & therapeutic potential. *Adv. Exp. Med. Biol.* **817**, 373–403 (2014).
62. Jianguo, L., Xueyang, J., Cui, W., Changxin, W. & Xuemei, Q. Altered gut metabolome contributes to depression-like behaviors in rats exposed to chronic unpredictable mild stress. *Transl. Psychiatry* **9**, 40 (2019).
63. Bravo, J. A. et al. Ingestion of *Lactobacillus* strain regulates emotional behavior and central GABA receptor expression in a mouse via the vagus nerve. *Proc. Natl Acad. Sci. USA* **108**, 16050–16055 (2011).
64. Dinan, T. G. & Cryan, J. F. Gut microbiomes and depression: still waiting for godot. *Brain Behav. Immun.* **79**, 1–2 (2019).

RAPID COMMUNICATION

(R)-Ketamine Rapidly Ameliorates the Decreased Spine Density in the Medial Prefrontal Cortex and Hippocampus of Susceptible Mice After Chronic Social Defeat Stress

Jiancheng Zhang, MD, PhD, Youge Qu, MS, Lijia Chang, MD, Yaoyu Pu, MD, and Kenji Hashimoto, PhD*

Division of Clinical Neuroscience, Chiba University Center for Forensic Mental Health, Chiba, Japan (Dr Zhang, Ms Qu, and Drs Chang, Pu, and Hashimoto); Department of Critical Care Medicine, Union Hospital, Tongji Medical College, Huazhong University of Science and Technology, Wuhan, China (Dr Zhang)

Correspondence: Kenji Hashimoto, PhD, Division of Clinical Neuroscience, Chiba University Center for Forensic Mental Health, 1-8-1 Inohana, Chiba 260-8670, Japan. (hashimoto@faculty.chiba-u.jp).

Abstract

Background: A recent study demonstrated that spine formation rates by ketamine in the prefrontal cortex (PFC) were not altered at 3–6 h following a single injection, but were markedly altered at 12–24 h. Here, we investigated the acute (3 h post-treatment) effects of (R)-ketamine in the decreased spine density in the medial PFC (mPFC) and hippocampus in susceptible mice after chronic social defeat stress (CSDS).

Methods: (R)-ketamine (10 mg/kg) or saline was administered intraperitoneally to CSDS-susceptible mice. Dendritic spine density in the mPFC and hippocampus was measured 3 h after a single injection.

Results: (R)-ketamine significantly ameliorated the decreased spine density in the prelimbic area of mPFC, Cornu Ammonis3, and dentate gyrus of the hippocampus of CSDS-susceptible mice

Conclusions: This study suggests that (R)-ketamine rapidly ameliorates the decreased spine density in the mPFC and hippocampus of CSDS-susceptible mice, resulting in its rapid-acting antidepressant effects.

Keywords: Rapid-acting antidepressant, dendritic spine density, (R)-ketamine, medial prefrontal cortex, hippocampus

Introduction

The discovery of the rapid-acting and sustained antidepressant effects of the N-methyl-D-aspartate receptor (NMDAR) antagonist ketamine in treatment-resistant patients with depression was serendipitous (Krystal et al., 2019). However, the precise molecular mechanisms underlying the antidepressant effect of ketamine remain to be elucidated (Hashimoto, 2019; Zhang and Hashimoto, 2019a). Chronic stress paradigms, such as chronic

social defeat stress (CSDS) and chronic unpredicted mild stress (CUMS), are known to profoundly reduce dendritic spine density and functions in the prefrontal cortex (PFC) and hippocampus; these effects could contribute to the morphological and functional alterations observed in patients with depression (Duman and Aghajanian, 2012; Duman and Duman, 2015). Ketamine (10 mg/kg, 24 h post-treatment) ameliorated the decreased spine

Received: August 14, 2019; Revised: August 24, 2019; Accepted: August 28, 2019

© The Author(s) 2019. Published by Oxford University Press on behalf of CINP.

This is an Open Access article distributed under the terms of the Creative Commons Attribution Non-Commercial License (<http://creativecommons.org/licenses/by-nc/4.0/>), which permits non-commercial re-use, distribution, and reproduction in any medium, provided the original work is properly cited. For commercial re-use, please contact journals.permissions@oup.com

Significance Statement

The discovery of rapid-acting and sustained antidepressant effects of ketamine in patients with treatment-resistant depression is serendipitous. A recent study using single-cell 2-photon calcium imaging demonstrated that spine formation rates in the prefrontal cortex (PFC) by (R,S)-ketamine were slow. Here, we report that (R)-ketamine rapidly (<3 h) ameliorates the decreased spine density in the medial PFC of susceptible mice after chronic social defeat stress. Therefore, it is likely that the rapid rescue of spine formation by (R)-ketamine contributes to its rapid-acting antidepressant effects.

synapse number in the medial PFC (mPFC) in mice after CUMS (Li et al., 2011), resulting in its sustained antidepressant effects. Notably, the rapid-acting antidepressant ketamine rapidly increases spine synapse numbers in the PFCs of rodents and reverses the effects of chronic stress. These findings support the neurotrophic and synaptogenic hypothesis of depression and rapid-acting antidepressant actions (Duman and Aghajanian, 2012; Duman and Duman, 2015).

(R,S)-ketamine ($K_i = 0.53 \mu\text{M}$ for NMDAR) is an equal amount mixture of (R)-ketamine (or arketamine: $K_i = 1.4 \mu\text{M}$ for NMDAR) and (S)-ketamine (or esketamine: $K_i = 0.3 \mu\text{M}$ for NMDAR; Hashimoto, 2019). On 5 March 2019, the United State Food Drug Administration approved (S)-ketamine nasal spray for treatment-resistant depression. However, preclinical studies demonstrated that (R)-ketamine has greater potency and longer lasting antidepressant effects than (S)-ketamine in rodent models of depression (Zhang et al., 2014a; Yang et al., 2015; Fukumoto et al., 2017; Yang et al., 2017; Yang et al., 2018). Importantly, the side effects of (R)-ketamine in rodents were less than those of (R,S)-ketamine and (S)-ketamine (Yang et al., 2015; Hashimoto et al., 2017; Tian et al., 2018a; Chang et al., 2019). We reported that ketamine and its 2 enantiomers ([R]-ketamine and [S]-ketamine; 10 mg/kg at 8 days post-treatment] significantly ameliorated the decreased spine density in the mPFC and hippocampus in CSDS-susceptible mice (Yang et al., 2015; Dong et al., 2017). Interestingly, (R)-ketamine elicited a more potent beneficial effect on the decreased dendritic spine density in the mPFC and hippocampus of CSDS-susceptible mice than (S)-ketamine (Yang et al., 2015). Compared with (S)-ketamine, it is possible that the greater potency of (R)-ketamine for dendritic spine formation contributes to its longer-lasting antidepressant effects (Yang et al., 2015; Hashimoto, 2019).

A recent study using single-cell 2-photon calcium imaging in awake mice showed that the effects of ketamine (10 mg/kg) on spine formation in the PFC were slower (Moda-Sava et al., 2019). Spine formation rates were not significantly altered at 3–6 h following a single injection of ketamine, but were markedly altered at 12–24 h (Moda-Sava et al., 2019). This study suggests that dendritic spine formation in the PFC was required for the sustained antidepressant effects of ketamine, but not for its acute antidepressant effects (Moda-Sava et al., 2019). Currently, there are no reports showing acute (3 h post-treatment) effects of ketamine on the decreased spine density in the brain after CSDS or CUMS.

The present study was performed to examine whether (R)-ketamine rapidly ameliorates the decreased spine density in the mPFC and hippocampus in CSDS-susceptible mice.

Methods and Materials

Animals

Male, adult, C57BL/6 mice aged 8 weeks (body weight 20–25 g; Japan SLC, Inc., Hamamatsu, Japan) and male, adult, CD1 (ICR)

mice aged 13–15 weeks (body weight >40 g; Japan SLC, Inc., Hamamatsu, Japan) were used. Animals were housed under controlled temperatures and 12 hour light/dark cycles (lights on between 07:00 a.m.–7:00 p.m.), with ad libitum food (CE-2; CLEA Japan, Inc., Tokyo, Japan) and water. The protocol was approved by the Chiba University Institutional Animal Care and Use Committee (permission number 1–376). This study was carried out in strict accordance with the recommendations in the Guide for the Care and Use of Laboratory Animals of the National Institutes of Health in the United States. Animals were deeply anaesthetized with isoflurane before being killed by cervical dislocation. All efforts were made to minimize suffering.

Materials

(R)-ketamine hydrochloride was prepared by recrystallization of (R,S)-ketamine (Ketalar ketamine hydrochloride, Daiichi Sankyo Pharmaceutical Ltd., Tokyo, Japan) and D-(-)-tartaric acid, as described previously (Zhang et al., 2014a). The dose (10 mg/kg as hydrochloride) of (R)-ketamine dissolved in the physiological saline was used as previously reported (Zhang et al., 2014a; Yang et al., 2015; Yang et al., 2017; Yang et al., 2018).

Chronic Social Defeat Stress Model

The procedure of CSDS was performed as previously reported (Figure 1; Yang et al., 2015; Dong et al., 2017; Yang et al., 2017; Qu et al., 2018; Yang et al., 2018). The C57BL/6 mice were exposed to a different CD1 aggressor mouse for 10 min per day for 10 consecutive days. When the social defeat session ended, the resident CD1 mouse and the intruder mouse were each housed in half of a cage, separated by a perforated Plexiglas divider to allow visual, olfactory, and auditory contact for the remainder of the 24-h period. At 24 h after the last session, all mice were housed individually. On Day 11, a social interaction test was performed to identify subgroups of mice that were susceptible and unsusceptible to social defeat stress. This was accomplished

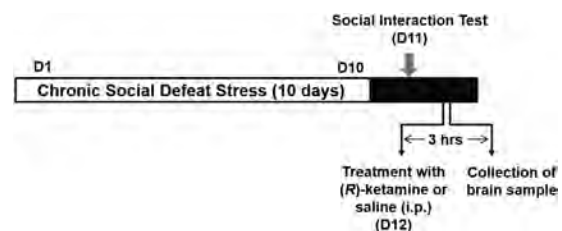


Figure 1. Schedule of CSDS, treatment, and brain collection. CSDS was performed from Day 1 to Day 10. A social interaction test was performed on Day 11 to select susceptible mice. On Day 12, saline (10 ml/kg) or (R)-ketamine (10 mg/kg) was administered i.p. to susceptible mice. Saline (10 ml/kg) was also administered i.p. to control (no CSDS) mice. Golgi-Cox staining in the control mice and CSDS-susceptible mice was performed 3 hours after a single administration of saline or (R)-ketamine. Abbreviations: CSDS, chronic social defeat stress; D, day; i.p., intraperitoneal.

by placing mice in an interaction test box (42 × 42 cm) with an empty wire-mesh cage (10 × 4.5 cm) located at an end. The movement of the mice was tracked for 2.5 min, followed by 2.5 min in the presence of an unfamiliar aggressor who was confined in the wire-mesh cage. The duration of the subject's presence in the "interaction zone" (defined as the 8 cm-wide area surrounding the wire-mesh cage) was recorded by a stopwatch. The interaction ratio was calculated as the time spent in an interaction zone with an aggressor/time spent in an interaction zone without an aggressor. An interaction ratio of 1 was set as the cut-off: mice with scores <1 were defined as "susceptible" to social defeat stress and those with scores ≥1 were defined as "resilient." Approximately 70–80% of mice were susceptible after CSDS. Susceptible mice were randomly divided in the subsequent experiments. Control C57BL/6 mice without CSDS were housed in the cage.

Golgi Staining

As previously reported (Zhang et al., 2014b; Yang et al., 2015; Dong et al., 2017; Qu et al., 2018), Golgi staining was performed using the FD Rapid Golgi Stain TM Kit (FD Neuro Technologies, Inc., Columbia, MD), following the manufacturer's instructions. At 3 h after a single intraperitoneal administration of saline (10 ml/kg) or (R)-ketamine (10 mg/kg), mice were deeply anesthetized with isoflurane and sodium pentobarbital; the brains were removed from the skull and rinsed in double-distilled water. Brains were immersed overnight in the impregnation solution, made by mixing equal volumes of Solution A and B, and were then stored in the dark in fresh solution for 2 weeks. Brains were transferred into Solution C overnight and then stored in the dark in fresh solution at 4°C for 1 week. Coronal brain sections (100 μm thickness) were cut on a cryostat (3050S, Leica Microsystems AG, Wetzlar, Germany), with the chamber temperature set at -20°C. Each section was mounted in Solution C, on saline-coated microscope slides. After absorption of excess solution, sections were dried naturally at room temperature. Dried sections were processed following the manufacturer's instructions. Briefly, images of dendrites within the prelimbic (PrL) area and infralimbic (IL) area of the mPFC, dentate gyrus (DG), Cornu Ammonis (CA1), and CA3 of the hippocampus were captured using a 100× objective with a Keyence BZ-9000 Generation microscope (Osaka, Japan). Spines were counted along mPFC, DG, CA1, and CA3 dendrites, starting from their point of origin from the primary dendrite, as previously reported (Yang et al., 2015; Dong et al., 2017; Qu et al., 2018). For spine density measurements, all clearly evaluable areas containing 50–100 μm of secondary dendrites from each imaged neuron were used. To determine the relative spine density, spines on multiple dendritic branches from a single neuron were counted to obtain an average spine number per 10 μm. For spine number measurements, only spines that emerged perpendicular to the dendritic shaft were counted. We analyzed 3 neurons per section and 3 sections per animal. The average value for each region was obtained in each individual. These individual averages were then combined to yield a grand average for each region.

Statistical Analysis

The data are shown as the mean ± standard error of the mean. An analysis was performed using PASW Statistics 20 (formerly SPSS Statistics). Comparisons between groups were performed using a 1-way analysis of variance, followed by a post hoc Tukey test. A *P* value of less than 0.05 was considered statistically significant.

Results

Dendritic spine densities in the PrL regions of the mPFC, CA3, and DG of the hippocampus from susceptible mice were significantly lower than those from control mice, consistent with previous reports (Figure 2A, D, and E; Yang et al., 2015; Dong et al., 2017; Qu et al., 2018). In contrast, spine densities in the IL regions of the mPFC and CA1 of the hippocampus from susceptible mice were not different from those in control mice, consistent with previous reports (Figure 2B and C; Yang et al., 2015; Dong et al., 2017; Qu et al., 2018). A single injection of (R)-ketamine (10 mg/kg at 3 h post-treatment) significantly ameliorated the decreased spine densities in the PrL areas of the mPFC, CA3, and DG of the hippocampus from susceptible mice (Figure 2A, D, and E).

Discussion

A recent study demonstrated that (R,S)-ketamine (10 mg/kg at 3–6 h post-treatment) did not affect the decreased spine density in the PFC of chronically corticosterone-treated mice, whereas (R,S)-ketamine markedly improved spine formation at 12–24 h (Moda-Sava et al., 2019). This observation suggests that spine formation is not involved in the rapid-acting antidepressant effects of (R,S)-ketamine, since (R,S)-ketamine (at 3–48 h post-treatment) rapidly attenuated the increased immobility time in the tail suspension test (TST).

In this study, we used (R)-ketamine, since (R)-ketamine elicited more potent antidepressant effects than (R,S)-ketamine and (S)-ketamine in a CSDS model (Chang et al., 2019). We found that (R)-ketamine (at 10 mg/kg) rapidly (<3 h) ameliorated the decreased spine densities in the PrL regions of the mPFC, CA3, and DG of the hippocampus in CSDS-susceptible mice. Furthermore, (R,S)-ketamine (or [R]-ketamine; at 10 mg/kg) rapidly (<3–4 h) attenuated the increased immobility time of TST in CSDS-susceptible mice (Tian et al., 2018b; Zhang and Hashimoto, 2019b). Although we did not investigate spines in the same regions of the same mice using the 2-photon imaging technique, it seems that (R)-ketamine could rapidly normalize the decreased spine densities of susceptible mice to control levels, resulting in its rapid-acting antidepressant effects.

It was reported that (R,S)-ketamine (5 mg/kg at 3 h post-treatment) rescued the decreased densities of thin spines, but not mushroom spines, in the mPFCs of male rats subjected to isolation stress (Sarkar and Kabbaj, 2016). Although the decline in total spine density was a cumulative effect of the declines in thin spines and mushroom spines, it has been suggested that the acute increase in spine density by ketamine was mediated mostly through an increase in thin spines (new, immature spines; Sarkar and Kabbaj, 2016). In addition, (S)-ketamine (15 mg/kg) reversed dendritic spine deficits in <1 h in CA1 pyramidal neurons of Flinders sensitive rats with a depression-like phenotype (Treccani et al., 2019). Cumulatively, it is likely that normalization of the decreased spine density in the brain by (R)-ketamine is more rapid.

Moda-Sava et al. (2019) used a chronic (21 days) corticosterone exposure model as a mouse model of depression. Chronic corticosterone treatment decreased dendritic spine density throughout the PFC, including in the anterior cingulate, PrL, and IL subregions, whereas ketamine had the opposite effect. Although ketamine showed a rapid (3 h post-treatment) antidepressant-like effect in TST, spine formation rates were not significantly altered at 3 to 6 hours post-treatment, but were markedly elevated at 12 to 24 hours. It has been suggested that the rescue of spine formation by ketamine is associated with

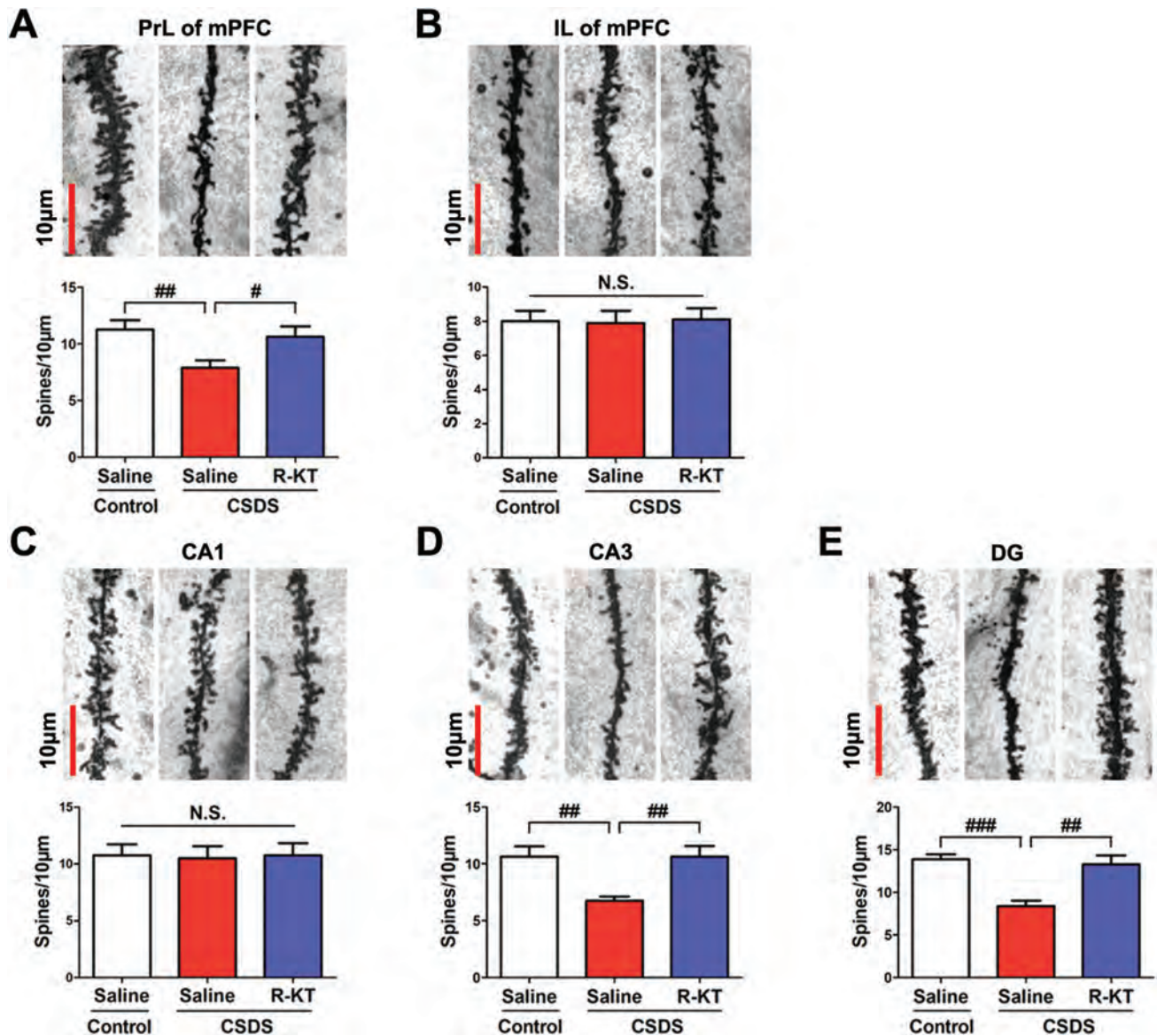


Figure 2. Rapid effects of (R)-ketamine on the decreased dendritic spine density in the prefrontal cortex and hippocampus in susceptible mice after CSDS. (A-E) Dendritic spine density in the PrL and IL regions of the mPFC, CA1, CA3, and DG of the hippocampus. The bar is 10 µm. (A) PrL region of mPFC (1-way ANOVA, $F_{2,21} = 4.825$; $P = 0.019$). (B) IL region of mPFC (1-way ANOVA, $F_{2,21} = 0.027$; $P = 0.973$). (C) CA1 of hippocampus (1-way ANOVA, $F_{2,21} = 0.019$; $P = 0.982$). (D) CA3 of hippocampus (1-way ANOVA, $F_{2,21} = 8.144$; $P = 0.002$). (E) DG of hippocampus (1-way ANOVA, $F_{2,21} = 14.070$; $P < 0.001$). The values represent the mean \pm standard error of the mean ($n = 8$ /group). * $P < 0.05$, ** $P < 0.01$, and *** $P < 0.001$, compared with saline-treated CSDS-susceptible mice. Abbreviations: ANOVA, analysis of variance; CSDS, chronic social defeat stress; DG, dentate gyrus; IL, infralimbic; mPFC, medial prefrontal cortex; N.S., not significant; PrL, prelimbic; R-KT, (R)-ketamine.

its behavioral changes (Li et al., 2011; Duman and Aghajanian, 2012; Duman and Duman, 2015). However, this paper showed that ketamine-induced spine formation affects the immobility time of TST, but not anhedonia, in the sucrose preference test, suggesting a specific role of the PFC and other regions for motivated escape behavior and anhedonia (Moda-Sava et al., 2019). Lipopolysaccharide (LPS) is known to produce depression-like behaviors in rodents 24 hours after a single dose (Dantzer et al., 2008; Zhang et al., 2014b). In addition, *in vivo* imaging using 2-photon microscopy showed long-term changes in dendritic spines in the mouse brain after a single dose of LPS (Kondo et al., 2011). Therefore, it is of interest to investigate the acute (<3 h) and sustained (<24 h) effects of ketamine and its enantiomers for spine formation in LPS-treated rodents, using single-cell 2-photon calcium imaging.

In this study, we did not examine the effects of (R)-ketamine in the spine formation of control mice, since (R)-ketamine did not show antidepressant-like effects in control (no CSDS) mice (Zhang et al., 2018). In addition, Nugent et al. (2019) reported that ketamine caused depressive symptoms (i.e., anhedonia) in healthy control subjects, indicating that ketamine does not have antidepressant effects in healthy control subjects. Nonetheless, it is also of interest to investigate whether (R)-ketamine can affect dendritic spine density in the control mice. In this study, we did not measure the synaptic proteins [i.e., PSD-95 (postsynaptic density protein 95) and GluA1 (α -amino-3-hydroxy-5-methyl-4-isoxazolepropionic acid receptor 1)] in the mPFC and hippocampus in CSDS-susceptible mice. It is of interest to examine whether (R)-ketamine can ameliorate the decreased

expression of these proteins in these regions, since ketamine and (R)-ketamine ameliorated these proteins (Duman and Aghajanian, 2012; Duman and Duman, 2015; Yang et al, 2015; Dong et al, 2017).

In conclusion, this study indicates that (R)-ketamine rapidly (<3 h) ameliorates the decreased spine densities in the PrL regions of the mPFC, CA3, and DG in susceptible mice after CSDS, suggesting this mechanism for its rapid-acting antidepressant effects. Further detailed study using single-cell 2-photon calcium imaging is needed to confirm the acute effects of ketamine and its enantiomers for spine formation in rodents with depression-like phenotypes.

Acknowledgments

This study was supported by Japan Agency for Medical Research and Development (grant number JP19dm0107119 to K. H.).

K. H. is an inventor on a filed patent application on “The use of R-ketamine in the treatment of psychiatric diseases” by Chiba University. The other authors have no conflicts of interest.

References

- Chang L, Zhang K, Pu Y, Qu Y, Wang SM, Xiong Z, Ren Q, Dong C, Fujita Y, Hashimoto K (2019) Comparison of antidepressant and side effects in mice after intranasal administration of (R,S)-ketamine, (R)-ketamine, and (S)-ketamine. *Pharmacol Biochem Behav* 181:53–59.
- Dantzer R, O'Connor JC, Freund GG, Johnson RW, Kelley KW (2008) From inflammation to sickness and depression: when the immune system subjugates the brain. *Nat Rev Neurosci* 9:46–56.
- Dong C, Zhang JC, Yao W, Ren Q, Ma M, Yang C, Chaki S, Hashimoto K (2017) Rapid and sustained antidepressant action of the mGlu2/3 receptor antagonist MGS0039 in the social defeat stress model: comparison with ketamine. *Int J Neuropsychopharmacol* 20:228–236.
- Duman RS, Aghajanian GK (2012) Synaptic dysfunction in depression: potential therapeutic targets. *Science* 338:68–72.
- Duman CH, Duman RS (2015) Spine synapse remodeling in the pathophysiology and treatment of depression. *Neurosci Lett* 601:20–29.
- Fukumoto K, Toki H, Iijima M, Hashihayata T, Yamaguchi JI, Hashimoto K, Chaki S (2017) Antidepressant potential of (R)-ketamine in rodent models: comparison with (S)-ketamine. *J Pharmacol Exp Ther* 361:9–16.
- Hashimoto K (2019) Rapid-acting antidepressant ketamine, its metabolites and other candidates: a historical overview and future perspective. *Psychiatry Clin Neurosci* doi:10.1111/pcn.12902
- Hashimoto K, Kakiuchi T, Ohba H, Nishiyama S, Tsukada H (2017) Reduction of dopamine D2/3 receptor binding in the striatum after a single administration of esketamine, but not R-ketamine: a PET study in conscious monkeys. *Eur Arch Psychiatry Clin Neurosci* 267:173–176.
- Kondo S, Kohsaka S, Okabe S (2011) Long-term changes of spine dynamics and microglia after transient peripheral immune response triggered by LPS in vivo. *Mol Brain* 4:27.
- Krystal JH, Abdallah CG, Sanacora G, Charney DS, Duman RS (2019) Ketamine: a paradigm shift for depression research and treatment. *Neuron* 101:774–778.
- Li N, Liu RJ, Dwyer JM, Banasr M, Lee B, Son H, Li XY, Aghajanian G, Duman RS (2011) Glutamate N-methyl-D-aspartate receptor antagonists rapidly reverse behavioral and synaptic deficits caused by chronic stress exposure. *Biol Psychiatry* 69:754–761.
- Moda-Sava RN, Murdock MH, Parekh PK, Fetcho RN, Huang BS, Huynh TN, Witzum J, Shaver DC, Rosenthal DL, Alway EJ, Lopez K, Meng Y, Nellissen L, Grosenick L, Milner TA, Deisseroth K, Bito H, Kasai H, Liston C (2019) Sustained rescue of prefrontal circuit dysfunction by antidepressant-induced spine formation. *Science* 364:eaat8078.
- Nugent AC, Ballard ED, Gould TD, Park LT, Moaddel R, Brutsche NE, Zarate CA Jr (2019) Ketamine has distinct electrophysiological and behavioral effects in depressed and healthy subjects. *Mol Psychiatry* 24:1040–1052.
- Qu Y, Yang C, Ren Q, Ma M, Dong C, Hashimoto K (2018) Regional differences in dendritic spine density confer resilience to chronic social defeat stress. *Acta Neuropsychiatr* 30:117–122.
- Sarkar A, Kabbaj M (2016) Sex differences in effects of ketamine on behavior, spine density, and synaptic proteins in socially isolated rats. *Biol Psychiatry* 80:448–456.
- Tian Z, Dong C, Fujita A, Fujita Y, Hashimoto K (2018a) Expression of heat shock protein HSP-70 in the retrosplenial cortex of rat brain after administration of (R,S)-ketamine and (S)-ketamine, but not (R)-ketamine. *Pharmacol Biochem Behav* 172:17–21.
- Tian Z, Dong C, Zhang K, Chang L, Hashimoto K (2018b) Lack of antidepressant effects of low-voltage-sensitive T-type calcium channel blocker ethosuximide in a chronic social defeat stress model: comparison with (R)-ketamine. *Int J Neuropsychopharmacol* 21:1031–1036.
- Treccani G, Ardalan M, Chen F, Musazzi L, Popoli M, Wegener G, Nyengaard JR, Müller HK (2019) S-ketamine reverses hippocampal dendritic spine deficits in Flinders sensitive line rats within 1 h of administration. *Mol Neurobiol*. Advance online publication. Retrieved 29 April 2019. doi:10.1007/s12035-019-1613-3.
- Yang C, Shirayama Y, Zhang JC, Ren Q, Yao W, Ma M, Dong C, Hashimoto K (2015) R-ketamine: a rapid-onset and sustained antidepressant without psychotomimetic side effects. *Transl Psychiatry* 5:e632.
- Yang C, Qu Y, Fujita Y, Ren Q, Ma M, Dong C, Hashimoto K (2017) Possible role of the gut microbiota-brain axis in the antidepressant effects of (R)-ketamine in a social defeat stress model. *Transl Psychiatry* 7:1294.
- Yang C, Ren Q, Qu Y, Zhang JC, Ma M, Dong C, Hashimoto K (2018) Mechanistic target of rapamycin-independent antidepressant effects of (R)-ketamine in a social defeat stress model. *Biol Psychiatry* 83:18–28.
- Zhang JC, Li SX, Hashimoto K (2014a) R (-)-ketamine shows greater potency and longer lasting antidepressant effects than S (+)-ketamine. *Pharmacol Biochem Behav* 116:137–141.
- Zhang JC, Wu J, Fujita Y, Yao W, Ren Q, Yang C, Li SX, Shirayama Y, Hashimoto K (2014b) Antidepressant effects of TrkB ligands on depression-like behavior and dendritic changes in mice after inflammation. *Int J Neuropsychopharmacol* 18:pyu077.
- Zhang K, Hashimoto K (2019a) An update on ketamine and its two enantiomers as rapid-acting antidepressants. *Expert Rev Neurother* 19:83–92.
- Zhang K, Hashimoto K (2019b) Lack of opioid system in the antidepressant actions of ketamine. *Biol Psychiatry* 85:e25–e27.
- Zhang K, Ma M, Dong C, Hashimoto K (2018) Role of inflammatory bone markers in the antidepressant actions of (R)-ketamine in a chronic social defeat stress model. *Int J Neuropsychopharmacol* 21:1025–1030.

The Chiba-Otawa Joint Session of Pharmacology 2019

Organizer: Naohiko Anzai, M.D., Ph.D.(Chiba University)
Date: Tuesday, July 23 to Wednesday, July 24, 2019
Place: Chiba University Graduate School of Medicine
(1-8-1 Inohana, Chuo-ku, Chiba 260-8670, Japan)

Schedule:
Day 1 (July 23)

- 14:00-14:40 Short Lecture at Department of Pharmacology
- "New Drug Development targeting Membrane Transporters"
Naohiko Anzai, M.D., Ph.D.
Professor of Department of Pharmacology,
Chiba University Graduate School of Medicine, Chiba, Japan
- 14:40-15:20 Young Investigator Session I at Department of Pharmacology
- "Characterization of the expression of LAT1 as a prognostic indicator and a therapeutic target in renal cell carcinoma"
Dr. Kosuke Higuchi (Department of Pharmacology)
- " Interactions of anti human immunodeficiency virus drugs with renal organic anion transporters"
Dr. Meika Kaneko (Department of Pharmacology)
- 15:20-15:40 Free Communication
- 15:40-16:00 Break
- 16:00-17:00 Lecture at Library Hall of Inohana Medical Library
- "Chemical probes for cell signaling and virus-induced cancer"
John Paul Pezacki, Ph.D.
Professor Department of Chemistry and Biomolecular Sciences
University of Ottawa, Canada
- Coorganized by Molecular Chirality Research Center, Chiba University, Molecular Signal Research Department,
"Physiological Function and Molecular Target Drug Discovery"
Group "Inohana Meeting"

Day 2 (July 24)

10:00-11:00 Young Investigator Session II at Seinan Seminar Room

“The inhibitory mechanism of lung mixed culture-derived epithelial cells (LMDEC) against pulmonary fibrosis”

Shuichi Matsuda, M.D. (Department of Biomedical Science / Respiriology)

"Biased adipocyte differentiation induces visceral adipose inflammation in obesity and aging"

Dr. Ryuzaburo Yuki (Department of Disease Biology and Molecular Medicine)

"Resident cardiac macrophages are involved in cardioprotection through metabolic regulation of cardiomyocytes"

Mr. Takahiro Ishii (Department of Disease Biology and Molecular Medicine, Department of Molecular Cardiovascular Pharmacology)

"Antidepressant actions of ketamine enantiomers"

Dr. Lijia Chang. (Center for Forensic Mental Health)

11:00-11:20 Free Communication

